



Hollandse Kust (west) Wind Farm Zone Extension Area

Geotechnical Advice

P904711/GA | 02 | 2 June 2021

Final

Rijksdienst voor Ondernemend Nederland



Rijksdienst voor Ondernemend
Nederland

Document Control

Document Information

Document Title	Hollandse Kust (west) Wind Farm Zone Extension Area Geotechnical Advice
Fugro Project No.	P904711
Fugro Document No.	P904711/GA
Issue Number	02
Issue Status	Final
Quality Management	Refer to appendix 'Supplementary Information about Document'
Fugro Project Lead	B.B. Klosowska – Principal Geologist

Client Information

Client	Rijksdienst voor Ondernemend Nederland
Client Address	Prinses Beatrixlaan 2 2595 AL Den Haag The Netherlands
Client Contact	Peter-Paul Lebbink
Client Document No.	WOZ2190153

Document History

Issue	Date	Status
02	02 June 2021	Final
01	30 April 2021	Complete

Contents

1. Introduction	1
1.1 Purpose of Report	1
1.2 Scope of Report	1
1.3 Project Responsibilities and Use of Report	2
2. Study Approach and Methodology	3
3. Site Conditions	4
3.1 Site Use	4
3.2 Seafloor Conditions	4
3.3 Soil Units	5
3.4 Geological Features	7
3.5 Soil Provinces	8
4. Comments on Site Suitability	10
5. Sources of Information and References	11

Figures in the Main Text

Figure 3.1: UHR MCS data example showing internal seismic character of Geological Soil Units A B, C1 and C2	6
Figure 3.2: UHR MCS data example showing internal seismic character of Geological Soil Units F and G	7
Figure 3.3: SBP data example showing buried channel in Geological Soil Unit B	8
Figure 3.4: UHR MCS data example showing peat / organic clay levels 2A, 2B and 2C	8

Tables in the Main Text

Table 1.1: Companion reports	1
Table 3.1: Seafloor conditions	4
Table 3.2: Soil units	5
Table 3.3: Soil provinces	9
Table 3.4: Depth to base of geotechnical soil unit per soil province	9

Appendices

Appendix A	Plates referenced in Main Text
Appendix B	In Situ Test Results
Appendix C	Descriptions of Methods and Practices
Appendix D	Supplementary Information about Document

1. Introduction

1.1 Purpose of Report

This report presents an assessment of site conditions for the Hollandse Kust (west) Wind Farm Zone Extension Area (HKW EA). The HKW EA is situated within the Hollandse Kust (west) Designated Wind Farm Zone (Plate A.1-1). The HKW EA borders with the Geotechnical Investigation Area, also referred to as Hollandse Kust (west) Wind Farm Zone (HKW WFZ).

The purpose of this report is to provide geotechnical information to aid conceptual design of structures in the HKW EA, including, but not limited to, foundations and cables.

1.2 Scope of Report

The scope of this report includes:

- Presentation of geological and geotechnical soil units, soil provinces and spatial zonation, for the purpose of efficient conceptual design of monopile and jacket pile foundations;
- Commentary on site suitability for wind farm foundations and cables;
- Results of one site-specific cone penetration test (CPT) to 60.3 m below seafloor (BSF).

The information presented here applies to a site defined by (1) an area demarcated as Hollandse Kust (west) Wind Farm Zone Extension Area (HKW EA), shown on Plate A.1-1 and (2) a depth coverage from seafloor to approximately 50 m BSF.

Plates A.1-2 and A.1-3 present details on positioning, water depth and geodetic parameters at the project-specific geotechnical test point. The results from a geotechnical investigation are included in Appendix B 'In Situ Test Results'.

This report has a companion digital deliverable, i.e. an ArcGIS database.

This report is supplementary to and must be read in conjunction with the companion reports listed in Table 1-1.

Table 1.1: Companion reports

Abbreviation	Reference
GGM report	<i>Geological Ground Model, Hollandse Kust (west) Wind Farm Zone Dutch Sector, North Sea</i> . Fugro Report No. P904711/06 (3), issued 12 May 2020 to RVO, Nootdorp, Fugro
GP report	<i>Geotechnical Parameters, Hollandse Kust (west) Wind Farm Zone Dutch Sector, North Sea</i> . Fugro Report No. P904711/07 (6), issued 7 October 2020 to RVO, Nootdorp, Fugro

1.3 Project Responsibilities and Use of Report

This report presents information according to a project specification determined and monitored by the client. The Main Text section titled 'Sources of Information and References' provides further details.

Read this report in its entirety. Particularly, take careful note of document titled 'Use of Geodata and Advice' in appendix titled 'Descriptions of Methods and Practices'.

Fugro understands that this report will be used for the purpose described in this Main Text section. That purpose was a significant factor in determining the scope and level of the services. Results must not be used if the purpose for which the report was prepared or the client's proposed development or activity changes. Results may possibly suit alternative use. Suitability must be verified.

2. Study Approach and Methodology

Refer to Section 2 of companion reports (Table 1.1) for details on study approach and methodology, where applicable.

Provision of a 3D model and synthetic CPT profiles is not part of the scope for this report.

3. Site Conditions

3.1 Site Use

No previous site use is known to Fugro, other than the intrusive geotechnical investigation activities within the HKW EA (Appendix B). These activities resulted in local soil disturbance.

No cables, pipelines and other infrastructure are present within and in close proximity of the site. This information relies on a geophysical survey (Fugro, 2019).

A client-provided database indicates three shipwrecks within the site. The presence of two wrecks was confirmed by the geophysical survey (Fugro, 2019).

An unexploded ordnance (UXO) desk study (REASeuro, 2018) contains information on the likelihood of encountering UXO. No project-specific UXO clearance survey has been conducted.

Fishing activity in the general area is evident from trawl marks observed in geophysical survey data. Trawl scars were observed close to the northern boundary of the site (Fugro, 2019).

Archaeological remains and prehistoric landscapes can be expected locally within the upper Pleistocene layers. The archaeological desk study (Periplus Archeomare, 2018) and archaeological assessment (Periplus Archeomare, 2019) discuss the possible presence of archaeological remains.

3.2 Seafloor Conditions

Table 3.1 presents seafloor conditions in the HKW EA. The information is based on a geophysical survey (Fugro, 2019), geotechnical results from location HKW119-PCPT and information presented in the GGM report.

The provided seafloor conditions relate to the time of the geophysical survey (Fugro, 2019).

Table 3.1: Seafloor conditions

Seafloor Conditions	Description
Bathymetry and morphology	Water depth varies between approximately 27 m and 36 m relative to LAT (Plate A.3-1). The seafloor is undulating as a result of bedforms: sand waves and superimposed megaripples. The sand waves have heights ranging from 1.5 m to 5 m (above surrounding seafloor) and average wavelengths between 150 m and 300 m. The megaripples have heights ranging from approximately 0.5 m to 1.5 m and average wavelengths between 10 m to 20 m. The orientation of the bedforms is generally south-west to north-east.
Gradient	The overall seafloor gradient is less than 6 degrees. The slopes of bedforms reach local values of up to about 12 degrees, related to lee sides of the sand waves (Plate A.3-2).
Soil type(s) at seafloor	Medium dense to very dense silica fine and medium SAND, with shells and shell fragments, with traces of organic matter.

Seafloor Conditions	Description
Objects	<p>Three (3) contacts were detected on the multibeam echosounder (MBES), seventeen (17) on the side scan sonar (SSS) and sixteen (16) on the magnetometer (MAG) datasets.</p> <p>Two wrecks were identified by clear outlines visible on the MBES and SSS data. The identified wrecks are associated with strong MAG signal and a few SSS contacts.</p>

Comments are as follows:

- Water depth changes locally over time as a result of seafloor mobility. The sand wave morphology indicates that the dominant migration direction is to the north-north-west;
- For details on the morphodynamics within the Hollandse Kust (west) Wind Farm Zone refer to Deltares (2020);
- Existing and future windfarms can act as hydraulic obstructions, which can contribute to changing near-seafloor hydrodynamic conditions. These in turn may change the general scheme of sediment deposition patterns and scour (in close vicinity of wind turbine foundations).

3.3 Soil Units

Six geological soil units and seven geotechnical soil units have been identified in the HKW EA to approximately 100 m below Lowest Astronomical Tide (LAT) (Table 3.2).

Plates A.3.-3 to A.3-14 present depth to base and thickness of geological soil units.

Information on the geological setting, seismostratigraphic framework and lithostratigraphic framework are provided in the GGM report. This information also applies to the HKW EA.

Table 3.2: Soil units

Geological Soil Unit [GGM report]	Geotechnical Soil Unit [GP report]	HKW119-PCPT		HKW EA	
		Depth to Base [m LAT] [m BSF]	Thickness [m]	Depth to Base [m LAT]	Thickness [m]
A	A	33.0 1.2	1.2	31 to 35	0.3 to 5
B	B1	-	-	33 to 35	0 to 2
	B2	35.0 3.2	2.0	33 to 43	1 to 10
C1	C1	37.7 5.9	2.7	36 to 41	0 to 6
C2	C2	40.0 8.2	2.3	37 to 42	0 to 4
F	F	58.4 26.6	18.4	55 to 62	15 to 24
G	G	> 92.1 > 60.3	> 33.7	> 90	> 35

Notes:

- Hyphen indicates that the associated soil unit or the unit's basal boundary has not been identified at the geotechnical location
- The base of Soil Unit G was not reached at the geotechnical location. The minimum unit thickness per location is presented where applicable

Comments are as follows:

- Geological Soil Units D and E, interpreted in the HKW WFZ, are not present in the HKW EA;
- Seismic character and geotechnical properties of the geological and geotechnical soil units as provided in the GGM and GP reports, apply to the HKW EA.
- Figures 3.1 and 3.2 show the general seismic character of the geological soil units present in the HKW EA;
- CPT parameters per geotechnical soil unit are within the range of values as presented for the HKW WFZ. Refer to the GP report for details;
- Geotechnical soil unit classification at location HKW119-PCPT follows expectations according to geotechnical soil unit classification at the HKW WFZ for the corresponding units (i.e. Geotechnical Soil Units A, B2, C1, C2, F and G).
- The following predominant soil behaviour types (SBT), based on results from the $Q_{tn}-F_r$ SBT classification chart (Robertson, 2016), are identified per geotechnical soil unit at location HKW119-PCPT:
 - Geotechnical Soil Unit A: Sand-like Dilative – 100 %;
 - Geotechnical Soil Unit B2: Sand-like Dilative – 98 %, Transitional Dilative – 2 %;
 - Geotechnical Soil Unit C1: Sand-like Dilative – 76 %, Transitional Dilative – 21%;
 - Geotechnical Soil Unit C2: Sand-like Dilative – 99 %;
 - Geotechnical Soil Unit F: Sand-like Dilative – 61 %, Transitional Contractive – 14 %, Clay-like Contractive – 12 %, Clay-like Dilative – 8 %;
 - Geotechnical Soil Unit G: Sand-like Dilative – 35 %, Transitional Contractive – 28 %, Clay-like Contractive Sensitive – 20 %, Clay-like Dilative – 5 %, Transitional Dilative – 5 %.

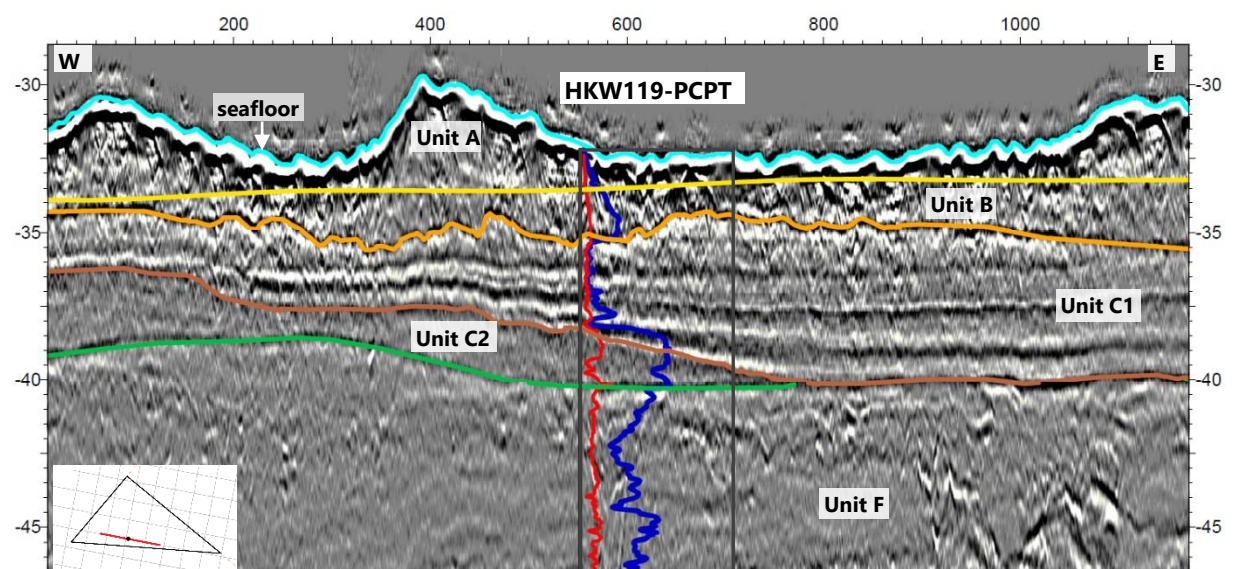


Figure 3.1: UHR MCS data example showing internal seismic character of Geological Soil Units A, B, C1 and C2

Line seq315_2X592infb. Vertical scale is in metres reduced to LAT. The horizontal scale shows relative distance in metres along the survey track line. Width of the CPT box shows cone resistance values (blue curve) within range of 0 to 60 MPa and sleeve friction values (red curve) from 0 to 1.0 MPa. The geotechnical location is within 5 m distance from the seismic line.

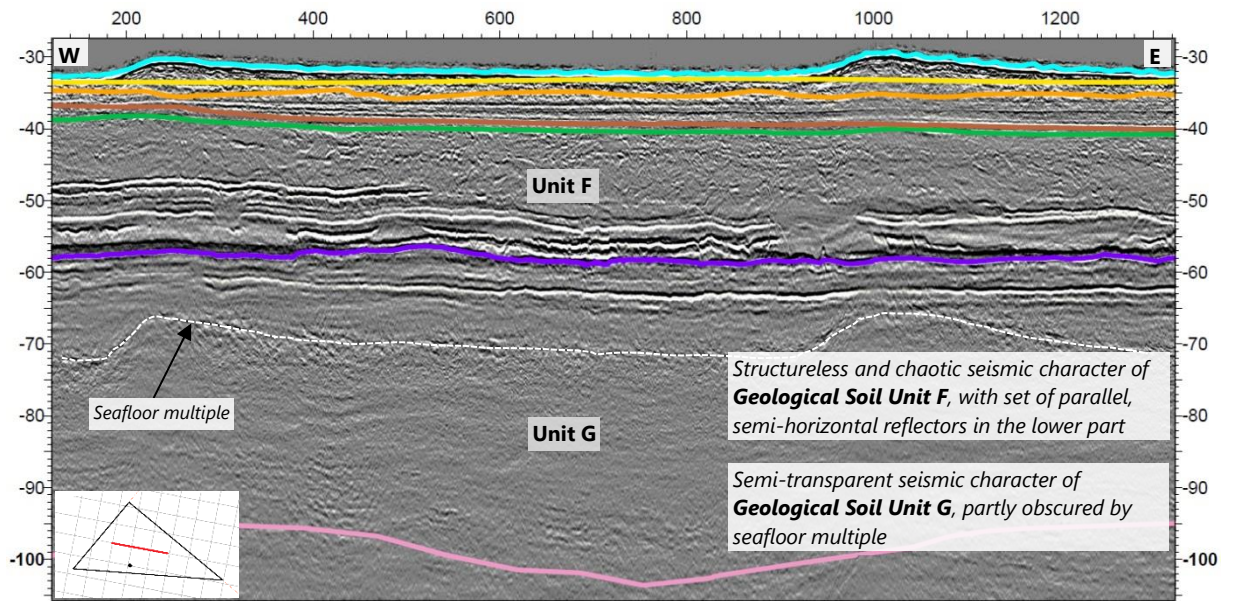


Figure 3.2: UHR MCS data example showing internal seismic character of Geological Soil Units F and G

Line seq417_2X593b. Vertical scale is in metres reduced to LAT. The horizontal scale shows relative distance in metres along the seismic line.

3.4 Geological Features

A map of geological features is presented on Plate A.3-15.

The following geological features were identified within the HKW EA:

- A buried channel in Geological Soil Unit B;
- A buried channel at the base of Geological Soil Unit B;
- Peat/organic clay associated with Geological Soil Unit F, i.e. levels 2A, 2B and 2C.

Figure 3.3 shows a buried channel in Geological Soil Unit B and Figure 3.4 shows peat/organic clay levels 2A, 2B and 2C.

Peat/organic clay level 2A is only occasionally present and of limited spatial extent.

Peat/organic clay levels 2B and 2C each form a thin layer (laminae to thin bed) that is present almost across the entire HKW EA.

No seismic anomalies (e.g. diffraction hyperbolas) suggesting boulders or cobbles were observed in seismic reflection data. Nevertheless, boulders or cobbles can occur in the HKW EA.

Glacial deformation features can be expected in the pre-Saalian sediments, i.e. Geological Soil Units F and G. However, no conclusive evidence for glacial deformation was observed on the seismic reflection data.

No evidence of faults was observed. However, the presence of faults cannot be ruled out, as they can remain undetected because of strong seafloor multiples and limited strength of seismic signal for the deeper strata.

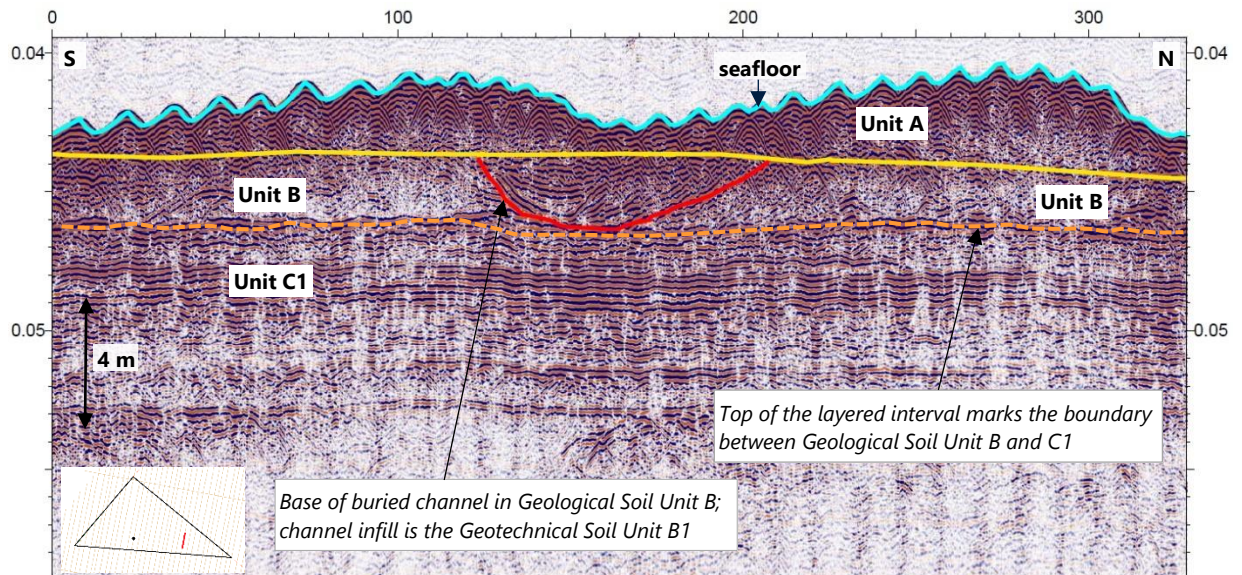


Figure 3.3: SBP data example showing buried channel in Geological Soil Unit B

Line SBP_T/1A038_HMP_101. Vertical scale is as shown. Horizontal scale shows relative distance in metres along the seismic line. The bar scale for depth represents 4 m for a seismic velocity of 1700 m/s.

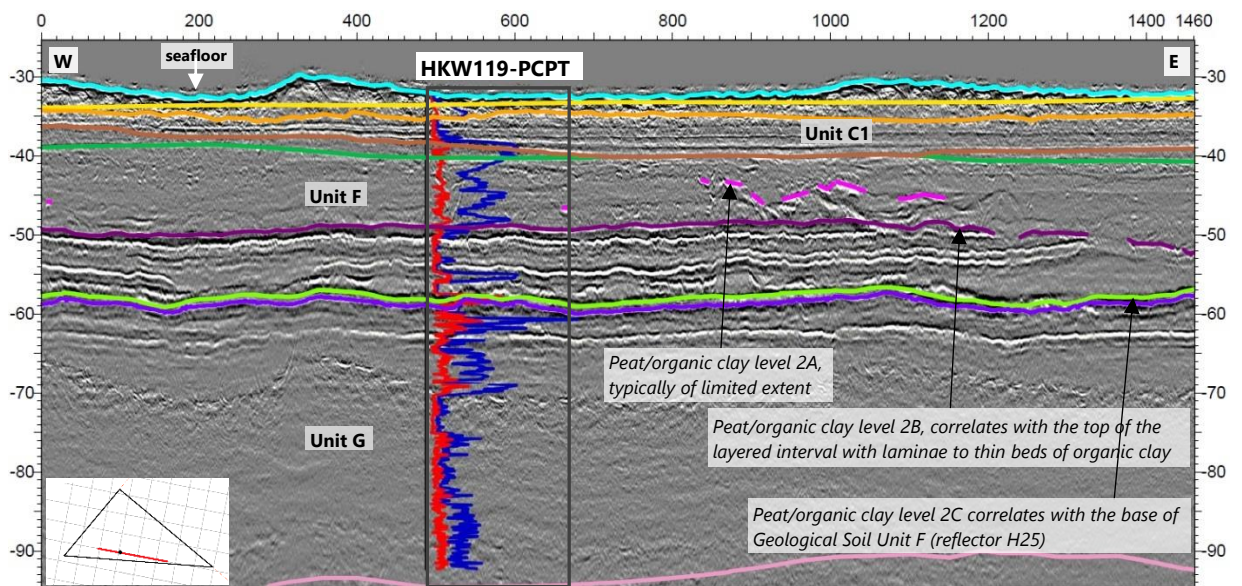


Figure 3.4: UHR MCS data example showing peat / organic clay levels 2A, 2B and 2C

Line seq315_2X592infb. Vertical scale for UHR MCS is in metres reduced to LAT. Horizontal scale shows relative distance in metres along the seismic line. Width of the CPT box shows cone resistance values (blue curve) within range of 0 to 80 MPa and sleeve friction values (red curve) from 0 to 2.5 MPa. The geotechnical location is within 5 m distance from the seismic line.

3.5 Soil Provinces

Plate A.3-16 and Table 3.3 present an overview of soil provinces identified in the HKW EA.

Location HKW119-PCPT belongs to Soil Province 4. Refer to the GP report for further details on geotechnical ground model and soil provinces.

Table 3.3: Soil provinces

Soil Province	Proportion of HKW EA [%]	Primary Feature / Comments
3	2.3	Presence of Geotechnical Soil Unit C2
4	96.5	Presence of Geotechnical Soil Unit C1
5	0.1	Presence of Geotechnical Soil Unit B2 with at least 7 m thickness
7	1.1	Presence of Geotechnical Soil Units B1 (internal channels) and C1

Table 3.4 provides depth to base of the geotechnical soil units per soil province present at the HKW EA. The ranges of depth to base values per soil unit per soil province at the HKW EA are within the corresponding ranges of depth to base values at the HKW WFZ (Fugro, 2020b).

Table 3.4: Depth to base of geotechnical soil unit per soil province

Geotechnical Soil Unit	Depth to Base of Geotechnical Soil Unit [m BSF]							
	Soil Province 3		Soil Province 4		Soil Province 5		Soil Province 7	
	Min	Max	Min	Max	Min	Max	Min	Max
A	1	5	0.5	5	1	2	0.5	4
B1	-	-	-	-	-	-	1	3
B2	4	8	2	6	8	10	3	5
C1	-	-	3	10	-	-	6	9
C2	7	11	6	11	-	-	8	11
D	-	-	-	-	-	-	-	-
E	-	-	-	-	-	-	-	-
F	26	29	23	30	26	27	25	28
G	> 50	> 50	> 50	> 50	> 50	> 50	> 50	> 50

Notes:

- Minimum and maximum depths are based on gridded geophysical horizons
- > 50 means that base of soil unit is below the depth coverage of the geotechnical ground model (i.e. 50 m BSF)
- Hyphen indicates that geotechnical soil unit is absent from the particular soil province

4. Comments on Site Suitability

All potential site-specific hazards and constraints for structures, as listed and described in Section 4 of the GGM report apply to HKW EA, with the exception of 'existing structures', e.g. cables, pipelines', which are not present in the HKW EA.

5. Sources of Information and References

Deltares. (2020). *Morphodynamics for Hollandse Kust (west) Wind Farm Zone*, Document No. 11204811-002-HYE-0001, Version 1.0 (Final), dated 06 July 2020.

Fugro. (2019). *Geophysical Results Report – Hollandse Kust (west) Wind Farm Zone Survey 2018*, Report No. P904162, Vol. 3, Revision 4 (Final), issued 19 August 2019 to RVO.

Fugro. (2020a). *Geological Ground Model, Hollandse Kust (west) Wind Farm Zone Dutch Sector, North Sea*. Report No. P904711/06, Issue 3 (Final), issued 12 May 2020 to RVO.

Fugro. (2020b). *Geotechnical Parameters, Hollandse Kust (west) Wind Farm Zone Dutch Sector, North Sea*. Report No. P904711/07, Issue 6 (Final), issued 7 October 2020 to RVO.

Periplus Archeomare. (2018). *Archaeological Desk Study Hollandse Kust (west) Wind Farm Zone*, Document No. 18A031-01, Issue 4 (Final), issued 18 December 2018 to RVO.

Periplus Archeomare. (2019). *Archaeological Assessment of gGeophysical Survey Results Hollandse Kust (west) Wind Farm Zone*, Document No. 19A015-01, Issue 3 (Final), issued 22 December 2019 to RVO.

REASeuro. (2018). *UXO Desk Study - Unexploded Ordnance - Site Data Hollandse Kust (west) Wind Farm Zone*, Document No. 73065/RO-180140, Issue 3 (Final), 7 August 2018.

Robertson, P.K. (2016). Cone penetration test (CPT)-based soil behaviour type (SBT) classification system – an update. *Canadian Geotechnical Journal* 53, 1910-1927 (2016), Published at www.nrcresearchpress.com/cgj on 14 July 2016.

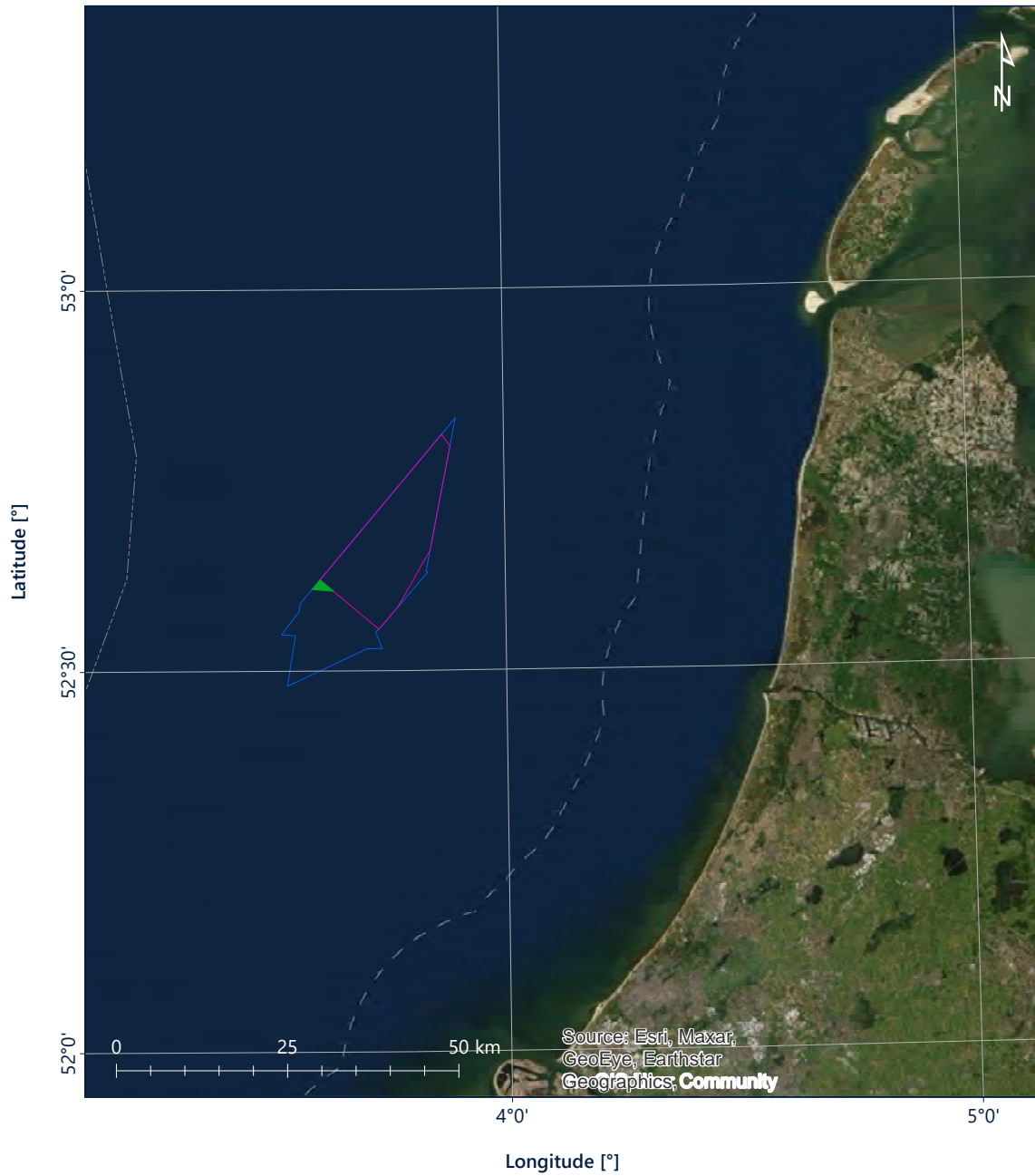
Appendix A

Plates referenced in Main Text

Contents Appendix A: Plates referenced in Main Text

List of Plates

Title	Plate
Vicinity Map	A.1-1
Coordinates and Water Depth at Geotechnical Location	A.1-2
Geodetic Parameters	A.1-3
Plan Overview and Bathymetry	A.3-1
Seafloor Gradient	A.3-2
UHR MCS Track Lines and Cross Section Lines	A.3-3
Cross Sections A-A' & B-B'	A.3-4
Depth to Base of Unit A	A.3-5
Depth to Base of Unit B	A.3-6
Depth to Base of Unit C1	A.3-7
Depth to Base of Unit C2	A.3-8
Depth to Base of Unit F	A.3-9
Thickness of Unit A	A.3-10
Thickness of Unit B	A.3-11
Thickness of Unit C1	A.3-12
Thickness of Unit C2	A.3-13
Thickness of Unit F	A.3-14
Geological Features	A.3-15
Soil Provinces	A.3-16



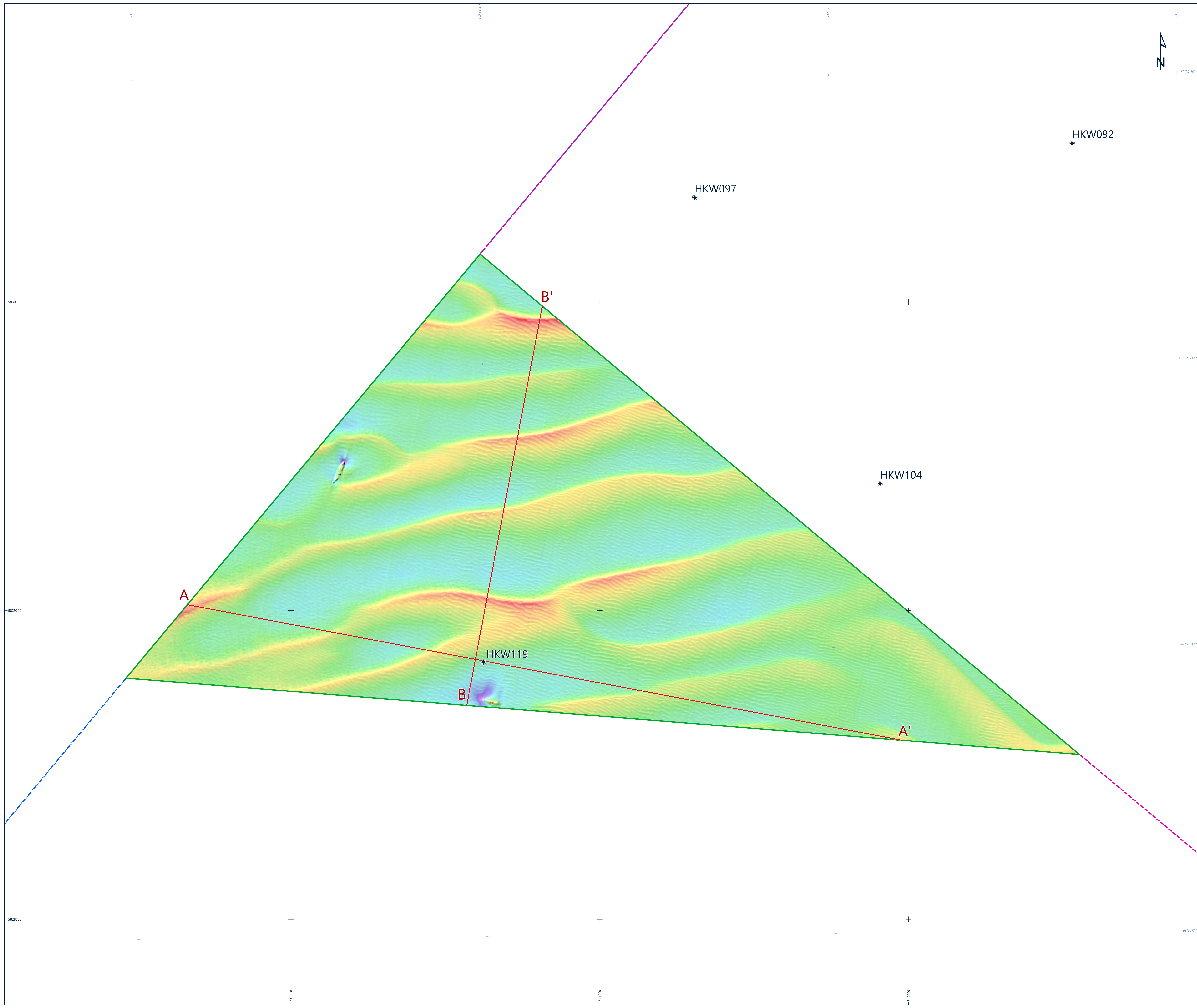
- Hollandse Kust (west) - Extension Area
- Hollandse Kust (west) - Geotechnical Investigation Area
- Hollandse Kust (west) - Designated Wind Farm Zone
- Maritime boundary
- 12 nautical mile zone

Datum : ETRS89
Spheroid : GRS80
Projection : UTM Zone 31N
Central Meridian: 3° East

Vicinity Map

DGPS Geodetic Parameters		
Datum	ITRF2014 (International Terrestrial Reference Frame 2014)	
Spheroid	GRS80 (Geodetic Reference System 1980)	
Semi-Major Axis, a	6 378 137.000 m	
Inverse Flattening, 1/f	298.257 222 101	
Transformation Parameters		
(from ITRF 2014 to Local Datum)		
Source Shift		
dX	+0.05582 m	
dY	+0.05332 m	
dZ	-0.09531 m	
Rotation and Scale		
rX	-0.0026051 "	
rY	-0.0157592 "	
rZ	+0.0254720 "	
dS (Scale Factor)	0.00334778 ppm	
Local Grid Geodetic Parameters		
Datum	ETRS89 (European Terrestrial Reference System 1989)	
Spheroid	GRS80 (Geodetic Reference System 1980)	
Semi-Major Axis, a	6 378 137.000 m	
Inverse Flattening, 1/f	298.257 222 101	
Local Projection Parameters		
Projection	UTM (Universal Transverse Mercator) zone 31N	
Hemisphere	Northern	
Central Meridian (CM)	003° 00' 00.0000" E	
Latitude of Origin	00° 00' 00.0000" N	
False Easting	500 000 m	
False Northing	0 m	
Scale Factor on CM	0.9996	
Units	metres	
Example Coordinates		
Local grid coordinates	Easting	540623.10 m
	Northing	5828832.73 m
Local geographical coordinates	Latitude	52° 36' 28.7533" N
	Longitude	003 ° 35' 59.6448" E
Global geographical coordinates	Latitude	52° 36' 28.8000" N
	Longitude	003 ° 35' 59.6000" E

Geodetic Parameters



LEGEND

GEOTECHNICAL LOCATIONS

- Geotechnical location
- Cross-section presented in the report

GENERAL

- Hollandse Kust (west) Wind Farm Zone Extension Area (HKW EA)
- Hollandse Kust (west) Wind Farm Zone (HKW WFZ)
- HKW - Designated Wind Farm Zone
- UTM grid
- Geographical grid

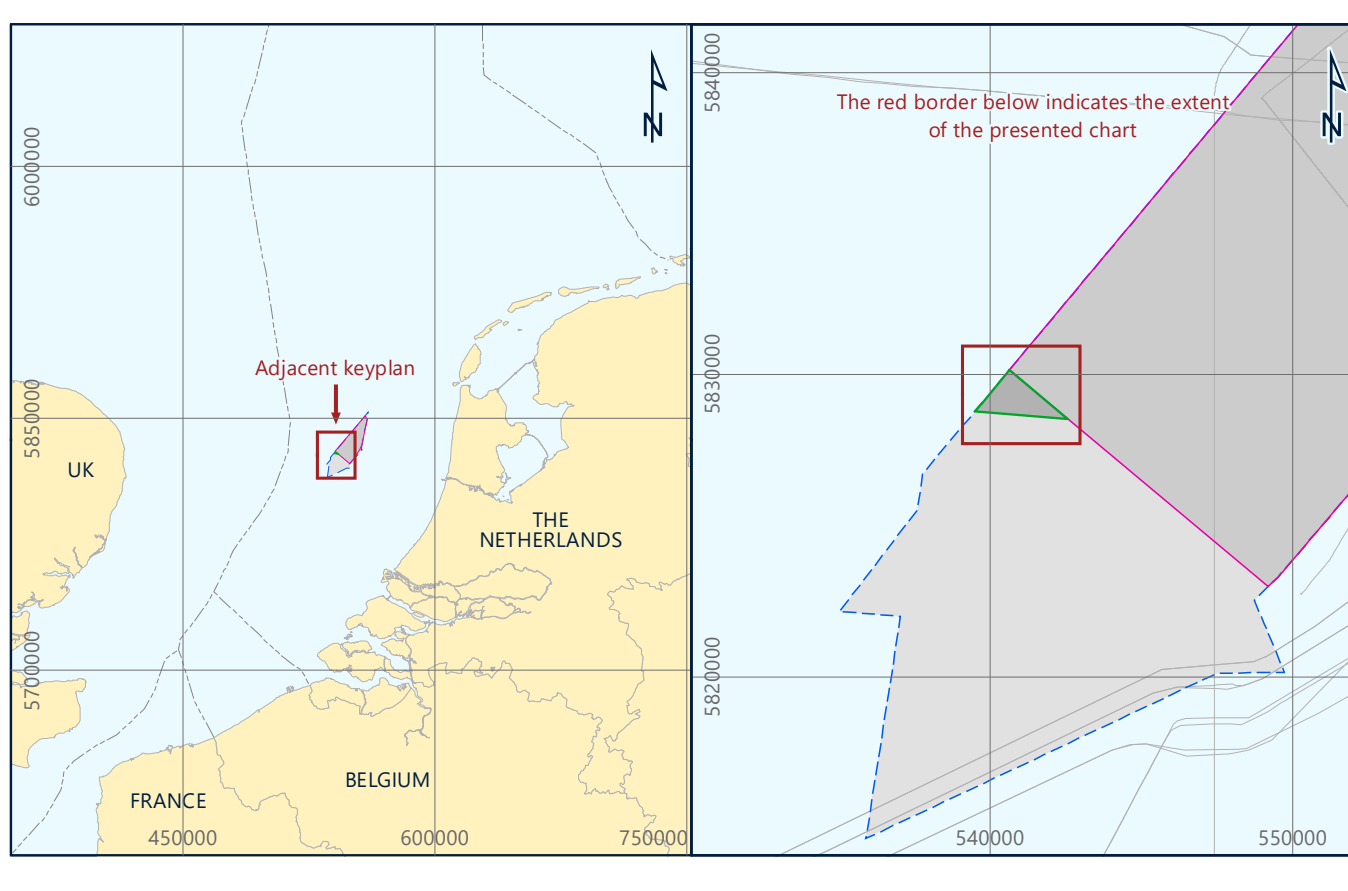


NOTES

- 1) Data acquired by multibeam echosounder (Fugro, 2019).
- 2) Resolution of bathymetry grid cells 0.5 m x 0.5 m.

GEODETIC PARAMETERS

GEODETIC DATUM	European Terrestrial Reference System 1989
ELLIPSOID	GRS 1980
Semi-Major Axis	6 378 137 000 m
Inverse Flattening	298.257 222 101
PROJECTION	ETRS 1989 / UTM Zone 31N (EPSG 25831)
Central Meridian (CM)	03°00'00" E
Latitude of Origin	00°00'00" N
Fake Easting	500 000 mE
Fake Northing	0 mN
Scale Factor at CM	0.9996
DATUM TRANSFORMATION	ITRS2014 to ETRS89 for Epoch 2017.4959
Source	dx = +0.05545 m, dy = +0.05295 m, dz = -0.08834 m, rx = -0.0023082", ry = -0.0139630", rz = -0.0225688", Scale = -0.00294455 ppm
VERTICAL DATUM	Lowest Astronomical Tide (LAT)



RVO
Rijksdienst voor Ondernemend Nederland

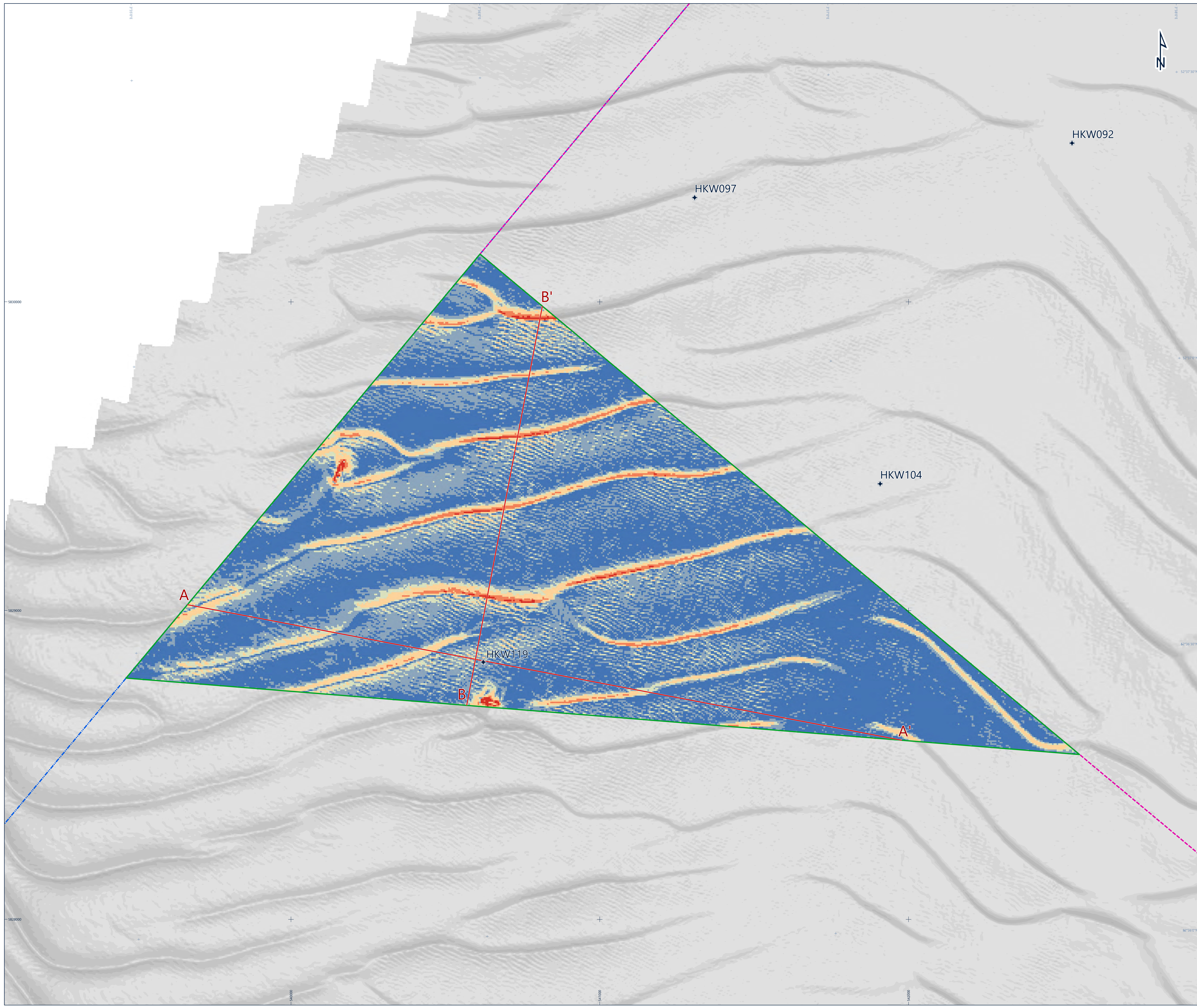
Fugro
Fugro Document No. P90471/GA/01

PLAN OVERVIEW AND BATHYMETRY

GEOTECHNICAL SITE INVESTIGATION
DUTCH SECTOR - NORTH SEA
HOLLANDE KUST (WEST) WIND FARM ZONE EXTENSION AREA

Scale 1 : 4 000 at original A0 page size

Fugro Document No. P90471/GA/01 Chart No. 1 of 1 Plate No. A3-1



LEGEND

GEOTECHNICAL LOCATIONS

- Geotechnical location
- Cross-section presented in the report

GENERAL

- Hollandse Kust (west) Wind Farm Zone Extension Area (HKW EA)
- Hollandse Kust (west) Wind Farm Zone (HKW WFZ)
- HKW - Designated Wind Farm Zone
- UTM grid
- Geographical grid

SEAFLOOR GRADIENT
[deg]

- > 0 - 1
- > 1 - 2
- > 2 - 3
- > 3 - 6
- > 6 - 9
- > 9

NOTES

1) Seafloor gradient derived from bathymetry data (Fugro, 2019).

GEODETIC PARAMETERS

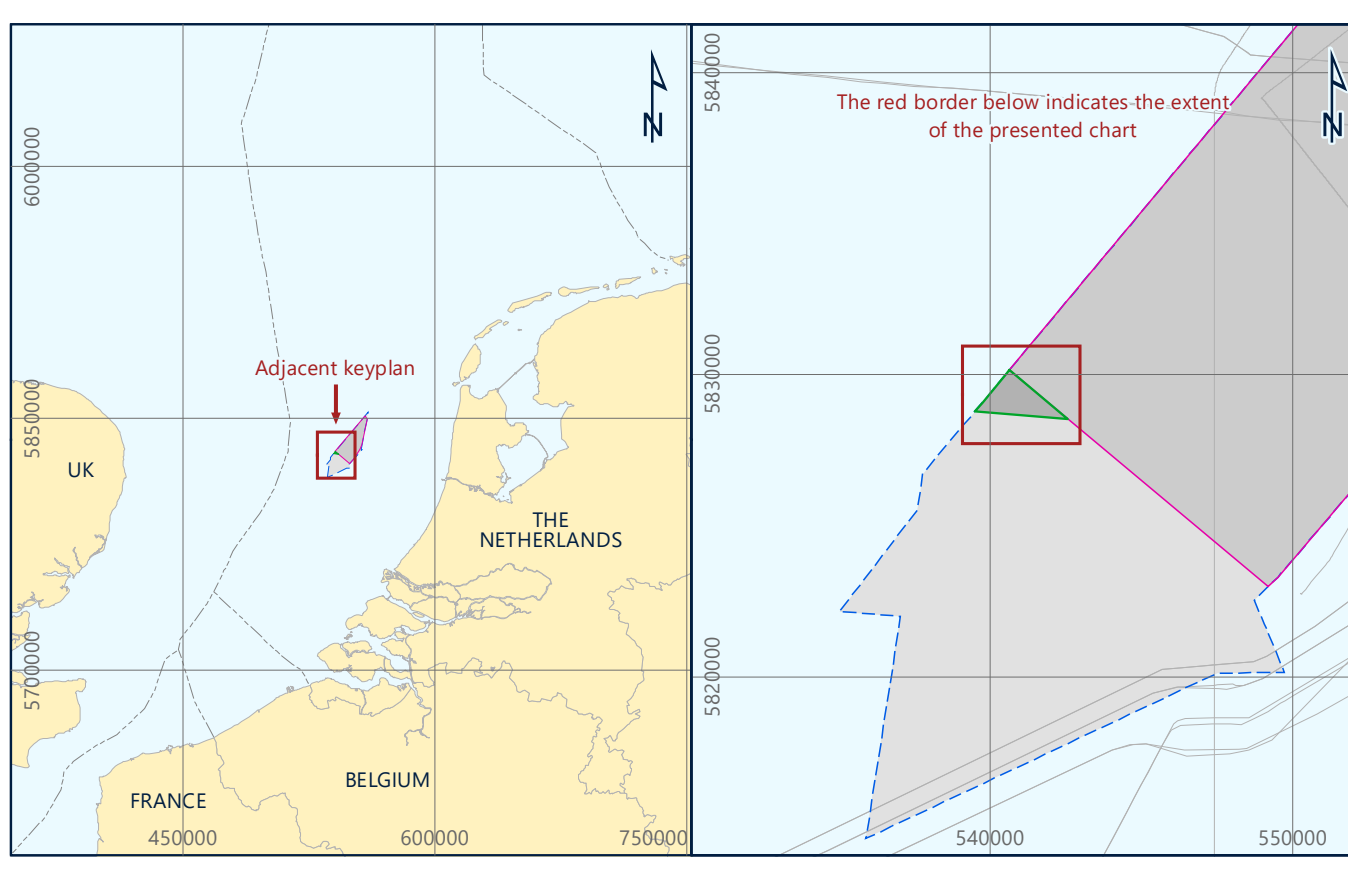
GEODETIC DATUM: European Terrestrial Reference System 1989

ELLIPSOID: GRS 1980
Semi-Major Axis: 6 378 137 000 m
Inverse Flattening: 298.257 222 101

PROJECTION: ETRS 1989 / UTM Zone 31N (EPSG 25831)
Central Meridian (CM): 03°00'00" E
Latitude of Origin: 00°00'00" N
False Easting: 500 000 mE
False Northing: 0 mN
Scale Factor at CM: 0.9996

DATUM TRANSFORMATION: ITRF2014 to ETRS89 for Epoch 2017.4959
Source: dx = +0.0545 m, dy = +0.05295 m, dz = -0.08834 m
rx = -0.0023082", ry = -0.0139630", rz = +0.0225688", Scale = +0.00294455 ppm

VERTICAL DATUM: Lowest Astronomical Tide (LAT)



RVO
Rijksdienst voor Ondernemend Nederland

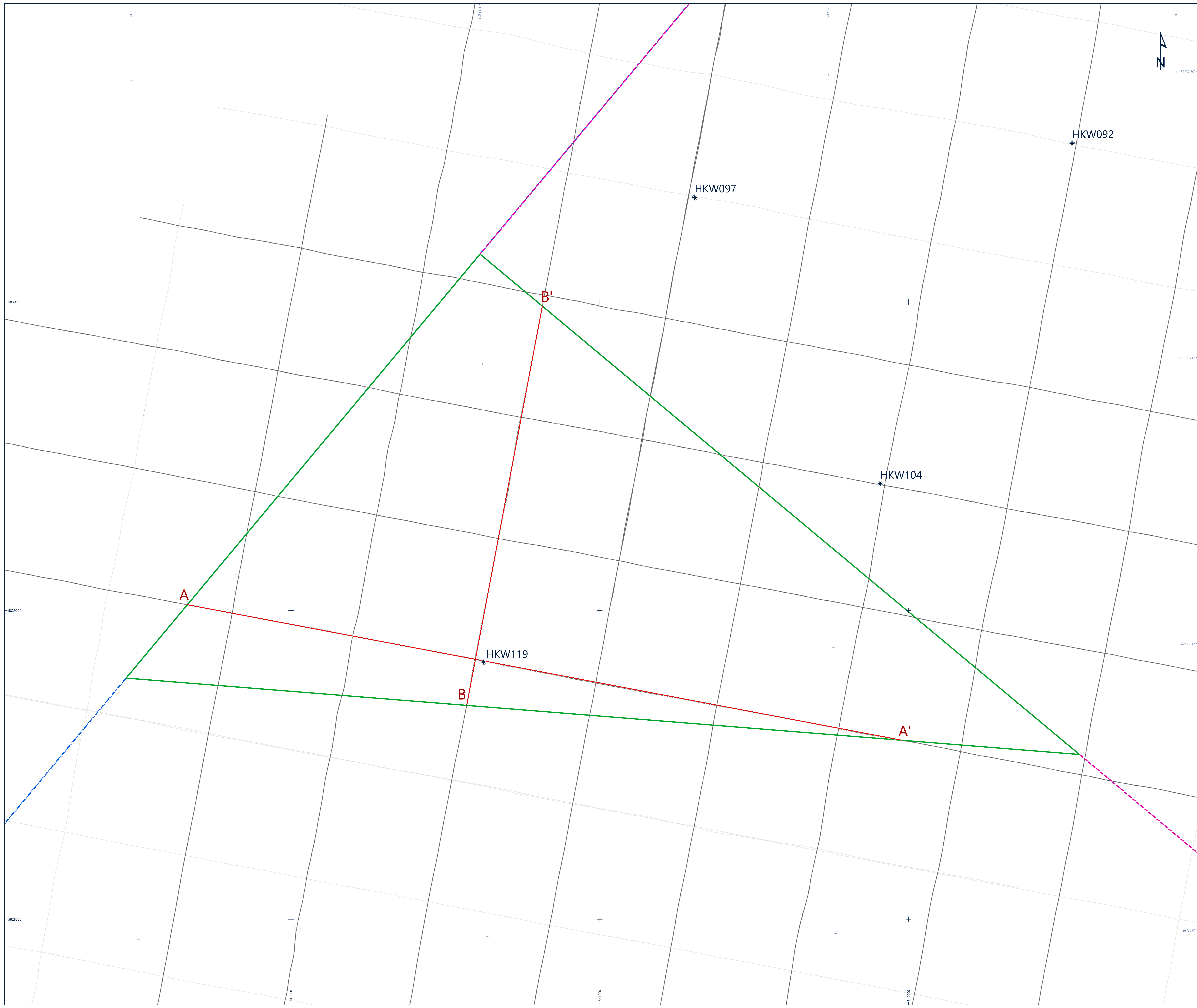
Fugro
Rijksdienst voor Ondernemend Nederland

SEAFLOOR GRADIENT
GEOTECHNICAL SITE INVESTIGATION
DUTCH SECTOR - NORTH SEA
HOLLANDE KUST (WEST) WIND FARM ZONE EXTENSION AREA

Scale 1 : 4 000 at original A0 page size

0 50 100 200 300 400 500 metres
0.02 0.04 0.06 0.08 0.1 0.12 0.14 0.16 0.18 0.2 nautical mile

Fugro Document No. P90471/GA/01 Chart No. 1 of 1 Plate No. A3-2



LEGEND

GEOTECHNICAL LOCATIONS

- Geotechnical location
- Cross-section presented in the report

GENERAL

- Hollandse Kust (west) Wind Farm Zone Extension Area (HKW EA)
- Hollandse Kust (west) Wind Farm Zone (HKW WFZ)
- HKW - Designated Wind Farm Zone
- UTM grid
- Geographical grid

TRACKS

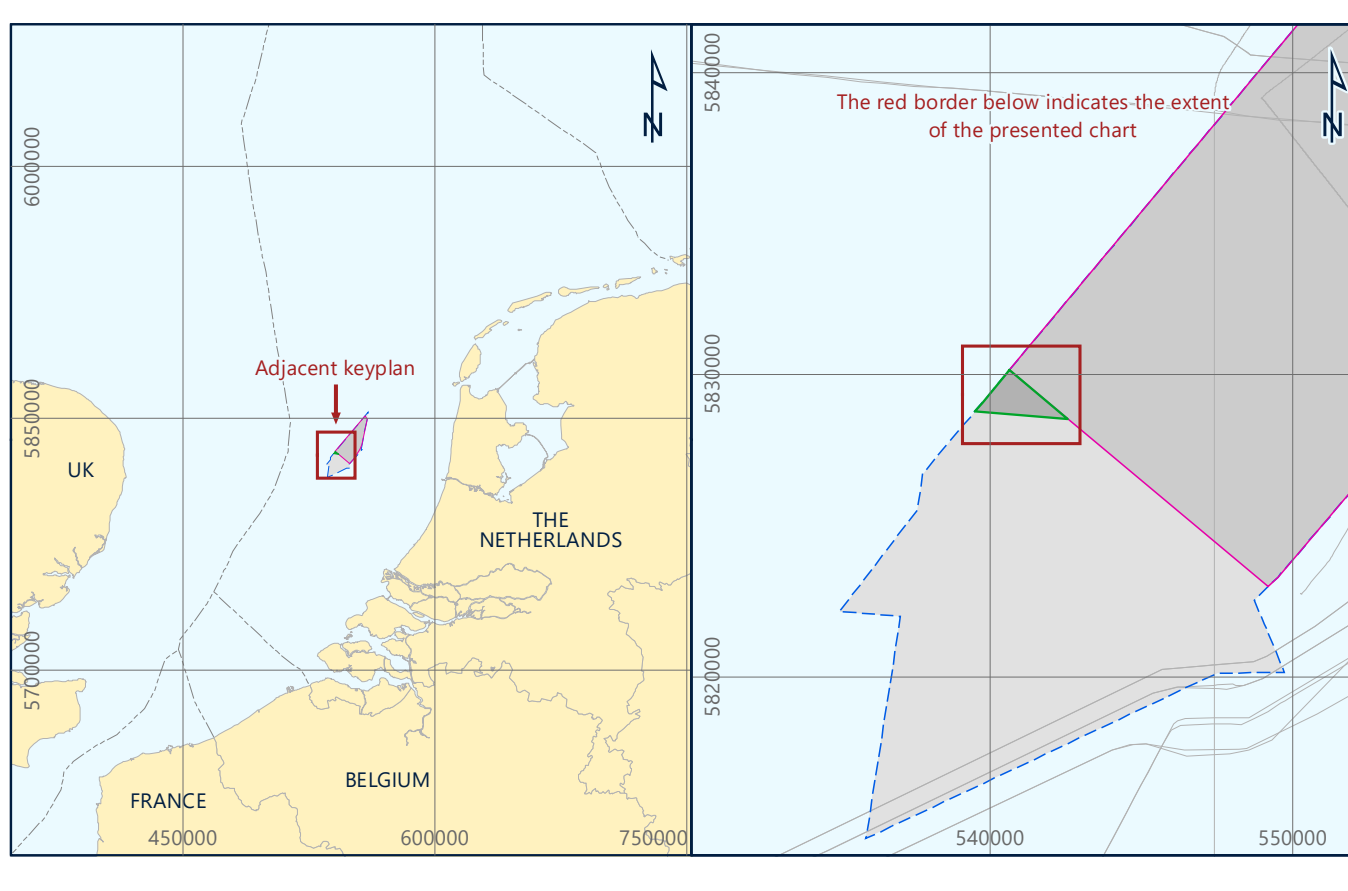
- UHR MCS track line

NOTES

1) Data acquired by Fugro (2019).

GEODETIC PARAMETERS

GEODETIC DATUM	European Terrestrial Reference System 1989
ELLIPSOID	GRS 1980
Semi-Major Axis	6 378 137 000 m
Inverse Flattening	298.257 222 101
PROJECTION	ETRS 1989 / UTM Zone 31N (EPSG 25831)
Central Meridian (CM)	03°00'00" E
Latitude of Origin	00°00'00" N
Fake Easting	500 000 mE
Fake Northing	0 mN
Scale Factor at CM	0.9996
DATUM TRANSFORMATION	ITRS2014 to ETRS89 for Epoch 2017.4959
Source	$dx = +0.0545$ m, $dy = +0.05295$ m, $dZ = -0.08834$ m $rx = -0.0023082''$, $ry = -0.0139630''$, $rz = -0.0225688''$; Scale = -0.00294455 ppm
VERTICAL DATUM	Lowest Astronomical Tide (LAT)

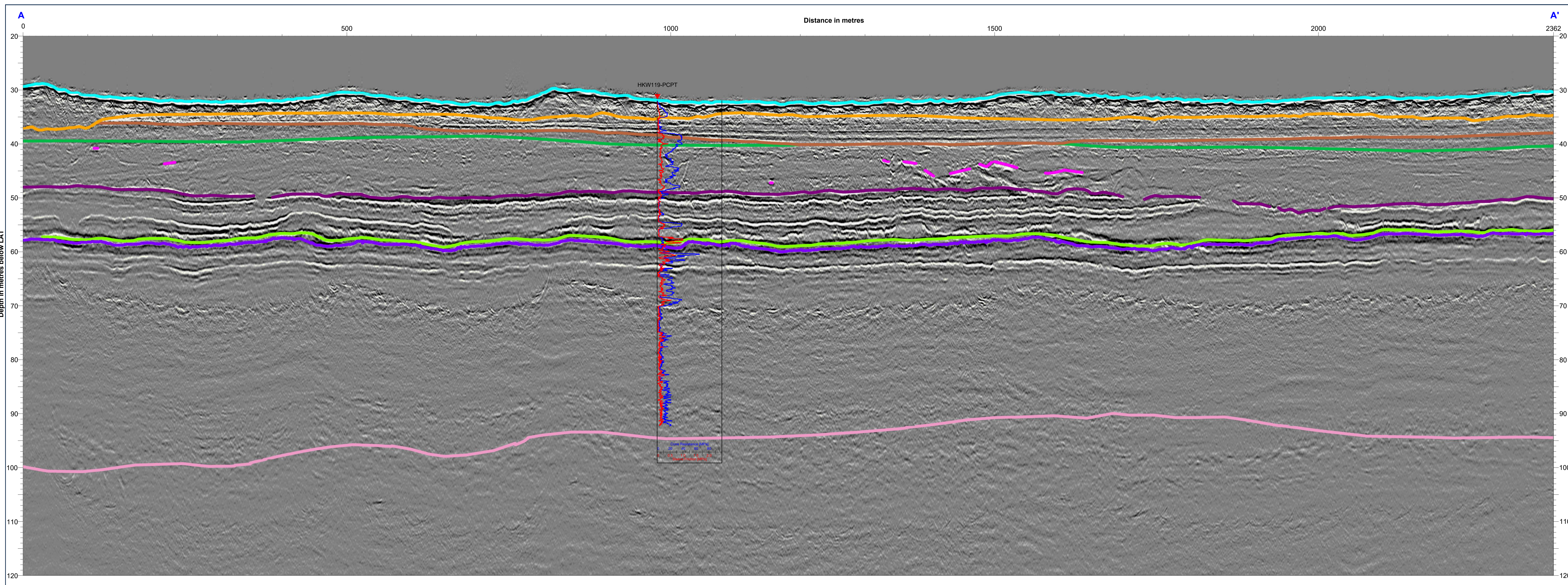


RVO
 Rijksoverheid
 Rijksdienst voor Ondernemend Nederland

Fugro
 Fugro

UHR-MCS TRACK LINES AND CROSS SECTION LINES
 GEOTECHNICAL SITE INVESTIGATION
 DUTCH SECTOR - NORTH SEA
 HOLLANDE KUST (WEST) WIND FARM ZONE EXTENSION AREA





LEGEND

SEISMIC PROFILE

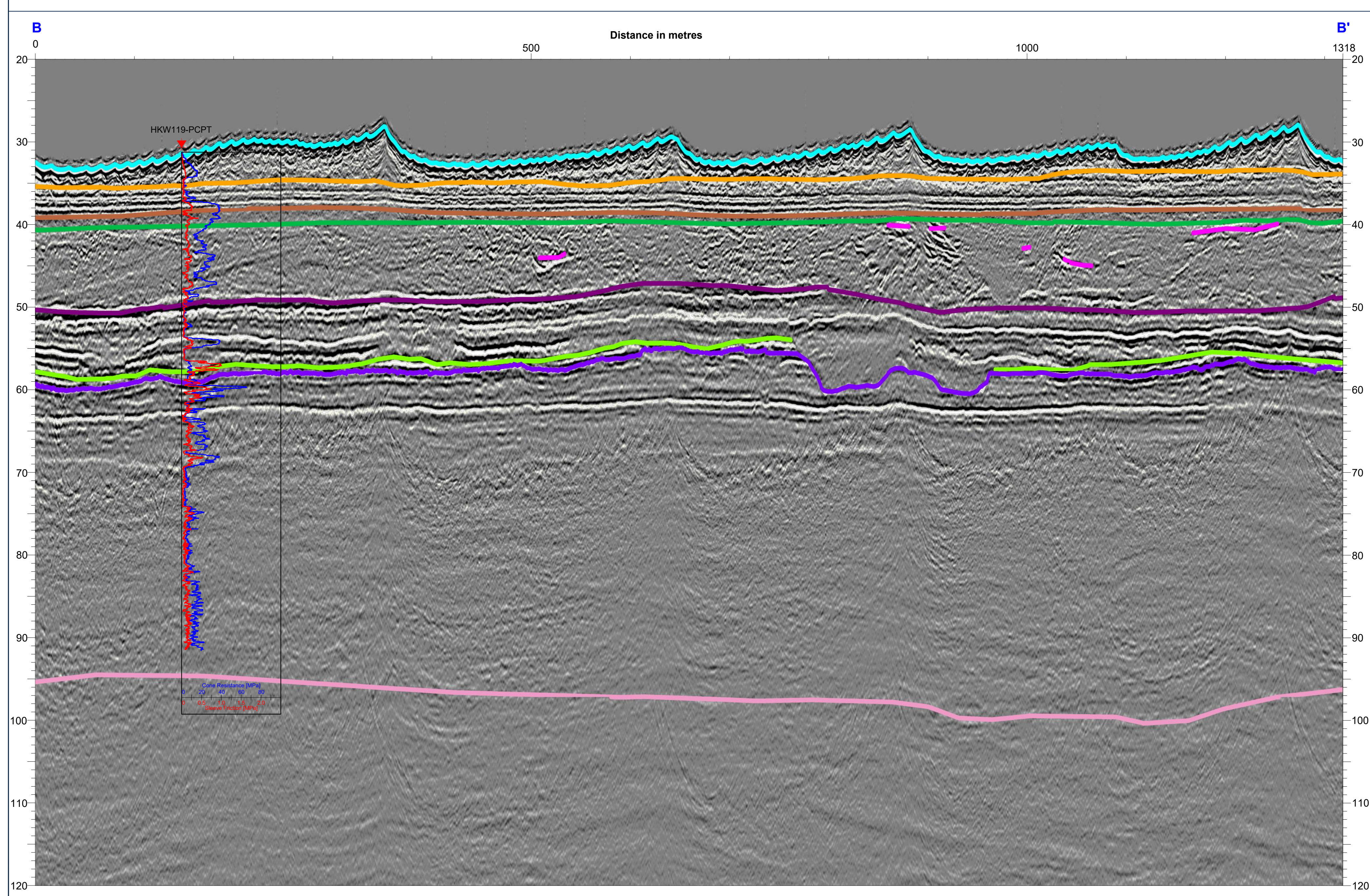
- Sea floor (from MBES)
- Base of Unit A (Horizon H02)
- Base of Unit B (Horizon H05)
- Base of Unit C1 (Horizon H09)
- Base of Unit C2 (Horizon H10)
- Base of Unit F (Horizon H25)
- Internal horizon in Unit G (H40)
- Peat / organic clay level 2A
- Peat / organic clay level 2B
- Peat / organic clay level 2C

CPT

- Cone resistance, q_c (MPa)
- Sleeve friction, f_s (MPa)

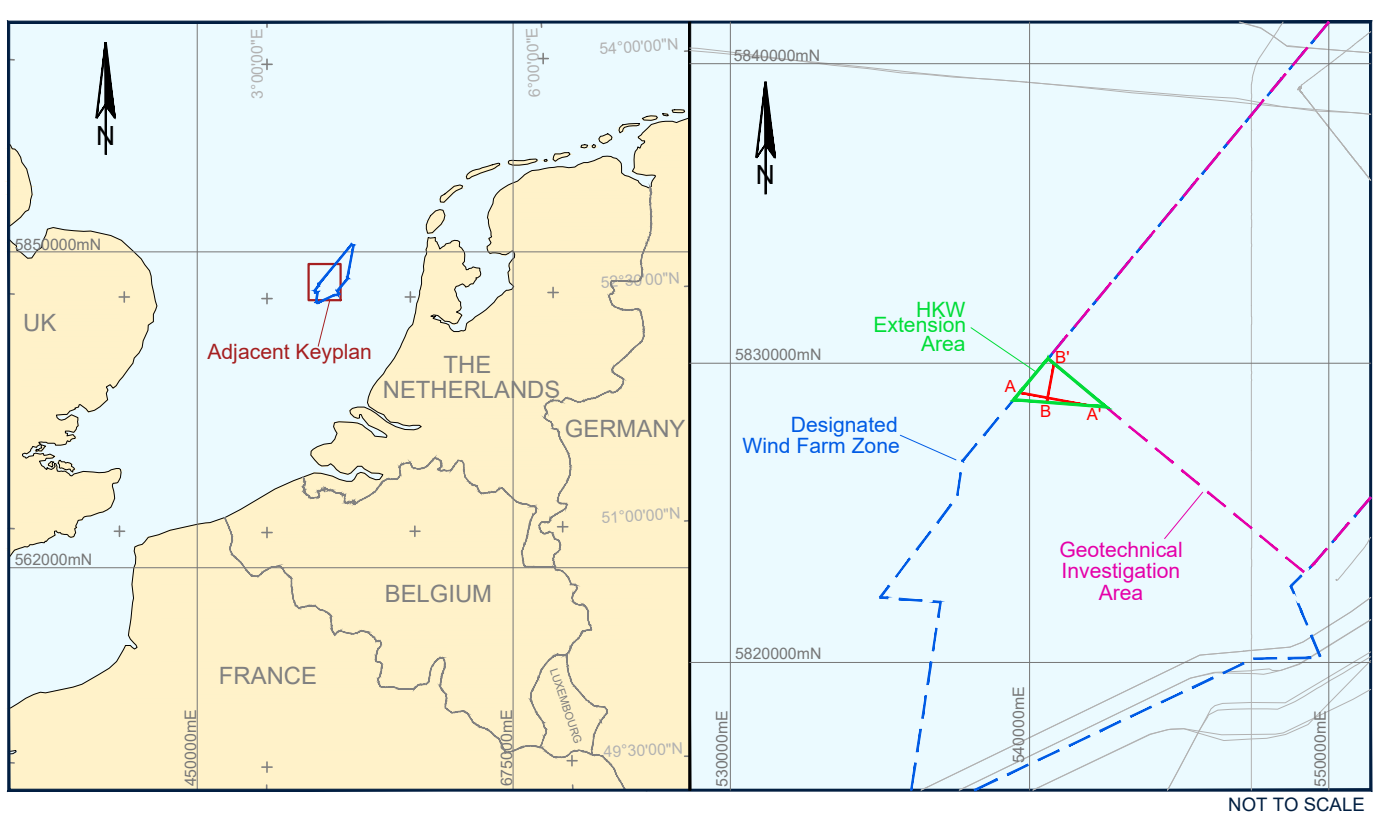
NOTES

- 1) Cross-section displays UHR MCS data (seismic lines 2X920rnb and 2A500fnta), with interpretation of geological soil units and geological features.
- 2) The vertical scale (in metres) was based on time-depth conversion using velocity fields from RMS velocity picking with 500 m increment on each UHR MCS line. Refer to geophysical survey report (Fugro, 2019) for details.
- 3) CPT data are projected on the cross-section. Refer to the geotechnical reports listed on Plate 1-3 in Fugro 2020a for details on the geotechnical data.
- 4) Geotechnical location is approximately 5m from the A-A' seismic line and approximately 30m from the B-B' seismic line.
- 5) Width of the CPT box shows cone resistance values (blue line) within range 0 to 100 MPa and sleeve resistance values (red curve) from 0 to 2.5 MPa.



GEODETTIC PARAMETERS

GEODETTIC DATUM		European Terrestrial Reference System 1989
ELLIPSOID	GRS 1980	
Semi-Major Axis	6,378,137.000 m	
Inverse Flattening	298.257222101	
PROJECTION		UTM Zone 11N (EPSG 25831)
Central Meridian (CM)	03°00'00" E	
Latitude of Origin	0 m	
Falsie Easting	500,000 mE	
Falsie Northing	0 mN	
Scale Factor at CM	0.9996	
DATUM TRANSFORMATION		ITRF2014 to ETRS89 for Epoch 2017.4959
dx	+0.0545 m	dy = +0.0295 m dz = -0.08834 m
rx	-0.0023968"	ry = -0.0136630" rz = +0.0022688"
Scale		+0.00294455 ppm
VERTICAL DATUM		LOWEST ASTRONOMICAL TIDE (LAT)



RVO
Prinses Beatrixlaan 2, 2596 AX, Den Haag, The Netherlands

Rijksdienst voor Ondernemend Nederland

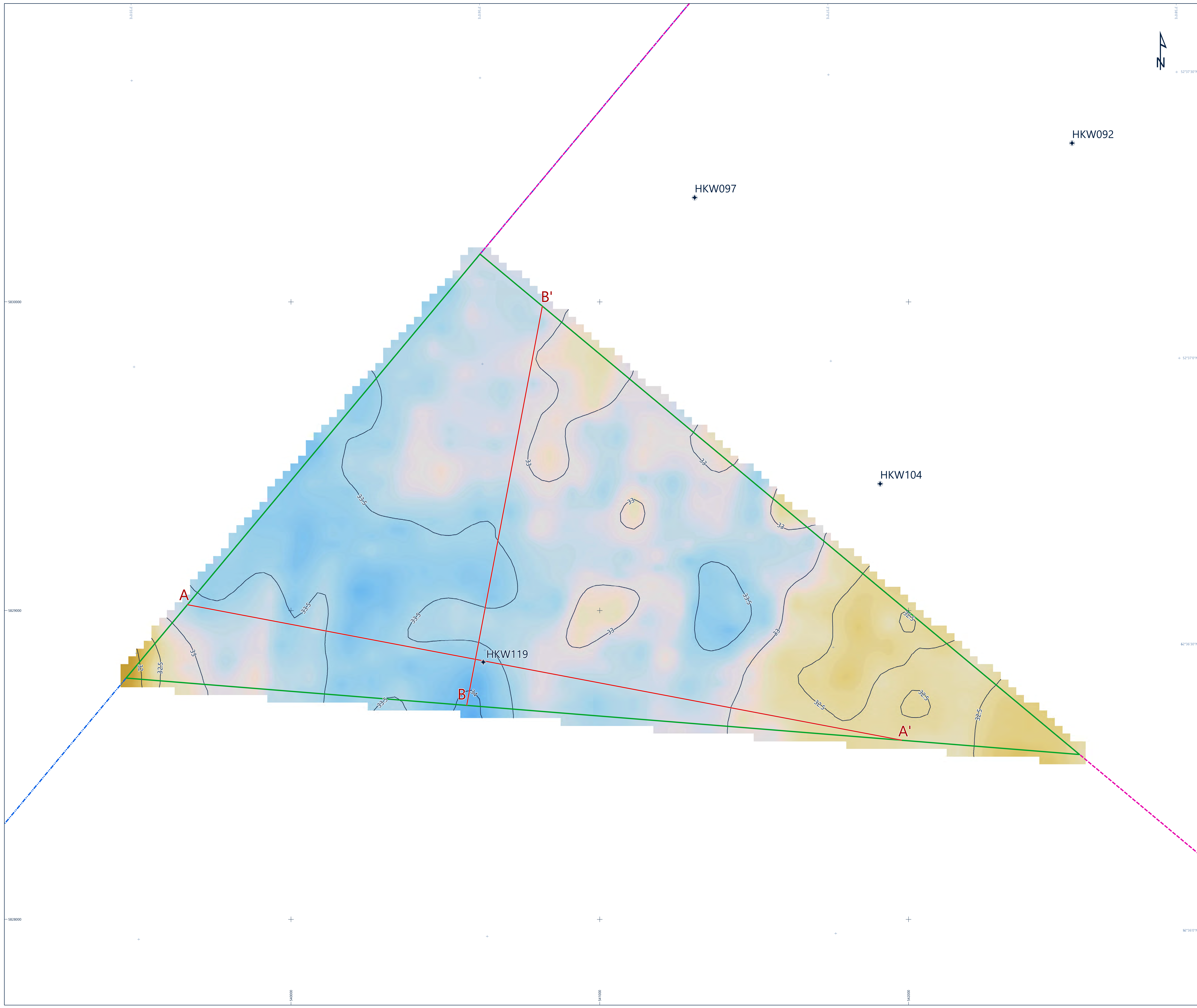
FUGRO
Ploegbaan 4, 2611 RT, Noordwijk, The Netherlands
Tel: +31 70 311 1444

CROSS-SECTIONS A - A' & B - B'
GEOTECHNICAL SITE INVESTIGATION
DUTCH SECTOR - NORTH SEA
HOLLANDE KUST (WEST) WIND FARM ZONE - EXTENSION AREA

HORIZONTAL SCALE: 1 : 2500 - VERTICAL SCALE: 1 : 300 - 8.3 VERTICAL EXAGGERATION

0 25 50 100 150 200 250 metres
0 50 100 150 200 250 feet

Fugro Document No. P904711/GA Issue: 1 Plate: 3-2



LEGEND

GEOTECHNICAL LOCATIONS

- Geotechnical location
- Cross-section presented in the report

GENERAL

- Hollande Kust (west) Wind Farm Zone Extension Area (HKW EA)
- Hollande Kust (west) Wind Farm Zone (HKW WFZ)
- HKW - Designated Wind Farm Zone
- UTM grid
- Geographical grid

DEPTH TO BASE OF UNIT A (METRES BELOW LAT)

Depth contour at 0.5 metres interval

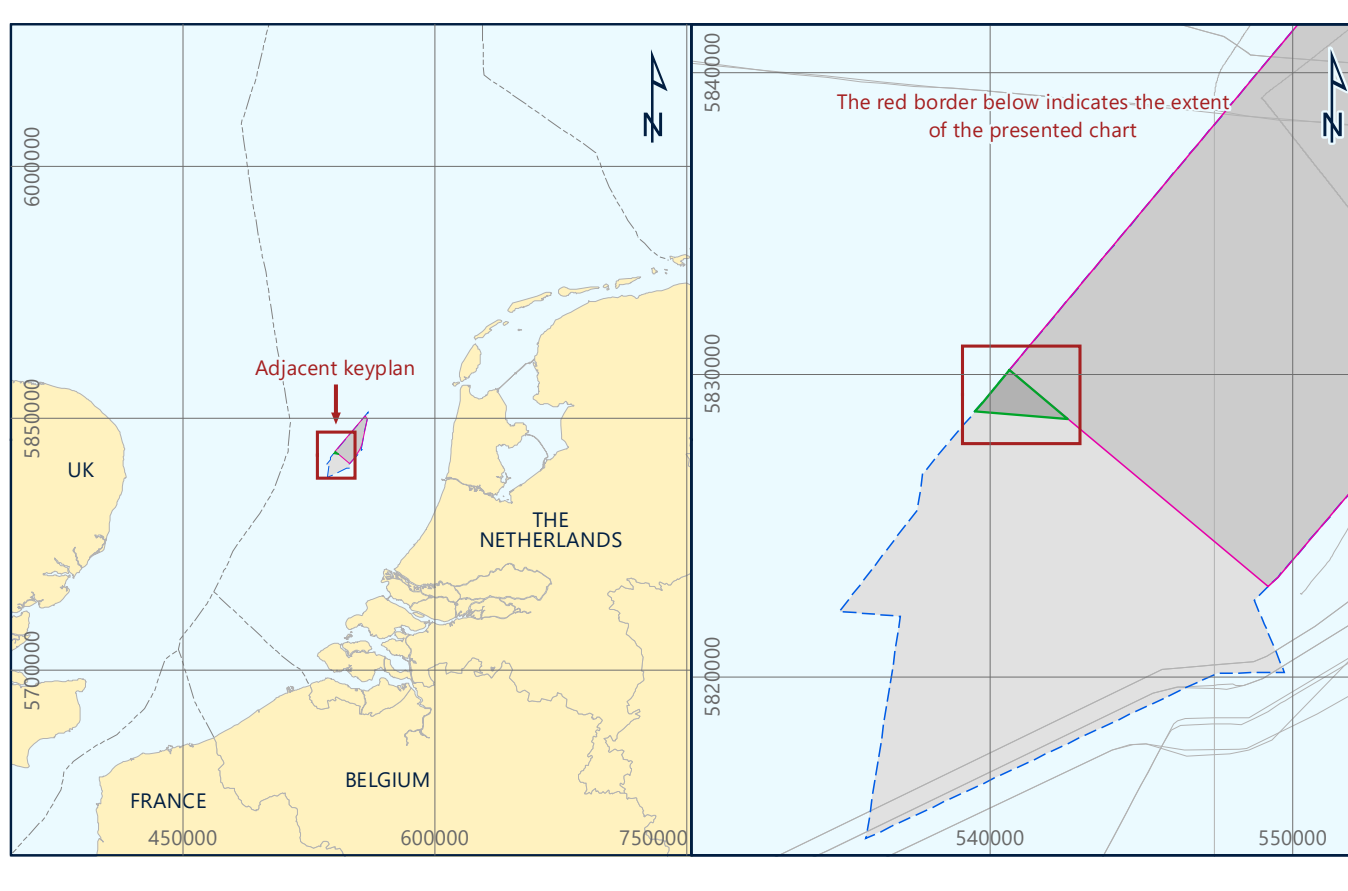
Depth to base [m below LAT]

NOTES

- Unit A is interpreted to be present across the entire HKW EA. Locally, the unit can be very thin. Detection of top layers <3.3 m thick is difficult on seismic reflection data.
- Interpretation based on SBP data. Time to depth conversion was performed using a fixed velocity of 1700 m/s.
- Gridding parameters: cell size 25 m x 25 m, fit to data 0.5, smoothing factor 6, search limit 105 m.

GEODETIC PARAMETERS

GEODETIC DATUM	European Terrestrial Reference System 1989
ELLIPSOID	GRS 1980
Semi-Major Axis	6 378 137 000 m
Inverse Flattening	298.257 222 101
PROJECTION	ETRS 1989 / UTM Zone 31N (EPSG 25831)
Central Meridian (CM)	03°00'00" E
Latitude of Origin	00°00'00" N
Fake Easting	500 000 mE
Fake Northing	0 mN
Scale Factor at CM	0.9996
DATUM TRANSFORMATION	ITRS2014 to ETRS89 for Epoch 2017.4959
Source	dx = +0.0545 m, dy = +0.05295 m, dz = -0.08834 m rx = -0.0023082", ry = -0.0139630", rz = +0.0225688", Scale = -0.00294455 ppm
VERTICAL DATUM	Lowest Astronomical Tide (LAT)



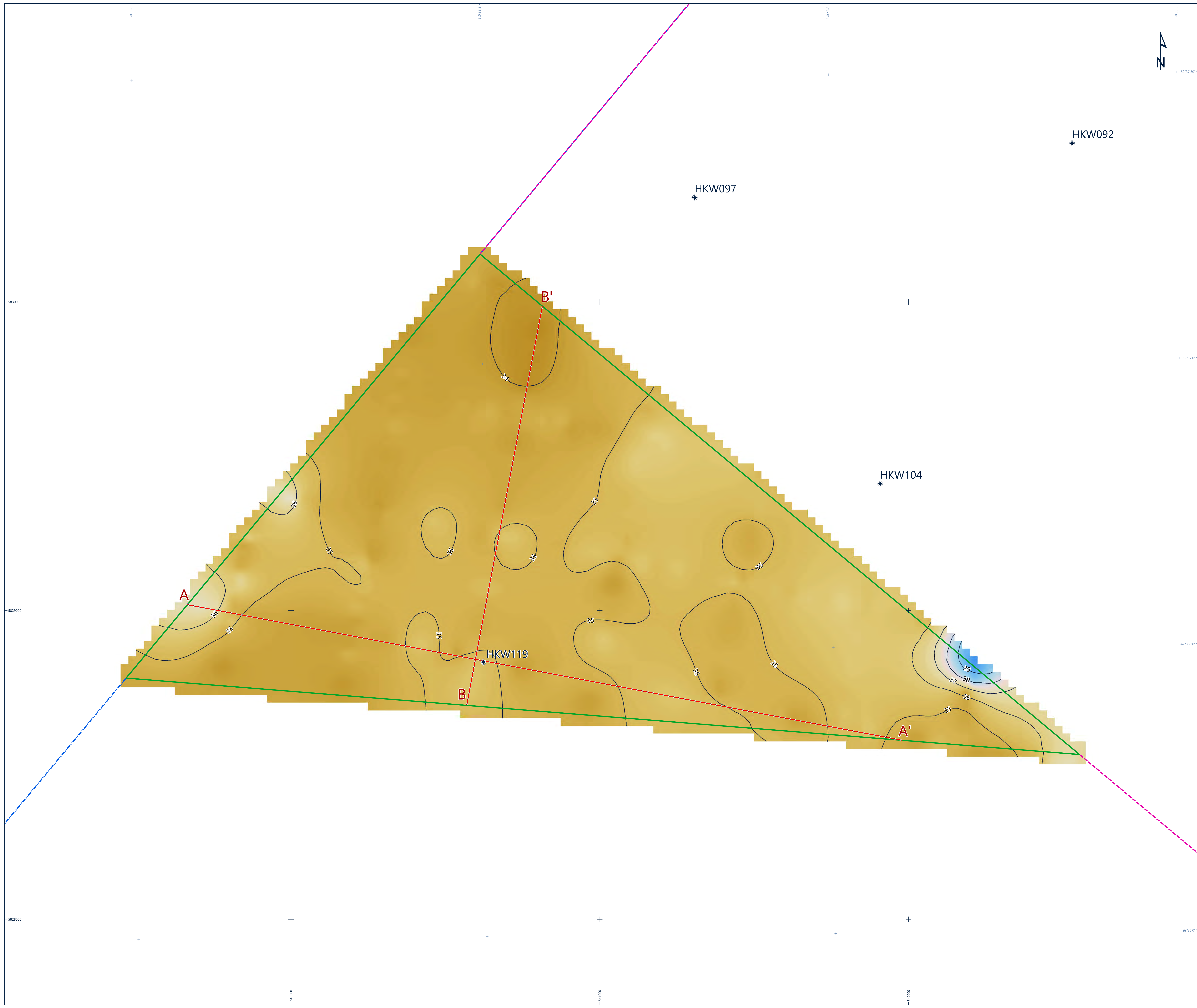
RVO
Rijksdienst voor Ondernemend Nederland

Fugro
Fugro Document No. P904711/GA/01

DEPTH TO BASE OF UNIT A (METRES BELOW LAT)
GEOTECHNICAL SITE INVESTIGATION
DUTCH SECTOR - NORTH SEA
HOLLANDE KUST (WEST) WIND FARM ZONE EXTENSION AREA

Scale 1 : 4 000 at original A0 page size

Fugro Document No. P904711/GA/01 Chart No. 1 of 1 Plate No. A3-5



LEGEND

GEOTECHNICAL LOCATIONS

- Geotechnical location
- Cross-section presented in the report

GENERAL

- Hollandse Kust (west) Wind Farm Zone Extension Area (HKW EA)
- Hollandse Kust (west) Wind Farm Zone (HKW WFZ)
- HKW - Designated Wind Farm Zone
- UTM grid
- Geographical grid

DEPTH TO BASE OF UNIT B (METRES BELOW LAT)

Depth contour at 1.0 metres interval

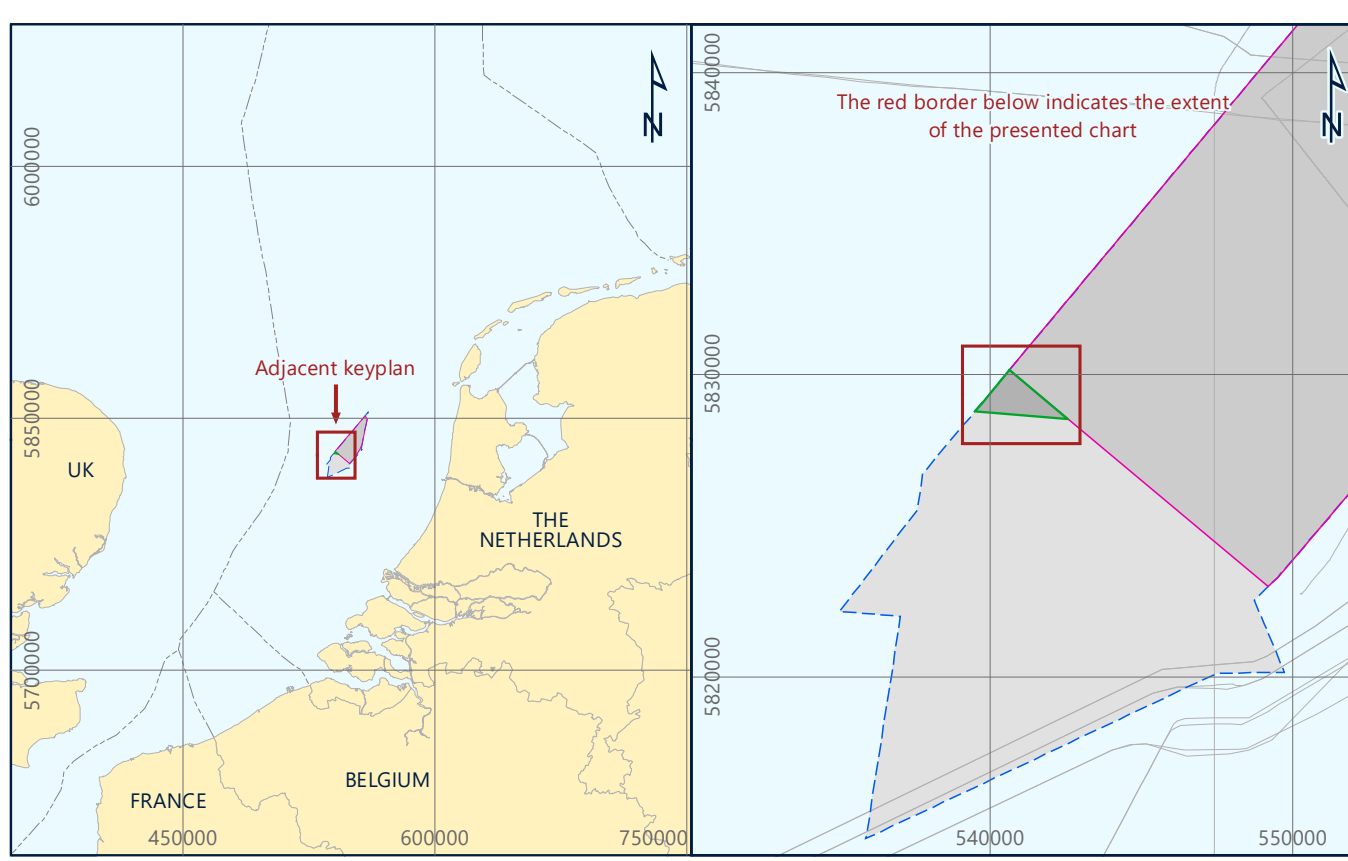
Depth to base [m below LAT]

NOTES

- Unit B is interpreted to be present across the entire HKW EA.
- Interpretation based on UHR-MCS data. Time to depth conversion was performed using an RMS interval velocity model (UHR-MCS). Refer to geophysical survey report (Fugro, 2019) for details.
- Gridding parameters: cell size 25 m x 25 m, fit to data 0.5, smoothing factor 6, search limit 200 m.

GEODETIC PARAMETERS

GEODETIC DATUM	European Terrestrial Reference System 1989
ELLIPSOID	GRS 1980
Semi-Major Axis	6 378 137 000 m
Inverse Flattening	298.257 222 101
PROJECTION	ETRS 1989 / UTM Zone 31N (EPSG 25831)
Central Meridian (CM)	03°00'00" E
Latitude of Origin	00°00'00" N
Fake Easting	500 000 mE
Fake Northing	0 mN
Scale Factor at CM	0.9996
DATUM TRANSFORMATION	ITRS2014 to ETRS89 for Epoch 2017.4959
Source	$dx = +0.0545$ m, $dy = +0.0295$ m, $dz = -0.08834$ m $rx = -0.0023082''$, $ry = -0.0139630''$, $rz = +0.0225688''$; Scale = -0.00294455 ppm
VERTICAL DATUM	Lowest Astronomical Tide (LAT)



RVO
 Prinses Beatrixlaan 2, 2595 AX Den Haag, The Netherlands
 www.rvo.nl

Rijksoverheid
 Rijksdienst voor Ondernemend Nederland

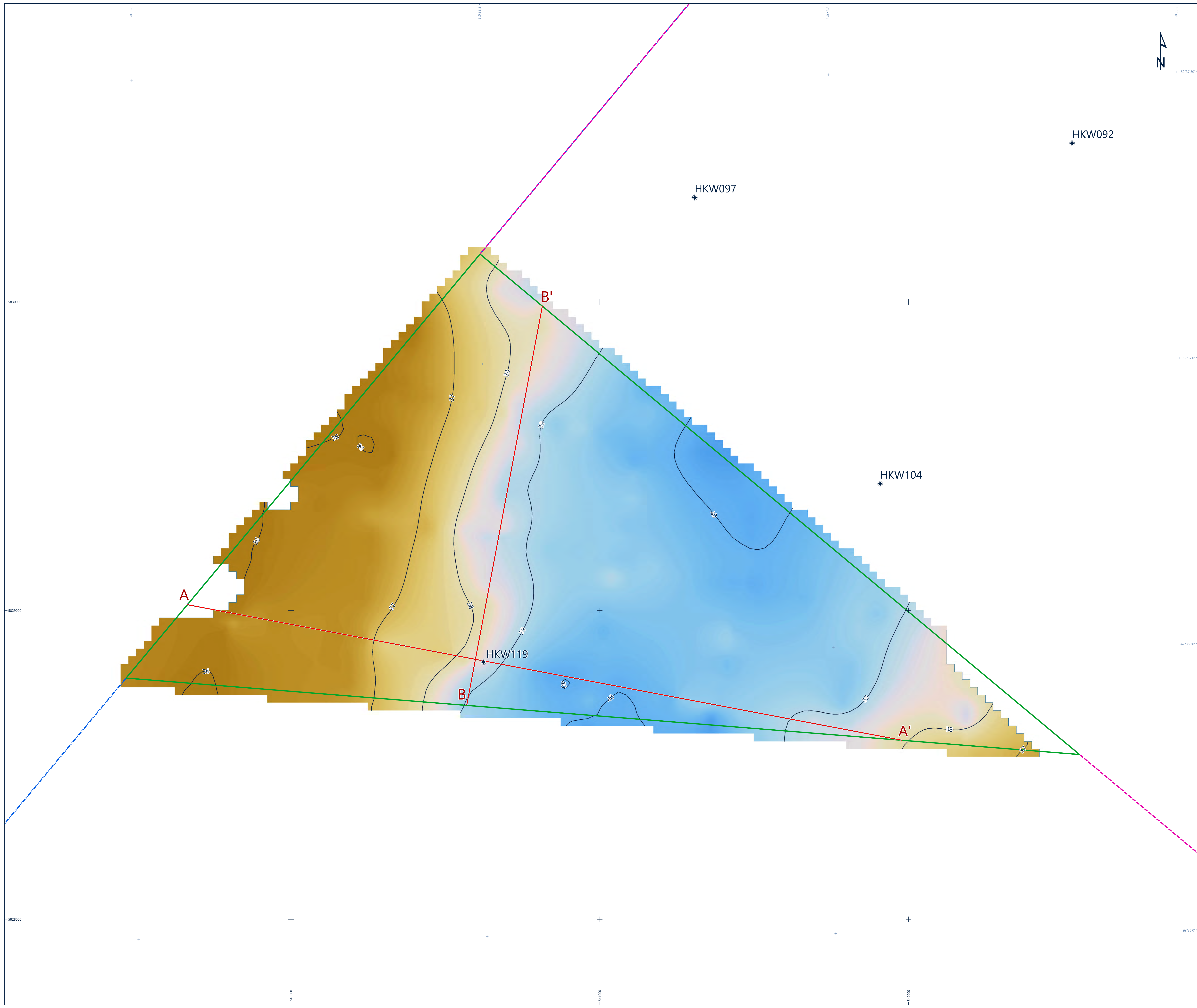
Fugro
 Prinsmastraat 4, 2611 RT Noordwijk, The Netherlands
 www.fugro.com

DEPTH TO BASE OF UNIT B (METRES BELOW LAT)

GEOTECHNICAL SITE INVESTIGATION
 DUTCH SECTOR - NORTH SEA
 HOLLANDE KUST (WEST) WIND FARM ZONE EXTENSION AREA

Scale 1 : 4 000 at original A0 page size

Fugro Document No. P904711/GA/01 Chart No. 1 of 1 Plate No. A3-6



LEGEND

GEOTECHNICAL LOCATIONS

- Geotechnical location
- Cross-section presented in the report

GENERAL

- Hollandse Kust (west) Wind Farm Zone Extension Area (HKW EA)
- Hollandse Kust (west) Wind Farm Zone (HKW WFZ)
- HKW - Designated Wind Farm Zone
- UTM grid
- Geographical grid

DEPTH TO BASE OF UNIT C1 (METRES BELOW LAT)

Depth contour at 1.0 metres interval

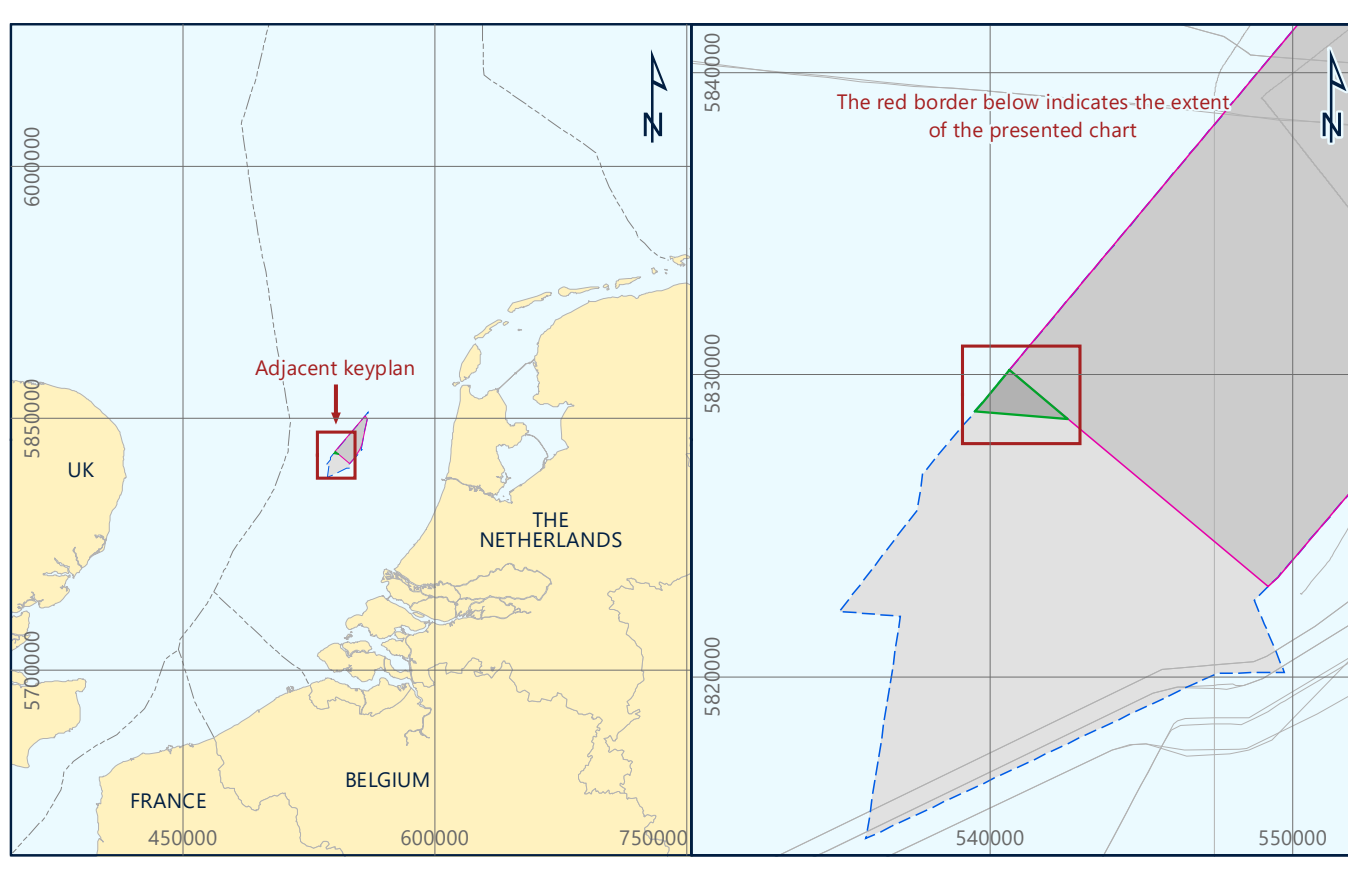
Depth to base [m below LAT]

NOTES

- Blank areas indicate where Unit C1 is interpreted to be absent.
- Interpretation based on UHR-MCS data. Time to depth conversion was based on an RMS interval velocity model. Refer to geophysical survey report (Fugro, 2019) for details.
- Gridding parameters: cell size 25 m x 25 m, fit to data 0.5, smoothing factor 6, search limit 200 m.

GEODETIC PARAMETERS

GEODETIC DATUM	European Terrestrial Reference System 1989
ELLIPSOID	GRS 1980
Semi-Major Axis	6 378 137 000 m
Inverse Flattening	298.257 222 101
PROJECTION	ETRS 1989 / UTM Zone 31N (EPSG 25831)
Central Meridian (CM)	03°00'00" E
Latitude of Origin	00°00'00" N
Fake Easting	500 000 mE
Fake Northing	0 mN
Scale Factor at CM	0.9996
DATUM TRANSFORMATION	ITRS2014 to ETRS89 for Epoch 2017.4959
Source	$dx = +0.0545$ m, $dy = +0.05295$ m, $dz = -0.08834$ m $rx = -0.0023082''$, $ry = -0.0139630''$, $rz = +0.0225688''$; Scale = 0.00294455 ppm
VERTICAL DATUM	Lowest Astronomical Tide (LAT)



RVO
Prinses Beatrixlaan 2, 2595 AX Den Haag, The Netherlands
www.rvo.nl

Rijksoverheid
Rijksdienst voor Ondernemend Nederland

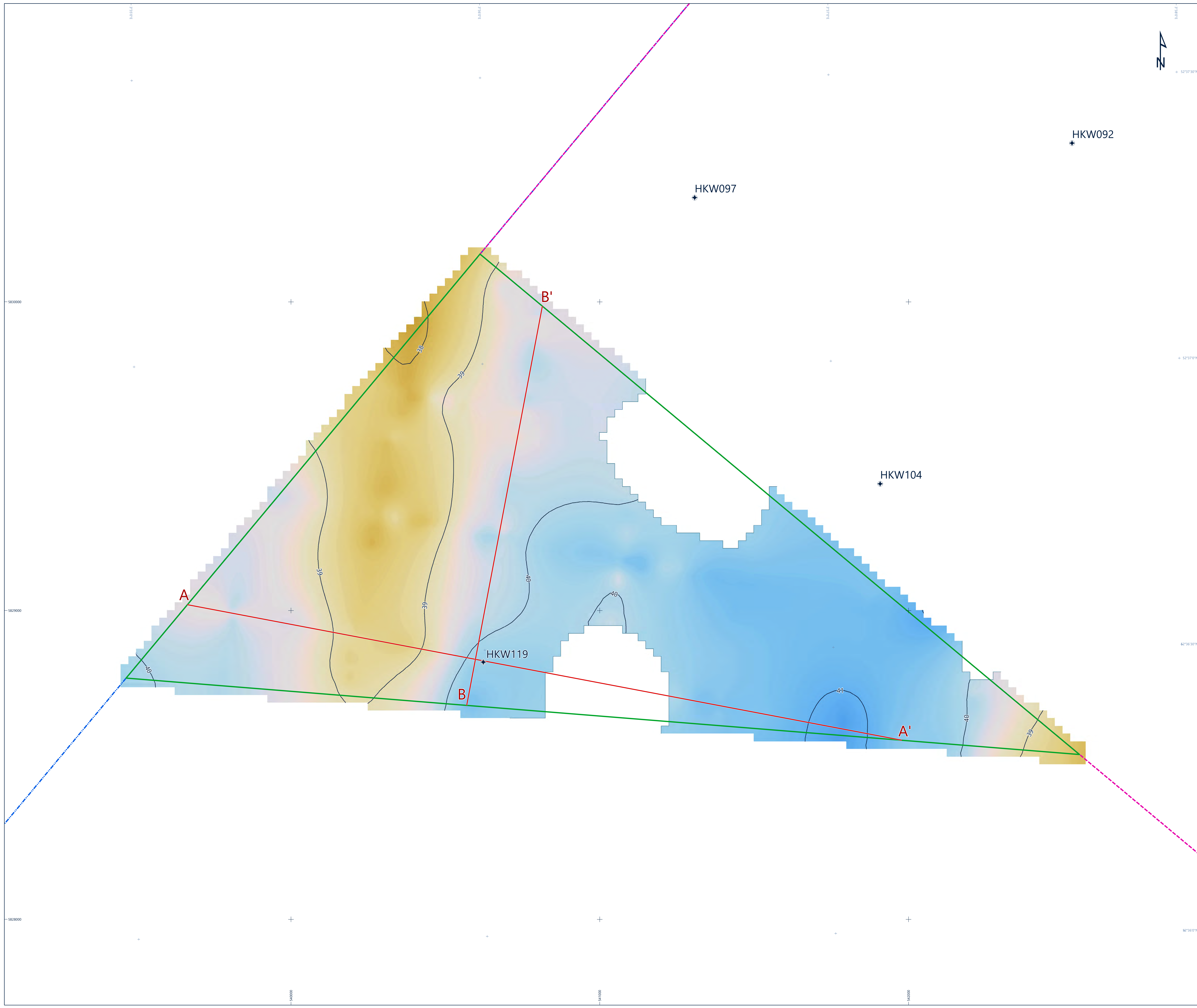
Fugro
Prinsmaatslaan 4, 2611 RT Noordwijk, The Netherlands
www.fugro.com

DEPTH TO BASE OF UNIT C1 (METRES BELOW LAT)

GEOTECHNICAL SITE INVESTIGATION
DUTCH SECTOR - NORTH SEA
HOLLANDE KUST (WEST) WIND FARM ZONE EXTENSION AREA

Scale 1 : 4 000 at original A0 page size

Fugro Document No. P90471/GA/01 Chart No. 1 of 1 Plate No. A3-7



LEGEND

GEOTECHNICAL LOCATIONS

- Geotechnical location
- Cross-section presented in the report

GENERAL

- Hollandse Kust (west) Wind Farm Zone Extension Area (HKW EA)
- Hollandse Kust (west) Wind Farm Zone (HKW WFZ)
- HKW - Designated Wind Farm Zone
- UTM grid
- Geographical grid

DEPTH TO BASE OF UNIT C2 (METRES BELOW LAT)

Depth contour at 1.0 metres interval

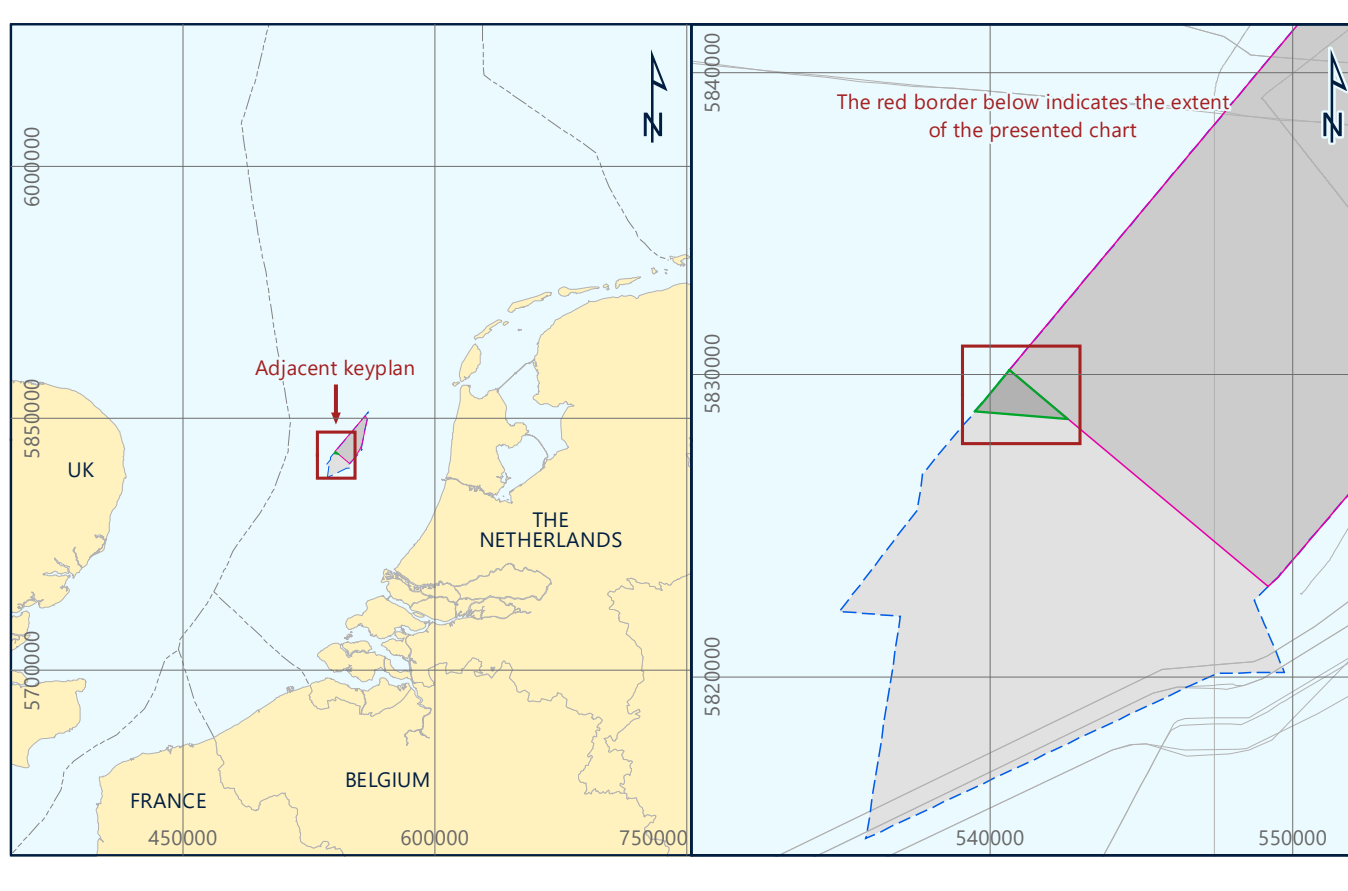
Depth to base [m below LAT]

NOTES

- Blank areas indicate where Unit C2 is interpreted to be absent.
- Interpretation based on UHR-MCS data. Time to depth conversion was based on an RMS interval velocity model. Refer to geophysical survey report (Fugro, 2019) for details.
- Gridding parameters: cell size 25 m x 25 m, fit to data 0.5, smoothing factor 6, search limit 200 m.

GEODETIC PARAMETERS

GEODETIC DATUM	European Terrestrial Reference System 1989
ELLIPSOID	GRS 1980
Semi-Major Axis	6 378 137 000 m
Inverse Flattening	298.257 222 101
PROJECTION	ETRS 1989 / UTM Zone 31N (EPSG 25831)
Central Meridian (CM)	03°00'00" E
Latitude of Origin	00°00'00" N
Fake Easting	500 000 mE
Fake Northing	0 mN
Scale Factor at CM	0.9996
DATUM TRANSFORMATION	ITRS2014 to ETRS89 for Epoch 2017.4959
Source	$dx = +0.0545$ m, $dy = +0.05295$ m, $dz = -0.08834$ m $rx = -0.0023082''$, $ry = -0.0139630''$, $rz = -0.0225688''$; Scale = -0.00294455 ppm
VERTICAL DATUM	Lowest Astronomical Tide (LAT)



RVO
Private Beeldruimte 2, 2995 AL Den Haag, The Netherlands
www.rvo.nl

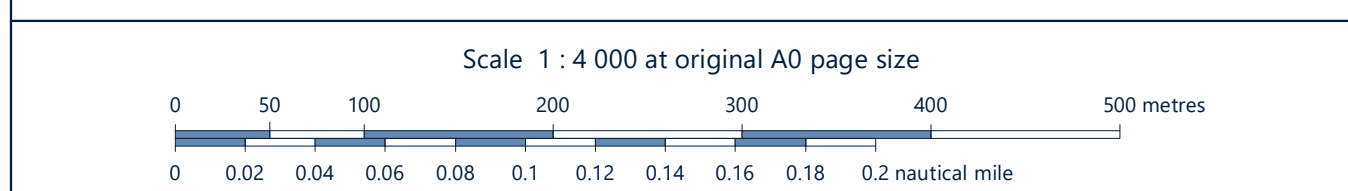
Rijksoverheid
Rijksdienst voor Ondernemend Nederland

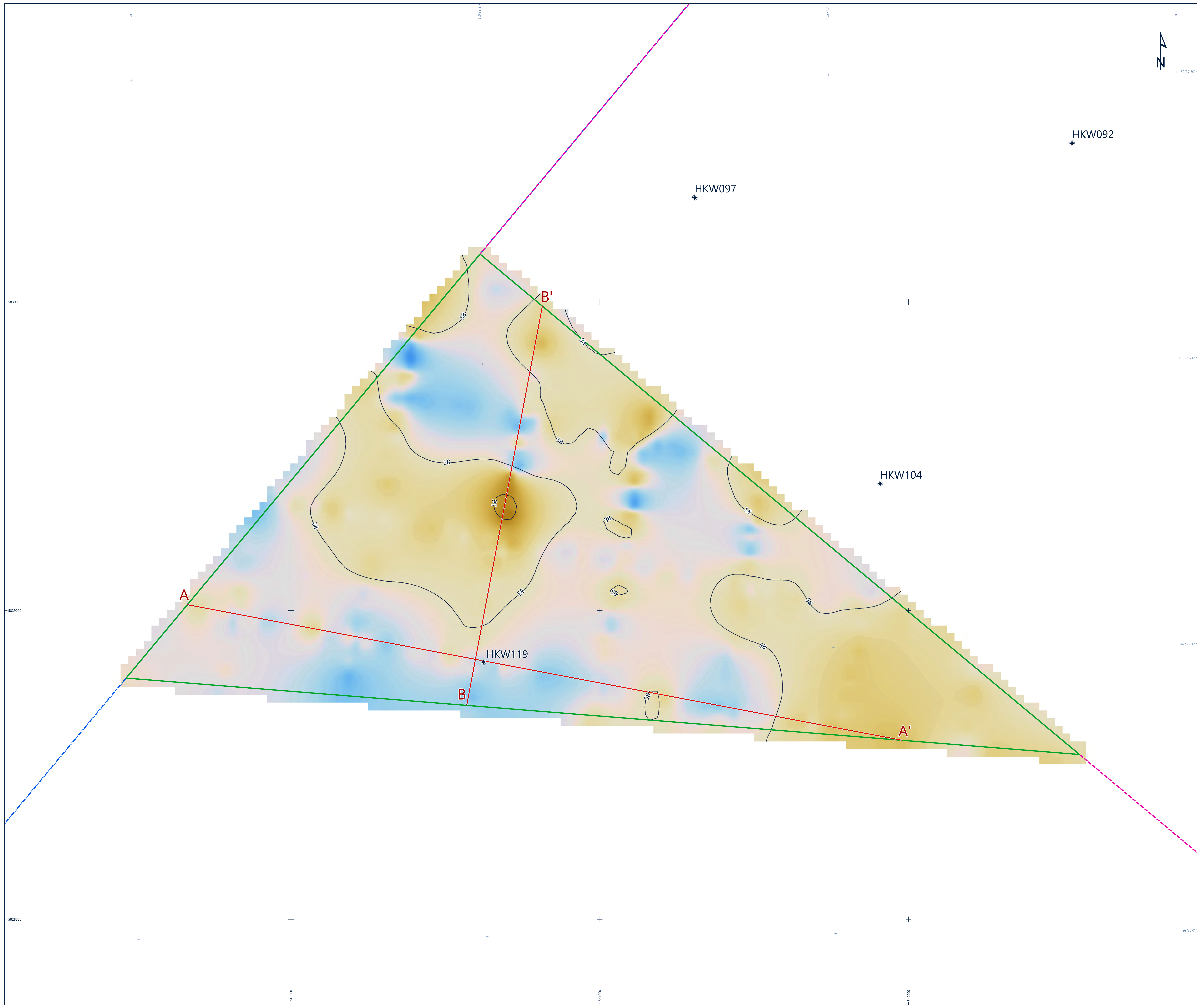
Fugro
Prinsmaats 4, 2611 RT Noordwijk, The Netherlands
www.fugro.com

FUGRO

DEPTH TO BASE OF UNIT C2 (METRES BELOW LAT)

GEOTECHNICAL SITE INVESTIGATION
DUTCH SECTOR - NORTH SEA
HOLLANDE KUST (WEST) WIND FARM ZONE EXTENSION AREA





LEGEND

GEOTECHNICAL LOCATIONS

- Geotechnical location
- Cross-section presented in the report

GENERAL

- Hollandse Kust (west) Wind Farm Zone Extension Area (HKW EA)
- Hollandse Kust (west) Wind Farm Zone (HKW WFZ)
- HKW - Designated Wind Farm Zone
- UTM grid
- Geographical grid

DEPTH TO BASE OF UNIT F (METRES BELOW LAT)

Depth contour at 2.0 metres interval

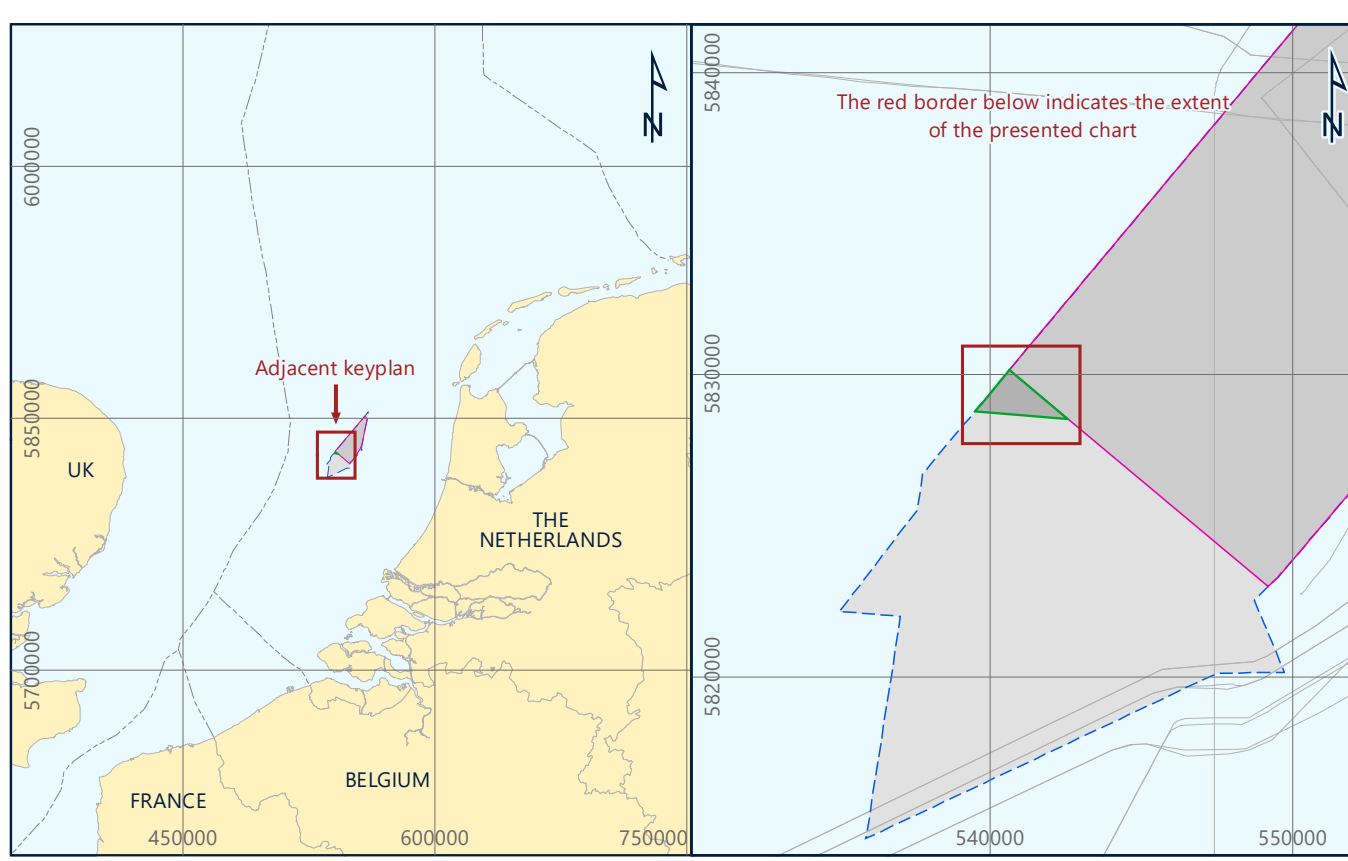
Depth to base [m below LAT]

NOTES

- Unit F is interpreted to be present across the entire HKW EA.
- Interpretation based on UHR-MCS data. Time to depth conversion was based on an RMS interval velocity model. Refer to geophysical survey report (Fugro, 2019) for details.
- Gridding parameters: cell size 25 m x 25 m, fit to data 0.5, smoothing factor 6, search limit 200 m.

GEODETIC PARAMETERS

GEODETIC DATUM	European Terrestrial Reference System 1989
ELLIPSOID	GRS 1980
Semi-Major Axis	6 378 137 000 m
Inverse Flattening	298.257 222 101
PROJECTION	ETRS 1989 / UTM Zone 31N (EPSG 25831)
Central Meridian (CM)	03°00'00" E
Latitude of Origin	00°00'00" N
Fake Easting	500 000 mE
Fake Northing	0 mN
Scale Factor at CM	0.9996
DATUM TRANSFORMATION	ITRS2014 to ETRS89 for Epoch 2017.4959
Source	$dx = +0.0545$ m, $dy = +0.05295$ m, $dz = -0.08834$ m $rx = -0.0023082''$, $ry = -0.0139630''$, $rz = -0.0225688''$, Scale = 0.00294455 ppm
VERTICAL DATUM	Lowest Astronomical Tide (LAT)



RVO
Prinses Beatrixlaan 2, 2595 AX Den Haag, The Netherlands
www.rvo.nl

Rijksoverheid
Rijksdienst voor Ondernemend Nederland

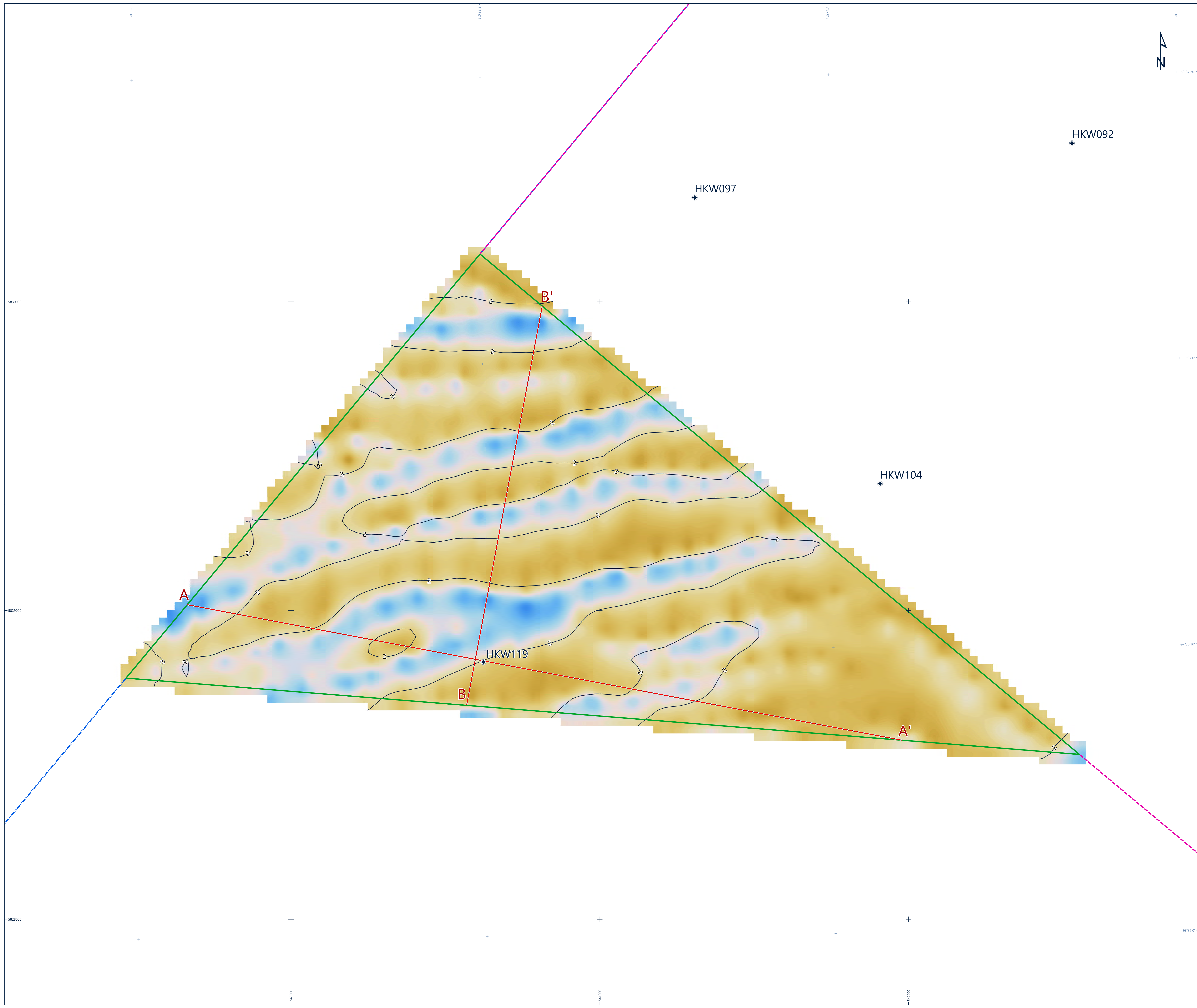
Fugro
Prinsmaatslaan 4, 2611 RT Noordwijk, The Netherlands
www.fugro.com

DEPTH TO BASE OF UNIT F (METRES BELOW LAT)

GEOTECHNICAL SITE INVESTIGATION
DUTCH SECTOR - NORTH SEA
HOLLANDE KUST (WEST) WIND FARM ZONE EXTENSION AREA

Scale 1 : 4 000 at original A0 page size

Fugro Document No. P904711/GA/01 Chart No. 1 of 1 Plate No. A3-9



LEGEND

GEOTECHNICAL LOCATIONS

- Geotechnical location
- Cross-section presented in the report

GENERAL

- Hollandse Kust (west) Wind Farm Zone Extension Area (HKW EA)
- Hollandse Kust (west) Wind Farm Zone (HKW WFZ)
- HKW - Designated Wind Farm Zone
- UTM grid
- Geographical grid

THICKNESS OF UNIT A

Thickness contour at 2.0 metres interval

Thickness [m]

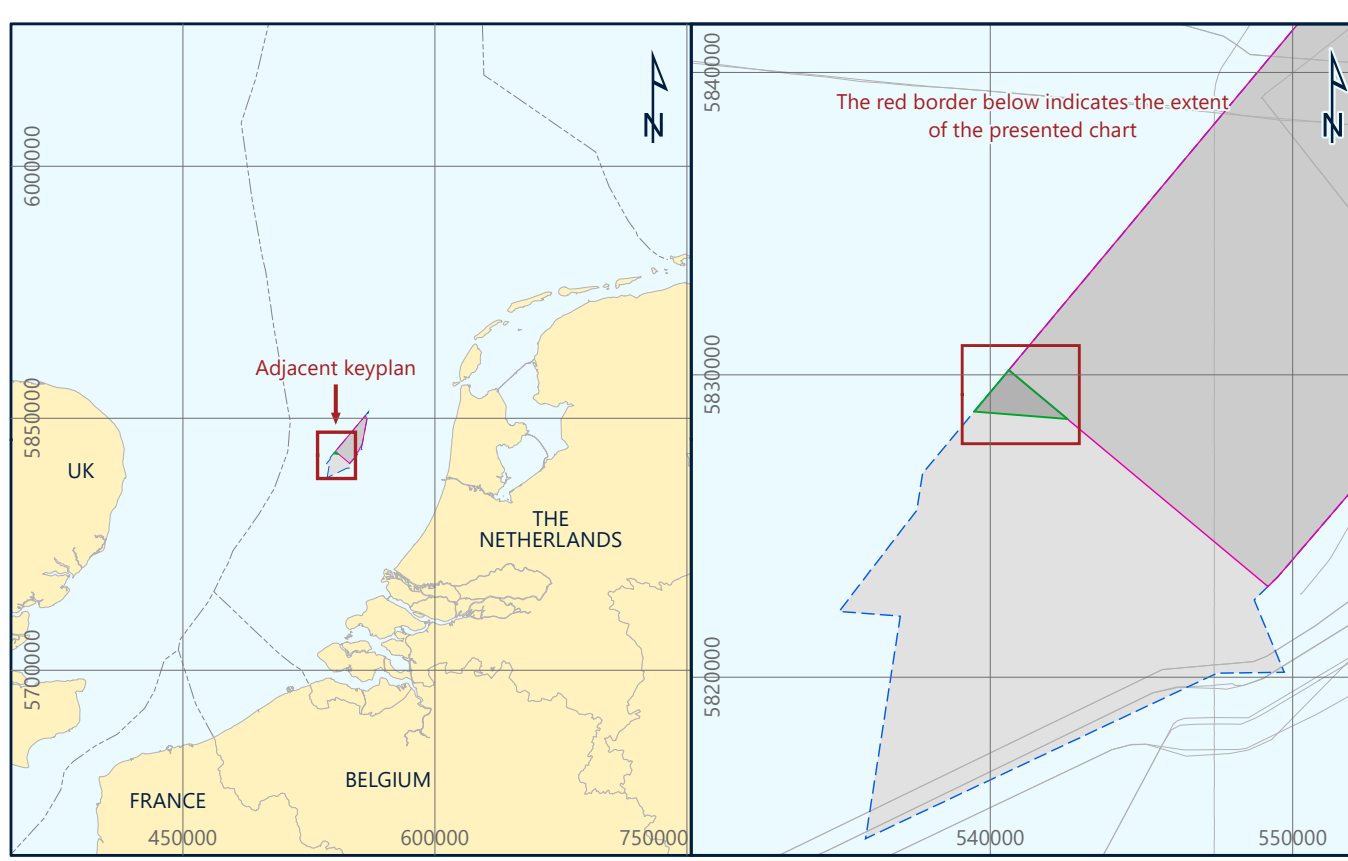
NOTES

1) Unit A is interpreted to be present across the entire HKW EA.

2) Gridding parameters: cell size 25 m x 25 m, fit to data 0.5, smoothing factor 6, search limit 200 m.

GEODETIC PARAMETERS

GEODETIC DATUM	European Terrestrial Reference System 1989
ELLIPSOID	GRS 1980
Semi-Major Axis	6 378 137 000 m
Inverse Flattening	298.257 222 101
PROJECTION	ETRS 1989 / UTM Zone 31N (EPSG 25837)
Central Meridian (CM)	03°00'00" E
Latitude of Origin	00°00'00" N
Fake Easting	500 000 mE
Fake Northing	0 mN
Scale Factor at CM	0.9996
DATUM TRANSFORMATION	ITRS2014 to ETRS89 for Epoch 2017.4959
Source	dx = +0.0545 m, dy = +0.05295 m, dz = -0.08834 m, rx = -0.0003087", ry = -0.0139630", rz = -0.0225688", Scale = -0.00294455 ppm
VERTICAL DATUM	Lowest Astronomical Tide (LAT)



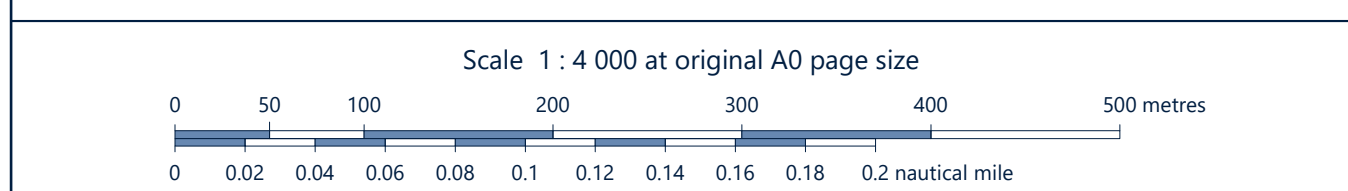
RVO
Prinses Beatrixlaan 2, 2595 AX Den Haag, The Netherlands
www.rvo.nl

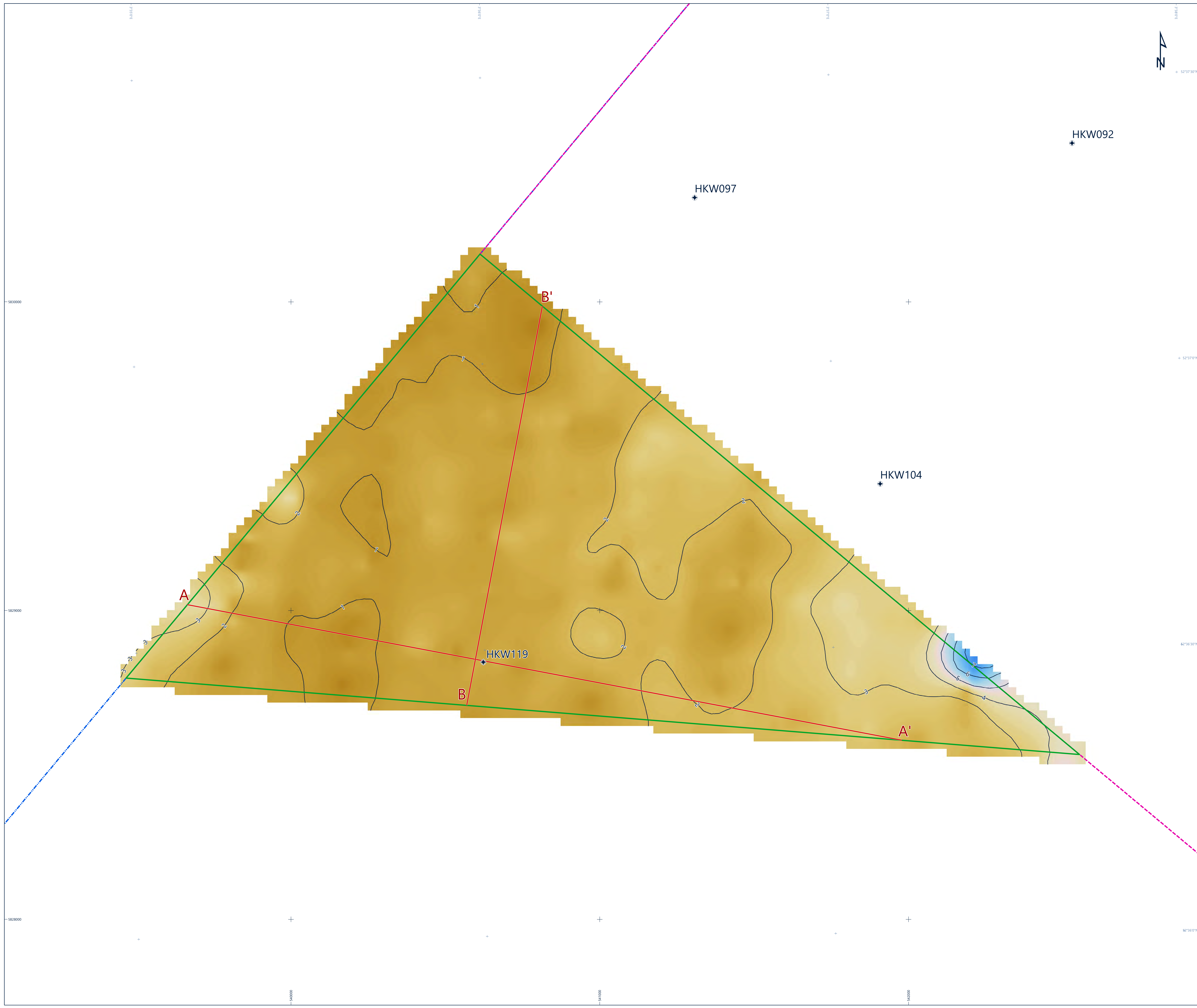
Rijksoverheid
Rijksdienst voor Ondernemend Nederland

Fugro
Prinsmaatslaan 4, 2031 RT Hoofddorp, The Netherlands
www.fugro.com

FUGRO

THICKNESS OF UNIT A
GEOTECHNICAL SITE INVESTIGATION
DUTCH SECTOR - NORTH SEA
HOLLANDE KUST (WEST) WIND FARM ZONE EXTENSION AREA





LEGEND

GEOTECHNICAL LOCATIONS

- Geotechnical location
- Cross-section presented in the report

GENERAL

- Hollandse Kust (west) Wind Farm Zone Extension Area (HKW EA)
- Hollandse Kust (west) Wind Farm Zone (HKW WFZ)
- HKW - Designated Wind Farm Zone
- UTM grid
- Geographical grid

THICKNESS OF UNIT B

Thickness contour at 1.0 metres interval

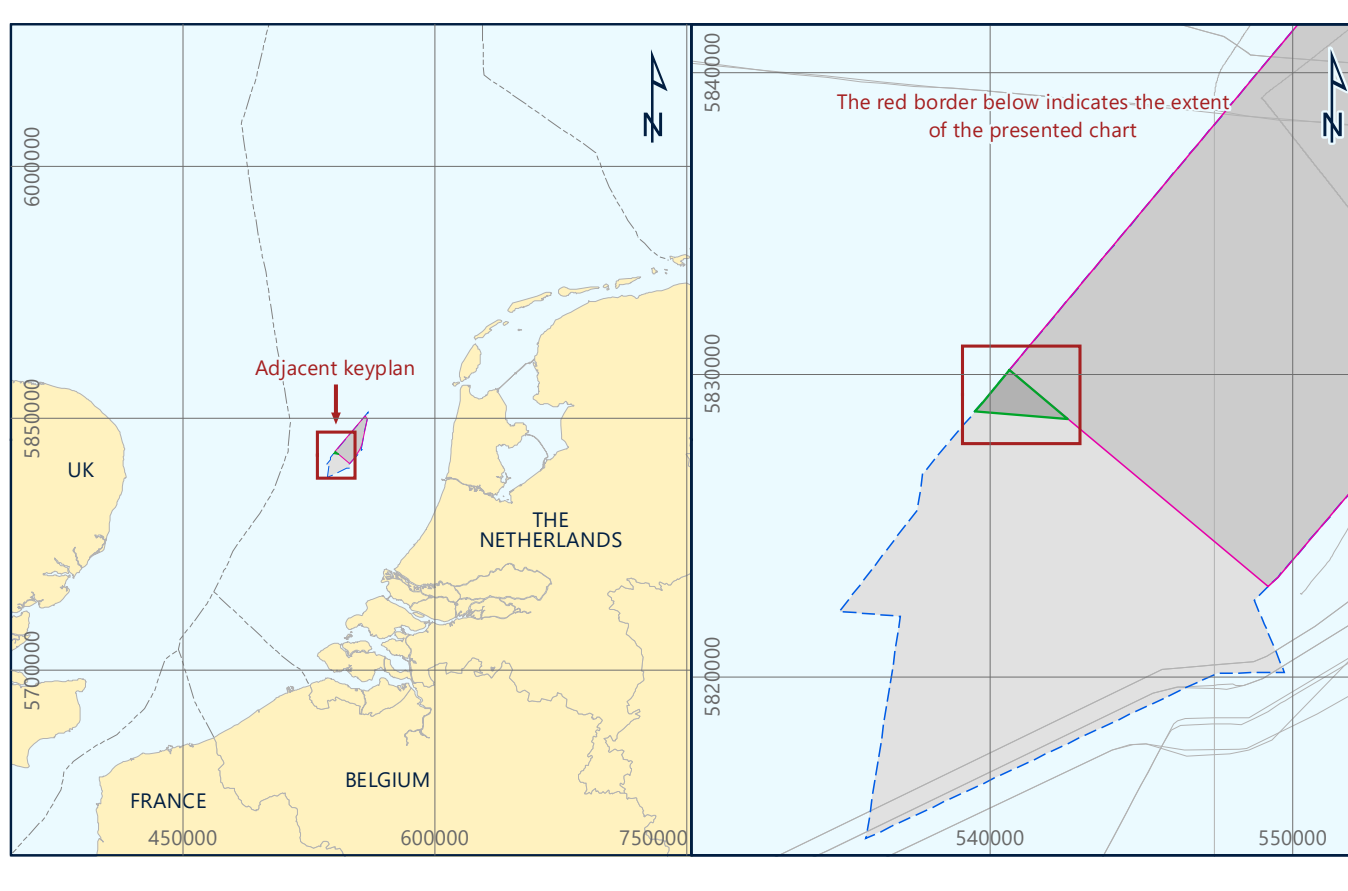
Thickness [m]

NOTES

- Unit B is interpreted to be present across the entire HKW EA.
- Gridding parameters: cell size 25 m x 25 m, fit to data 0.5, smoothing factor 6, search limit 200 m.

GEODETIC PARAMETERS

GEODETIC DATUM	European Terrestrial Reference System 1989
ELLIPSOID	GRS 1980
Semi-Major Axis	6 378 137 000 m
Inverse Flattening	298.257 222 101
PROJECTION	ETRS 1989 / UTM Zone 31N (EPSG 25831)
Central Meridian (CM)	03°00'00" E
Latitude of Origin	00°00'00" N
Fake Easting	500 000 mE
Fake Northing	0 mN
Scale Factor at CM	0.9996
DATUM TRANSFORMATION	ITRS2014 to ETRS89 for Epoch 2017.4959
Source	$dx = +0.0545$ m, $dy = +0.05295$ m, $dz = -0.08834$ m $rx = -0.0023082''$, $ry = -0.0139630''$, $rz = -0.0225688''$, Scale = -0.00294455 ppm
VERTICAL DATUM	Lowest Astronomical Tide (LAT)



RVO
 Prinses Beatrixlaan 2, 2595 AX Den Haag, The Netherlands
 www.rvo.nl

Rijksoverheid
 Rijksdienst voor Ondernemend Nederland

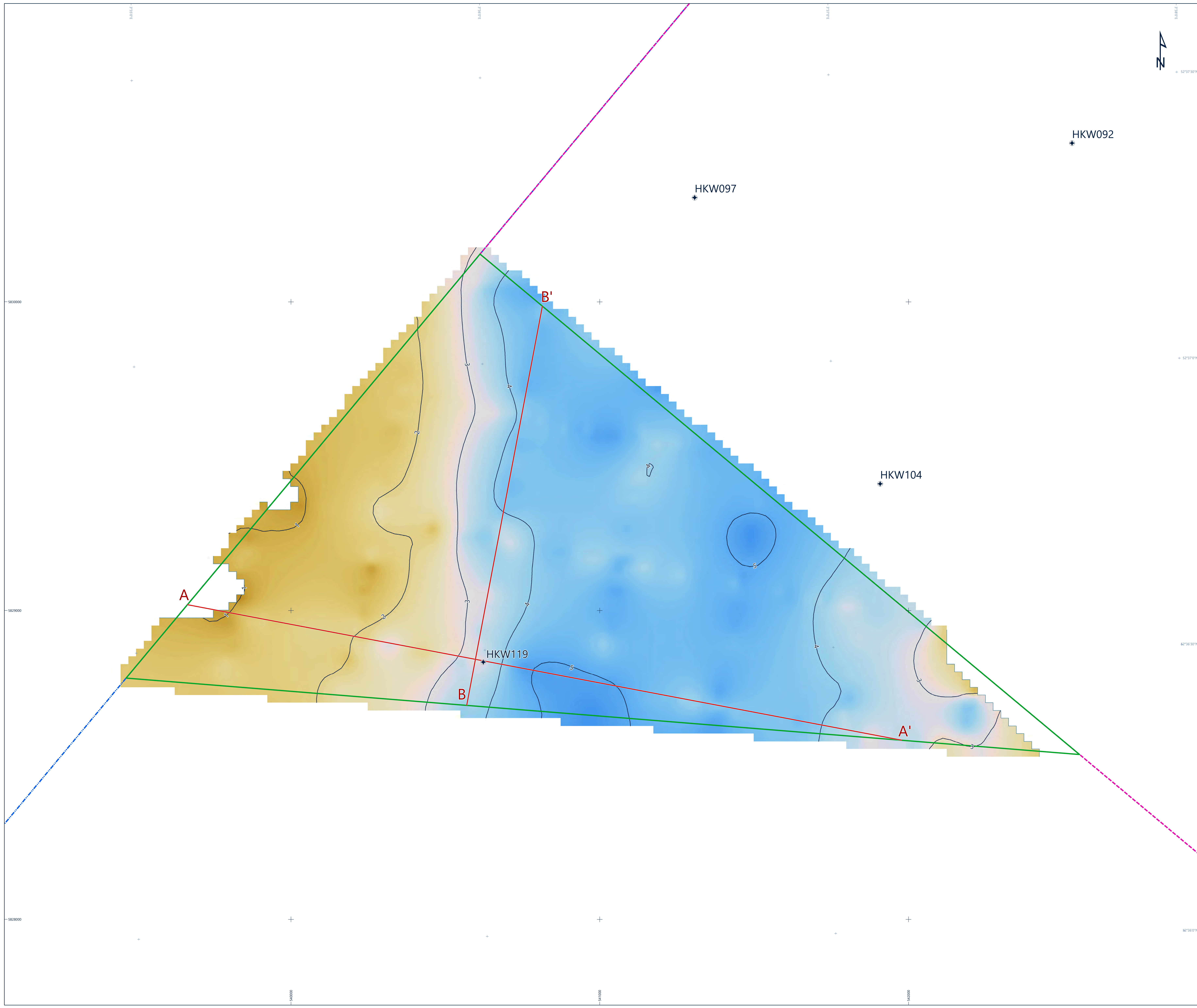
Fugro
 Prinsmaatslaan 4, 2611 RT Noordwijk, The Netherlands
 www.fugro.com

FUGRO

THICKNESS OF UNIT B
 GEOTECHNICAL SITE INVESTIGATION
 DUTCH SECTOR - NORTH SEA
 HOLLANDE KUST (WEST) WIND FARM ZONE EXTENSION AREA

Scale 1 : 4 000 at original A0 page size

Fugro Document No. P904711/GA/01 Chart No. 1 of 1 Plate No. A3-11



LEGEND

GEOTECHNICAL LOCATIONS

- Geotechnical location
- Cross-section presented in the report

GENERAL

- Hollandse Kust (west) Wind Farm Zone Extension Area (HKW EA)
- Hollandse Kust (west) Wind Farm Zone (HKW WFZ)
- HKW - Designated Wind Farm Zone
- UTM grid
- Geographical grid

THICKNESS OF UNIT C1

Thickness contour at 1.0 metres interval

Thickness [m]

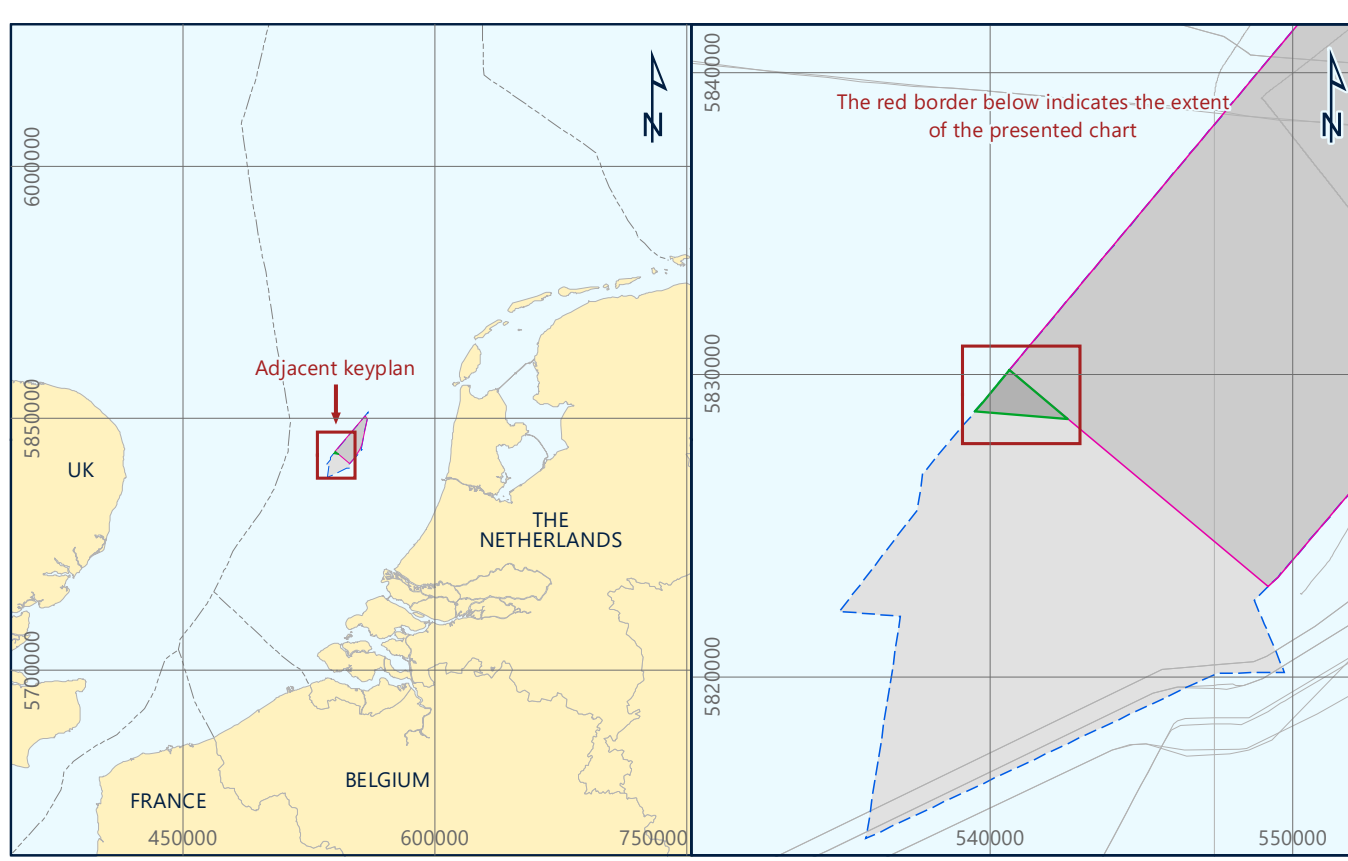
- > 0
- 1
- 2
- 3
- 4
- 5
- 6

NOTES

- Blank areas indicate where Unit C1 is interpreted to be absent.
- Gridding parameters: cell size 25 m x 25 m, fit to data 0.5, smoothing factor 6, search limit 200 m.

GEODETIC PARAMETERS

GEODETIC DATUM	European Terrestrial Reference System 1989
ELLIPSOID	GRS 1980
Semi-Major Axis	6 378 137 000 m
Inverse Flattening	298.257 222 101
PROJECTION	ETRS 1989 / UTM Zone 31N (EPSG 25831)
Central Meridian (CM)	03°00'00" E
Latitude of Origin	00°00'00" N
Fake Easting	500 000 mE
Fake Northing	0 mN
Scale Factor at CM	0.9996
DATUM TRANSFORMATION	ITRS2014 to ETRS89 for Epoch 2017.4959
Source	dx = +0.0545 m, dy = +0.05295 m, dz = -0.08834 m, rx = -0.0023082", ry = -0.0139630", rz = -0.0225688", Scale = -0.00294455 ppm
VERTICAL DATUM	Lowest Astronomical Tide (LAT)



RVO
 Private Beeldruimte 2, 2595 AL Den Haag, The Netherlands
 www.rvo.nl

Rijksoverheid
 Rijksdienst voor Ondernemend Nederland

Fugro
 Prinsmaats 4, 2611 RT Noordwijk, The Netherlands
 www.fugro.com

FUGRO

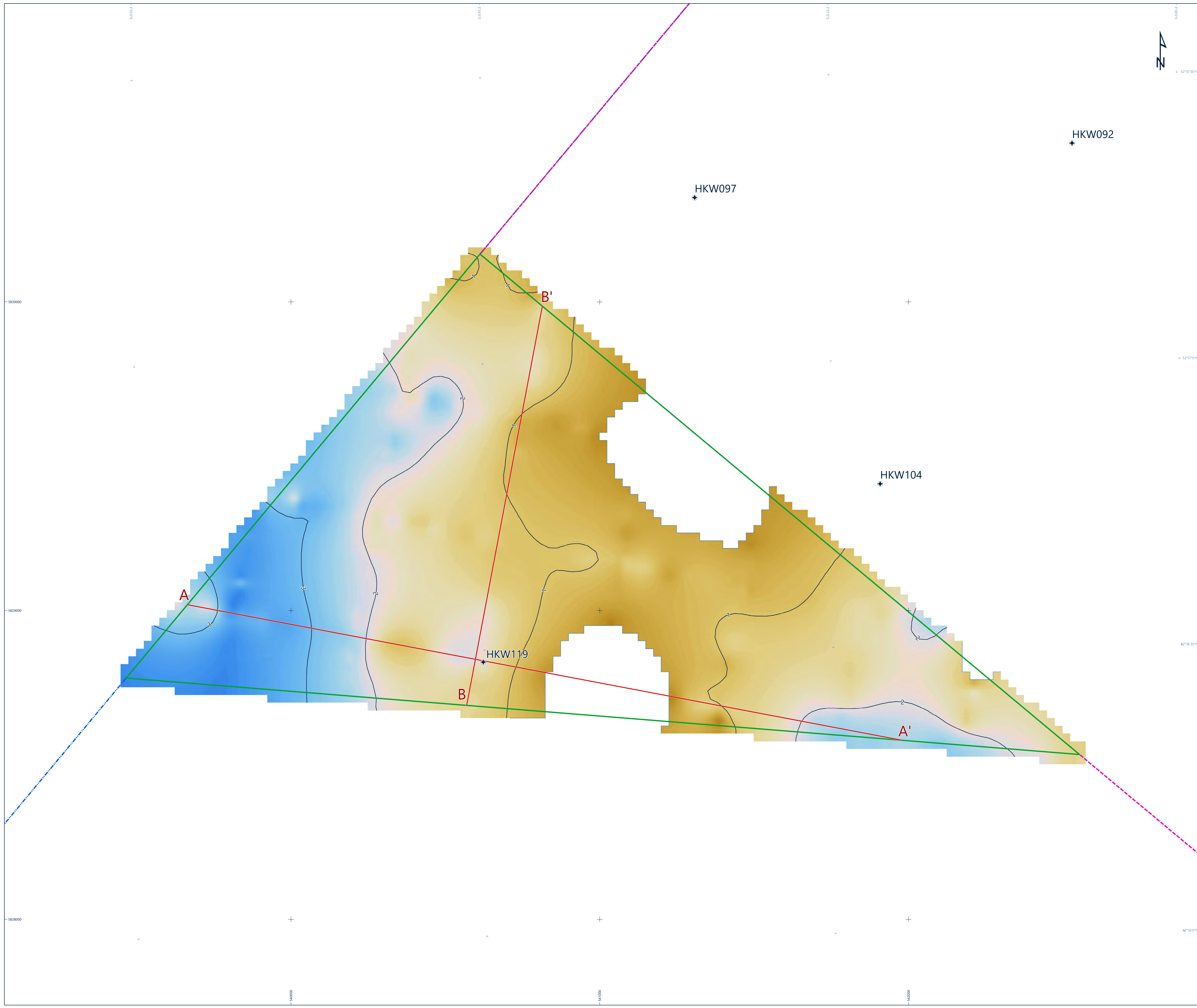
THICKNESS OF UNIT C1

GEOTECHNICAL SITE INVESTIGATION
 DUTCH SECTOR - NORTH SEA
 HOLLANDE KUST (WEST) WIND FARM ZONE EXTENSION AREA

Scale 1 : 4 000 at original A0 page size

0 50 100 200 300 400 500 metres
 0 0.02 0.04 0.06 0.08 0.1 0.12 0.14 0.16 0.18 0.2 nautical miles

Fugro Document No. P90471/GA/01 Chart No. 1 of 1 Plate No. A3-12



LEGEND

GEOTECHNICAL LOCATIONS

- Geotechnical location
- Cross-section presented in the report

GENERAL

- Hollandse Kust (west) Wind Farm Zone Extension Area (HKW EA)
- Hollandse Kust (west) Wind Farm Zone (HKW WFZ)
- HKW - Designated Wind Farm Zone
- UTM grid
- Geographical grid

THICKNESS OF UNIT C2

Thickness contour at 1.0 metres interval

Thickness [m]

> 0

1

2

3

4

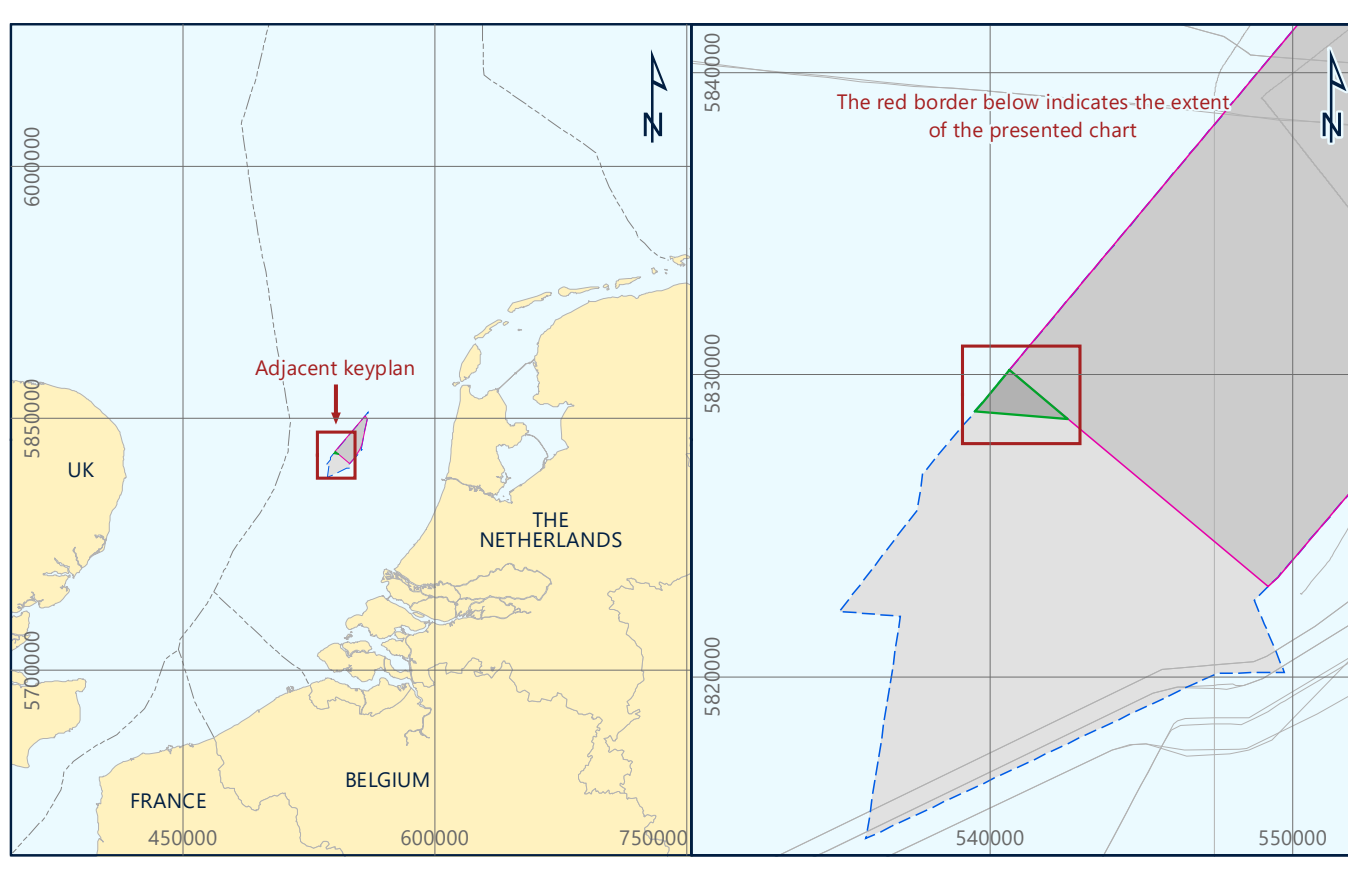
NOTES

1) Blank areas indicate where Unit C2 is interpreted to be absent.

2) Gridding parameters: cell size 25 m x 25 m, fit to data 0.5, smoothing factor 6, search limit 200 m.

GEODETIC PARAMETERS

GEODETIC DATUM	European Terrestrial Reference System 1989
ELLIPSOID	GRS 1980
Semi-Major Axis	6 378 137 000 m
Inverse Flattening	298.257 222 101
PROJECTION	ETRS 1989 / UTM Zone 31N (EPSG 25831)
Central Meridian (CM)	03°00'00" E
Latitude of Origin	00°00'00" N
Fake Easting	500 000 mE
Fake Northing	0 mN
Scale Factor at CM	0.9996
DATUM TRANSFORMATION	ITRS2014 to ETRS89 for Epoch 2017.4959
Source	$dx = +0.0545$ m, $dy = +0.05295$ m, $dz = -0.08834$ m $kx = -0.0023082$, $ky = -0.0139630$, $kz = -0.0225688$; Scale = -0.00294455 ppm
VERTICAL DATUM	Lowest Astronomical Tide (LAT)



RVO
 Private Beeldruimte 2, 2595 AL Den Haag, The Netherlands
 www.rvo.nl

Rijksoverheid
 Rijksdienst voor Ondernemend Nederland

Fugro
 Prinsmaatsla 4, 2611 RT Noordwijk, The Netherlands
 www.fugro.com

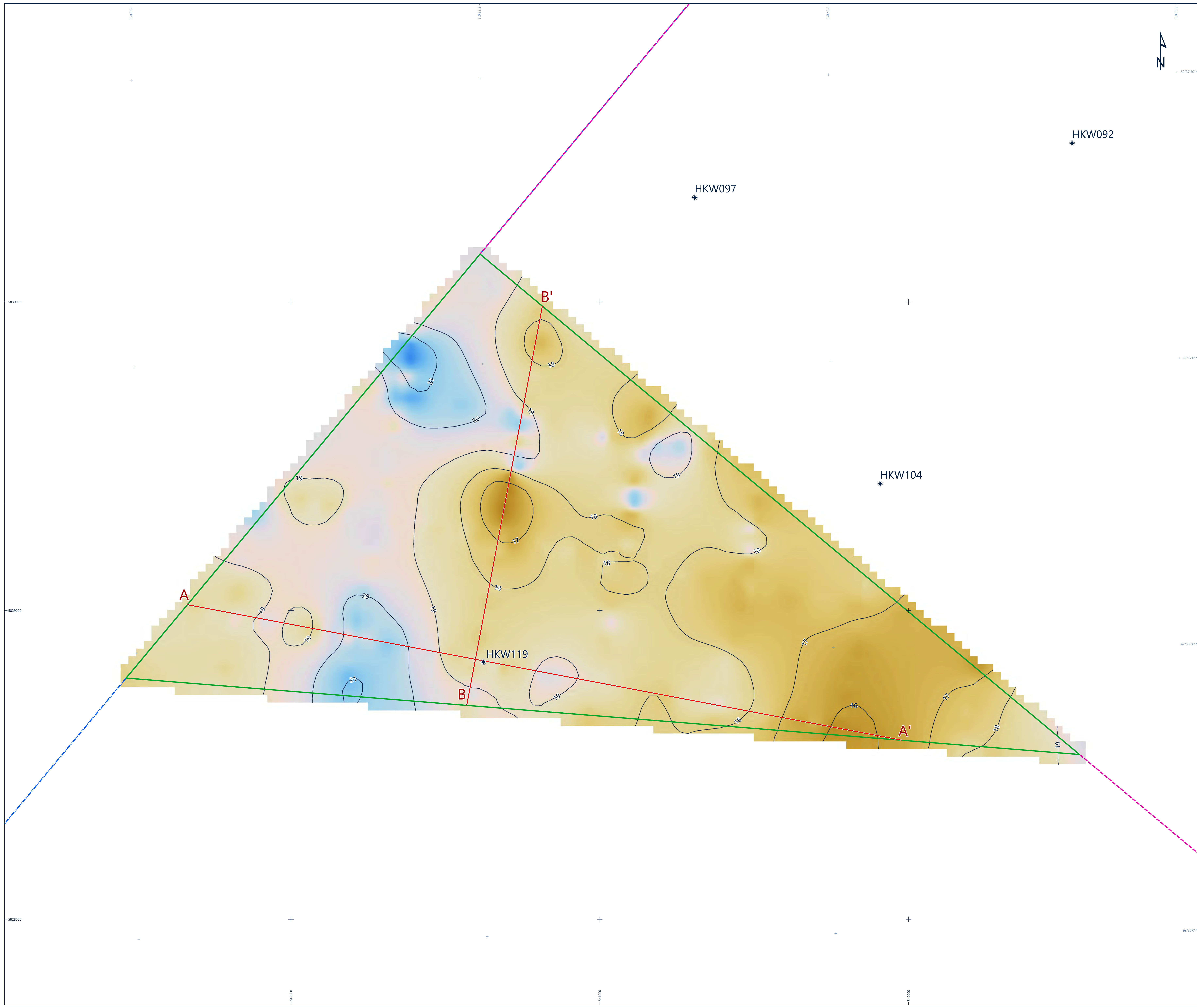
FUGRO

THICKNESS OF UNIT C2
 GEOTECHNICAL SITE INVESTIGATION
 DUTCH SECTOR - NORTH SEA
 HOLLANDE KUST (WEST) WIND FARM ZONE EXTENSION AREA

Scale 1 : 4 000 at original A0 page size

0 50 100 200 300 400 500 metres
 0 0.02 0.04 0.06 0.08 0.1 0.12 0.14 0.16 0.18 0.2 nautical mile

Fugro Document No. P90471/GA/01 Chart No. 1 of 1 Plate No. A3-13



LEGEND

GEOTECHNICAL LOCATIONS

- Geotechnical location
- Cross-section presented in the report

GENERAL

- Hollandse Kust (west) Wind Farm Zone Extension Area (HKW EA)
- Hollandse Kust (west) Wind Farm Zone (HKW WFZ)
- HKW - Designated Wind Farm Zone
- UTM grid
- Geographical grid

THICKNESS OF UNIT F

Thickness contour at 1.0 metres interval

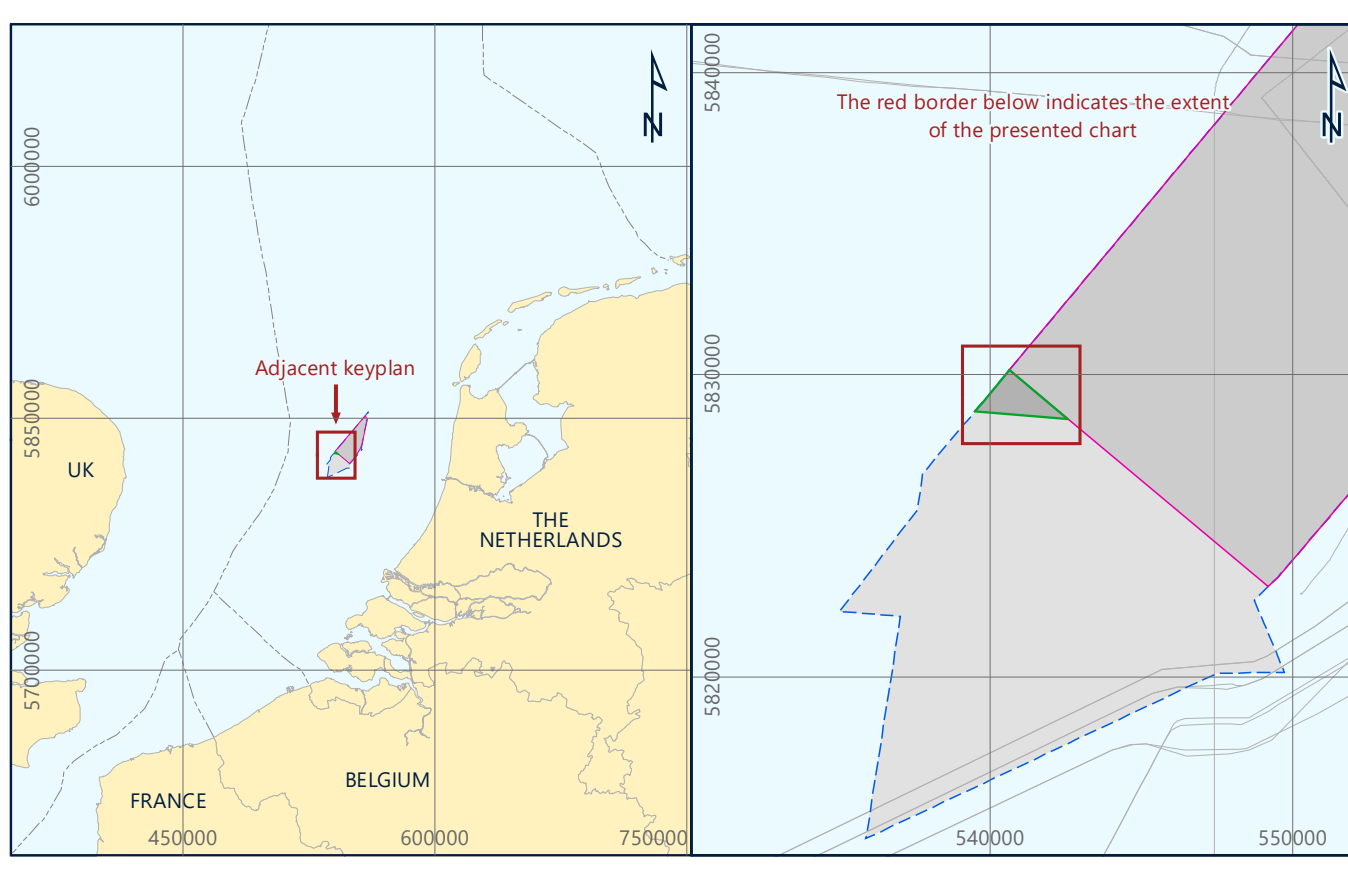
Thickness [m]

NOTES

- Unit F is interpreted to be present across the entire HKW EA.
- Gridding parameters: cell size 25 m x 25 m, fit to data 0.5, smoothing factor 6, search limit 200 m.

GEODETIC PARAMETERS

GEODETIC DATUM	European Terrestrial Reference System 1989
ELLIPSOID	GRS 1980
Semi-Major Axis	6 378 137 000 m
Inverse Flattening	298.257 222 101
PROJECTION	ETRS 1989 / UTM Zone 31N (EPSG 25831)
Central Meridian (CM)	03°00'00" E
Latitude of Origin	00°00'00" N
Fake Easting	500 000 mE
Fake Northing	0 mN
Scale Factor at CM	0.9996
DATUM TRANSFORMATION	ITRS2014 to ETRS89 for Epoch 2017.4959
Source	dx = +0.05545 m, dy = +0.05295 m, dz = -0.08834 m rx = -0.0023082", ry = -0.0139630", rz = -0.0225688", Scale = -0.00294455 ppm
VERTICAL DATUM	Lowest Astronomical Tide (LAT)



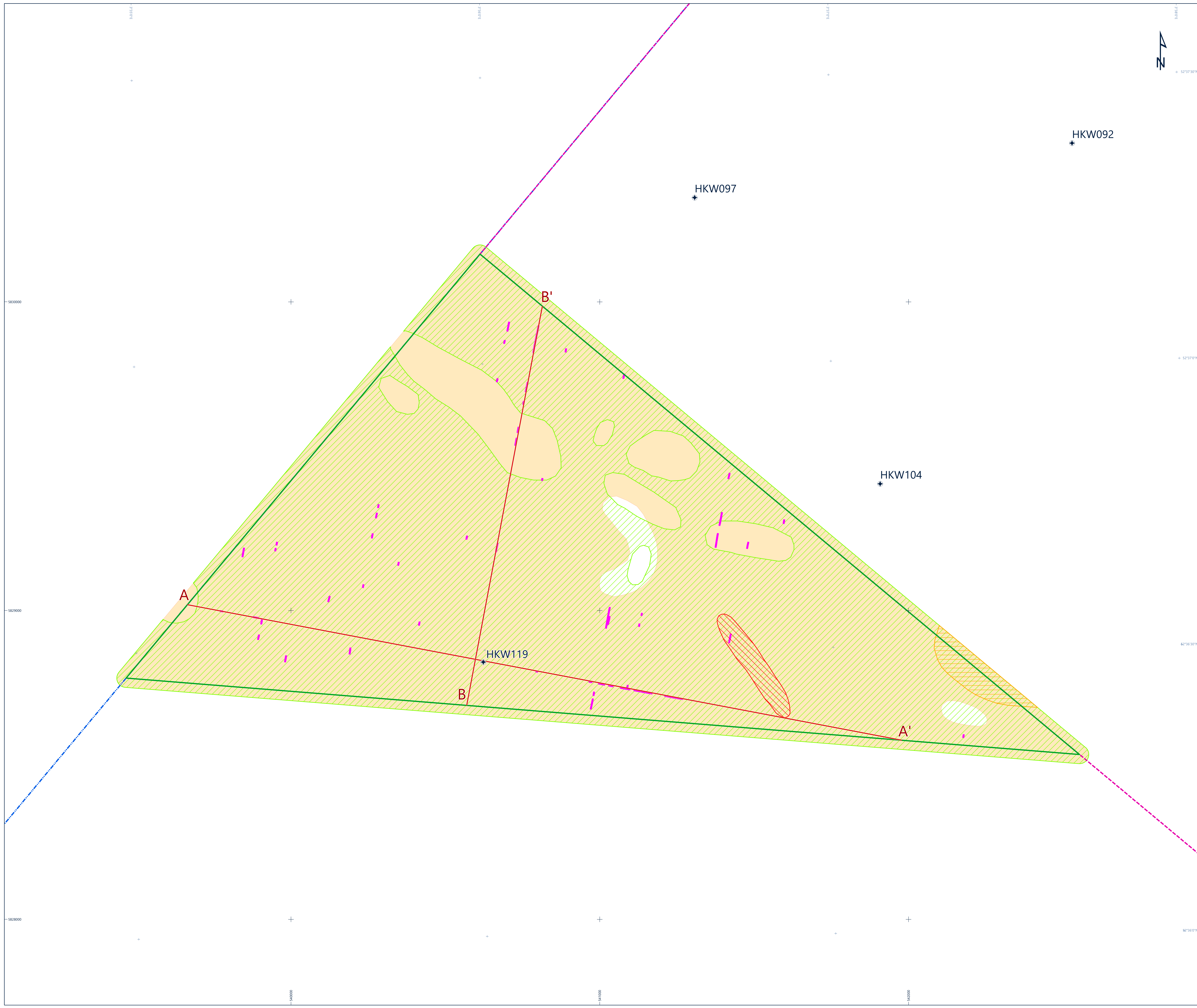
RVO
Rijksdienst voor Ondernemend Nederland

Fugro
Fugro Document No. P90471/GA/01

THICKNESS OF UNIT F
GEOTECHNICAL SITE INVESTIGATION
DUTCH SECTOR - NORTH SEA
HOLLANDE KUST (WEST) WIND FARM ZONE EXTENSION AREA

Scale 1 : 4 000 at original A0 page size

Fugro Document No. P90471/GA/01 Chart No. 1 of 1 Plate No. A3-14



LEGEND

GEOTECHNICAL LOCATIONS

- Geotechnical location
- Cross-section presented in the report

GENERAL

- Hollandse Kust (west) Wind Farm Zone Extension Area (HKW EA)
- Hollandse Kust (west) Wind Farm Zone (HKW WFZ)
- HKW - Designated Wind Farm Zone
- UTM grid
- Geographical grid

GEOLOGICAL FEATURES

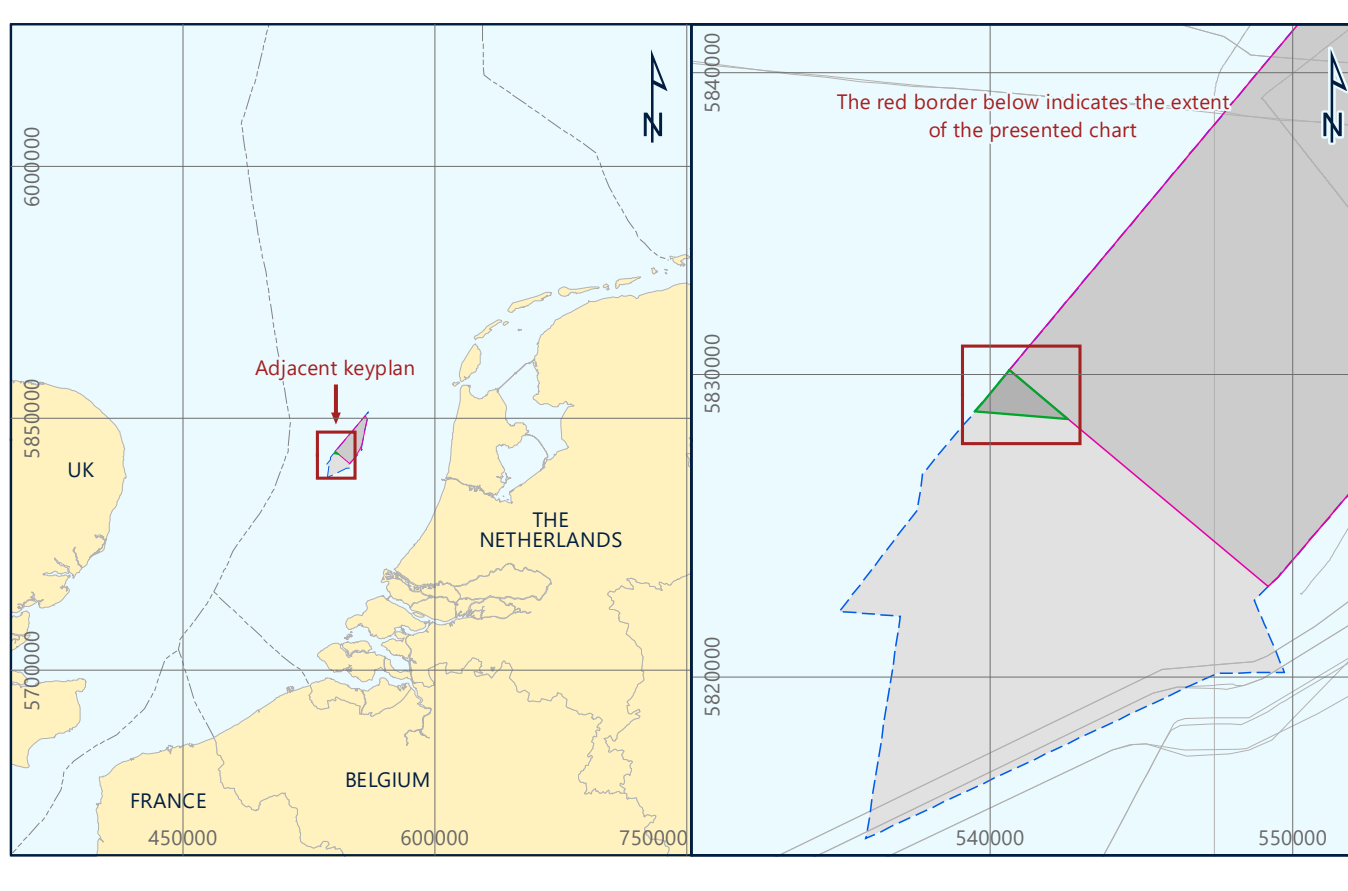
- Buried channel in Unit B
- Buried channel at the base of Unit B
- Peat / organic clay level 2A
- Peat / organic clay level 2B
- Peat / organic clay level 2C (at the base of Unit F)

NOTES

- Blank areas indicate where geological features are interpreted to be absent. Refer to Main Text for details.
- Buried channels may occur at other locations than those interpreted from the seismic reflection and geotechnical data.
- The presented information shows amplitude anomalies which were identified on seismic data. Peat / organic clay beds were observed in geotechnical data with no corresponding seismic response. Peat / organic clay may occur more frequently than interpreted from seismic reflection data alone.
- Due to the limited lateral extent, peat / organic clay level 2A is presented as points, where this level was interpreted.

GEODEIC PARAMETERS

GEODETIC DATUM	European Terrestrial Reference System 1989
ELLIPSOID	GRS 1980
Semi-Major Axis	6 378 137 000 m
Inverse Flattening	298.257 222 101
PROJECTION	ETRS 1989 / UTM Zone 31N (EPSG 25831)
Central Meridian (CM)	03°00'00" E
Latitude of Origin	00°00'00" N
Fake Easting	500 000 mE
Fake Northing	0 mN
Scale Factor at CM	0.9996
DATUM TRANSFORMATION	ITRS2014 to ETRS89 for Epoch 2017.4959
Source	$dx = +0.0545$ m, $dy = +0.05295$ m, $dz = -0.08834$ m $rx = -0.0023082''$, $ry = -0.0139630''$, $rz = -0.0225688''$, Scale = 0.00294455 ppm
VERTICAL DATUM	Lowest Astronomical Tide (LAT)



RVO
 Prinses Beatrixlaan 2, 2595 AX Den Haag, The Netherlands
 www.rvo.nl

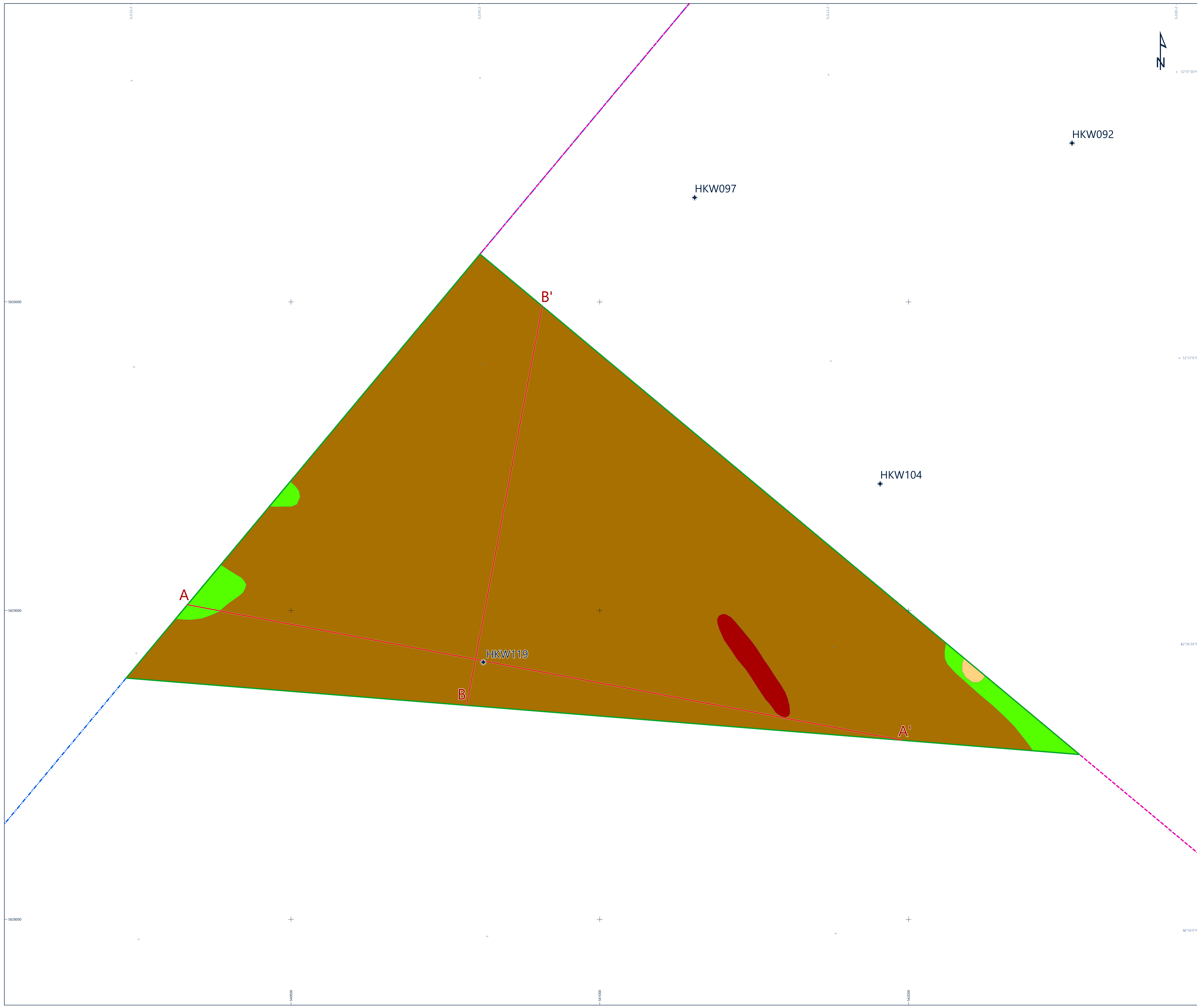
Rijksoverheid
 Rijksdienst voor Ondernemend Nederland

Fugro
 Prinsmaatslaan 4, 2611 RT Noordwijk, The Netherlands
 www.fugro.com

FUGRO

GEOLOGICAL FEATURES
 GEOTECHNICAL SITE INVESTIGATION
 DUTCH SECTOR - NORTH SEA
 HOLLANDE KUST (WEST) WIND FARM ZONE EXTENSION AREA





LEGEND

GEOTECHNICAL LOCATIONS

- Geotechnical location
- Cross-section presented in the report

GENERAL

- Hollandse Kust (west) Wind Farm Zone Extension Area (HKW EA)
- Hollandse Kust (west) Wind Farm Zone (HKW WFZ)
- HKW - Designated Wind Farm Zone
- UTM grid
- Geographical grid

SOIL PROVINCES

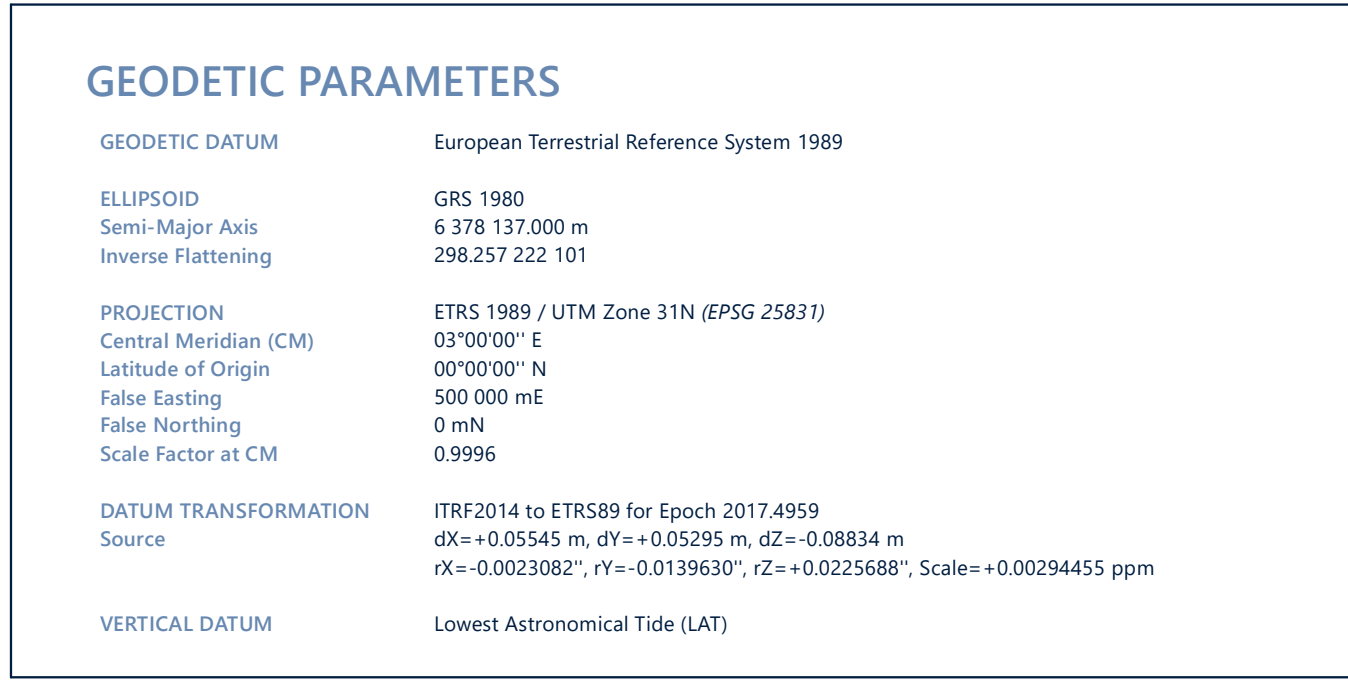
- Soil Province 3
- Soil Province 4
- Soil Province 5
- Soil Province 7

NOTES

1) Refer to Main Text for details.

GEODETIC PARAMETERS

GEODETIC DATUM	European Terrestrial Reference System 1989
ELLIPSOID	GRS 1980
Semi-Major Axis	6 378 137 000 m
Inverse Flattening	298.257 222 101
PROJECTION	ETRS 1989 / UTM Zone 31N (EPSG 25831)
Central Meridian (CM)	03°00'00" E
Latitude of Origin	00°00'00" N
Fake Easting	500 000 mE
Fake Northing	0 mN
Scale Factor at CM	0.9996
DATUM TRANSFORMATION	ITRS2014 to ETRS89 for Epoch 2017.4959
Source	$dx = +0.05545$ m, $dy = +0.05295$ m, $dz = -0.38834$ m $rx = -0.0023082''$, $ry = -0.0139630''$, $rz = -0.0225688''$; Scale = -0.00294455 ppm
VERTICAL DATUM	Lowest Astronomical Tide (LAT)



RVO
 Rijksdienst voor Ondernemend Nederland

Fugro
 Prinsmaats 4, 2611 RT Noordwijk, The Netherlands

SOIL PROVINCES

GEOTECHNICAL SITE INVESTIGATION
 DUTCH SECTOR - NORTH SEA
 HOLLANDE KUST (WEST) WIND FARM ZONE EXTENSION AREA

Scale 1 : 4 000 at original A0 page size

Fugro Document No. P904711/GA/01 Chart No. 1 of 1 Plate No. A3-16

Appendix B

In Situ Test Results

Contents Appendix B.1: Geotechnical Logs

	Page
B.1 Geotechnical Logs	1
B.1.1 Practice for Geotechnical Log	1
B.1.2 Comments on Results	2
B.1.3 References	2

List of Plates

Title	Plate
Geotechnical Log	B.1-1 to B.1-3

B.1 Geotechnical Logs

B.1.1 Practice for Geotechnical Log

Approach

Purpose:	Refer to Main Text
General Procedure:	<ul style="list-style-type: none"> ■ Refer to document titled 'Geotechnical Log' presented in appendix titled 'Descriptions of Methods and Practices' ■ According to ISO (2014)

Results – Cone Penetration Test – Non-drilling Deployment

Data Processing and Interpretation:	<ul style="list-style-type: none"> ■ Discovery – GeoVisual software ■ Graphical scales selected to suit general presentation of data ■ No display of data outside of chart limits, i.e. some values may not be shown
Data Format(s):	<ul style="list-style-type: none"> ■ PDF for viewing and printing (this primary document)
Ground Description:	<ul style="list-style-type: none"> ■ According to ISO (2014) and Robertson (2010) ■ No ground description may be presented where data are outside of limits of the Robertson methods ■ No verification with physical samples and laboratory test results
Unit Weight derived from In Situ Test:	Not applicable
Relative Density derived from In Situ Test:	<p>If applicable:</p> <ul style="list-style-type: none"> ■ refer to document titled 'Cone Penetration Test Interpretation' presented in appendix titled 'Descriptions of Methods and Practices' ■ according to Jamiolkowski et al. (2003) for saturated coarse-grained, frictional soil behaviour ■ based on earth pressure coefficient values $K_0 = 0.5$ and 1.0 ■ relative density presented where soil behaviour type index $I_c < 2.6$ (or ISBT < 2.6 where applicable) ■ no calculation of relative density for initial penetration to a depth equivalent to five times diameter of deployed cone penetrometer ■ presented values represent results of correlation(s), i.e. not an expected range

Undrained Shear Strength derived from In Situ Test:	<p>If applicable:</p> <ul style="list-style-type: none"> ■ refer to document titled 'Cone Penetration Test Interpretation' presented in appendix titled 'Descriptions of Methods and Practices' ■ applies to interpreted fine-grained, cohesive soil behaviour ■ based on cone factor of $N_{kt} = 11$ and $N_{kt} = 17$ ■ target reference strength is laboratory consolidated (an)isotropic undrained triaxial compression on undisturbed sample, recompressed to estimated in situ stress conditions ■ undrained shear strength presented where soil behaviour type index $I_c > 2.05$ (or $I_{SBT} > 2.05$ where applicable) ■ no calculation of undrained shear strength for initial penetration to a depth equivalent to five times diameter of deployed cone penetrometer ■ presented values represent results of correlation(s), i.e. not an expected range
Other Parameters Derived from In Situ Test:	Not applicable
Coordinates and Water Depth:	Applicable to CPT location
Water Depth Reference:	As inferred from conductivity, temperature, and depth (CTD) measurements at start of testing/sampling, reduced to LAT
Depth Reference Correction:	None applied, CPT assumed continuous from seafloor to recovery depth, with no continuity gaps

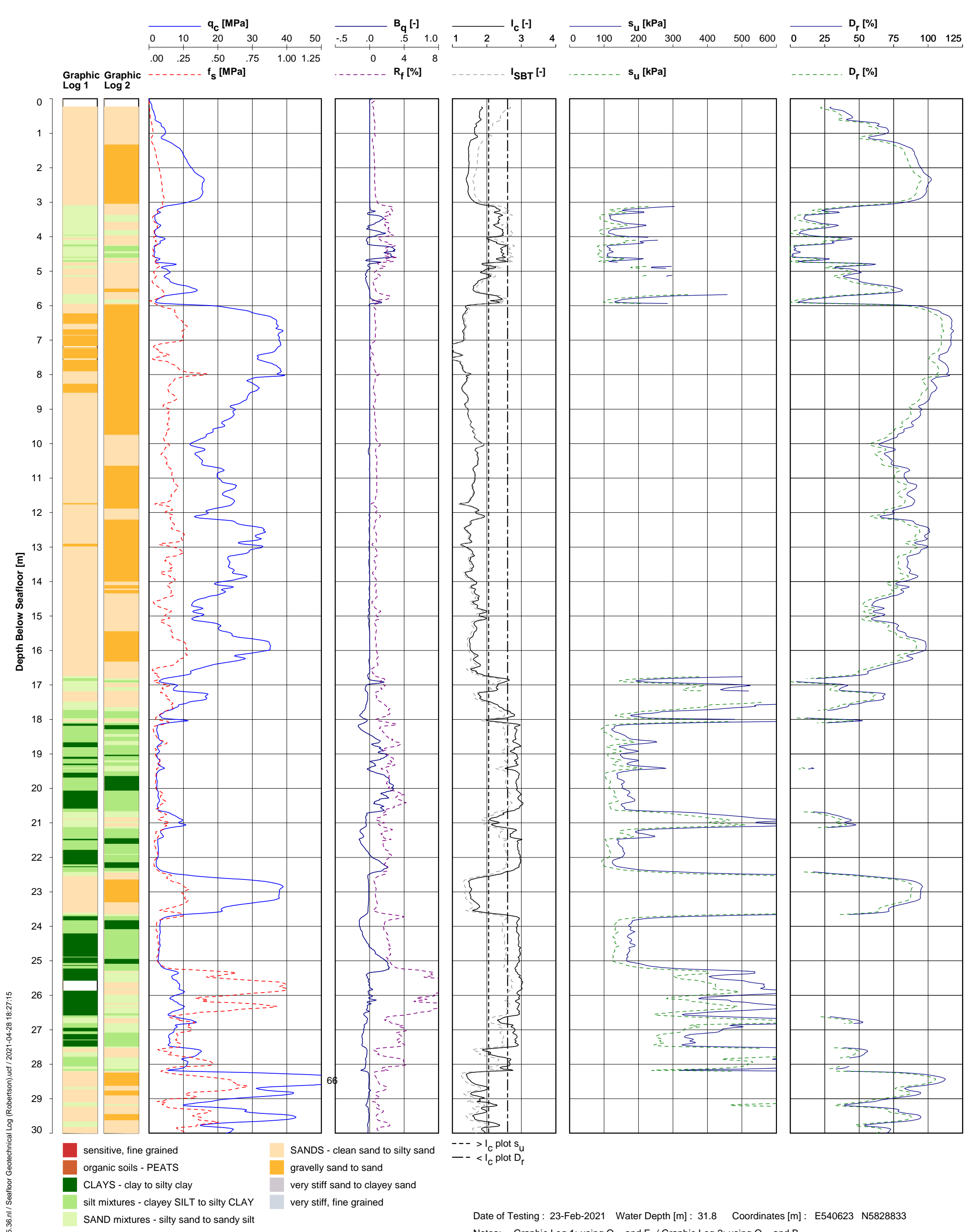
B.1.2 Comments on Results

The interpreted ground model and associated strata descriptions presented in the geotechnical log consider soil layers with a minimum thickness of 0.2 m.

B.1.3 References

- Computer Program 'Discovery GeoVisual', *Processing, Presentation and Analysis of In Situ Test Data*.
- International Organization for Standardization (2014). *Petroleum and natural gas industries – specific requirements for offshore structures – part 8: marine soil investigations* (ISO 19901-8:2014). <https://www.iso.org/standard/61145.html>
- Jamiolkowski, M., Lo Presti, D.C.F., & Manassero, M. (2003). Evaluation of relative density and shear strength of sands from CPT and DMT. In J.T. Germaine, T.C. Sheahan & R.V. Whitman (Eds.), *Soil behavior and soft ground construction* (pp. 201–238). American Society for Civil Engineers. <https://doi.org/10.1061/9780784406595>

- Robertson, P.K. (2009). Performance based earthquake design using the CPT. In Kokusho, T., Tsukamoto, Y. and Yoshimine, M. Eds. *Performance-Based Design in Earthquake Geotechnical Engineering – from Case History to Practice*: Proceedings of the International Conference on Performance-Based Design in Earthquake Geotechnical Engineering ISTokyo 2009), 15-18 June 2009, Boca Raton: CRC Press, pp. 3-20.
- Robertson, P.K. (2010). Soil behaviour type from the CPT: an update. In *2nd International symposium on cone penetration testing, Huntington Beach, CA, Vol. 2.* (pp. 575-583)

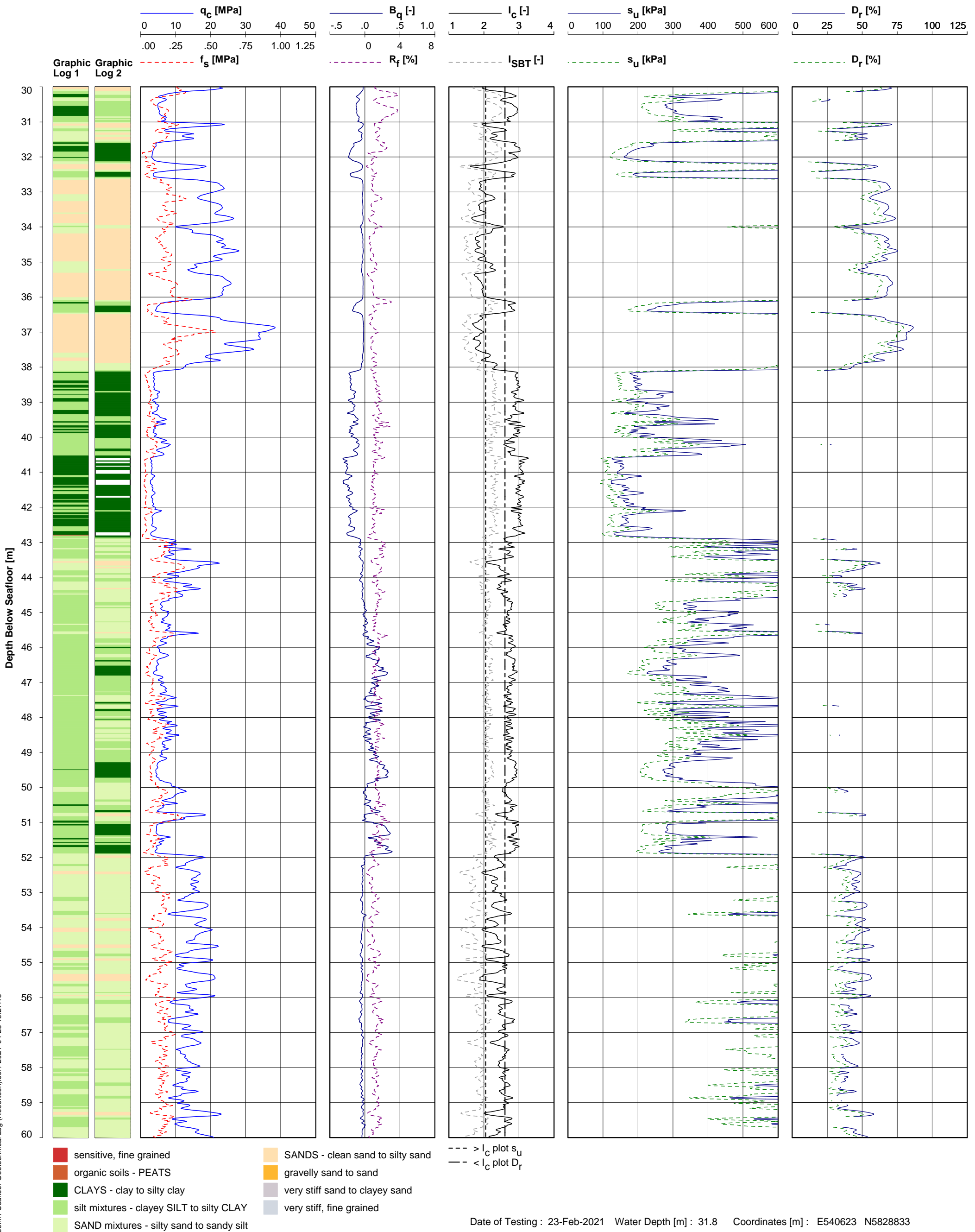


UNIPLOT 05.36.nl / Seafloor Geotechnical Log (Robertson).ucf / 2021-04-28 18:27:15

GEOTECHNICAL LOG
HKW119-PCPT

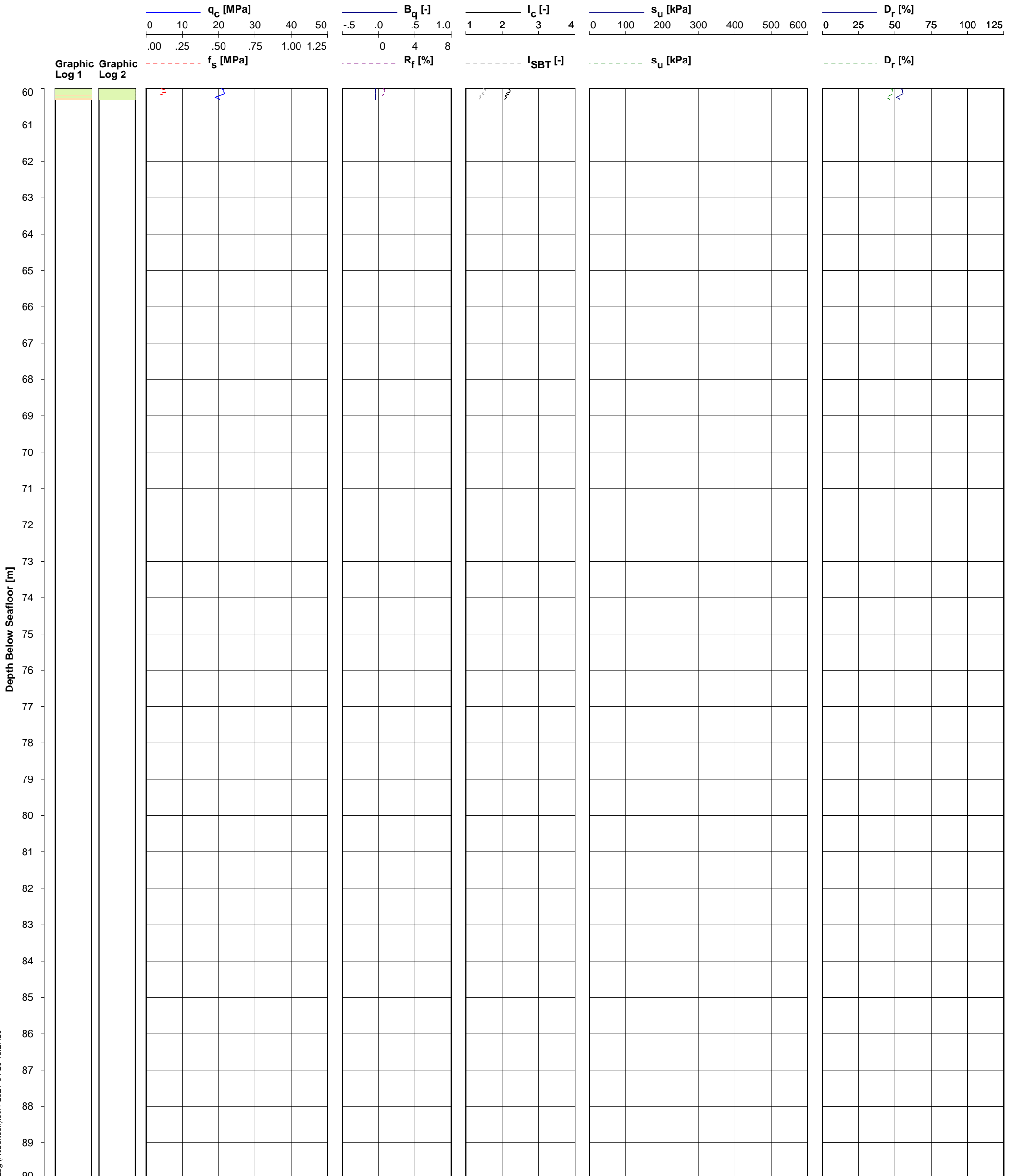


UNIPLOT 05.36.nl / Seafloor Geotechnical Log (Robertson).ucf / 2021-04-28 18:27:18



GEOTECHNICAL LOG
 HKW119-PCPT

UNIPLOT 05.36.nl / Seafloor Geotechnical Log (Robertson).ucf / 2021-04-28 18:27:20



- | | | |
|---|--|------------------|
| ■ sensitive, fine grained | ■ SANDS - clean sand to silty sand | --- > Ic plot su |
| ■ organic soils - PEATS | ■ gravelly sand to sand | --- < Ic plot Dr |
| ■ CLAYS - clay to silty clay | ■ very stiff sand to clayey sand | |
| ■ silt mixtures - clayey SILT to silty CLAY | ■ very stiff, fine grained | |
| ■ SAND mixtures - silty sand to sandy silt | | |

Date of Testing : 23-Feb-2021 Water Depth [m] : 31.8 Coordinates [m] : E540623 N5828833
 Notes: - Graphic Log 1: using Q_{tn} and F_r / Graphic Log 2: using Q_{tn} and B_q
 - Refer to Appendix Text for details

GEOTECHNICAL LOG
 HKW119-PCPT



Contents Appendix B.2: Results of Cone Penetration Tests

	Page
B.2 Results of Cone Penetration Tests	1
B.2.1 Practice for Cone Penetration Test	1
B.2.2 Comments on Results	2
B.2.3 References	3

List of Plates

Title	Plate
Cone Penetration Test; q_c , f_s and u_2	B.2 to B.2-10
Cone Penetration Test; q_t , q_n , R_f and B_q	B.2-11 to B.2-20
Parameter Values for Net Cone Resistance Calculation	B.2-21 to B.2-25
Cone Penetration Test - Zero Drift	B.2-26

B.2 Results of Cone Penetration Tests

B.2.1 Practice for Cone Penetration Test

Test Overview

General Procedure:	<ul style="list-style-type: none"> ■ According to ISO (2014) ■ Refer to document titled 'Cone Penetration Test' presented in appendix titled 'Descriptions of Methods and Practices'
Target Application Class:	Class 2 of ISO (2014), refer to document titled 'Cone Penetration Test' presented in appendix titled 'Descriptions of Methods and Practices'
Set-up Stage:	Location as directed by client
Additional Measurements:	Not applicable
Test Stage:	No project-specific practice
Test Termination:	Refer to document titled 'Cone Penetration Test' presented in Appendix C
Drill-Out:	Not applicable
Test Site Restoration:	<ul style="list-style-type: none"> ■ No backfill of test hole ■ Local seabed disturbance ■ Possibility of local seafloor depression(s)

CPT Apparatus

Thrust Machine:	SEACALF® MkV Constant Drive System with nominal 200 kN thrust capacity and with > 50 m continuous push/retraction capacity
Mounting of Thrust Machine	SEACALF® unit ballasted to maximum 260 kN underwater weight, upward heave compensation of 20 kN to 30 kN, 3 m by 3 m in plan with 8.7 m ² for seafloor support
Reaction Equipment:	Weight of thrust machine, equivalent to a maximum of 260 kN underwater weight
Push Rod:	38 mm push rod outer diameter
Push Rod Casing:	To a maximum of 0.5 m below seafloor
Friction Reducer:	Applicable
Penetrometer Type:	<ul style="list-style-type: none"> ■ Type CP15-CF150PB20SN2-P1E2M4-V2 piezo-cone penetrometer, 150 kN load sensors (200 kN for overloading), 20 MPa pressure sensor, HDPE filter in cylindrical extension above base of cone, 1500 mm² cone base area, 20 000 mm² sleeve area ■ Net area ratio for cone tip as per plate(s) titled 'Cone Penetration Test – Zero Drift'

Test Results

Data Processing and Management:	<ul style="list-style-type: none"> ■ Refer to document titled 'Cone Penetration Test' presented in Appendix C ■ Discovery GeoVisual software ■ Graphical scales selected to suit general presentation of data and requirements of standards, where practicable ■ No display of data outside of chart limits, i.e. some values may not be shown
Data Format(s):	<ul style="list-style-type: none"> ■ PDF for viewing and printing (this primary document) ■ AGS 4.0 (AGS, 2011) digital tabular data (separate deliverables) ■ ASCII (ANSI, 2007) digital tabular data (separate deliverables)
Water Depth Reference:	As inferred from Conductivity Temperature Density (CTD) measurements at start of testing, reduced to LAT
Depth Reference Level:	Seafloor, particularly: <ul style="list-style-type: none"> ■ No evidence of extremely soft ground at seafloor ■ Base of seabed frame assumed level with seafloor at start of testing ■ Depth accuracy assessment of 'Non-Drilling – Favourable'; refer to document titled 'Positioning Survey and Depth Measurement' presented in Appendix C
Depth Correction for Penetrometer Inclination:	Applicable
Parameter Values for Data Processing:	<ul style="list-style-type: none"> ■ Refer to plate(s) titled 'Cone Penetration Test' showing soil behaviour type index, soil unit weight and supplementary normalised parameter values, where applicable ■ Soil unit weight assumed constant with depth at 20 kN/m³ ■ Hydrostatic pore pressure conditions with zero at seafloor and unit weight of (pore)water of 10 kN/m³

B.2.2 Comments on Results

Seafloor in situ testing was performed from MV Despina on 23 February 2021.

CPTs can show negative pore pressures upon penetration of dense to very dense and/or (silty) fine sands. Interpretation of the pore pressure profiles suggests that some of these occurrences led to a locally sluggish pore pressure response, particularly between 17 m BSF and 43 m BSF. This is not uncommon. Refer to the document titled 'Cone Penetration Test' in Appendix C for details, including effects on derived values such as corrected cone resistance q_t .

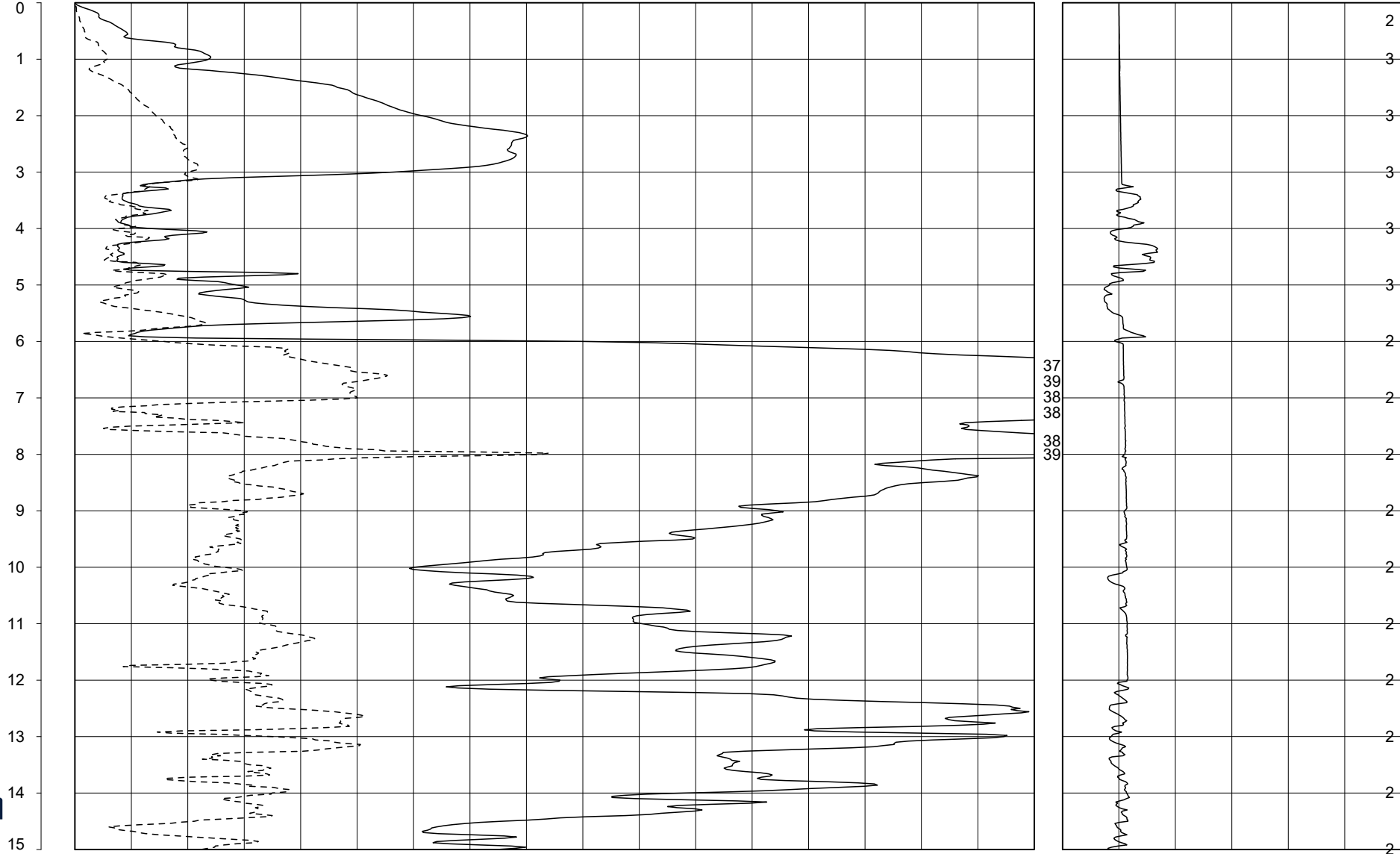
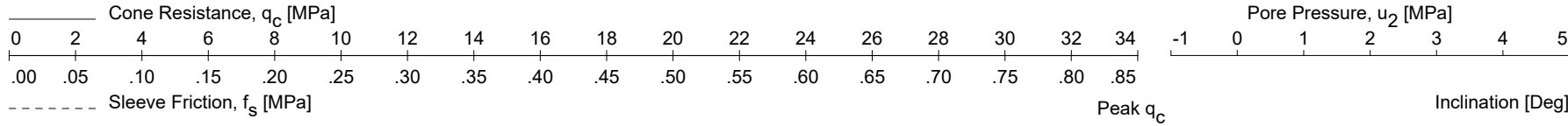
B.2.3 References

- AGS Association of Geotechnical and Geoenvironmental Specialists (2011). *Electronic Transfer of Geotechnical and Geoenvironmental Data*, AGS Edition 4.0.
- American National Standards Institute (2007). *American National Standard for Information Systems - Coded Character Sets – 7-Bit American National Standard Code for Information Interchange (7-Bit ASCII)*. (ANSI X3.4-1986 (R2007)).
<https://webstore.ansi.org/Standards/INCITS/ANSIX31986R1997>
- Computer Program Discovery Geovisual, Processing of CPT data
- International Organization for Standardization (2014). *Petroleum and natural gas industries – specific requirements for offshore structures – part 8: marine soil investigations* (ISO 19901-8:2014). <https://www.iso.org/standard/61145.html>.

Plate B.2-1

P904711/GA | 01

Depth Below Seafloor [m]

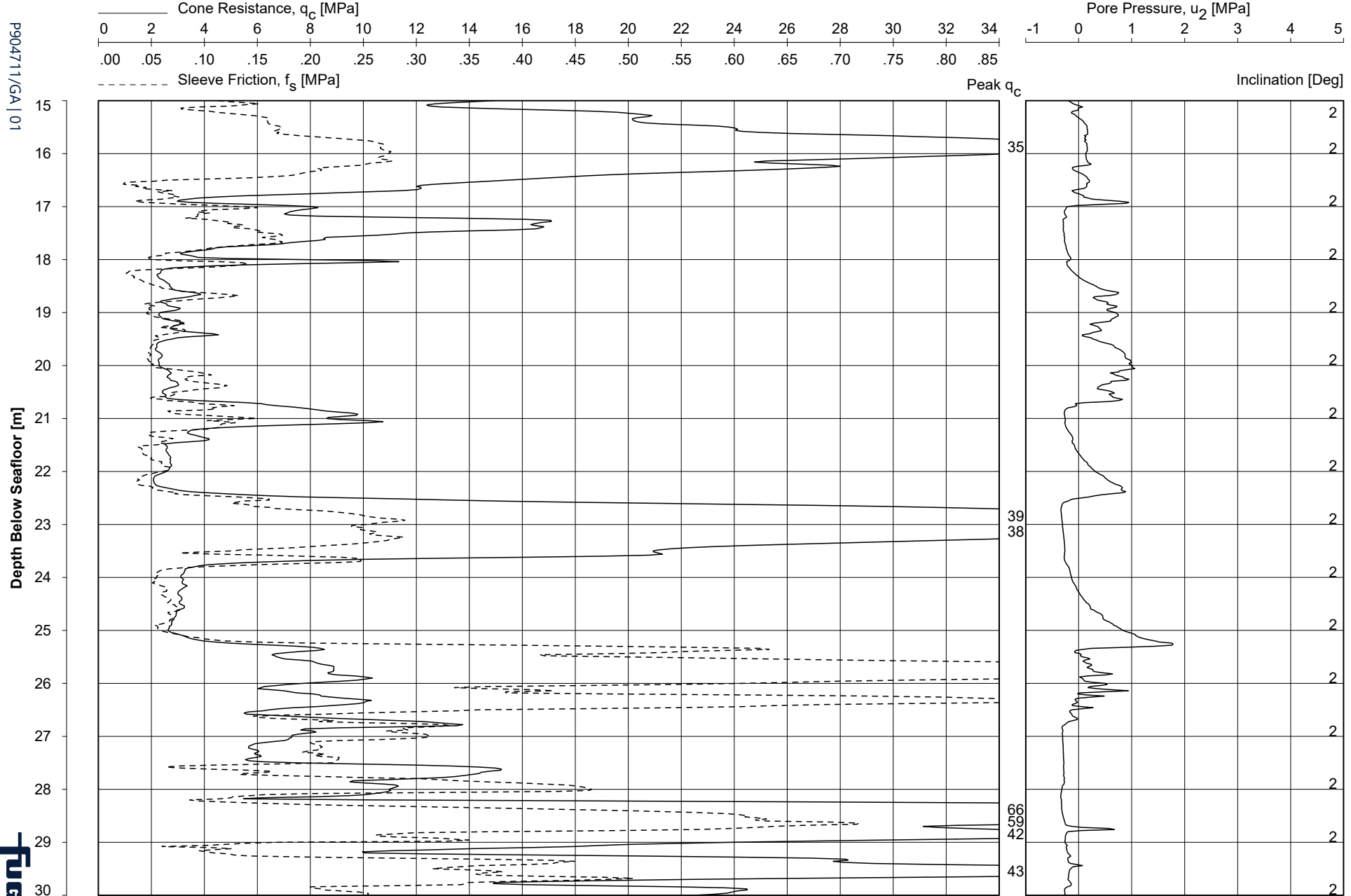


Date of Testing : 23-Feb-2021
 Water Depth [m LAT] : 31.8
 Coordinates [m] : E 540623 N 5828833

Probe Type : CP15-CF150PB20SN2
 Cone Base Area [mm²] : 1510

CONE PENETRATION TEST
 HKW119-PCPT





Date of Testing : 23-Feb-2021
 Water Depth [m LAT] : 31.8
 Coordinates [m] : E 540623 N 5828833

Probe Type : CP15-CF150PB20SN2
 Cone Base Area [mm²] : 1510

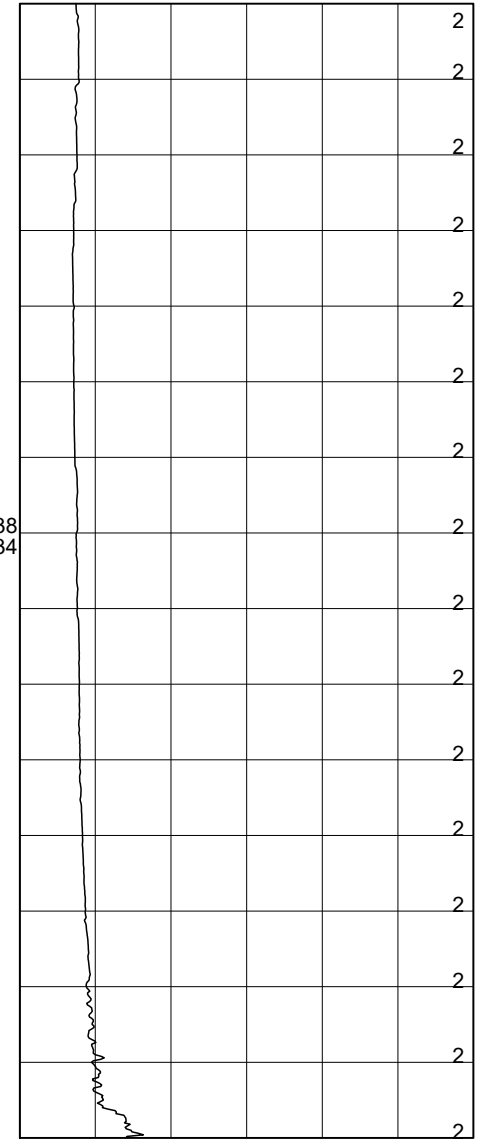
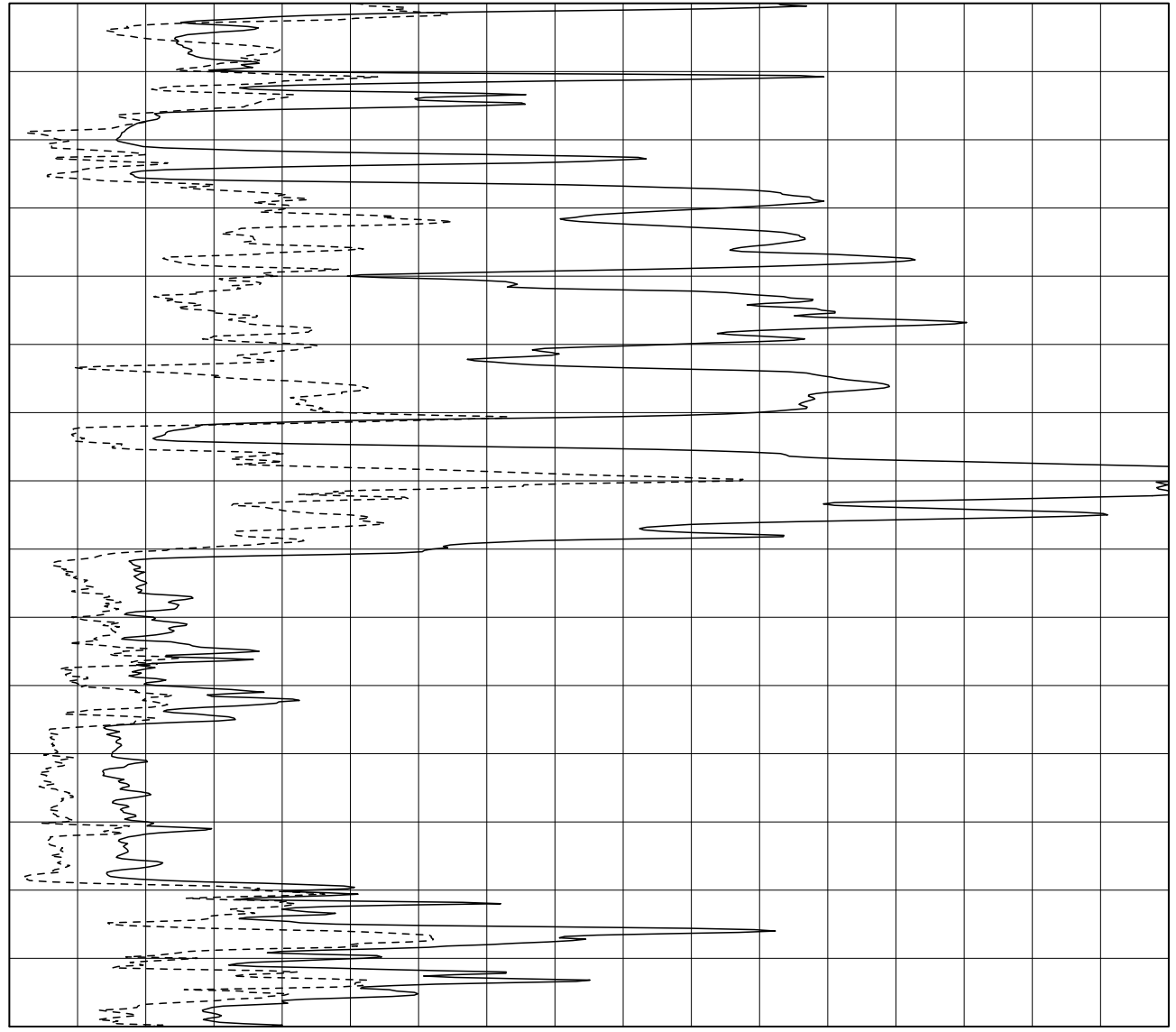
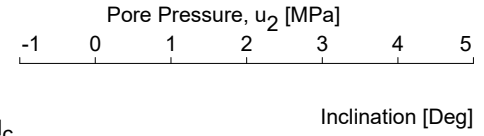
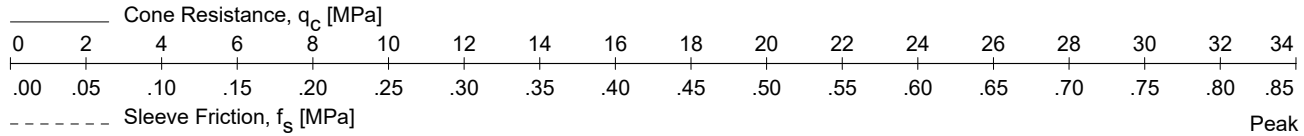
CONE PENETRATION TEST
 HKW119-PCPT



Plate B-2-3

P904711/GA | 01

Depth Below Seafloor [m]



Date of Testing : 23-Feb-2021
 Water Depth [m LAT] : 31.8
 Coordinates [m] : E 540623 N 5828833
 Probe Type : CP15-CF150PB20SN2
 Cone Base Area [mm²] : 1510

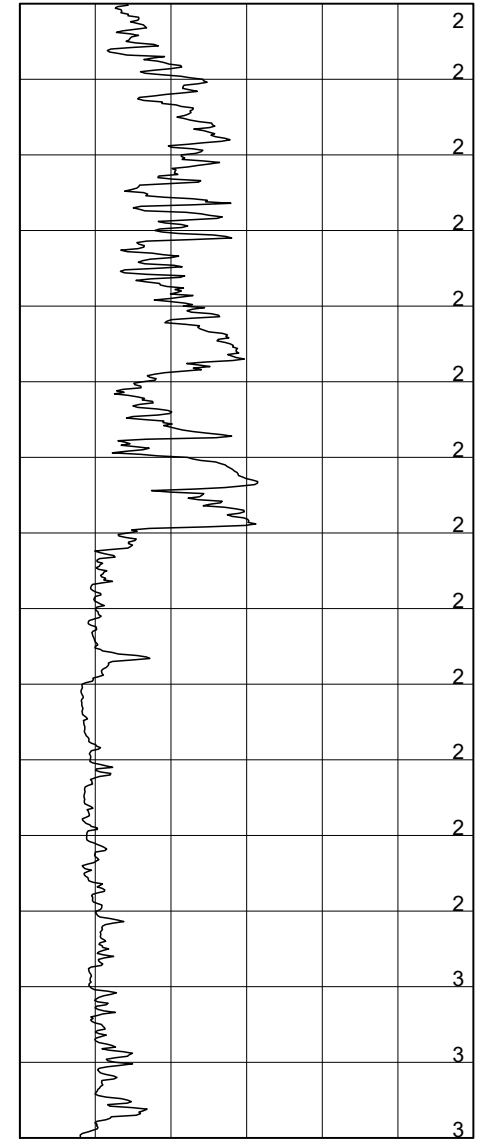
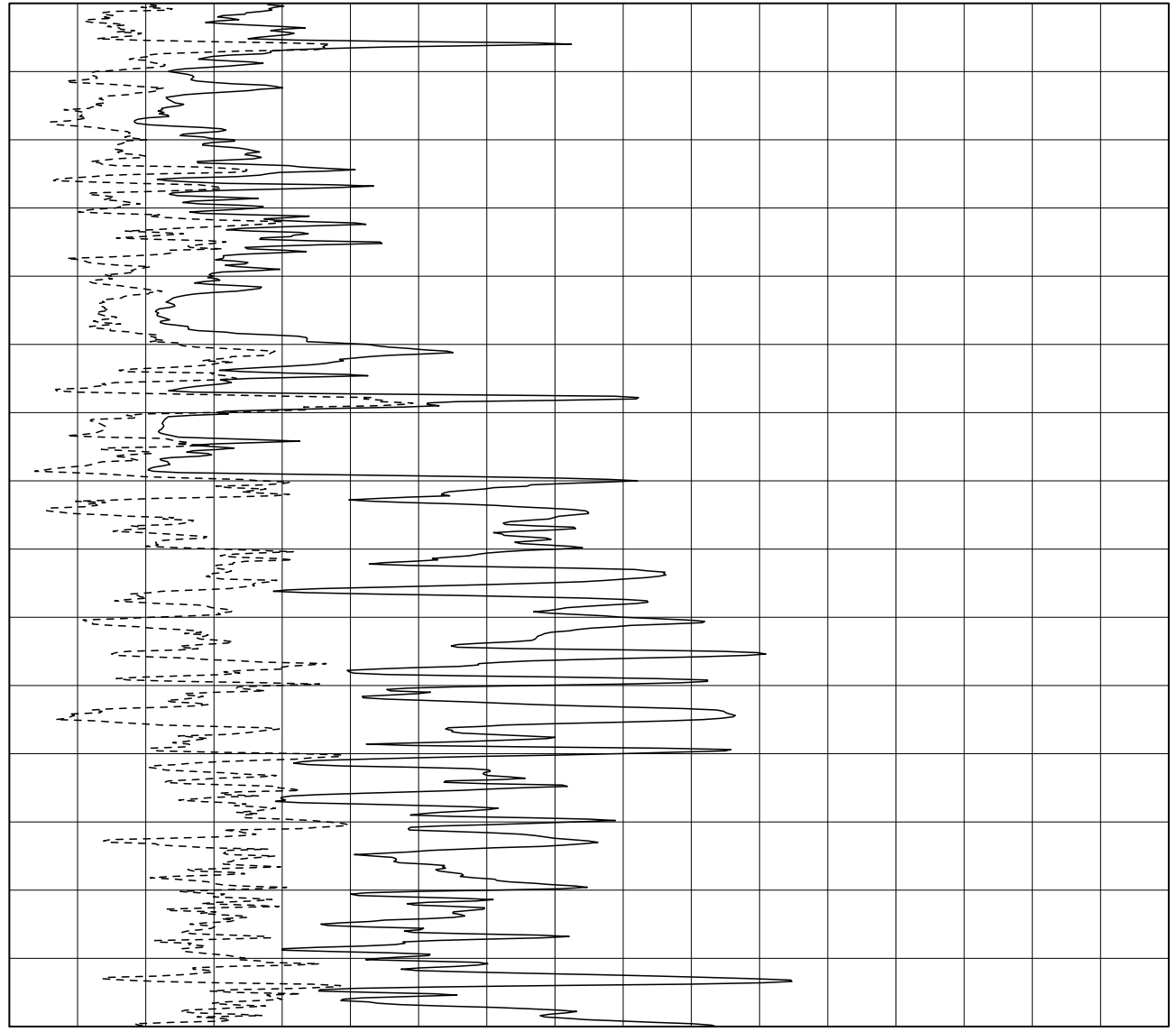
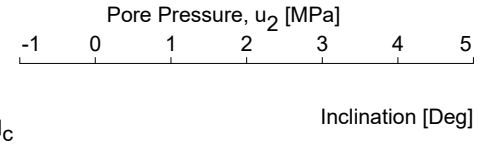
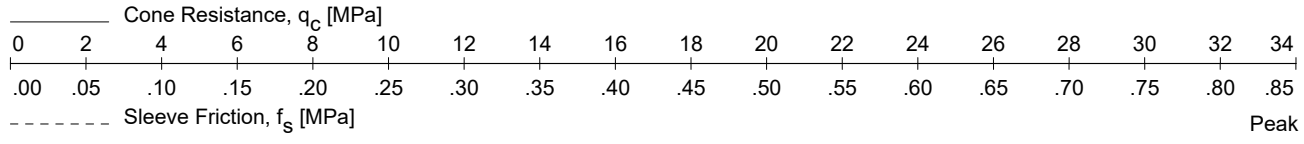
CONE PENETRATION TEST
HKW119-PCPT



Plate B.2-4

P904711/GA | 01

Depth Below Seafloor [m]



Date of Testing : 23-Feb-2021
 Water Depth [m LAT] : 31.8
 Coordinates [m] : E 540623 N 5828833

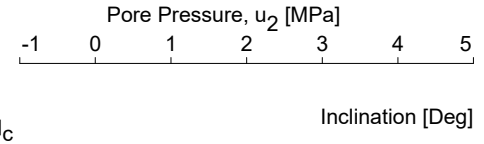
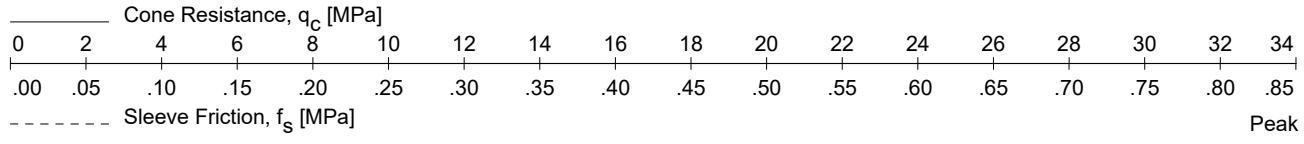
Probe Type : CP15-CF150PB20SN2
 Cone Base Area [mm²] : 1510

CONE PENETRATION TEST
 HKW119-PCPT

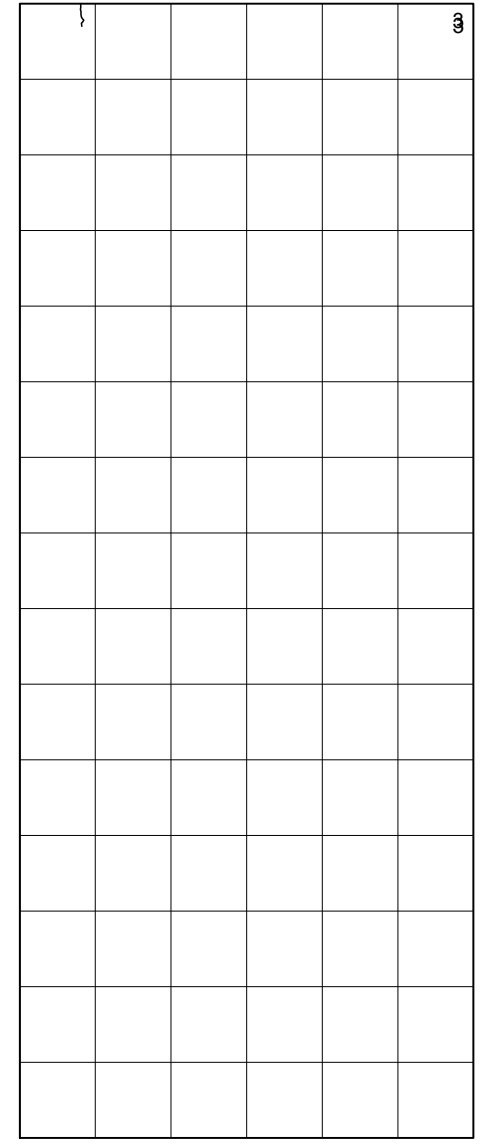
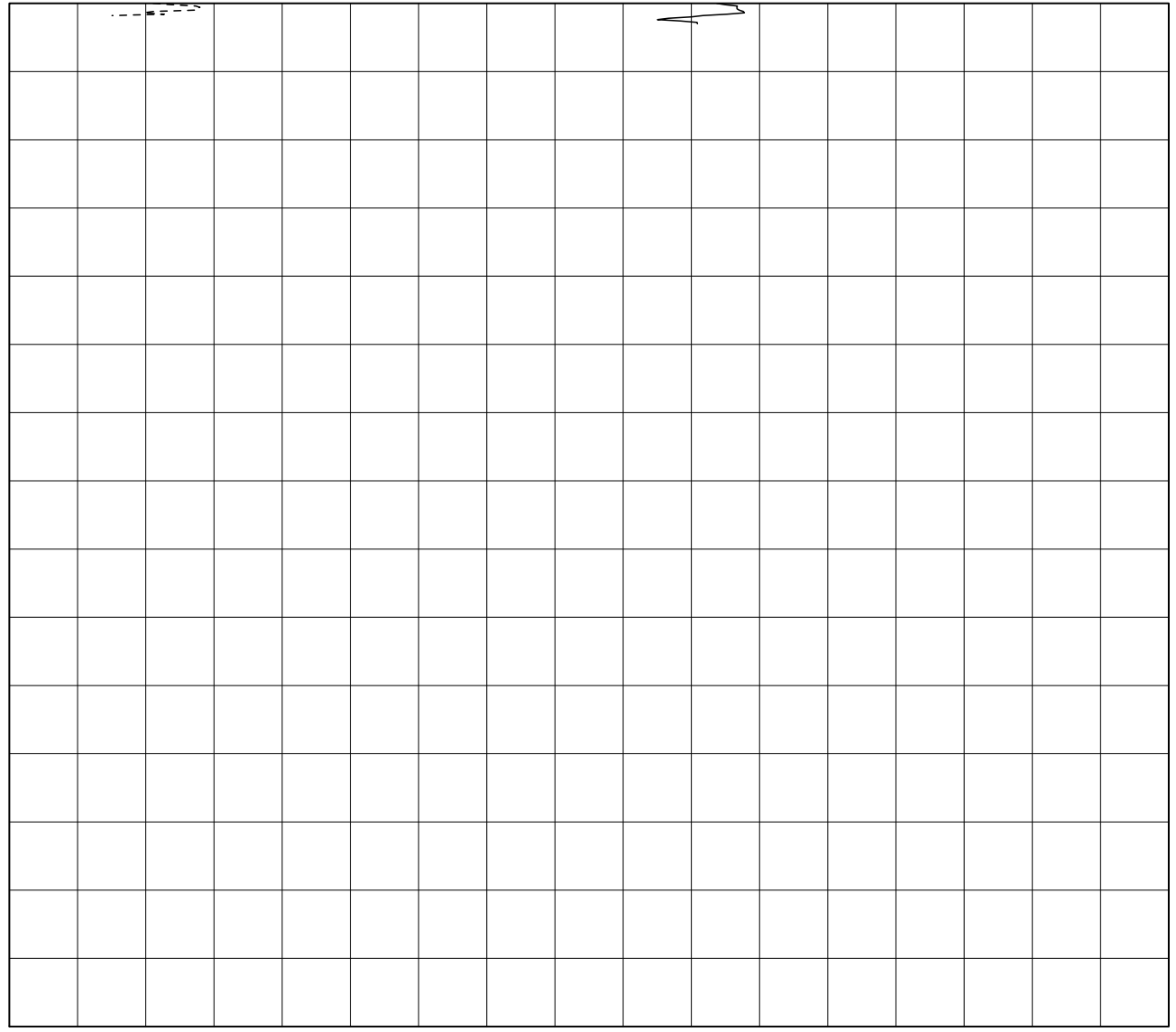


Plate B.2-5

P904711/GA | 01



Depth Below Seafloor [m]



Date of Testing : 23-Feb-2021
 Water Depth [m LAT] : 31.8
 Coordinates [m] : E 540623 N 5828833

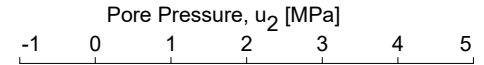
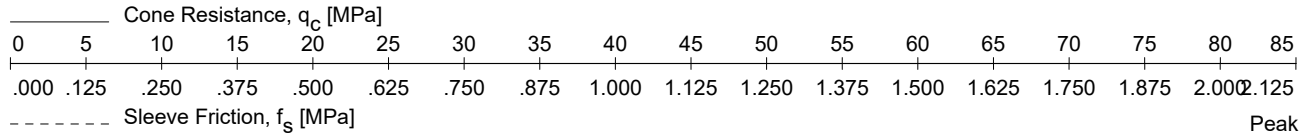
Probe Type : CP15-CF150PB20SN2
 Cone Base Area [mm²] : 1510

CONE PENETRATION TEST
 HKW119-PCPT

Plate B.2-6

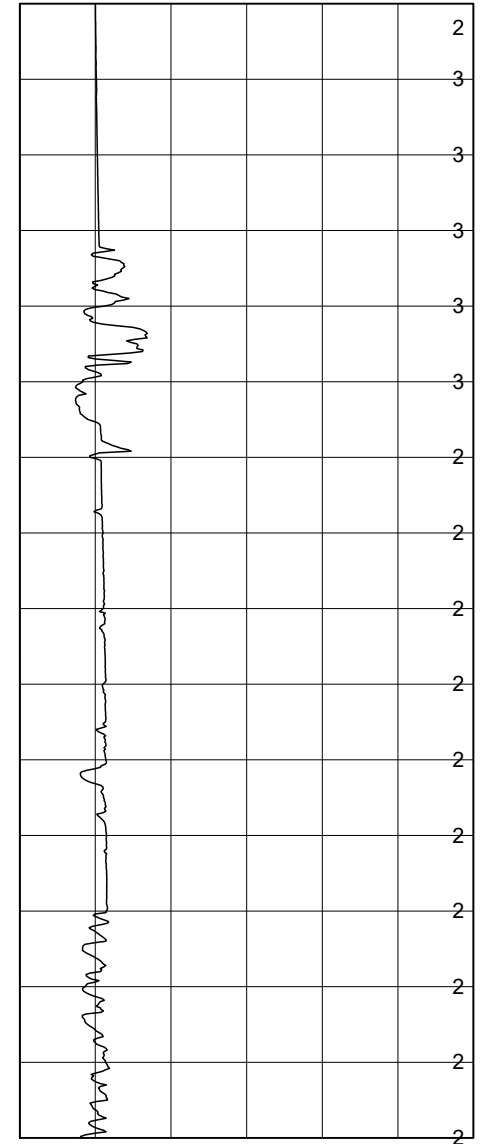
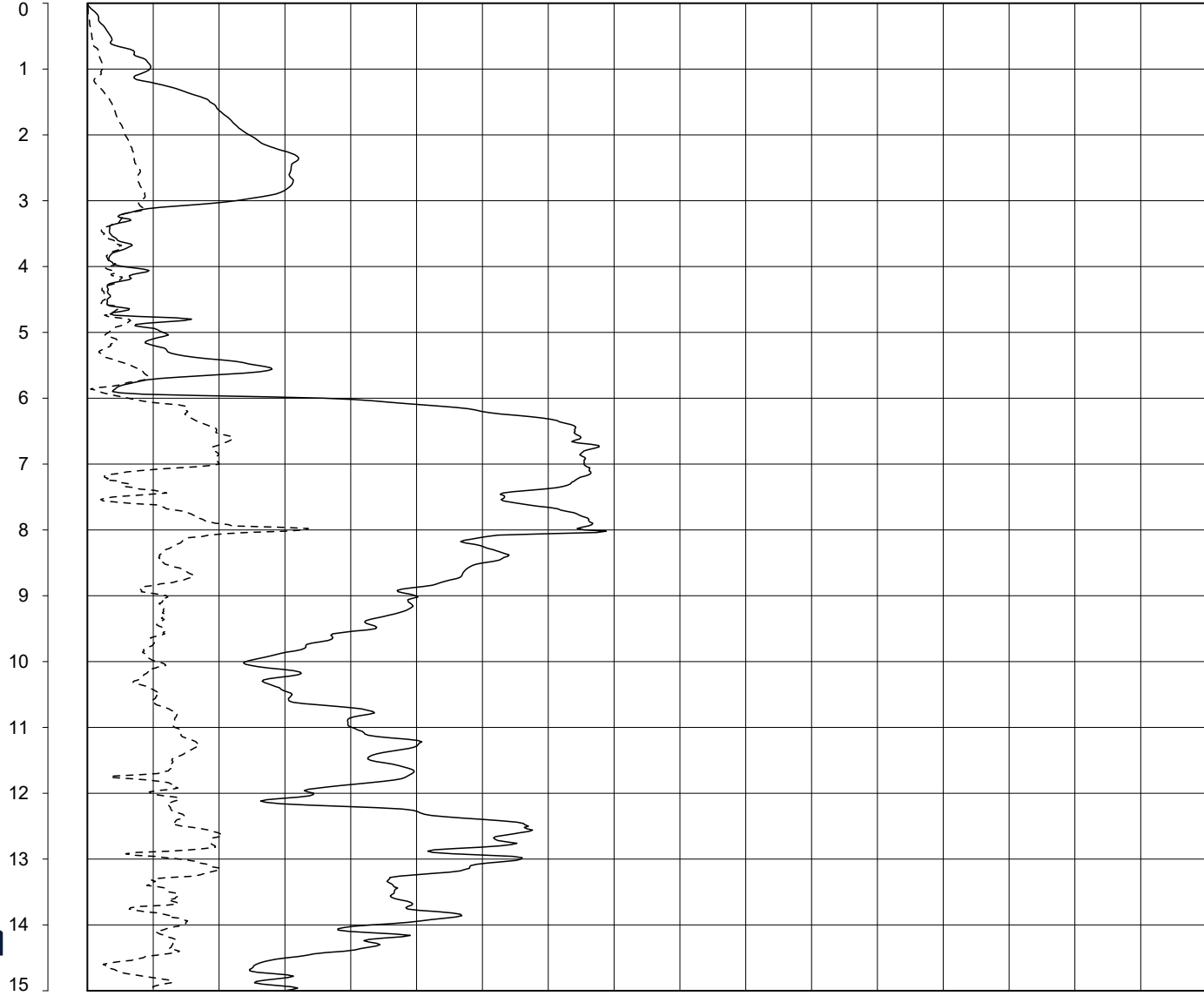
P904711/GA | 01

Depth Below Seafloor [m]



Peak q_c

Inclination [Deg]



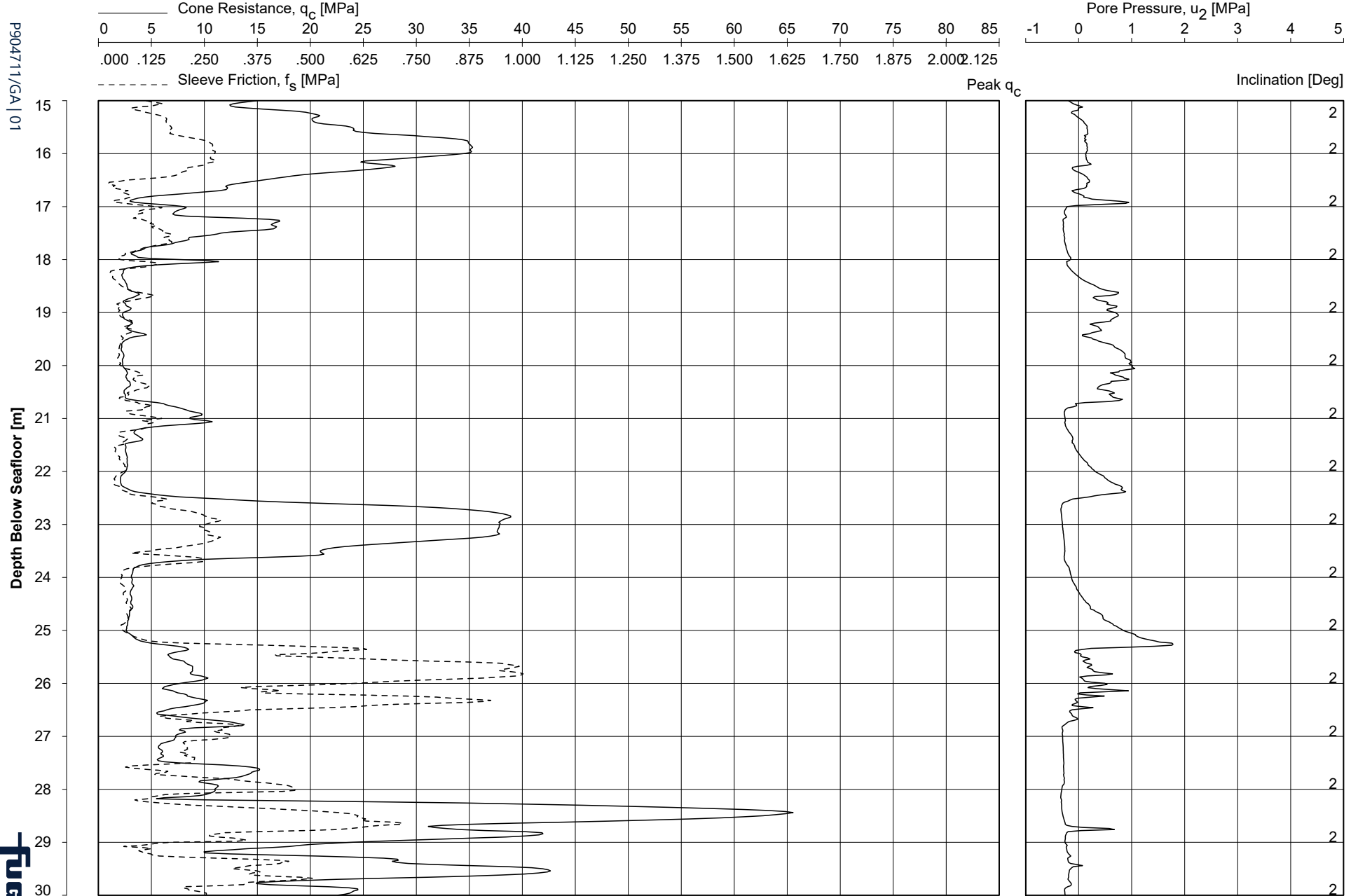
Date of Testing : 23-Feb-2021
 Water Depth [m LAT] : 31.8
 Coordinates [m] : E 540623 N 5828833

Probe Type : CP15-CF150PB20SN2
 Cone Base Area [mm²] : 1510

CONE PENETRATION TEST
 HKW119-PCPT



Plate B.2-7



Date of Testing : 23-Feb-2021
 Water Depth [m LAT] : 31.8
 Coordinates [m] : E 540623 N 5828833

Probe Type : CP15-CF150PB20SN2
 Cone Base Area [mm²] : 1510

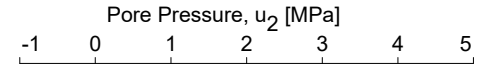
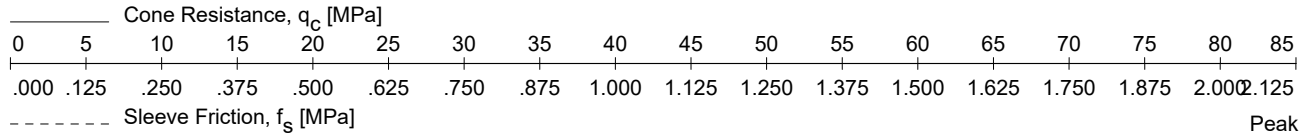
CONE PENETRATION TEST
 HKW119-PCPT



Plate B.2-8

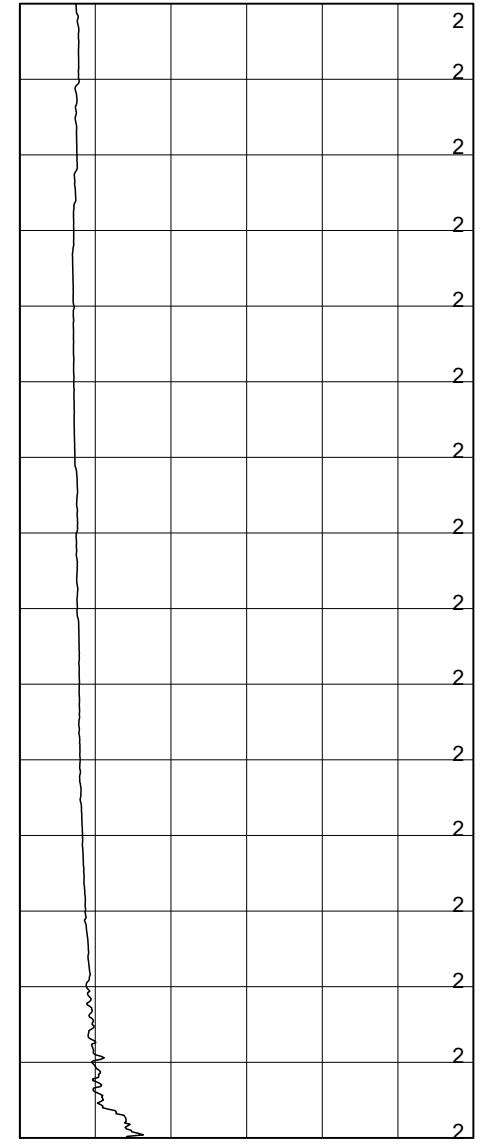
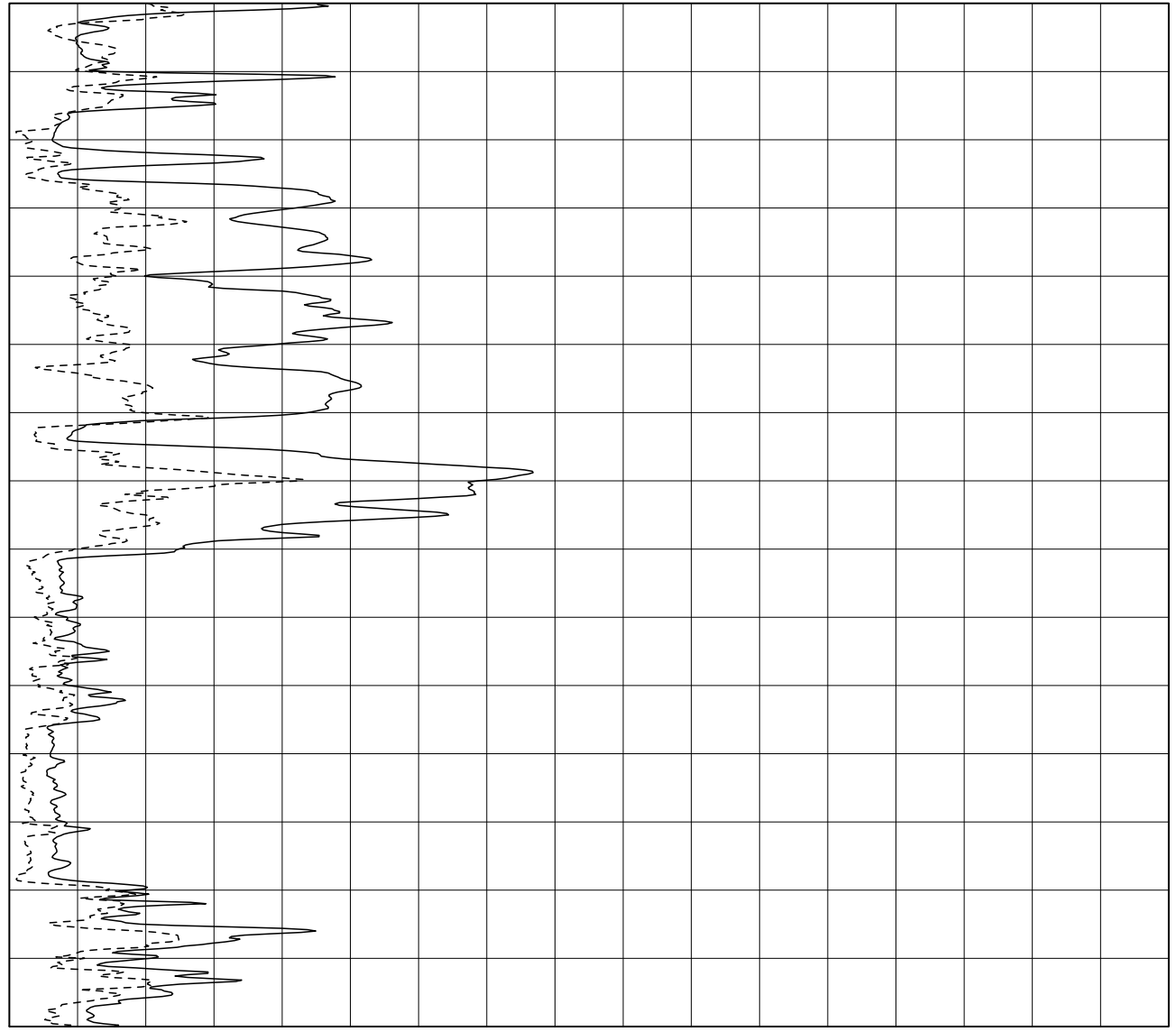
P90471/GA | 01

Depth Below Seafloor [m]



Peak q_c

Inclination [Deg]



Date of Testing : 23-Feb-2021
 Water Depth [m LAT] : 31.8
 Coordinates [m] : E 540623 N 5828833

Probe Type : CP15-CF150PB20SN2
 Cone Base Area [mm²] : 1510

CONE PENETRATION TEST
 HKW119-PCPT

Plate B.2-9

P904711/GA | 01

Depth Below Seafloor [m]

Cone Resistance, q_c [MPa]

0 5 10 15 20 25 30 35 40 45 50 55 60 65 70 75 80 85

.000 .125 .250 .375 .500 .625 .750 .875 1.000 1.125 1.250 1.375 1.500 1.625 1.750 1.875 2.000 2.125

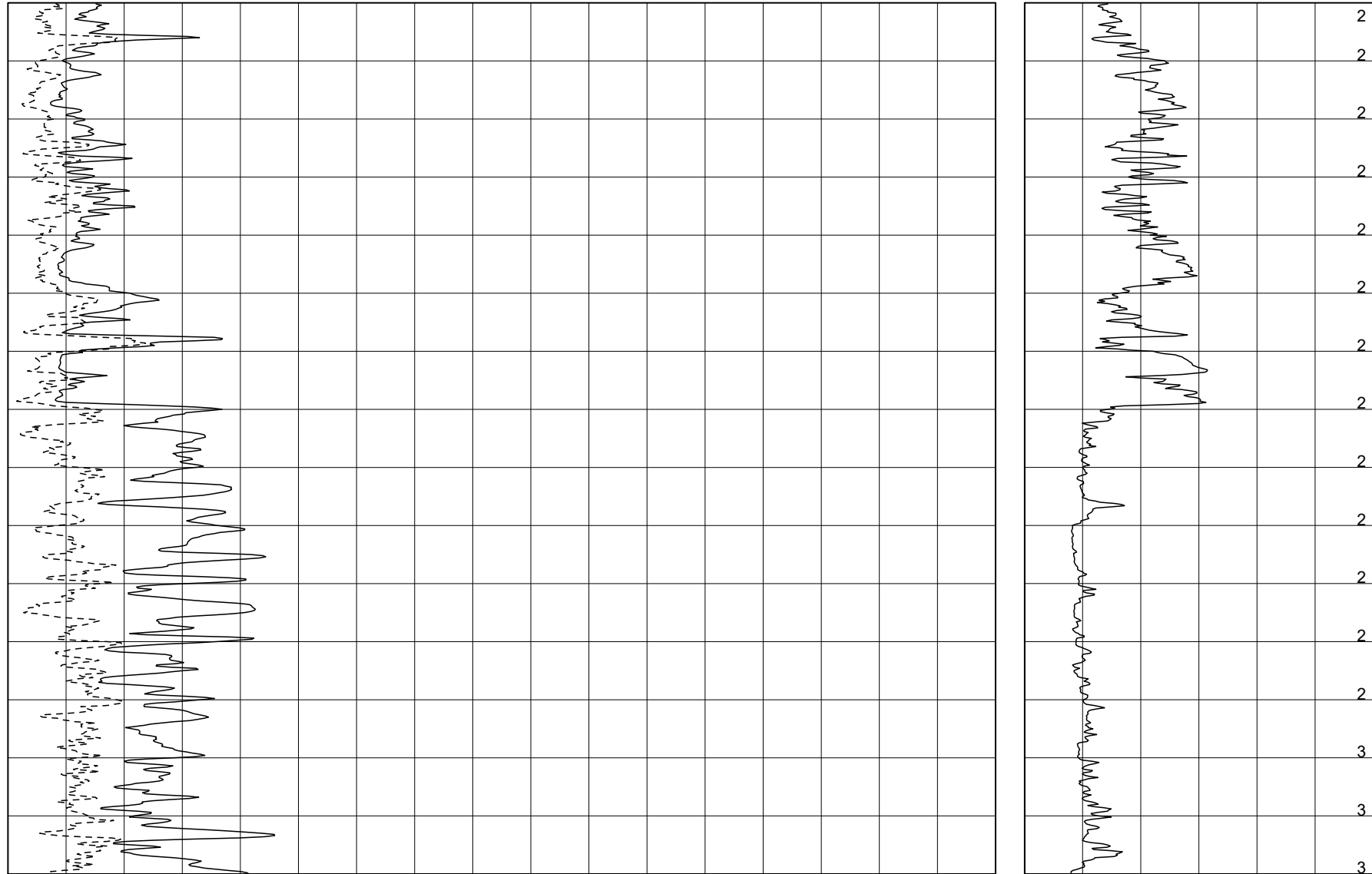
Sleeve Friction, f_s [MPa]

Pore Pressure, u_2 [MPa]

-1 0 1 2 3 4 5

Peak q_c

Inclination [Deg]



Date of Testing : 23-Feb-2021

Water Depth [m LAT] : 31.8

Coordinates [m] : E 540623 N 5828833

Probe Type : CP15-CF150PB20SN2

Cone Base Area [mm²] : 1510

CONE PENETRATION TEST

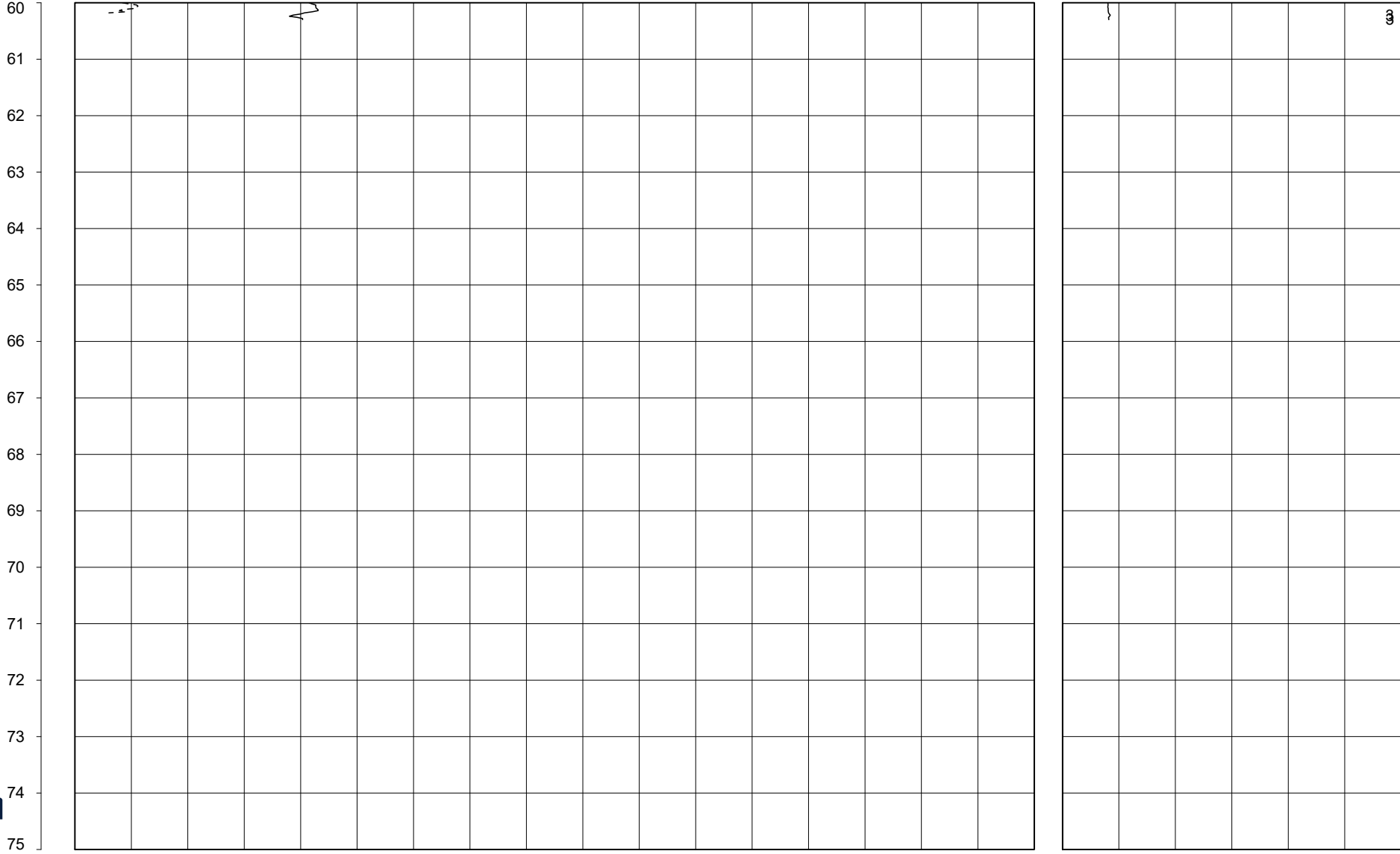
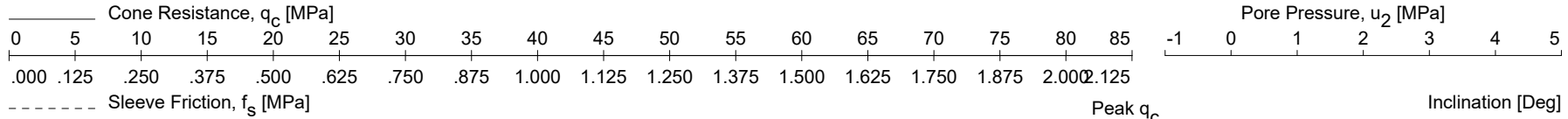
HKW119-PCPT



Plate B.2-10

P90471/GA | 01

Depth Below Seafloor [m]



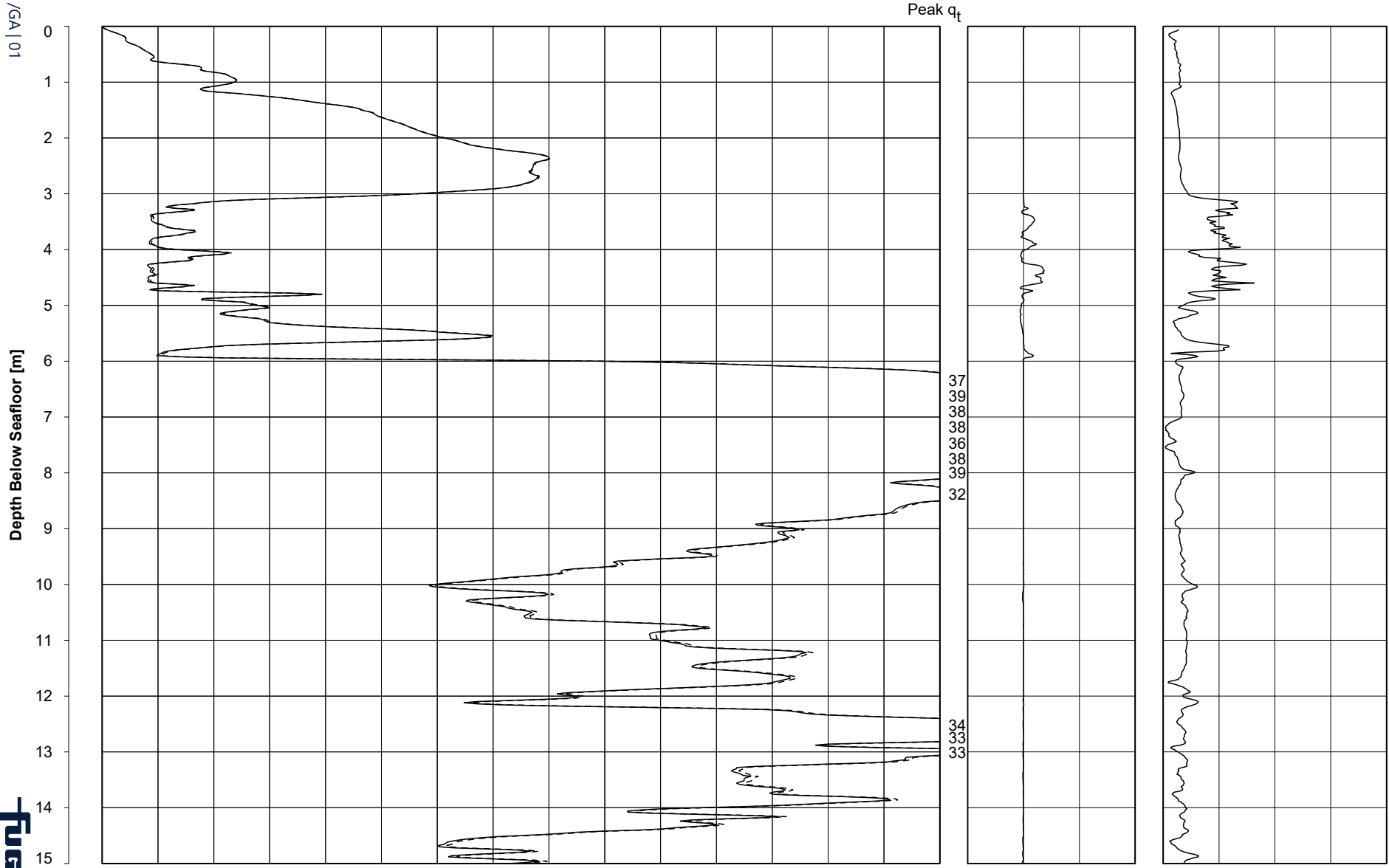
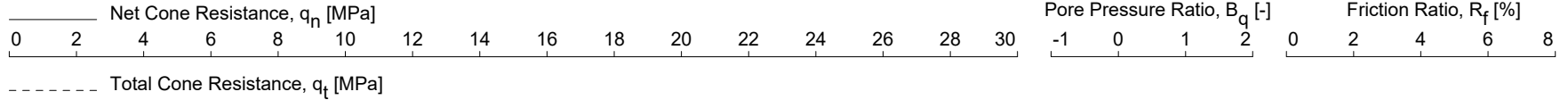
Date of Testing : 23-Feb-2021
 Water Depth [m LAT] : 31.8
 Coordinates [m] : E 540623 N 5828833

Probe Type : CP15-CF150PB20SN2
 Cone Base Area [mm²] : 1510

CONE PENETRATION TEST
 HKW119-PCPT



P90471/GA | 01
 Plate B.2-11



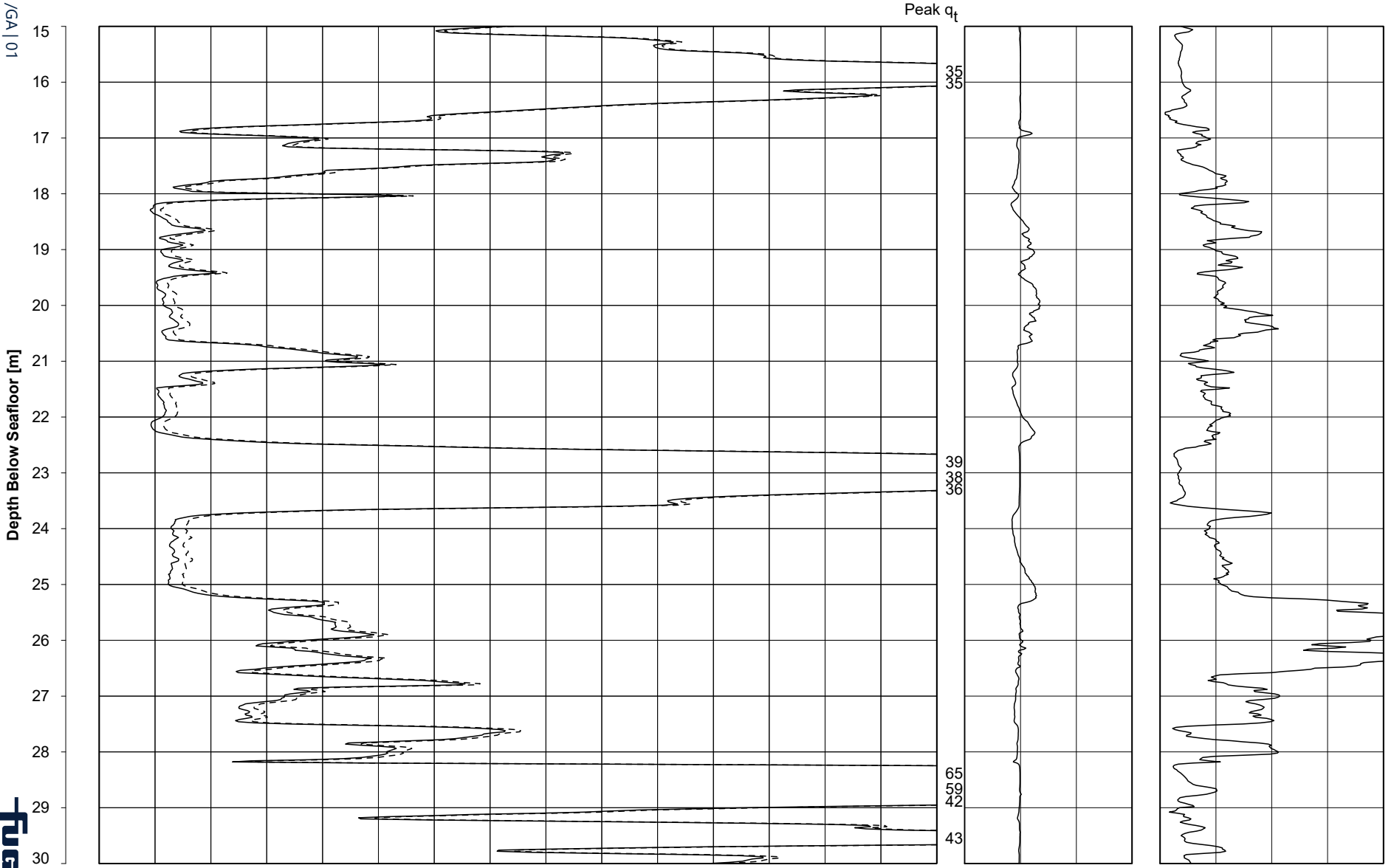
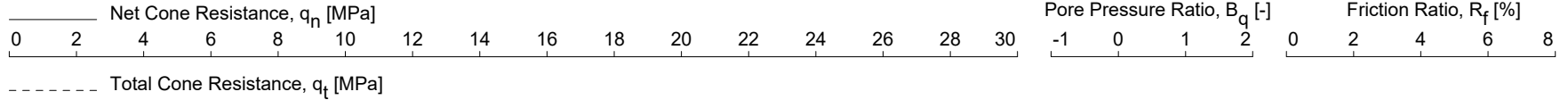
Date of Testing : 23-Feb-2021 Probe Type : CP15-CF150PB20SN2
 Water Depth [m LAT] : 31.8 Cone Base Area [mm²] : 1510
 Coordinates [m] : E 540623 N 5828833

CONE PENETRATION TEST
 HKW119-PCPT



Plate B.2-12

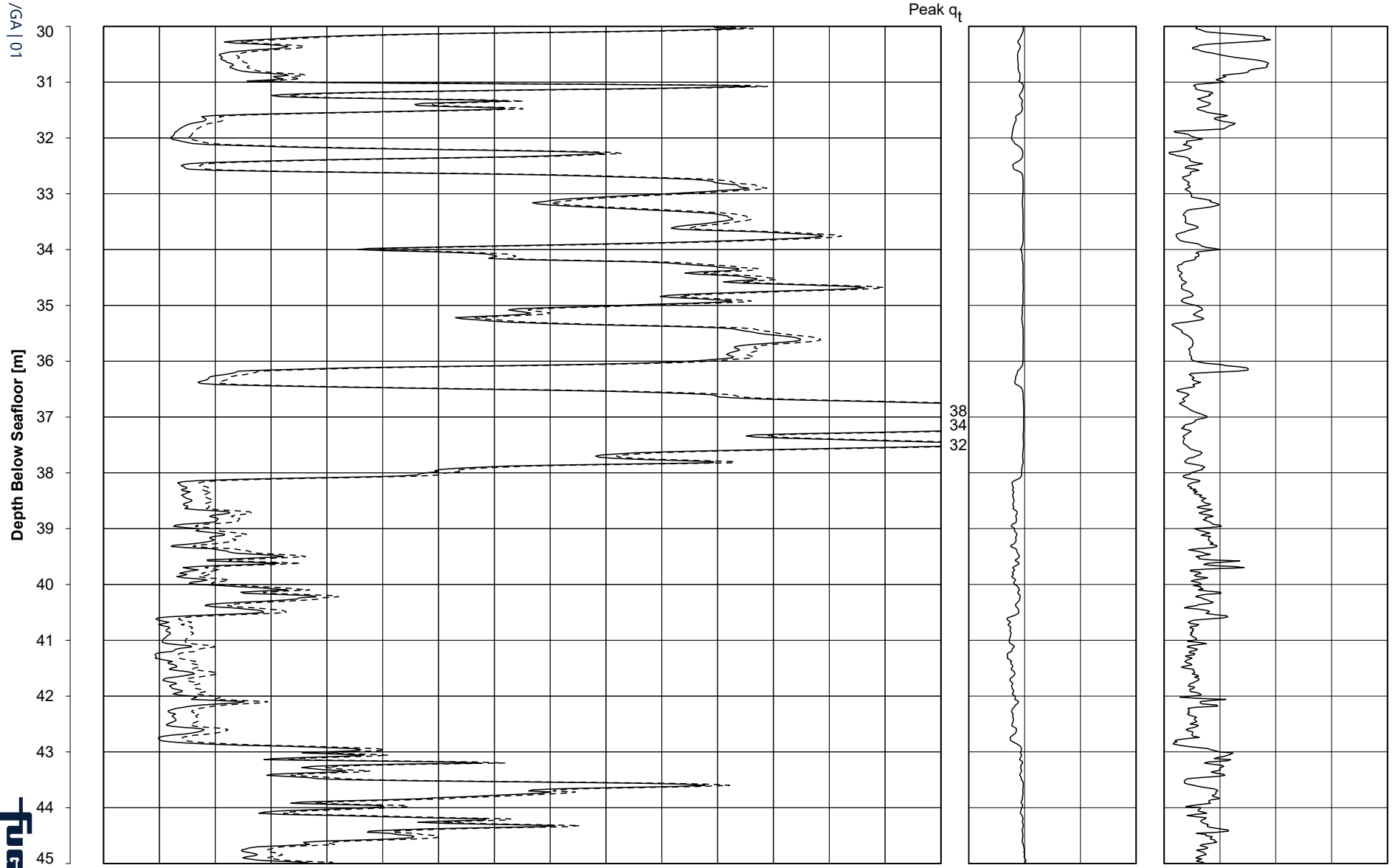
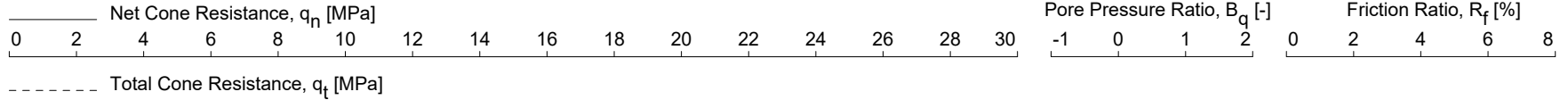
P90471/GA | 01



Date of Testing : 23-Feb-2021
 Water Depth [m LAT] : 31.8
 Coordinates [m] : E 540623 N 5828833
 Probe Type : CP15-CF150PB20SN2
 Cone Base Area [mm²] : 1510

CONE PENETRATION TEST
HKW119-PCPT

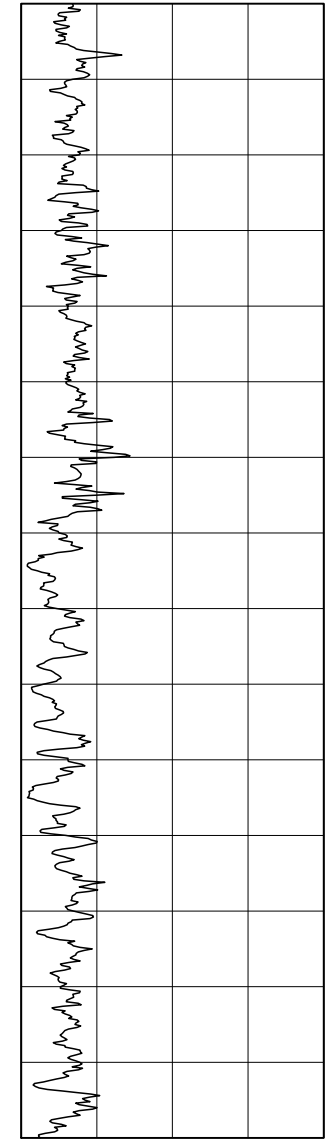
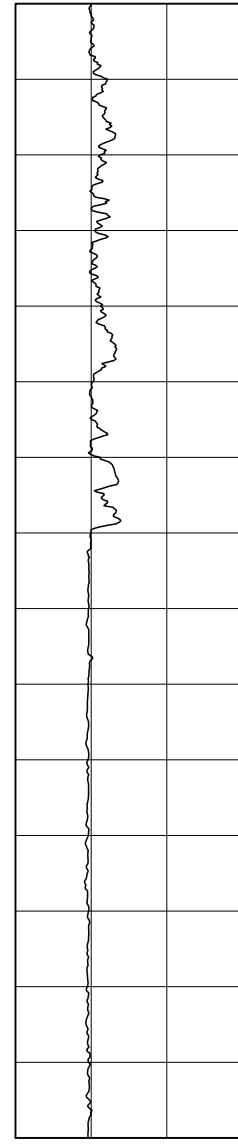
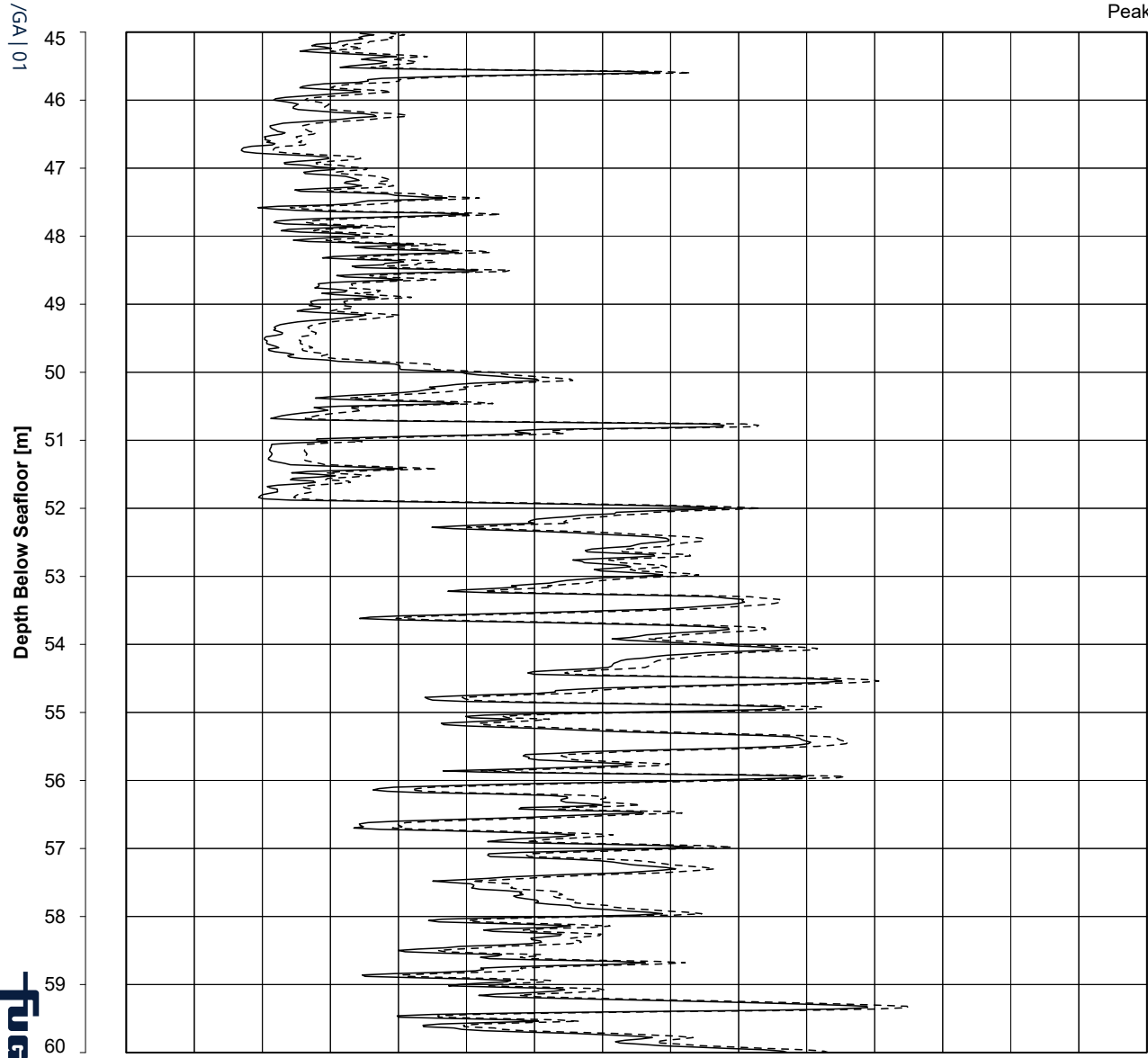
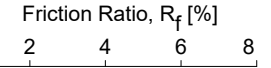
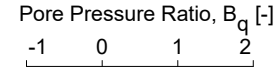
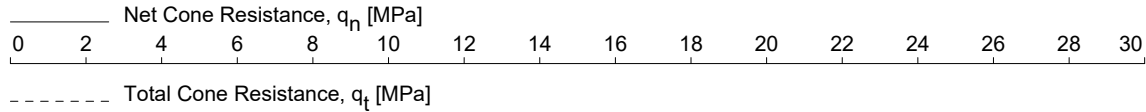




Date of Testing : 23-Feb-2021
 Water Depth [m LAT] : 31.8
 Coordinates [m] : E 540623 N 5828833
 Probe Type : CP15-CF150PB20SN2
 Cone Base Area [mm²] : 1510

CONE PENETRATION TEST
 HKW119-PCPT





Date of Testing : 23-Feb-2021
 Water Depth [m LAT] : 31.8
 Coordinates [m] : E 540623 N 5828833

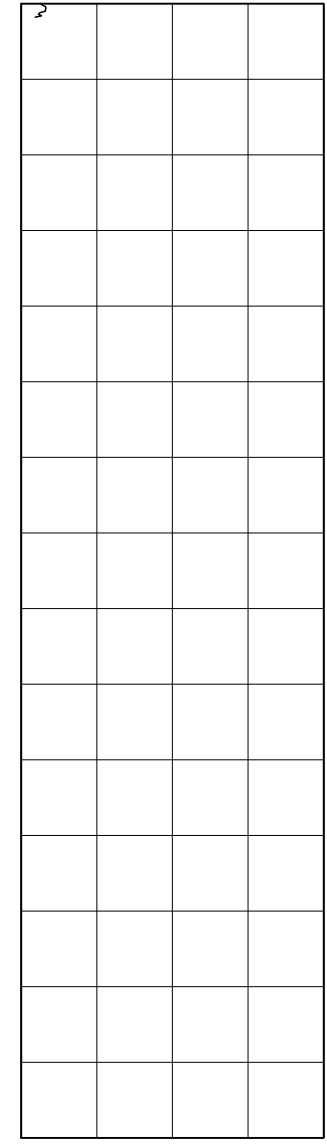
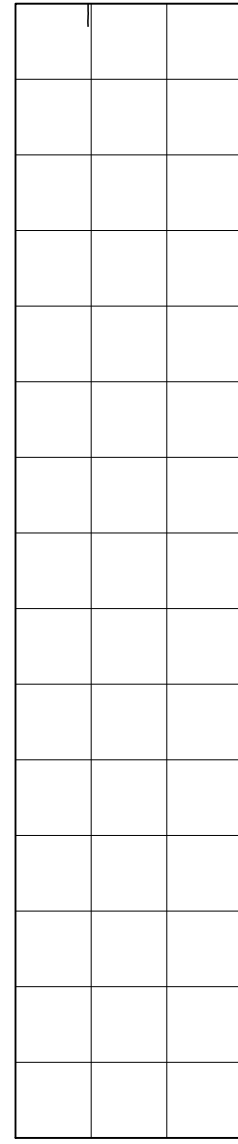
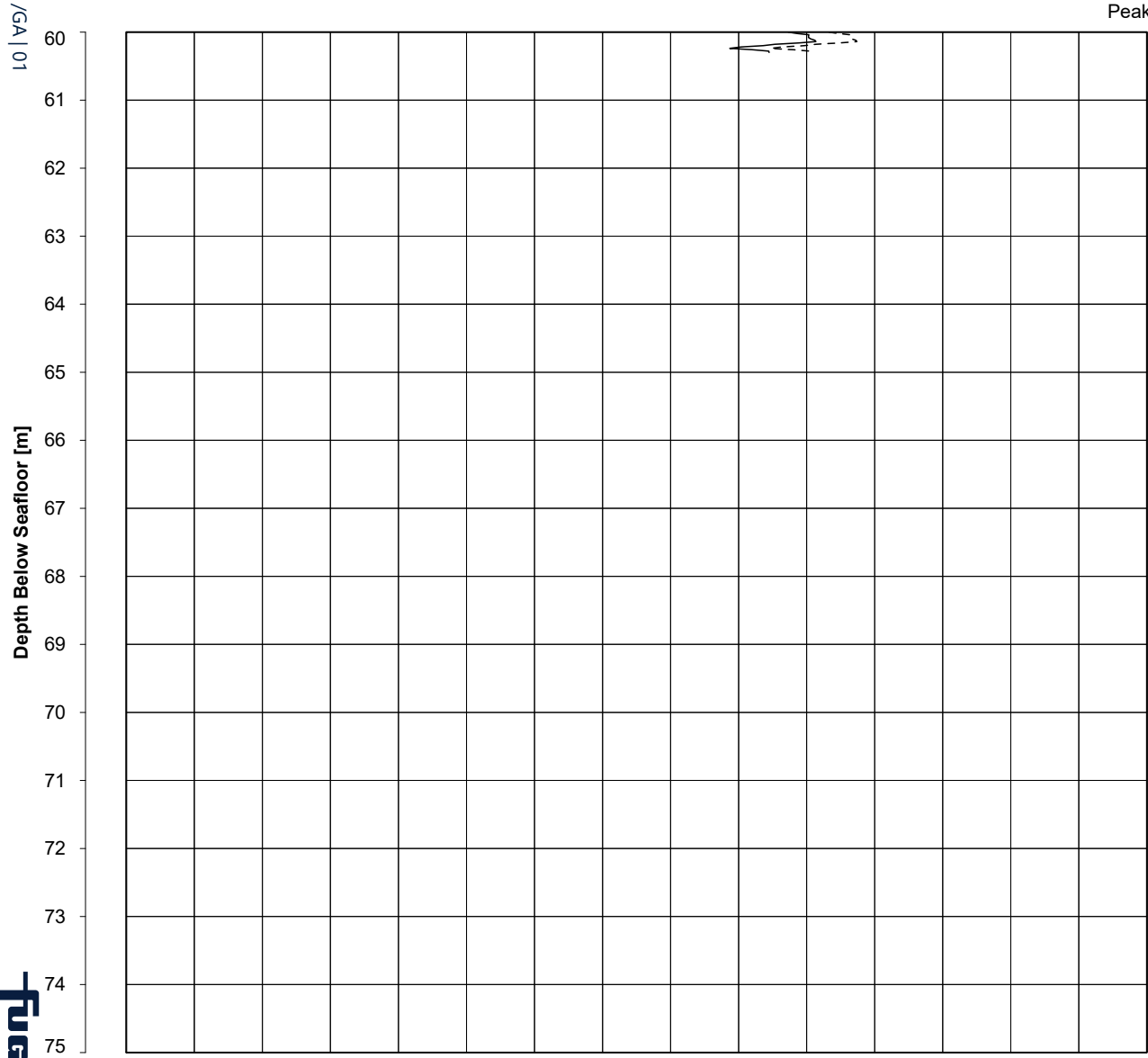
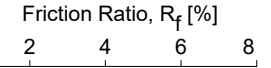
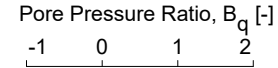
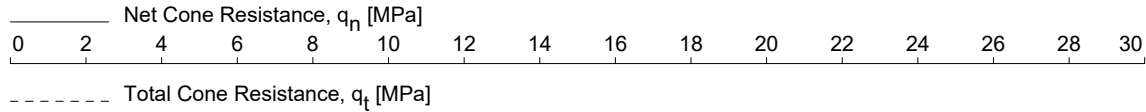
Probe Type : CP15-CF150PB20SN2
 Cone Base Area [mm²] : 1510

CONE PENETRATION TEST
 HKW119-PCPT



Plate B.2-15

P90471/GA | 01



Date of Testing : 23-Feb-2021
 Water Depth [m LAT] : 31.8
 Coordinates [m] : E 540623 N 5828833

Probe Type : CP15-CF150PB20SN2
 Cone Base Area [mm²] : 1510

CONE PENETRATION TEST
 HKW119-PCPT

Net Cone Resistance, q_n [MPa]

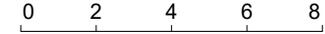


Total Cone Resistance, q_t [MPa]

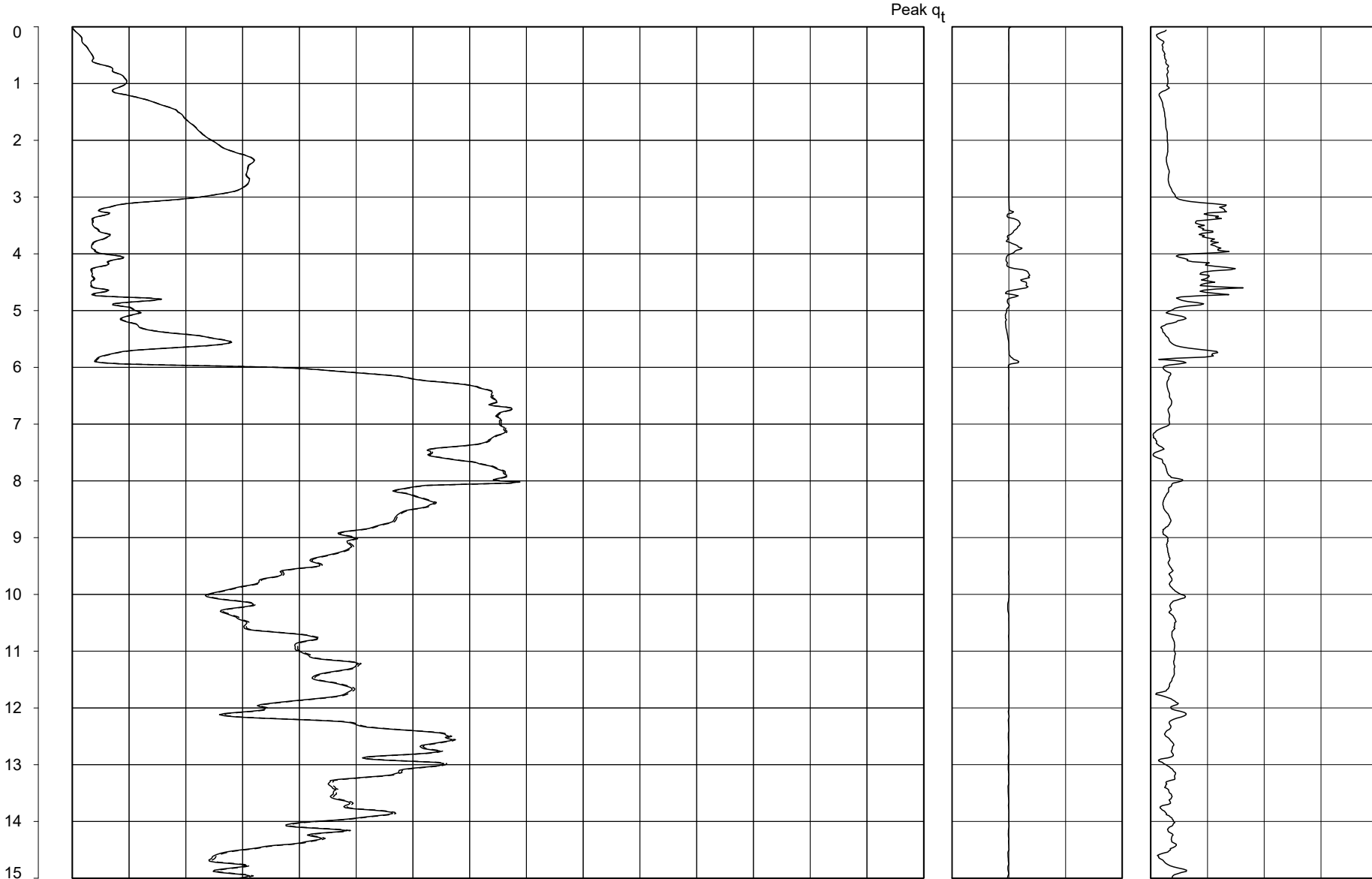
Pore Pressure Ratio, B_q [-]



Friction Ratio, R_f [%]



Depth Below Seafloor [m]



Date of Testing : 23-Feb-2021

Water Depth [m LAT] : 31.8

Coordinates [m] : E 540623 N 5828833

Probe Type : CP15-CF150PB20SN2

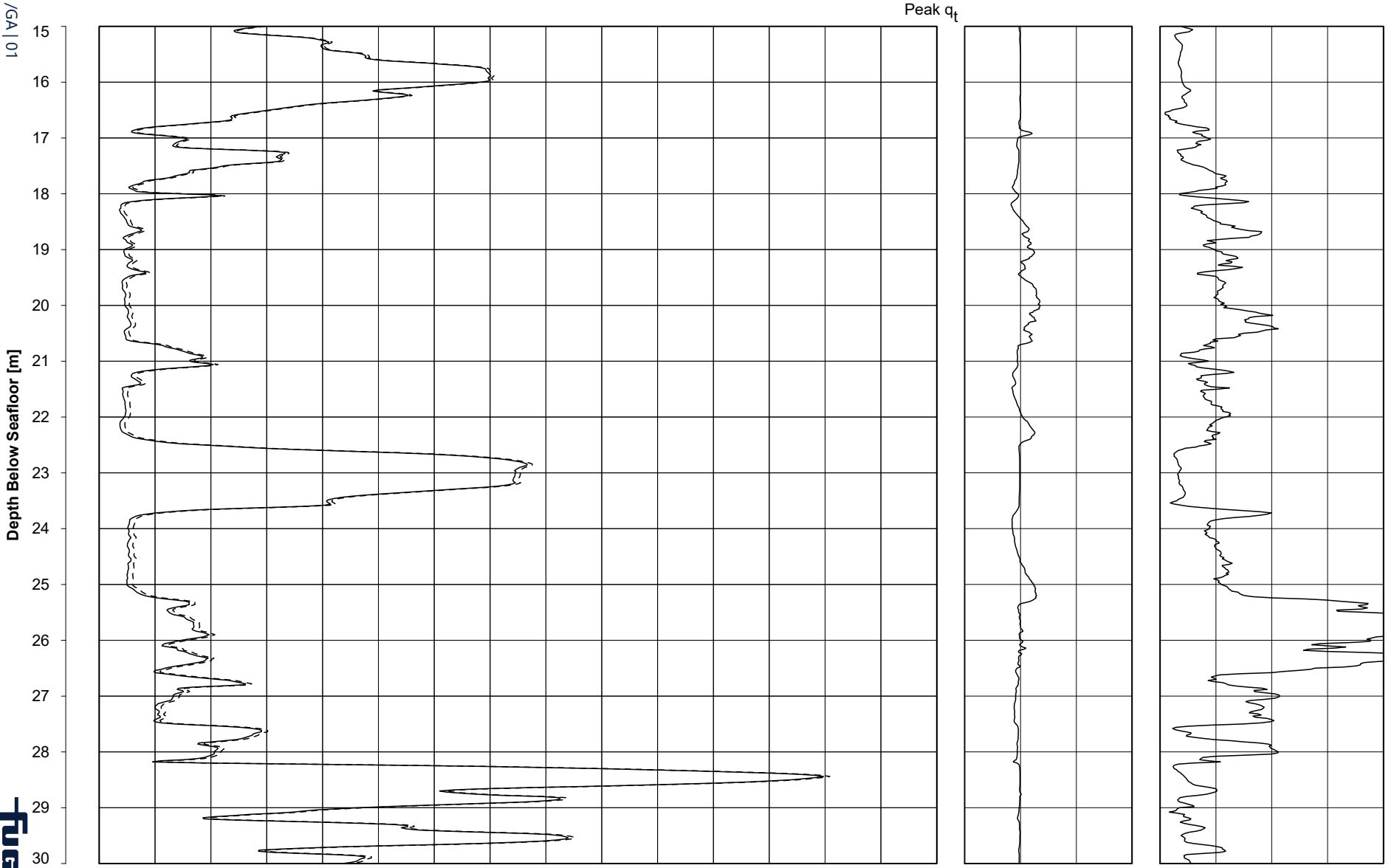
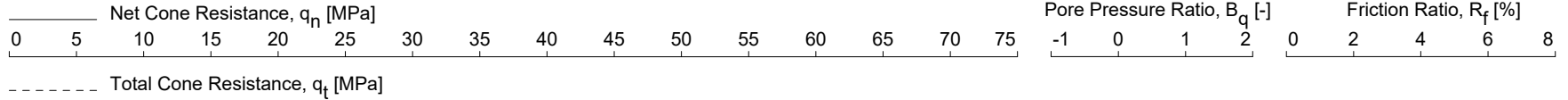
Cone Base Area [mm²] : 1510

CONE PENETRATION TEST

HKW119-PCPT

Plate B.2-17

P90471/GA | 01



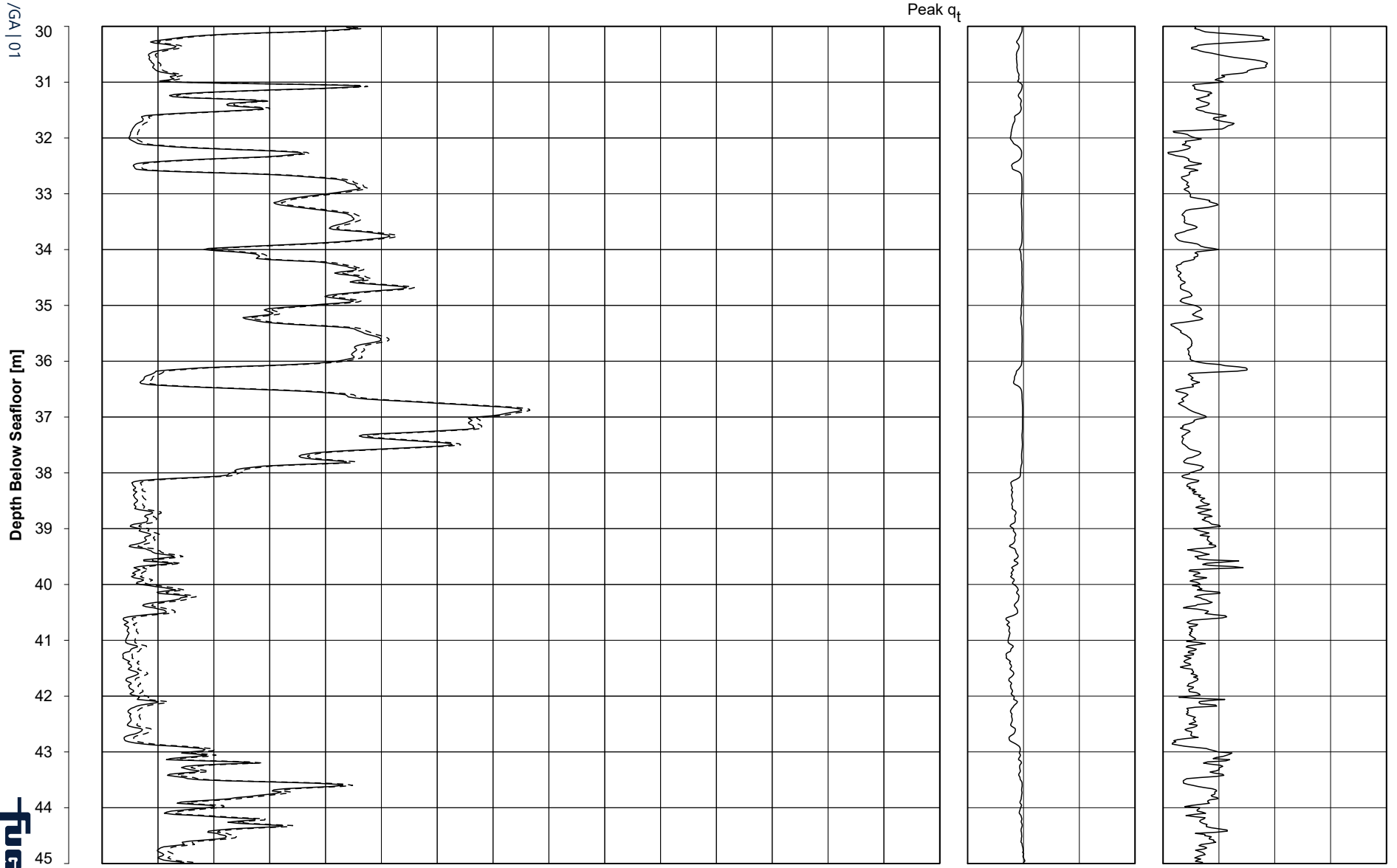
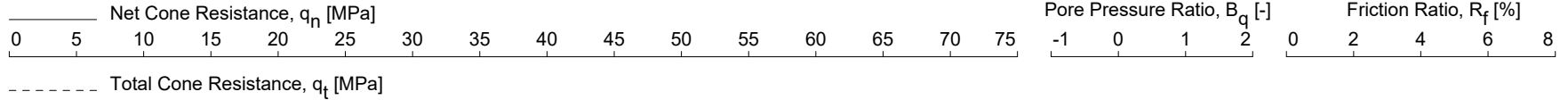
Date of Testing	: 23-Feb-2021	Probe Type	: CP15-CF150PB20SN2
Water Depth [m LAT]	: 31.8	Cone Base Area [mm ²]	: 1510
Coordinates [m]	: E 540623 N 5828833		

CONE PENETRATION TEST
HKW119-PCPT



Plate B.2-18

P90471/GA | 01



Date of Testing : 23-Feb-2021
 Water Depth [m LAT] : 31.8
 Coordinates [m] : E 540623 N 5828833
 Probe Type : CP15-CF150PB20SN2
 Cone Base Area [mm²] : 1510

CONE PENETRATION TEST
HKW119-PCPT



Plate B.2-19

P904711/GA | 01

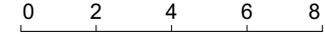
Net Cone Resistance, q_n [MPa]



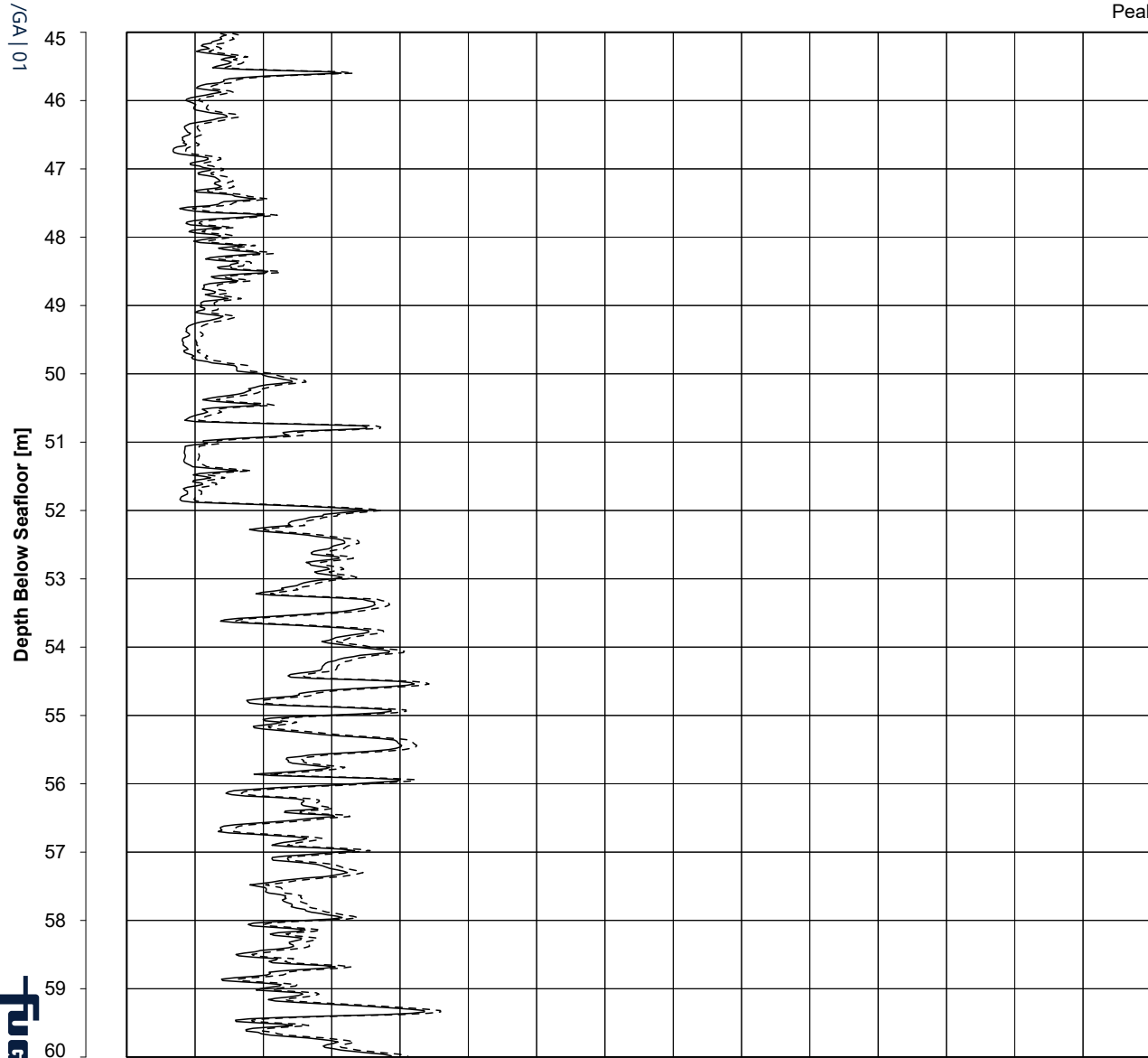
Pore Pressure Ratio, B_q [-]



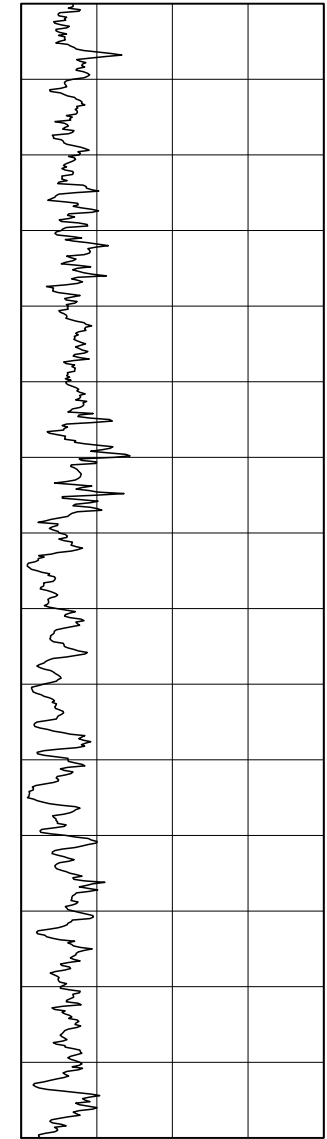
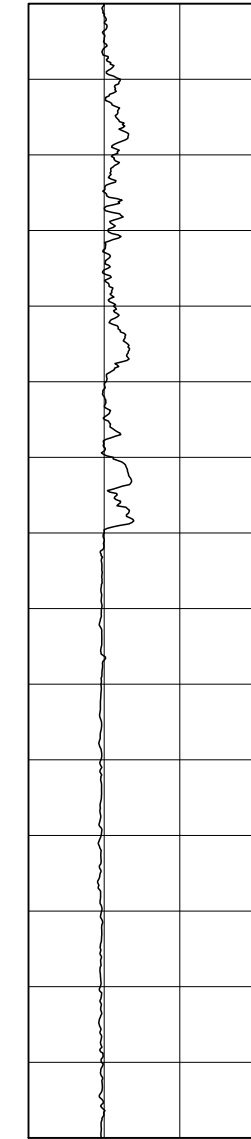
Friction Ratio, R_f [%]



----- Total Cone Resistance, q_t [MPa]



Peak q_t



Date of Testing : 23-Feb-2021

Water Depth [m LAT] : 31.8

Coordinates [m] : E 540623 N 5828833

Probe Type : CP15-CF150PB20SN2

Cone Base Area [mm²] : 1510

CONE PENETRATION TEST

HKW119-PCPT



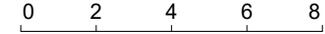
Net Cone Resistance, q_n [MPa]



Pore Pressure Ratio, B_q [-]



Friction Ratio, R_f [%]



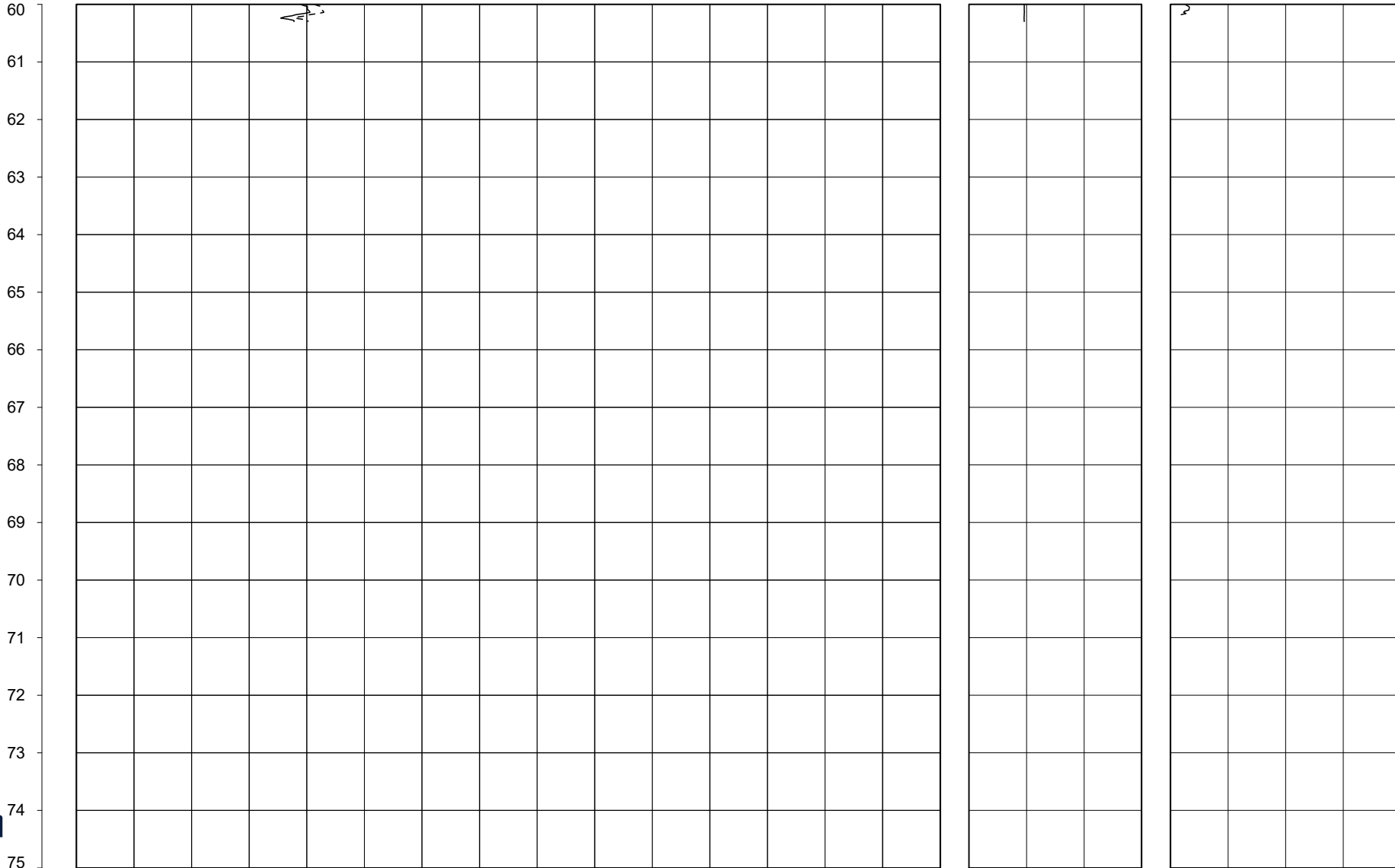
Total Cone Resistance, q_t [MPa]

Peak q_t

Plate B.2-20

P90471/GA | 01

Depth Below Seafloor [m]



Date of Testing : 23-Feb-2021

Water Depth [m LAT] : 31.8

Coordinates [m] : E 540623 N 5828833

Probe Type : CP15-CF150PB20SN2

Cone Base Area [mm²] : 1510

CONE PENETRATION TEST

HKW119-PCPT



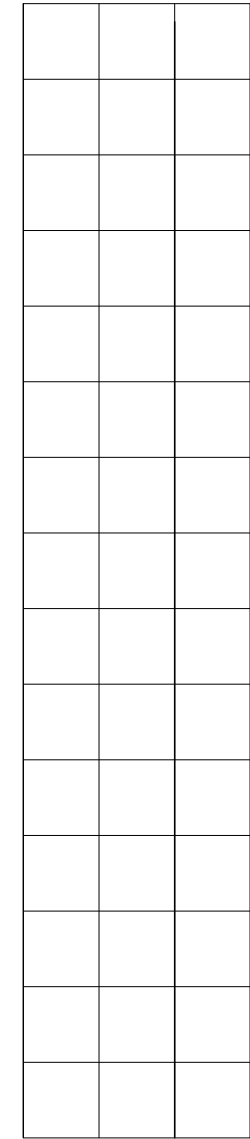
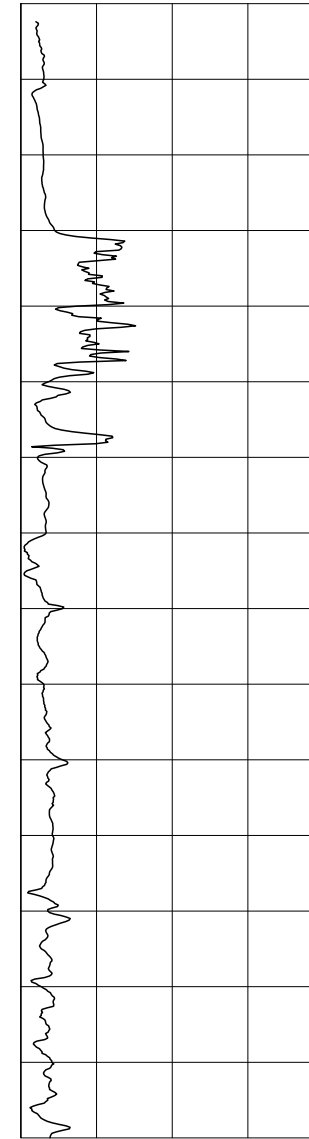
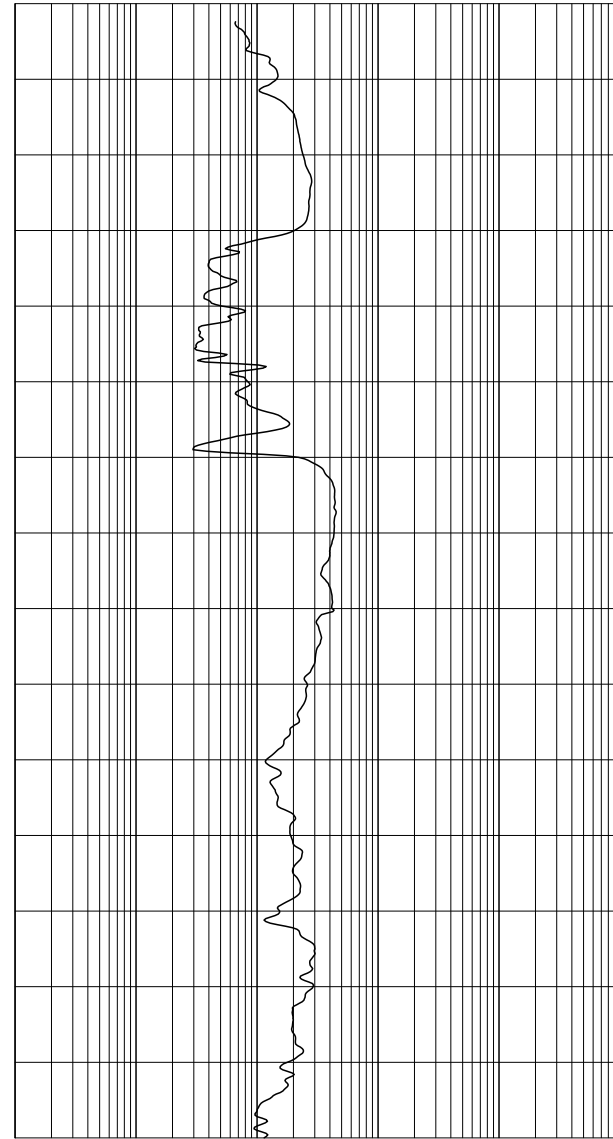
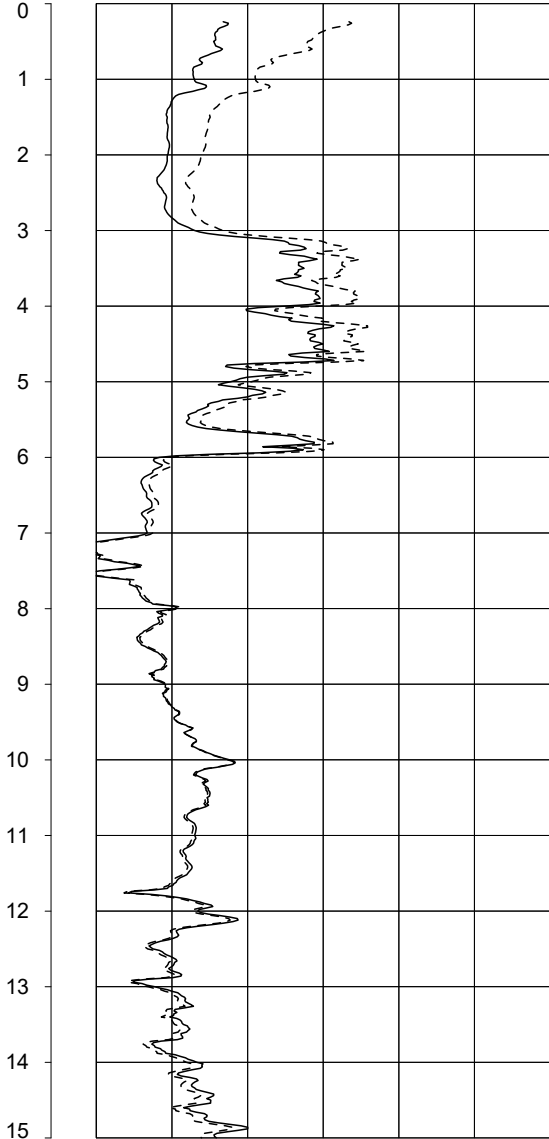
Soil Behaviour Type Index, I_c [-]
 1.0 1.5 2.0 2.5 3.0 3.5 4.0

Soil Behaviour Type Index, I_{SBT} [-]

Normalised Cone Resistance, Q_{tn} [-]
 10^0 10^1 10^2 10^3 10^4 10^5

Normalised Friction Ratio, F_r [%]
 0 2 4 6 8

Unit Weight, γ [kN/m^3]
 10 15 20 25



Date of Testing : 23-Feb-2021
 Water Depth [m LAT] : 31.8
 Coordinates [m] : E 540623 N 5828833

Probe Type : CP15-CF150PB20SN2
 Cone Base Area [mm^2] : 1510

CONE PENETRATION TEST
 HKW119-PCPT



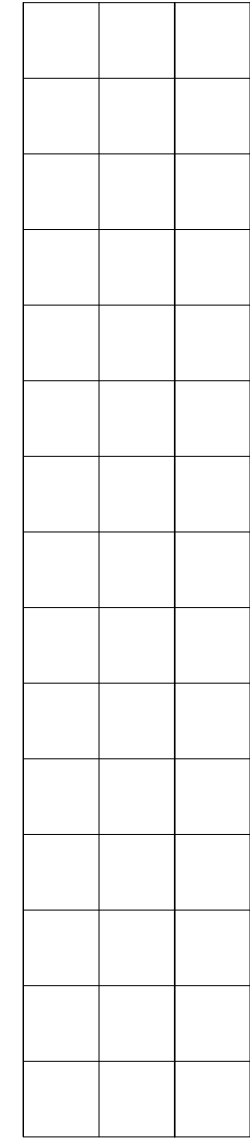
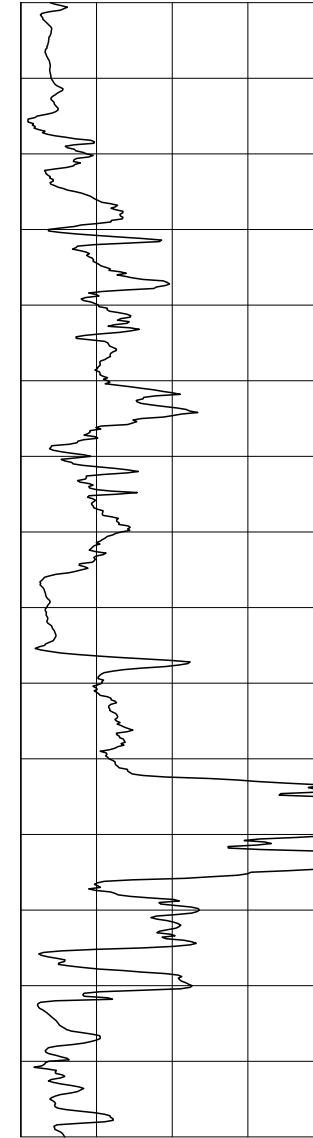
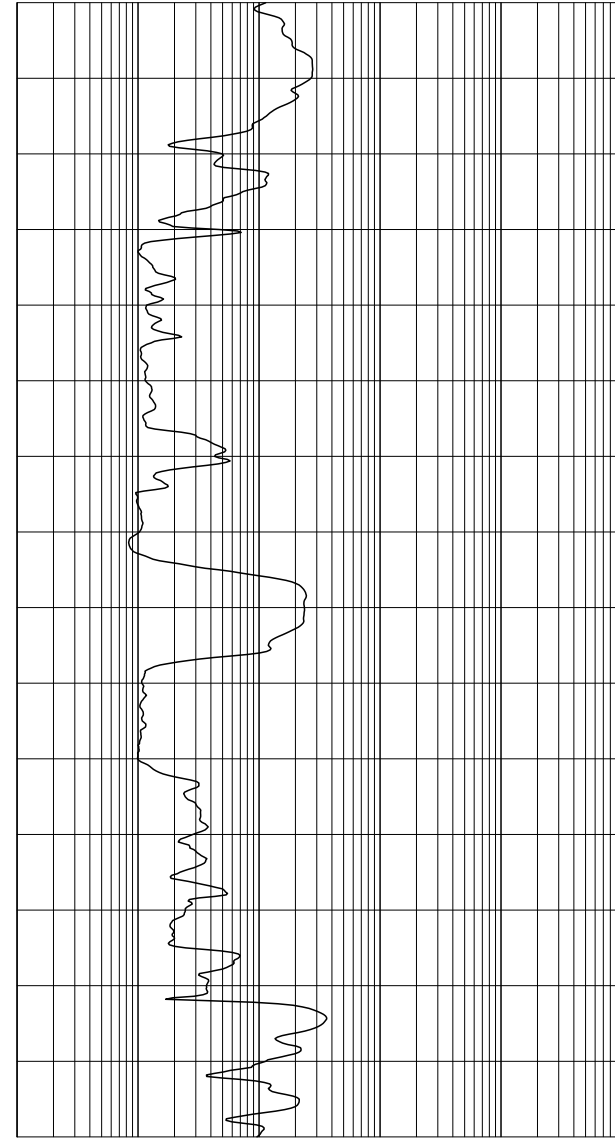
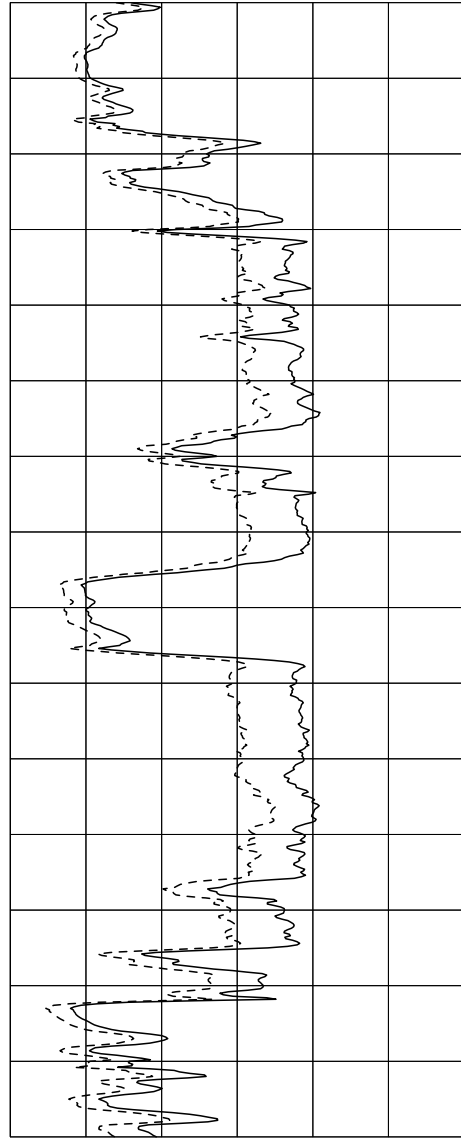
— Soil Behaviour Type Index, I_c [-]
 1.0 1.5 2.0 2.5 3.0 3.5 4.0

--- Soil Behaviour Type Index, I_{SBT} [-]

Normalised Cone Resistance, Q_{tn} [-]
 10^0 10^1 10^2 10^3 10^4 10^5

Normalised Friction Ratio, F_r [%]
 0 2 4 6 8

Unit Weight, γ [kN/m^3]
 10 15 20 25



Date of Testing : 23-Feb-2021
 Water Depth [m LAT] : 31.8
 Coordinates [m] : E 540623 N 5828833

Probe Type : CP15-CF150PB20SN2
 Cone Base Area [mm²] : 1510

CONE PENETRATION TEST
 HKW119-PCPT



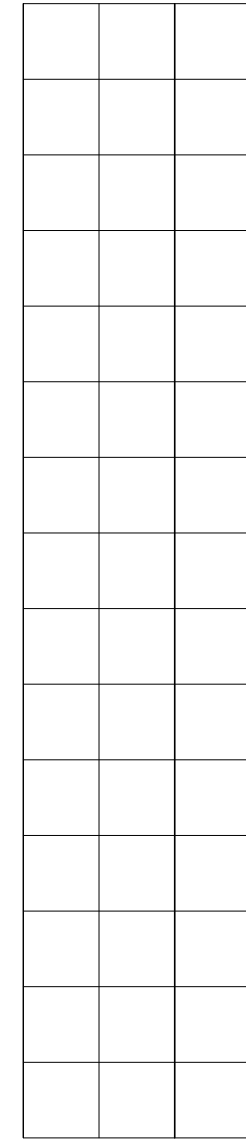
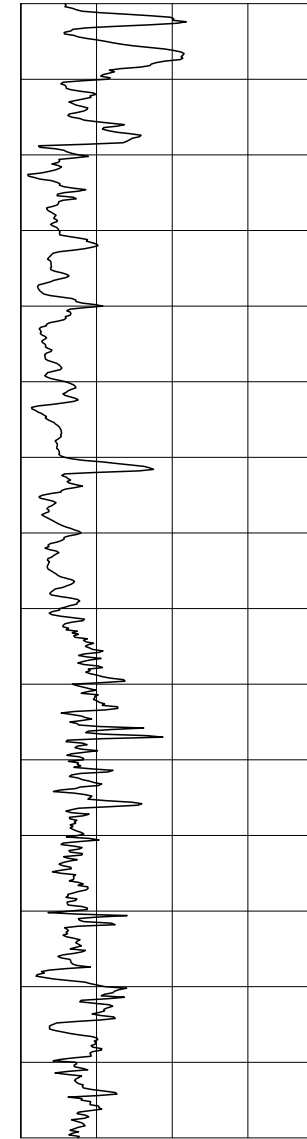
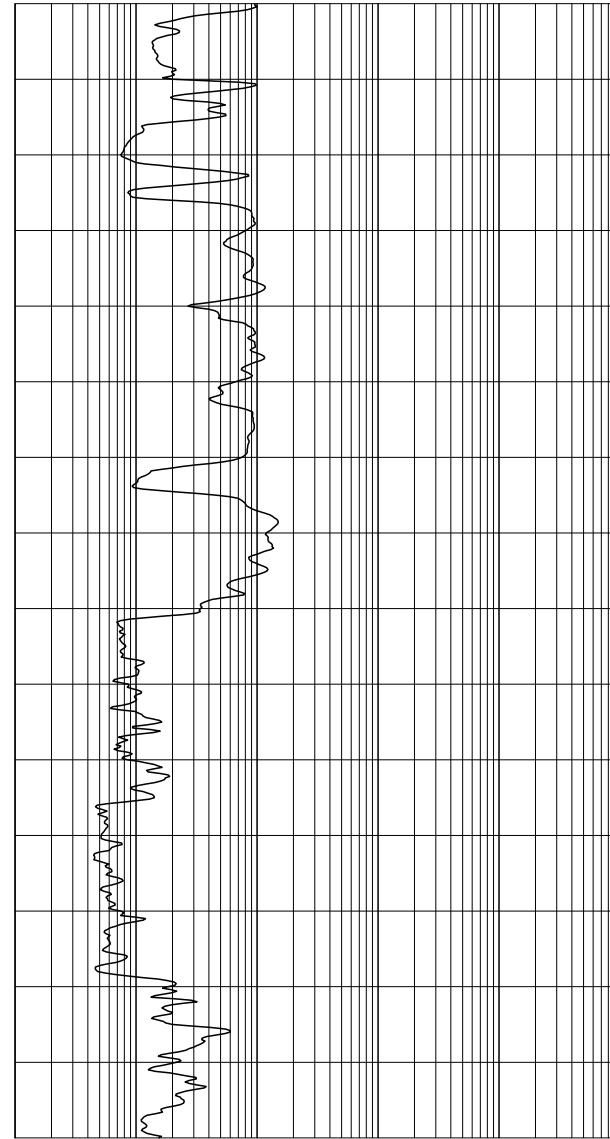
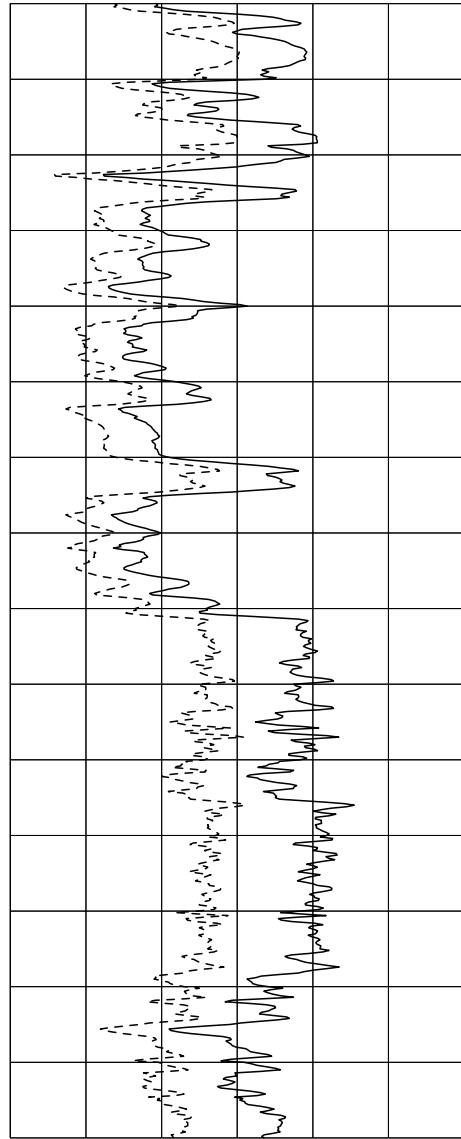
— Soil Behaviour Type Index, I_c [-]
 1.0 1.5 2.0 2.5 3.0 3.5 4.0

--- Soil Behaviour Type Index, I_{SBT} [-]

Normalised Cone Resistance, Q_{tn} [-]
 10^0 10^1 10^2 10^3 10^4 10^5

Normalised Friction Ratio, F_r [%]
 0 2 4 6 8

Unit Weight, γ [kN/m^3]
 10 15 20 25



Date of Testing : 23-Feb-2021
 Water Depth [m LAT] : 31.8
 Coordinates [m] : E 540623 N 5828833

Probe Type : CP15-CF150PB20SN2
 Cone Base Area [mm^2] : 1510

CONE PENETRATION TEST
 HKW119-PCPT



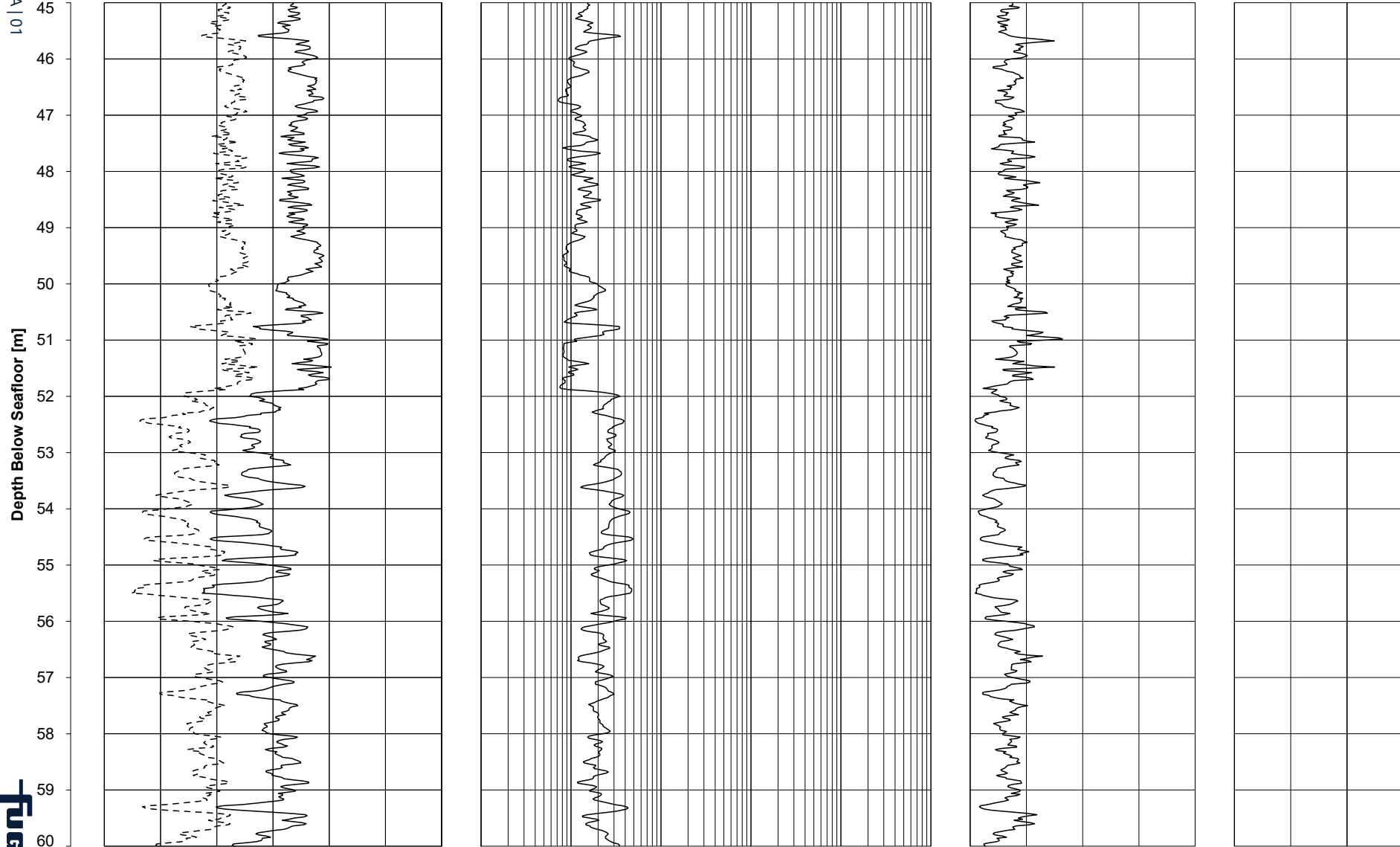
Soil Behaviour Type Index, I_c [-]
 1.0 1.5 2.0 2.5 3.0 3.5 4.0

Soil Behaviour Type Index, I_{SBT} [-]

Normalised Cone Resistance, Q_{tn} [-]
 10^0 10^1 10^2 10^3 10^4 10^5

Normalised Friction Ratio, F_r [%]
 0 2 4 6 8

Unit Weight, γ [kN/m^3]
 10 15 20 25

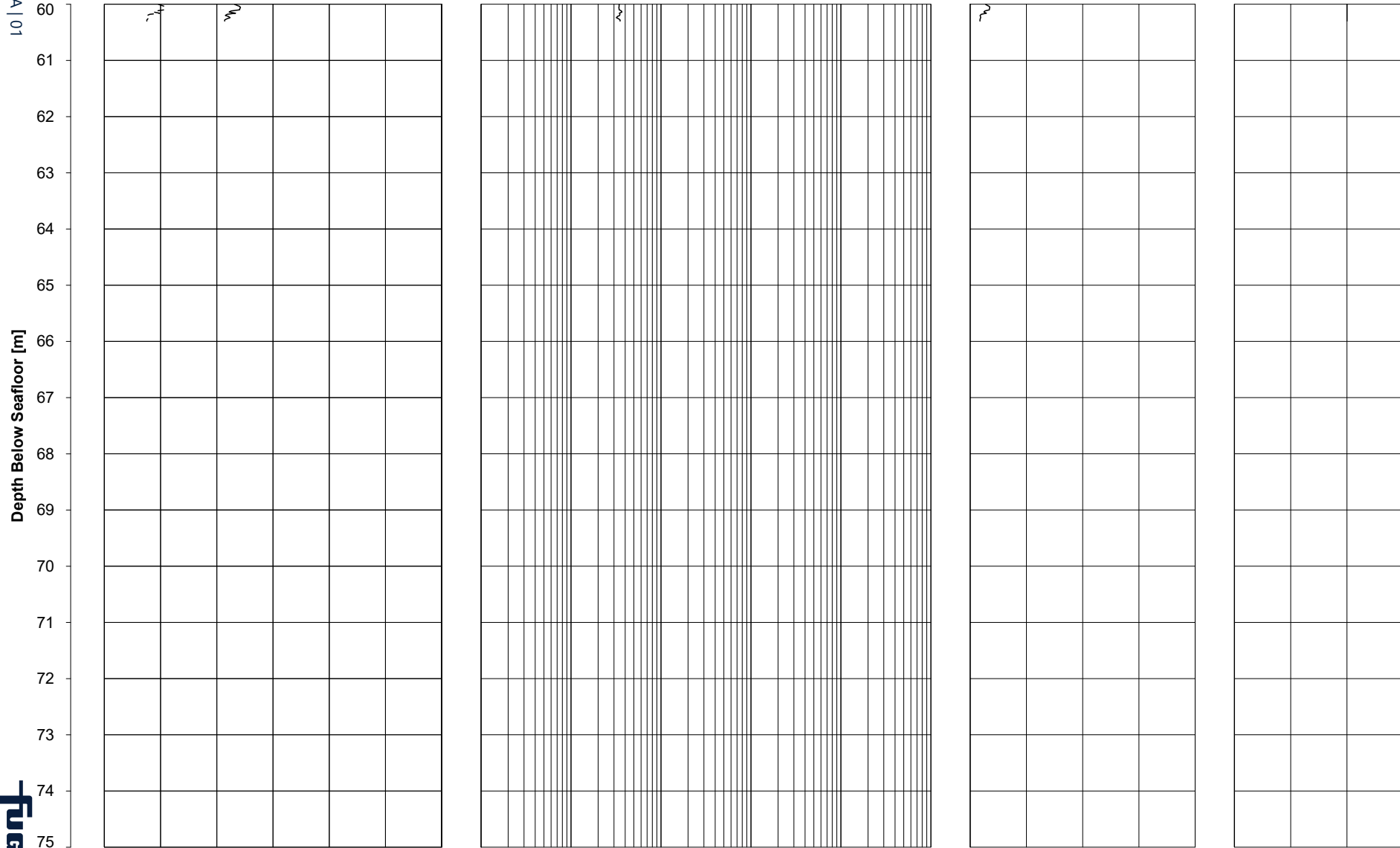
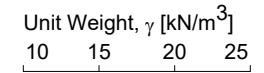
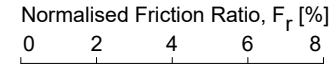
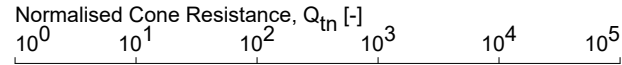
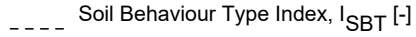
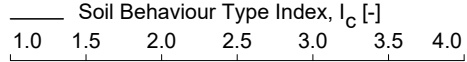


Date of Testing : 23-Feb-2021
 Water Depth [m LAT] : 31.8
 Coordinates [m] : E 540623 N 5828833

Probe Type : CP15-CF150PB20SN2
 Cone Base Area [mm^2] : 1510

CONE PENETRATION TEST
 HKW119-PCPT





Date of Testing : 23-Feb-2021
 Water Depth [m LAT] : 31.8
 Coordinates [m] : E 540623 N 5828833

Probe Type : CP15-CF150PB20SN2
 Cone Base Area [mm²] : 1510

CONE PENETRATION TEST
 HKW119-PCPT



Borehole/ Location	Zero Reading at Start of Test			Zero Drift			Probe	Net Area Ratio a [-]
	q _c [MPa]	f _s [MPa]	u [MPa]	q _c [MPa]	f _s [MPa]	u [MPa]		
HKW119-PCPT	0.104	0.002	-0.022	-0.034	-0.002	0.002	CP15-CF150PB20SN2 1701-3263	0.580

CONE PENETRATION TEST - ZERO DRIFT

Key:

q_c : cone resistance f_s : sleeve friction u : pore water pressure

Note:

- Zero Drift is the difference between the zero output at the start of the test and the zero output at the end of the test. Offshore tests may show Reference Readings. The Zero Reading or Reference Reading at Start of Test is a value presented in units of measurement result. The value itself is a conversion from system output, usually in mV. It has no explicit physical meaning.
- : Zero Drift was not monitored. The drift can be assessed from the start values of successive tests.

Appendix C

Descriptions of Methods and
Practices

Contents Appendix C: Descriptions of Methods and Practices

List of Documents

Use of Geodata and Advice	FNLM-GEO-APP-077
Abbreviations	FNLM-GEO-APP-080
Symbols	FNLM-GEO-APP-017
Geotechnical Log	FNLM-GEO-APP-078
Soil Description and Classification	FNLM-GEO-APP-005
Cone Penetration Test	FNLM-GEO-APP-001
Cone Penetration Test Interpretation	FNLM-GEO-APP-012
Positioning Survey and Depth Measurement	FNLM-GEO-APP-029
Marine Reflection Seismics	FNLM-GEO-APP-016
Site Characterisation	FNLM-GEO-APP-075
Geotechnical Analysis	FNLM-GEO-APP-052

This appendix presents important guidance and method statements that are generally familiar to expert users of the information.

Use of Geodata and Advice

Introduction

This document provides important information regarding the use of Fugro geodata, analyses and advice.

Site-specific acquisition of geodata can include metocean monitoring, geophysical seafloor mapping, subsurface mapping, logging of boreholes, in situ testing, laboratory testing of samples and monitoring of structures or elements of structures.

The cost of geodata acquisition, interpretation and monitoring is a small portion of the total cost of a development such as a construction project. By contrast, the costs of correcting a wrongly designed programme or mobilising alternative construction methods are often far greater than the cost of the original investigation for a site or structure.

Attention and adherence to the information presented in this document can reduce delays and cost overruns related to site-specific factors.

The focus of this document is on construction projects. This document also applies to information and advice related to asset integrity and decommissioning.

Requirements for Quality Geodata

Project quality management should follow ISO 9001 quality principles for project management and ISO 2394 for general principles on reliability for structures. Project activities usually comprise part of specific phases of a construction project. The quality plan for the entire construction project should incorporate geodata input in every phase - from the feasibility planning stages to project completion. The parties involved should do the following:

- Provide complete and accurate information necessary to plan an appropriate site investigation.

- Describe the purpose(s), type(s) and construction methods of planned structures in detail.
- Provide the time, financial, personnel and other resources necessary for the planning, execution and follow-up of a site investigation programme.
- Understand the limitations and degree of accuracy inherent in geodata.
- Understand the limitations and degree of accuracy inherent in the advice based upon site investigation data.
- During all design and construction activities, be aware of the limitations of site investigation data and analyses/ advice, and use appropriate preventative measures.
- Incorporate all geodata input in the design, planning, construction and other activities involving the site and structures. Provide the entire (set of) document(s), including digital files where applicable, to parties involved in site selection, design and construction.
- Use the site investigation data and advice for only the structures, site and activities which were described to Fugro prior to and for the purpose of planning the site investigation or the programme of analysis and advice.

Authority, Time and Resources Necessary for Site Investigations

Adequate designation of authority and accountability for site-specific aspects of construction projects is necessary. This way, an appropriate investigation can be performed, and the use of the results by project design and construction professionals can be optimised.

Figure 1 illustrates the importance of the initial project phases for gathering adequate geodata for a project. The initial phases, when site investigation requirements are defined and resources are allocated, are represented by more than 50 % of the Quality Triangle (Figure 1). Decisions and actions made during these phases have a large impact of the outcome and thus the potential of the investigation to meet project requirements.

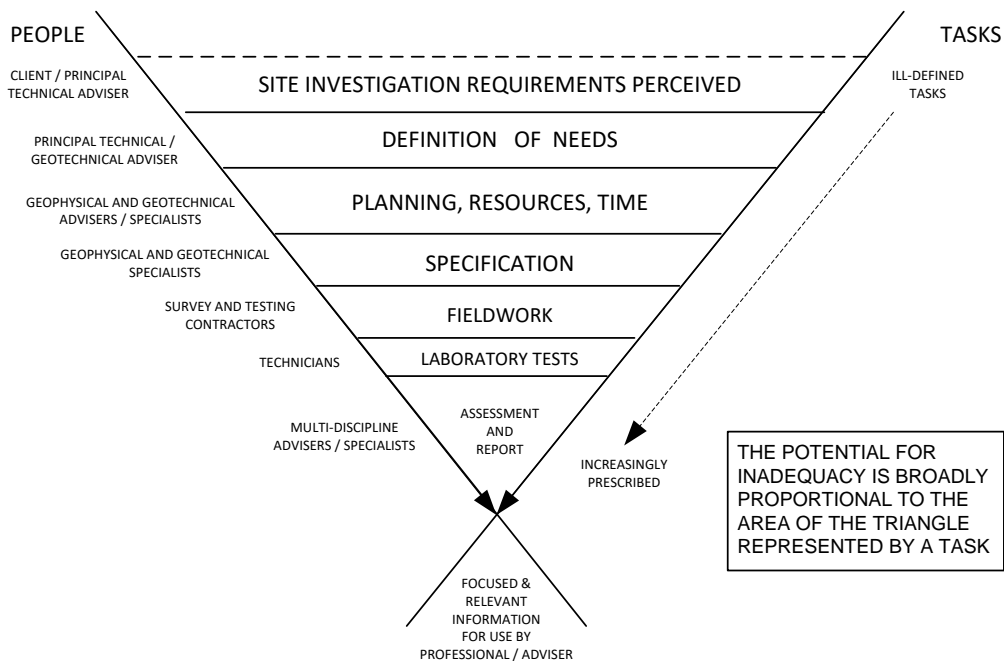


Figure 1: Quality of Site Investigation (adapted from SISG¹).

¹ Site Investigation Steering Group SISG (1993). *Site investigation in construction 2: planning, procurement and quality management*. Thomas Telford.

Data Acquisition and Monitoring Programmes

Site-specific investigations, such as geophysical and geotechnical investigations, are operations of discovery. Investigation should proceed in logical stages. Planning should allow operational adjustments deemed necessary by newly available information. This observational approach permits the development of a sound engineering strategy and reduces the risk of discovering unexpected (geo)hazards during or after construction.

Data Types and Limitations

1. Reliability of Supplied Information

Analysis and advice can involve the use of information and physical material that is publicly available or supplied by the client. Examples are geodetic data, geological maps, geophysical records, earthquake data, earlier geotechnical logs and soil samples. Fugro endeavours to identify potential anomalies but does not independently verify the accuracy or completeness of public or client-supplied information unless indicated otherwise. This information, therefore, can limit the accuracy of the geodata, analyses and advice.

2. Complexity of Ground Conditions

There are hazards associated with the ground. An adequate understanding of these hazards can help to minimize risks to a project and the site. The ground is a vital element of all structures which rest on or in the ground. Information about ground behaviour is necessary to achieve a safe and economical structure. Often less is known about the ground than for any other element of a structure.

3. Site Investigation - Spatial Coverage Limitations

Geophysical investigations typically provide information about ground conditions along survey track lines. Geotechnical investigations collect data at specific test locations. Interpretation of ground conditions away from survey track lines and test locations is a matter of extrapolation and judgement based on geological and geotechnical knowledge, as well as on experience. Nevertheless, actual conditions in untested areas may differ from predictions. For example, the interface between ground materials may be far more gradual or abrupt than indicated by the geodata. It is not realistic to expect a site investigation to reveal or anticipate every detail of ground conditions. Nevertheless, an investigation can reduce the residual risk associated with unforeseen conditions to a tolerable level. If ground problems do arise, it is important to have relevant expertise available to help reduce and mitigate safety and financial risks.

4. Role of Judgement and Opinion In Analysis and Advice

Analysis and advice that involve geodata are less exact than most other design disciplines. Extensive judgement and opinion are often required. Therefore, geodata, analyses and advice may contain definitive statements that identify where the responsibility of Fugro begins and ends. These are not exculpatory clauses designed to transfer liabilities to another party, but they are statements that can help all parties involved to recognise their individual responsibilities and take appropriate actions.

Complete Information should be Available to all Parties Involved

To prevent costly construction problems, construction contractors should have access to the best available information. They should have access to the complete original (set of) documents including digital files where applicable, to prevent or minimize any misinterpretation of site conditions and advice. To prevent errors or omissions that could lead to misinterpretation, geophysical sections, geotechnical logs and illustrations should not be redrawn, and users of geodata and advice should confer with the authors when applying the geodata and/or advice.

Information is Project-Specific

Fugro's investigative programmes, analyses and advice are designed and conducted specifically for the client described project and conditions. Thus the geodata, analyses and advice present information for a unique construction project. Project-specific factors for a structure include but are not limited to:

- location
- size and configuration of structure
- type and purpose or use of structure
- other facilities or structures in the area.

Any factor that changes subsequent to the preparation of the geodata, analyses and advice may affect its applicability. A specialised review of the impact of changes would be necessary. Fugro is not responsible for conditions which develop after change of any factor in site investigation programming, development or structure.

For purposes or parties other than the original project or client, the geodata, analyses and advice may not be adequate and should not be used.

Changes in Site Conditions Affect the Accuracy/Suitability of the Data

Ground is complex and can be changed by natural phenomena such as earthquakes, floods, seabed scour and groundwater fluctuations. Construction operations at or near the site can also change ground conditions. The geodata, analyses and advice consider conditions at the time of investigation. Construction decisions should consider any changes in site conditions, regulatory provisions, technology or economic conditions subsequent to the investigation. In general, two years after the date of geodata, analyses and advice, the information may be considered inaccurate or unreliable. A specialist should be consulted regarding the adequacy of the geodata, analyses and advice for use after any passage of time.

Abbreviations

I – General

1D	one-dimensional
2D	two-dimensional
3D	three-dimensional
API	American Petroleum Institute
ASTM	American Society for Testing and Materials
BSI	British Standards Institution
COV	coefficient of variation
FEED	front-end engineering design
GIS	geographical information system
ISO	International Organization for Standardization
SD	standard deviation

II – Geodetics

BGL	below ground level
BSF	below seafloor
CD	chart datum
CM	central meridian
DGPS	Differential Global Positioning System
CRS	coordinate reference system
E	east
ED	European Datum
ETRS	European terrestrial reference system
GNSS	Global Navigation Satellite System
GPS	Global Positioning System
GRS	Geodetic Reference System
INS	inertial navigation system
KP	kilometre point
LAT	Lowest Astronomical Tide
MSL	Mean Sea Level
N	north
S	south
TM	Transverse Mercator
USBL	ultra short baseline
UTC	Coordinated Universal Time
UTM	Universal Transverse Mercator
W	west
WGS	World Geodetic System

III – Site Investigation

ABI	acoustic borehole imager
ASV	autonomous surface vehicle
AUV	autonomous underwater vehicle
BC	box core(r)
BH	borehole
BGL	borehole geophysical logging
BPT	ball penetration test
CAL	caliper tool
CDP	common depth point
CMP	common mid-point
CPT	cone penetration test
CPTU	piezocone penetration test (or PCPT)
CTD	conductivity temperature depth
FFP	free-fall penetration test
FLPC	Fugro large piston core(r)
GC	gravity core(r)
GR	natural gamma radiation
GS	grab sample(r)
HRS	high resolution seismic reflection
ID	inner diameter
LDPC	large diameter piston core(r)
LGPC	large gravity piston core(r)

MAG	magnetometer
MBES	multibeam echosounder
MBPT	miniature ball penetration test
MCS	multichannel seismic reflection
MTPT	miniature T-bar penetration test
MV	motor vessel
OD	outer diameter
PC	piston core(r)
PPDT	pore pressure dissipation test
PSSL	P and S suspension logger
RC	rotary core(r)
ROV	remotely operated vehicle
SBES	single beam echosounder
SBF	seabed frame
SBP	sub-bottom profiler, seismic reflection
SCPT	seismic cone penetration test
SCS	single channel seismic reflection
SGR	spectral gamma radiation
SIR	strong impedance reflector
SSDM	Seabed Survey Data Model
SSS	side scan sonar
STACOR®	stationary piston gravity core(r)
SV	sailing vessel
SVP	sound velocity profiler
TCPT	temperature cone penetration test
TPT	T-bar penetration test
TWTT	two-way travel time, seismic reflection
UHRs	ultra high resolution seismic reflection
VC	vibrocore(r)
VST	vane shear test
WISON®	wireline sounding tool
WIP	wireline push sampler

IV – Site Characterisation

BP	before present
DTM	digital terrain model
Fm	geological formation
LGM	last glacial maximum
Mb	geological formation member
MDAC	methane-derived authigenic carbonate
MTD	mass transport deposit
UXO	unexploded ordnance

V – Geotechnical Analysis

ALS	accidental limit state
ASD	allowable stress design
FLS	fatigue limit state
LSD	limit state design
PFD	partial factor design
SLS	serviceability limit state
ULS	ultimate limit state
WSD	working stress design

Symbols

<u>Symbol</u>	<u>Unit</u>	<u>Quantity</u>
I - General		
A	m^2	Area
L	m	Length
B	m	Width
D	m	Diameter
U	-	Uncertainty of parameter value
V	m^3	Volume
W	kN	Weight
a	m/s^2	Acceleration
d	m	Depth
g	m/s^2	Acceleration due to gravity ($g = 9.81 m/s^2$)
h	m	Height or thickness
i	-	Inclination
m	kg	Mass
t	s	Time
t	a	Time, mean Julian year
v	m/s	Velocity
z	m	Penetration or depth below reference level (usually ground surface)
$\dot{\epsilon}$	s^{-1}	Rate of strain (length)
ρ	kg/m^3	Density
π	-	Mathematical constant (= 3.14159)
e	-	Base of natural logarithm (= 2.71828)
ln	-	Natural logarithm
log	-	Logarithm base 10
II - Stress and Strain		
P_a	kPa	Atmospheric pressure
u	MPa	Pore pressure
u_o	MPa	Hydrostatic pore pressure relative to seafloor or phreatic surface
u_f	MPa	Pore pressure at failure
Δu	MPa	Change in pore pressure or excess pore pressure
σ	kPa	Total stress
σ'	kPa	Effective stress
τ	kPa	Shear stress
τ_{peak}	kPa	Peak shear stress
$\sigma_1, \sigma_2, \sigma_3$	kPa	Principal stresses
σ_h	kPa	Total horizontal stress
$\Delta\sigma_h$	kPa	Change in total horizontal stress
σ_v	kPa	Total vertical stress
$\Delta\sigma_v$	kPa	Change in total vertical stress
σ_{h0}	kPa	Total in situ horizontal stress relative to ground surface or phreatic surface
σ'_{h0}	kPa	Effective in situ horizontal stress
σ_{v0}	kPa	Total in situ vertical stress relative to ground surface or phreatic surface
σ'_{v0}	kPa	Effective in situ vertical stress (or p'_0)
σ'_h	kPa	Effective horizontal stress
σ'_v	kPa	Effective vertical stress
σ'_r	kPa	Effective radial stress
σ'_a	kPa	Effective axial stress
r_u	-	Pore pressure ratio [= u/σ_{v0}]
p'	kPa	Mean effective stress [= $(\sigma'_1 + \sigma'_2 + \sigma'_3)/3$]
q	kPa	Principal deviator stress [= $\sigma'_1 - \sigma'_3$] or [= $\sigma_1 - \sigma_3$]
q_{ref}	kPa	Reference principal deviator stress
s'	kPa	Mean effective stress in $s' - t$ space [= $(\sigma'_1 + \sigma'_3)/2$]
t	kPa	Shear stress in $s' - t$ space [= $(\sigma'_1 - \sigma'_3)/2$] or [= $(\sigma_1 - \sigma_3)/2$]

<u>Symbol</u>	<u>Unit</u>	<u>Quantity</u>
ε	-	Linear strain
$\varepsilon_1, \varepsilon_2, \varepsilon_3$	-	Principal strains
ε_v	-	Vertical strain (or volumetric strain)
ε_{vol}	-	Volumetric strain
γ	-	Shear strain
γ_c	-	Shear strain at maximum shear stress
ν	-	Poisson's ratio
ν_u	-	Poisson's ratio for undrained stress change
ν_d	-	Poisson's ratio for drained stress change
E	MPa	Modulus of linear deformation (Young's modulus)
E_{max}	MPa	Modulus of linear deformation at small strain
E_u	MPa	Modulus of linear deformation (Young's modulus for undrained stress change)
E_d	MPa	Modulus of linear deformation (Young's modulus for drained stress change)
G	MPa	Modulus of shear deformation (shear modulus)
G_{max}	MPa	Shear modulus at small strain
I_r	-	Rigidity index [= G/τ_{max} or G/s_u]
K	MPa	Modulus of compressibility (bulk modulus)
M	MPa	Constrained modulus [= $1/m_v$]
M_{max}	MPa	Constrained modulus at small strain
μ	-	Coefficient of friction
η	kPa.s	Coefficient of viscosity

III - Physical Characteristics of Ground

(a) Density and Unit Weights

γ	kN/m ³	Unit weight of ground (or bulk unit weight or total unit weight)
γ_d	kN/m ³	Unit weight of dry ground
γ_s	kN/m ³	Unit weight of solid particles
γ_w	kN/m ³	Unit weight of water
γ_{pf}	kN/m ³	Unit weight of pore fluid
γ_{dmin}	kN/m ³	Minimum index (dry) unit weight
γ_{dmax}	kN/m ³	Maximum index (dry) unit weight
γ'	kN/m ³	Unit weight of submerged ground (or γ_{sub})
ρ	Mg/m ³ [= t/m ³]	Density of ground (or bulk density)
ρ_d	Mg/m ³ [= t/m ³]	Density of dry ground
ρ_s	Mg/m ³ [= t/m ³]	Density of solid particles (or G_s)
ρ_w	Mg/m ³ [= t/m ³]	Density of water
D_r	-, %	Relative density [= $I_D = \gamma_{dmax}(\gamma_d - \gamma_{dmin})/\gamma_d(\gamma_{dmax} - \gamma_{dmin}) = (e_{max} - e)/(e_{max} - e_{min})$]
v	-	Specific volume [= $1 + e$]
e	-	Void ratio
e_0	-	Initial void ratio
$e_{\sigma'_{v0}}$	-	Void ratio at σ'_{v0} (or e_0)
e_{max}	-	Maximum index void ratio
e_{min}	-	Minimum index void ratio
G_s	-	Specific gravity of solid particles
I_D	-, %	Density index [= D_r]
R_D	-, %	Dry density ratio [= γ_d/γ_{dmax}]
n	-, %	Porosity
w	%	Water content
S_r	%	Degree of saturation
r	-, g/kg	Salinity of pore fluid [= ratio of mass of salt to mass of pore fluid]
R	g/l	Salinity of fluid [= ratio of mass of salt to volume of distilled water]
s	g/l	Salinity of fluid [= ratio of mass of salt to volume of fluid]
S	g/kg	Salinity of seawater [= ratio of mass of salt to mass of seawater]

<u>Symbol</u>	<u>Unit</u>	<u>Quantity</u>
(b) Consistency		
w_L	%	Liquid limit
w_P	%	Plastic limit
I_P	%	Plasticity index [= $w_L - w_P$]
I_L	%	Liquidity index [= $(w - w_P)/(w_L - w_P)$]
I_C	%	Consistency index [= $(w_L - w)/(w_L - w_P)$]
A	-, %	Activity [= ratio of plasticity index to percentage by weight of clay-size particles]
(c) Particle Size		
D	mm	Particle diameter
D_n	mm	Particle diameter, where n% of the dry mass of ground has a smaller particle diameter
C_u	-	Uniformity coefficient [= D_{60}/D_{10}]
C_c	-	Curvature coefficient [= $(D_{30})^2/D_{10}D_{60}$]
(d) Acoustic Properties		
S_{vh}	-	S-wave propagating in the vertical direction with particle motion in the horizontal direction
S_{hh}	-	S-wave propagating in the horizontal direction with particle motion in the horizontal direction
S_{hv}	-	S-wave propagating in the horizontal direction with particle motion in the vertical direction
v_p	m/s	P-wave velocity (compression wave velocity)
v_s	m/s	S-wave velocity (shear wave velocity)
v_{s1}	m/s	S-wave velocity normalised to 100 kPa in situ vertical stress
v_{vh}	m/s	S-wave velocity, vertically (v) propagated, horizontally (h) polarised
(e) Hydraulic Properties		
k	m/s	Coefficient of permeability
k_v	m/s	Coefficient of vertical permeability
k_h	m/s	Coefficient of horizontal permeability
i	-	Hydraulic gradient
(f) Thermal and Electrical Properties		
T	K, °C	Temperature
k	W/(m·K)	Thermal conductivity
a_L	1/°C	Thermal expansion coefficient (linear)
α	m ² /s	Thermal diffusion coefficient
C	MJ/m ³ K	Volumetric heat capacity
ρ	Ω m	Electrical resistivity
K	S/m	Electrical conductivity
(g) Magnetic Properties		
B	T	Magnetic flux density (or magnetic induction)
(h) Radioactive Properties		
γ	CPS	Natural gamma ray

IV - Mechanical Characteristics of Ground

(a) Cone Penetration Test (CPT)

q_c	MPa	Cone resistance
q_{c1}	MPa	Cone resistance normalised to 100 kPa effective in situ vertical stress
f_s	MPa	Sleeve friction
f_t	MPa	Sleeve friction corrected for pore pressures acting on the end areas of the friction sleeve
R_f	%	Ratio of sleeve friction to cone resistance
R_{ft}	%	Ratio of sleeve friction to corrected cone resistance (f_s/q_c or f_t/q_t)
u_1	MPa	Pore pressure at the face of the cone
u_2	MPa	Pore pressure at the cylindrical extension above the base of the cone or in the gap between the friction sleeve and the cone

<u>Symbol</u>	<u>Unit</u>	<u>Quantity</u>
u_2^*	MPa	Pore pressure u_2 , but derived rather than measured
u_3	MPa	Pore pressure immediately above the friction sleeve or in the gap above the friction sleeve
K	-	Adjustment factor for ratio of pore pressure at u_1 to u_2 location
q_n	MPa	Net cone resistance
q_t	MPa	Corrected cone resistance (or total cone resistance)
B_q	-	Pore pressure ratio
Q_t	-	Normalized cone resistance [= q_n/σ'_{v0}]
Q_{tn}	-	Normalized cone resistance with variable stress exponent
F_r	%	Normalized friction ratio [= f_t/q_n]
I_c	-	Soil behaviour type index (for Q_{tn} and F_r)
I_{SBT}	-	Soil behaviour type index (for q_c and R_f)
N_c	-	Cone factor between q_c and s_u
N_{kt}	-	Cone factor between q_n and s_u (or N_k)
$N_{\Delta u}$	-	Pore pressure factor between $u_2 - u_0$ and s_u

(b) Standard Penetration Test (SPT)

N	Blows/0.3 m	SPT blow count
N_{60}	Blows/0.3 m	SPT blow count normalised to 60 % energy
$N_{1,60}$	Blows/0.3 m	SPT blow count normalised to 60 % energy and to 100 kPa effective in situ vertical stress

(c) Strength and Stiffness of Soil – Static

s_u	kPa	Undrained shear strength (or c_u)
s_{uC}	kPa	Undrained shear strength in laboratory triaxial compression (or c_{uC})
s_{uD}	kPa	Undrained shear strength in laboratory direct simple shear (or c_{uD})
s_{uE}	kPa	Undrained shear strength in laboratory triaxial extension (or c_{uE})
$s_{u,ref}$	kPa	Reference undrained shear strength
s_u/σ'_{v0}	-	Undrained strength ratio
κ	kPa/m	Rate of increase of undrained shear strength with depth (linear)
c'	kPa	Effective cohesion intercept
ϕ'	°(deg)	Effective angle of internal friction (or ϕ')
ϕ'_{cv}	°(deg)	Effective angle of internal friction at large strain (or ϕ'_{cv})
ϕ'_R	°(deg)	Effective angle of internal friction at residual shear conditions (or ϕ'_R)
ψ	°(deg)	Angle of dilation (or dilatancy angle)
ϵ_{50}	%	External axial strain at half the maximum deviator stress (or ϵ_c)
ϵ_c	%	External axial strain at the maximum deviator stress
E_{50}	MPa	Secant Young's modulus at half the maximum deviator stress
$s_{u,r}$	kPa	Undrained shear strength of remoulded soil
$s_{u,ar}$	kPa	Undrained shear strength of aged remoulded soil
s_R	kPa	Undrained residual shear strength
S_t	-	Sensitivity [= $s_u/s_{u,r}$ or s_u/s_R]
T_x	-	Thixotropy strength ratio [$T_x(t) = s_{u,ar}(t)/s_{u,r}$]
M	-	Gradient of critical state line when projected onto a constant volume plane
A	-	Pore pressure coefficient for anisotropic pressure increment
B	-	Pore pressure coefficient for isotropic pressure increment

(d) Strength and Stiffness of Soil – Cyclic and Dynamic

N	-	Number of cycles (or cycle number)
N_f	-	Number of cycles to soil failure or final number of cycles
N_{eq}	-	Equivalent number of cycles
τ_0	kPa	Initial shear stress
τ_{av}	kPa	Average shear stress or constant shear stress (or τ_a)
τ_{cy}	kPa	Cyclic shear stress amplitude [= $(\tau_{max} - \tau_{min})/2$]
$\tau_{cy,f}$	kPa	Cyclic shear strength at a specified failure criterion [= $(\tau_{av} + \tau_{cy})_f$]
τ_{max}	kPa	Maximum shear stress
τ_{min}	kPa	Minimum shear stress
γ_{av}	%	Average shear strain (or γ_a) [= $(\gamma_{max} + \gamma_{min})/2$]
γ_{cy}	%	Cyclic shear strain amplitude [= $(\gamma_{max} - \gamma_{min})/2$]
γ_{max}	%	Maximum shear strain
γ_{min}	%	Minimum shear strain
γ_p	%	Permanent shear strain

<u>Symbol</u>	<u>Unit</u>	<u>Quantity</u>
σ'_{ac}	kPa	Effective axial consolidation stress
σ'_{rc}	kPa	Effective radial consolidation stress
σ'_{ref}	kPa	Reference effective stress
q_{cy}	kPa	Cyclic deviator stress amplitude [= $(q_{max} - q_{min})/2$]
q_{max}	kPa	Maximum deviator stress
q_{min}	kPa	Minimum deviator stress
q_{av}	kPa	Average deviator stress [= $(q_{max} + q_{min})/2$]
ε_{cy}	%	Cyclic axial strain (or cyclic vertical strain) amplitude [= $(\varepsilon_{max} - \varepsilon_{min})/2$]
ε_{max}	%	Maximum axial strain (or maximum vertical strain)
ε_{min}	%	Minimum axial strain (or minimum vertical strain)
ε_{av}	%	Average axial strain (or average vertical strain) [= $(\varepsilon_{max} + \varepsilon_{min})/2$]
ε_a	%	External axial strain at N_f (or external vertical strain at N_f)
E_{ext}	MPa	Young's modulus derived from loop stiffness and external axial strain
E_{loc}	MPa	Young's modulus derived from loop stiffness and local axial strain
u_a	kPa	Average pore pressure
u_{cy}	kPa	Cyclic pore pressure amplitude [= $(u_{max} - u_{min})/2$]
u_{max}	kPa	Maximum pore pressure
u_{min}	kPa	Minimum pore pressure
u_p	kPa	Permanent pore pressure
λ	-, %	Damping ratio of ground (or D)
λ_{ext}	%	Damping ratio derived from external axial strain
λ_{loc}	%	Damping ratio derived from local axial strain

(e) Strength of Rock

σ_c	MPa	Uni-axial compressive strength
$I_{s(50)}$	MPa	Point load strength index
NPR	N/mm	Needle point resistance

(f) Consolidation (One Dimensional)

σ'_{hc}	kPa	Effective horizontal consolidation stress
σ'_{vc}	kPa	Effective vertical consolidation stress
σ'_p	kPa	Effective preconsolidation stress (or effective vertical yield stress in situ)
σ^*_{ve}	kPa	Effective vertical stress on ICL at e_0
σ'_{vy}	kPa	Effective vertical yield stress in situ (or effective preconsolidation stress)
C_c	-	Compression index
C^*_c	-	Intrinsic compression index [= $e^*_{100} - e^*_{1000}$]
C_s	-	Swelling index (or re-compression)
CR	-	Primary compression ratio [= $C_c/(1 + e_0)$]
RR	-	Recompression ratio [= $C_s/(1 + e_0)$]
e_L	-	Void ratio at liquid limit w_L
e^*_{100}	-	Void ratio at $\sigma'_v = 100$ kPa during one-dimensional intrinsic compression
e^*_{1000}	-	Void ratio at $\sigma'_v = 1000$ kPa during one-dimensional intrinsic compression
C_α	-	Coefficient of secondary compression (primary compression)
$C_{\alpha s}$	-	Coefficient of secondary compression (swelling/re-compression)
c_v	m ² /s	Coefficient of consolidation
H	m	Drainage path length
ICL	-	Intrinsic compression line (Burland, 1990)
I_v	-	Void index [= $(e_0 - e^*_{100})/C^*_c$]
m_v	m ² /MN	Coefficient of volume compressibility
M	MPa	Constrained modulus [= $1/m_v$]
p	kPa	Vertical pressure
OCR	-	Overconsolidation ratio [= σ'_p/σ'_{v0}] (or yield stress ratio)
SCC	-	Sedimentation compression curve
SCL	-	Sedimentation compression line (Burland, 1990)
S_σ	-	Stress sensitivity [= $\sigma'_{vy}/\sigma^*_{ve}$]
YSR	-	Yield stress ratio [= $\sigma'_{vy}/\sigma'_{v0}$] (or overconsolidation ratio)

<u>Symbol</u>	<u>Unit</u>	<u>Quantity</u>
---------------	-------------	-----------------

V - Geotechnical Design

(a) Partial Factors

γ_d	-	Factor related to model uncertainty or other circumstances
γ_f	-	Partial action factor (load factor)
γ_m	-	Partial material factor (partial safety factor)
γ_R	-	Partial resistance factor (partial safety factor)

(b) Seismicity

a_g	m/s ²	Effective peak ground acceleration (design ground acceleration)
d_g	m	Peak ground displacement
α	-	Acceleration ratio [= a_g/g]
τ_c	kPa	Seismic shear stress

(c) Compaction

ρ_{dmax}	Mg/m ³ [= t/m ³]	Maximum dry density
ρ_{max}	Mg/m ³ [= t/m ³]	Maximum density
w_{opt}	%	Optimum moisture content

(d) Earth Pressure

δ	°(deg)	Angle of interface friction (between ground and foundation)
K	-	Coefficient of lateral earth pressure
K_a	-	Coefficient of active earth pressure
K_{ac}	-	Coefficient of active earth pressure for total stress analysis
K_p	-	Coefficient of passive earth pressure
K_{pc}	-	Coefficient of passive earth pressure for total stress analysis
K_0	-	Coefficient of earth pressure at rest
K_{0nc}	-	K_0 for normally consolidated soil
K_{0oc}	-	K_0 for overconsolidated soil

(e) Foundations

A	m ²	Total foundation area
A'	m ²	Effective foundation area
B'	m	Effective width of foundation
E_s	MN/m ³	Modulus of subgrade reaction
k	MPa/m	Rate of change of modulus of subgrade reaction E_s with depth z
L'	m	Effective length of foundation
H	MN	Horizontal external force or action
V	MN	Vertical external force or action
M	MN.m	External moment
T	MN.m	External torsion moment
Q	MN	Total vertical resistance of a foundation/pile
Q_p	MN	End bearing of pile
Q_s	MN	Shaft resistance of pile
q_p	MPa	Unit end bearing
q_{lim}	MPa	Limit unit end bearing
f	kPa	Unit skin friction (or q_s)
f_{lim}	kPa	Limit unit skin friction
p	MN/m	Lateral resistance per unit length of pile
p_{lim}	MN/m	Limit lateral resistance per unit length of pile
s	m	Settlement
t	MN/m	Skin friction per unit length of pile
y	mm	Lateral pile deflection
z	mm	Axial pile displacement
α	-	Adhesion factor between ground and foundation (= f/s_u)
β	-	Adhesion factor between ground and foundation (= f/σ'_v or f/σ'_{v0})
δ	°(deg)	Angle of interface friction (between ground and foundation)
δ_{cv}	°(deg)	Constant volume or critical-state angle of interface friction (between ground and foundation)

N_c, N_q, N_γ	-	Bearing capacity factors
K_c, K_q, K_γ	-	Bearing capacity correction factors for inclined forces or actions, foundation shape and depth of embedment
i_c, i_q, i_γ	-	Bearing capacity correction factors for external force inclined from vertical shape
S_c, S_q, S_γ	-	Bearing capacity correction factors for foundation shape
d_c, d_q, d_γ	-	Bearing capacity correction factors for foundation embedment

Signs:

- A "prime" applies to effective stress.
- A "bar" above a symbol relates to average properties.
- A "dot" above a symbol denotes derivative with respect to time.
- The prefix " Δ " denotes an increment or a change.
- A "star" after a symbol denotes value corrected for pore fluid salinity.

Geotechnical Log

Introduction

A geotechnical log presents a one-dimensional, typically vertical, profile of ground strata and water level measurements, where applicable. In addition, it may include the principal details of operational activities for acquisition of the information shown on the geotechnical log.

Other terms for geotechnical log used in practice include core log, borehole log, drilling log, sample log, geohazard core log, geological log and wireline log.

Table 1: Levels of Integration

Integration Level	Integration Type	Description
1	Bundled Information	Each data acquisition activity is interpreted and reported separately. No specific effort is made to consider and reconcile potential conflicts between information sources.
2	Stratigraphic Integration	This level of integration specifically focusses on achieving stratigraphic alignment between (1) sub-surface/sub-bottom profiles obtained by non-intrusive geophysical techniques (e.g. seismostratigraphy) and (2) stratigraphic interpretation from results of ground investigation obtained at specific locations (e.g. geotechnical soil unitisation). The stratigraphic alignment considers vertical zonation of a site.
3	Geotechnical Zonation	This level of integration provides a vertical and horizontal geotechnical zoning of a site. The horizontal zonation comprises a delineation and mapping of 'soil provinces'. Each soil province has a representative vertical soil profile and envelopes of ground characterisation such as shear strength, relative density, friction angle, unit weight, etc. The 'horizontal and vertical zoning' facilitates selection of engineering criteria (e.g. geotechnical parameter values/ ranges) for analysis of trenchability, anchor holding capacity, foundation bearing resistance, etc.
4	Geotechnical Zonation and Analysis	This level of integration not only provides geotechnical zonation but also incorporates engineering assessments of specific project requirements such as bearing resistance, trenching resistance, anchor holding capacity, upheaval buckling resistance, scour potential, etc. These requirements are usually specific to the type of facility, construction method and project phase.

A basic geotechnical log can consist of descriptions limited to e.g. "soil" and "rock" or a value such as soil behaviour type index I_c , in combination with corresponding depths below ground surface or seafloor.

A comprehensive geotechnical log is an interpretation of selected, processed data. The procedure for interpretation typically includes ranking of information for quality and importance and, where applicable, selection of primary depth values and aligning other depth data with the primary reference. The selected data can include:

- geological information;
- 2D/ 3D geophysical data;
- results of nearby geotechnical investigation locations;
- borehole geophysical logging data;
- in situ test data;
- laboratory test results;
- drilling parameters such as torque, feed, drill fluid pressure and drilling time.

A geotechnical log can apply to:

- a single investigation location, such as a borehole or cone penetration test (CPT);
- a location cluster comprising two or more investigation locations;
- a soil province, site or region.

A comprehensive geotechnical log can include mm-scale geological descriptions, geotechnical strata, data points of

Procedure

Preparation of geotechnical logs is based on ISO, CEN, BSI and ASTM standards.

The format and detail of a geotechnical log depends on an agreed project specification. Integration Level 1 of Table 1 applies, unless indicated otherwise.

A geotechnical log typically considers a specific purpose, for example presentation of geotechnical information for design of a pile foundation. The geotechnical log should not be used for another purpose without appropriate verification.

laboratory test results and multiple profiles of borehole geophysical logging and interpretive results of in situ testing.

The level of detail and accuracy of a geotechnical log depends on factors such as sample size, quality, coverage of samples and test data and integration with any supplementary information. For example, interfaces between strata may be more gradual than a geotechnical log indicates. The selected method for data presentation can also influence the level of detail. For example, graphical presentation will be constrained by the selected vertical depth scale and horizontal scale(s). Any graphical presentation of test results considers values within the scale limits only. No automatic scaling applies, unless indicated otherwise. Tabular presentation of a geotechnical log (no linear depth scale and no fixed horizontal scales) imposes fewer constraints.

Example Information - Geotechnical Logs

Depth

A geotechnical log typically presents depths below ground surface or seafloor as positive values in the downward direction. Information can also be presented relative to a vertical datum such as mean sea level. This gives increasing values for elevation in the upward direction.

The penetration depth shown on a (vertical) geotechnical log is defined as the deepest point reached by drilling, sampling or in situ testing. The recovery depth is the deepest point for which investigation data (logging, sample and test data) are presented.

In some cases, geotechnical logs can include geotechnical interpretations derived from geophysical data.

Unless indicated otherwise, recovery of a borehole tube sample or a core sample is assumed and shown to be continuous from the starting depth of sampling. Similarly, sample recovery for a seafloor sampler is assumed to be continuous from seafloor to recovery depth. In other words, the geotechnical log ignores possible plugging, flow-in and/or wash-out.

Geotechnical logs for a soil province, site or region can include multiple top and bottom depths for a single stratum or ground unit.

Operational Activities

A geotechnical log can include documentation of operational activities, such as details on drilling, sampling and in situ testing. Figure 1 shows examples for presentation of operational information.



Figure 1: Symbols for identification of samples and in situ tests

Drilling Parameters

Measurement while drilling (MWD) parameters for rotary drilling or percussion drilling can help characterisation of ground conditions such as cemented strata, weak rock and formations with cavities. Recording can be manually or by means of an automated recording system. Recorded parameter values are typically qualitative, i.e. no calibration of sensors would apply. Presentation of factual and/or interpreted results is usually in graphical format.

Rock Coring Parameters

ASTM International (2017) provides descriptions for rock core quality as follows:

- TCR Total Core Recovery: the total core length divided by the core run length
- SCR Solid Core Recovery: the total length of the pieces of solid core that have a complete circumference divided by the core run length
- RQD Rock Quality Designation: the total length of the pieces of sound core over 100 mm long along the centreline divided by the core run lengths per stratum or core run; sound core includes core with obvious drilling breaks
- I_F Fracture Index: spacing of natural discontinuities.

Table 2 shows a classification of rock quality according to ASTM International (2017).

Table 2: Classification of Rock Quality

RQD	Classification of Rock Quality
0 % to 25 %	Very poor
25 % to 50 %	Poor
50 % to 75 %	Fair
75 % to 90 %	Good
90 % to 100 %	Excellent

Geotechnical Description

Geotechnical description can be presented by text, numerical test values and by graphic logs.

Cone penetration test data allow software algorithms for geotechnical description of soil. Widely used systems are those by proposed by Robertson (2009, 2010, 2016). These systems include numerical test values, such as soil behaviour type index I_c as geotechnical description.

A geotechnical log can consist of or include a graphic log of ground conditions. Figures 2 through 4 present examples of symbols used in graphic logs.

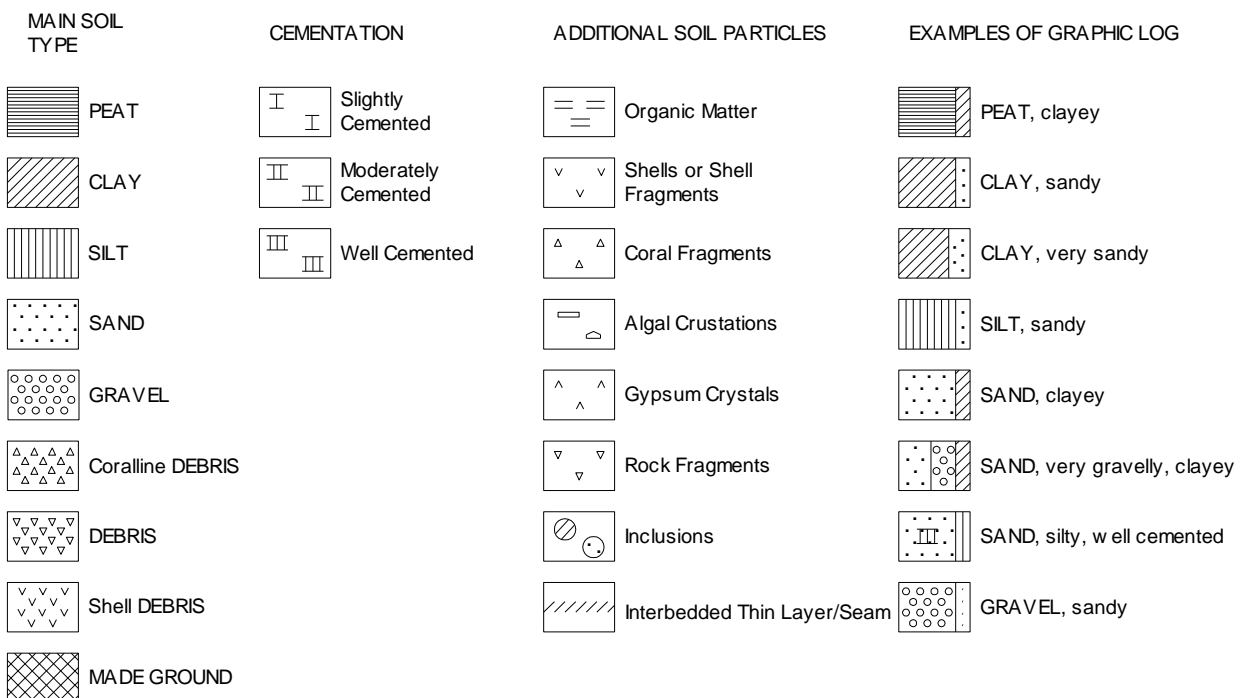


Figure 2: Symbols for soils

© Fugro 1996-2021

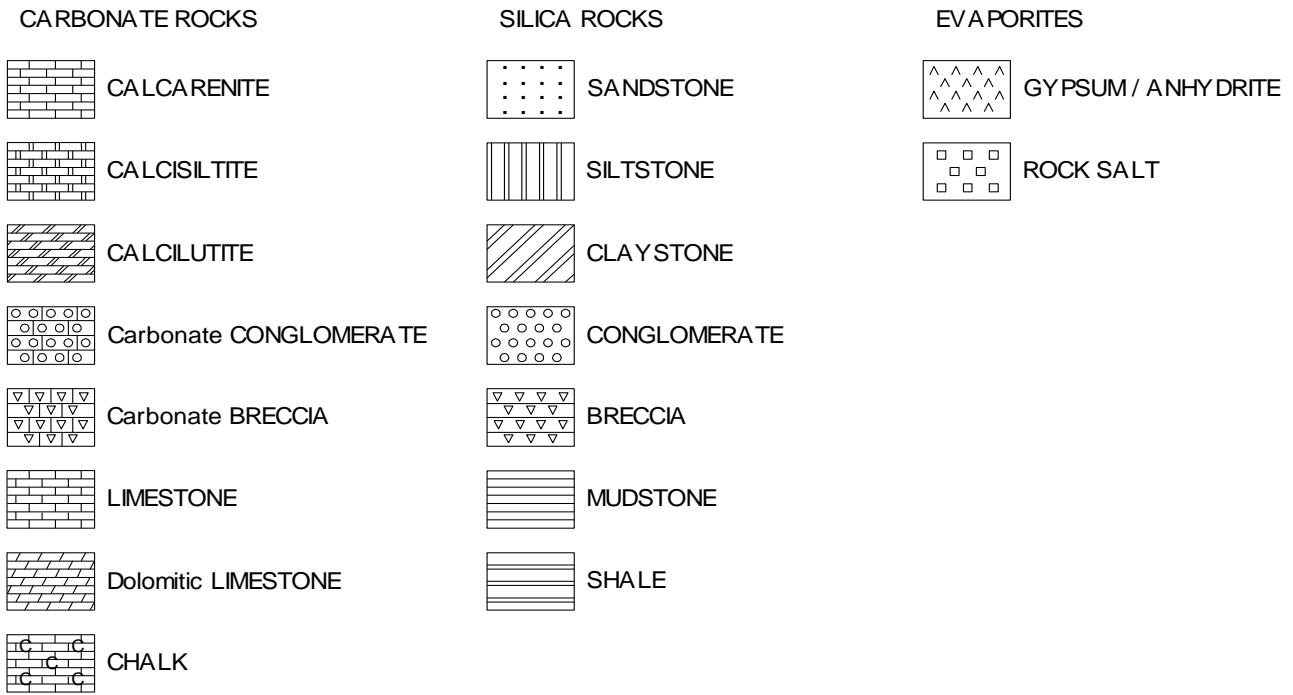


Figure 3: Symbols for sedimentary rocks

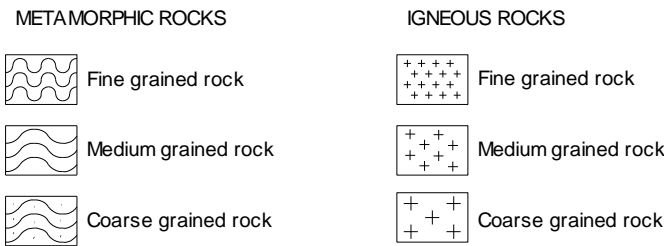


Figure 4: Symbols for metamorphic and igneous rocks

Water Level

Water level measurements taken in boreholes can be valuable. Interpretation of water levels requires due caution. They may or may not be representative of the ground water levels. In any case, water levels apply to the time and date of the measurements only. They will vary due to seasonal and other environmental influences, including construction activities.

Results of Geotechnical Tests and Correlations

A geotechnical log can include results of geotechnical tests and correlations, presented as numerical values and/or by graphic logs. Common examples are derived values of water content, soil unit weight, undrained shear strength, relative density and uniaxial compressive strength.

Test results and correlations for undrained shear strength are commonly shown for a main soil type shown as CLAY. Test results and correlations for relative density are commonly shown for a main soil type shown as SAND. In some cases, e.g. for transitional soils and layered soils, values of both undrained strength and relative density can be shown for CLAY, for SILT and for SAND. Specific decisions on presentation can be made by judgement and by algorithms. An example of a decision algorithm is CPT-based calculation using soil behaviour type index I_c .

References

ASTM International (2017). *Standard test method for determining rock quality designation (RQD) of rock core.* (ASTM D6032/D6032M-17). <https://www.astm.org/Standards/D6032.htm>.

BSI. (2020). *Code of practice for ground investigations* (BS 5930:2015+A1:2020). <https://shop.bsigroup.com/ProductDetail/?pid=000000000030400754>

European Committee for Standardization (2010). *Eurocode 7 - geotechnical design – part 2: ground investigation and testing* (EN 1997-2:2007+ AC:2010) https://standards.cen.eu/dyn/www/f?p=204:110:0:::FSP_PROJECT_FSP_ORG_ID:23735.6231&cs=14A2DCCA6BF367BFBD54D9FC0822BE0ED.

International Organization for Standardization (2006). *Geotechnical investigation and testing - sampling methods and groundwater measurements - part 1: technical principles for execution* (ISO 22475-1:2006) <https://www.iso.org/standard/36244.html>.

International Organization for Standardization (2014). *Petroleum and natural gas industries – specific requirements for offshore structures – part 8: marine soil investigations* (ISO 19901-8:2014). <https://www.iso.org/standard/61145.html>.

Robertson, P.K. (2009). Performance based earthquake design using the CPT. In T. Kokusho, Y. Tsukamoto & M. Yoshimine (Eds.), *Performance-based design in earthquake geotechnical engineering: From case history to practice* (pp. 3–20). CRC Press.

Robertson, P.K. (2010). Soil behaviour type from the CPT: an update. In *2nd International symposium on cone penetration testing, Huntington Beach, CA, Vol. 2.* (pp. 575-583).

Robertson, P.K. (2016). Cone penetration test (CPT)-based soil behaviour type (SBT) classification system — an update. *Canadian Geotechnical Journal*, 53(12) 1910-1927
<https://doi.org/10.1139/cgj-2016-0044>

Soil Description and Classification

Scope

This document applies to soil description and classification as laboratory test methods, particularly:

- sample description;
- soil specimen description, whereby a specimen can be all or part of sample.

This document excludes:

- CPT-based description of soil behaviour type;
- rock description and classification;
- specific engineering geological classification systems, such as those for detailed identification of peat, chalk and micaceous sand;
- soil stratum description, for example in the format of a geotechnical log.

Standards for Soil Description and Classification

Fugro employs a range of industry-standard systems for soil description, with additional refinements. The more important systems are:

- British Standards Institution (BSI) standard BS 5930:2015+A1:2020 (Code of Practice for Ground Investigations);
- American Society for Testing and Materials (ASTM) standards D2487-17 (Standard Practice for Classification of Soils for Engineering Purposes – United Soil Classification System) and D2488-17e1 (Standard Practice for Description and Identification of Soils – Visual-Manual Procedures);
- International Organization for Standardization (ISO) standards ISO 14688-1:2017 (Geotechnical Investigation and Testing - Identification and Classification of Soil. Part 1: Identification and Description) and ISO 14688-2:2017 (Geotechnical Investigation and Testing - Identification and Classification of Soil. Part 2: Principles for a Classification);
- International Organization for Standardization (ISO) standard ISO 19901-8:2014 (Petroleum and Natural Gas Industries - Specific Requirements for Offshore Structures. Part 8: Marine Soil Investigations).

The standards are similar, as they are (1) based on the Unified Soil Classification System (Casagrande, 1947), (2) rely on a range of relatively simple visual and manual observations, and (3) classify soils primarily according to particle size distribution and plasticity. Laboratory particle size distribution and Atterberg limits tests are used to confirm the observations. In addition, the standards include organic soils characterisation under soil particle type description.

Significant differences between the standards include the particle size boundaries and the degree to which plasticity is used as a basis for description and classification.

Where applicable, a classification system for calcareous soil can be integrated (for example based on Clark & Walker, 1977). The characteristics of calcareous soil deposits can differ substantially from those of silica-based soil deposits, primarily because of cementation and differences in void ratios.

Based on identification and description of soils, the standards given above provide a means by which soils can be classified into

groups of similar composition and geotechnical characteristics.

General Procedure

The general procedure for soil description and classification is as follows:

1. Select ISO, BS or ASTM based on local geotechnical practice or project specifications and follow the appropriate descriptive procedure; for calcareous soils, the process described by Clark & Walker (1977) may be used as an alternative.
2. Measure or estimate the particle size distribution and plasticity for use in defining the primary and secondary soil fractions.
3. Measure or estimate soil strength according to one of the following: (1) relative density of coarse soils, (2) consistency and/or undrained shear strength of fine soils, (3) cementation of cemented soils, or (4) lithification of soils undergoing diagenesis.
4. Complete the description and classification using additional terms for the soil mass characteristics and other features such as bedding, colour, and particle shape.

Soil Description and Classification using BS 5930:2015+A1:2020, ISO 14688-1:2017 and ISO 14688-2:2017

Soil Group

Soil group subdivides soils into very coarse, coarse, fine, organic, and anthropogenic soils.

Very coarse soils consist of cobbles and boulders, with particles larger than 63 mm in diameter. These soil particles are rarely sampled using standard soil sampling techniques. They are described separately, and not included when determining the proportions of the other soil components.

Characteristics of fine and coarse soils are based on particle size distribution of the coarser particles and plasticity of the finer particles. A first appraisal of physical properties is made from visual description of the soil's nature and composition, assisted by a few simple hand tests. Soils that stick together when wet and can be rolled into a thread that supports the soil's own weight (i.e. they have cohesion and plasticity) are matrix-supported and are described as fine soils. Soils that do not exhibit these properties are clast-supported and are described as coarse soils. The boundary between fine and coarse soils is on the basis of behaviour, not by weight percentage.

Organic soils contain usually small quantities of dispersed organic matter that can have a significant effect on soil plasticity and may produce a distinctive odour and have a dark grey, dark brown or dark bluish grey colour. Increasing quantities of organic matter enhance effects. Soils with a high organic content might oxidize and change colour rapidly. Organic soil descriptions in BS 5930 are based on organic content by weight determined by loss on ignition. Where organic matter is present as a secondary constituent in inorganic soil, the terms in Table 1 are used.

Soils with organic contents of up to approximately 30 % by mass and water contents of up to about 250 % behave largely as inorganic soils and are described using the terms given in Table 1. Such materials are usually transported (geologically) and would not be described as peat.

Soils comprising mainly organic materials are termed peats. They are of low density, typically 1.01 Mg/m³ to 1.1 Mg/m³. Peat consists predominantly of plant remains, is usually dark brown or black, and has a distinctive smell. It is generally classified

according to the degree of decomposition (fibrous, pseudo-fibrous, or amorphous) and strength (firm, spongy, or plastic).

Table 1: Description of secondary organic matter in an inorganic soil (BS 5930:2015+A1:2020)

Term	Typical Colour	Organic Content	Approximate % of dry mass
Slightly organic	Grey	Low organic content	2 to 6
Organic	Dark grey	Medium organic content	6 to 20
Very organic	Black	High organic content	> 20

The description and classification of the carbonate content of soils is made using the terms given in Table 2.

Table 2: Carbonate content classification (based on ISO 14688-1:2017 and ISO 14688-2:2017)

Description	Carbonate Content [% CaCO ₃]	Reaction with HCl (10 %)
Slightly calcareous	1 to 5	Addition of HCl produces weak or sporadic effervescence
Calcareous	5 to 25	Addition of HCl produces clear but not sustained effervescence
Highly calcareous	25 to 50	Addition of HCl produces strong and sustained effervescence
Very highly calcareous or Carbonate	> 50	Addition of HCl produces strong and sustained effervescence

Primary Soil Fraction

Classification of coarse soils, fine soils and composite mixtures is based both on particle size distribution and on plasticity, unless determination of plasticity is irrelevant or not feasible. Classification of fine soil is based on either particle size distribution and/or on plasticity.

Where a soil (omitting any boulders or cobbles) 'sticks together when wet, and remoulds' it is described as a fine soil ('CLAY' or 'SILT', dependent on its plasticity). When it does not stick together and remould, it is described as a coarse soil ('SAND' or 'GRAVEL' depending on its particle size distribution). The primary soil fraction which dominates the soil behaviour and the secondary fractions that modify that behaviour are described.

Coarse Soils

The primary soil fraction in coarse soils is sand if the dry weight of the sand fraction (0.063 mm to 2 mm particle sizes) exceeds that of the gravel fraction (2 mm to 63 mm particle sizes), and vice versa for gravel.

Particle size distribution of coarse soils can be designated based on uniformity coefficient (C_u) and coefficient of curvature (C_c) from particle size distribution curves, as presented in Table 3.

Table 3: Shape of grading curve (ISO 14688-2:2017)

Term	C_u	C_c
Uniformly graded	< 3	< 1
Poorly graded	3 to 6	< 1
Medium graded	6 to 15	< 1

Term	C_u	C_c
Well graded	> 15	1 to 3
Gap graded	> 15	< 0.5

Sands and gravels are subdivided into coarse, medium, and fine, as defined in Table 4. Predominant size fractions are stated as, for example, 'fine and medium GRAVEL' or 'fine to coarse SAND'. The use of the conjunctions 'and' or 'to' allows differentiation between predominant fractions and a range of sizes.

Table 4: Particle size fractions of coarse soils (ISO 14688-1:2017)

Soil	Particle Size Range [mm]		
	Coarse	Medium	Fine
Gravel	63 to 20	20 to 6.3	6.3 to 2
Sand	2 to 0.63	0.63 to 0.2	0.2 to 0.063

Fine Soils

Fine soils are classified as clay or silt based on their plasticity. The description of plasticity on-site can be carried out using the terms low plasticity or high plasticity, based on hand tests. In a laboratory, plasticity can be determined based on the results of Atterberg limits tests (Table 5).

Table 5: Plasticity classification (ISO 14688-2:2017)

Term	Liquid Limit, w_L [%]
Low Plasticity	< 35
Medium Plasticity	35 to 50
High Plasticity	50 to 70
Very High Plasticity	> 70

Soils consisting solely of coarse silt may not demonstrate plasticity. They are described as silt rather than fine sand, if the grains cannot be seen with the naked eye. The distinction between clay and silt is often taken as the 'A-line', defined as $I_p = 0.73 (w_L - 20)$, on a plasticity chart. Fine soil is classified as clay if:

$$I_p \geq 6 \text{ and } I_p \geq 0.73 (w_L - 20)$$

where:

- I_p = plasticity index [%]
- w_L = liquid limit [%]

A plasticity chart may also show a 'U-line' defined (in percentages) as $I_p = 0.9 (w_L - 8)$ and $w_L \geq 16$ %, according to Casagrande (1948). The U-line represents an approximate upper limit of correlation between plasticity index and liquid limit for natural soils.

Secondary descriptors in a fine soil may be used for materials that show behaviour that is borderline between those showing clay-like and silt-like behaviour, hence 'silty CLAY' or 'clayey SILT'. These terms are qualitative only.

Particle Shape

Description of particle shape applies to gravel, cobbles and boulders. It typically covers the angularity of the particles (degree of rounding at edges and corners), the general form, and surface characteristics. The terms in Table 6 can be used, where appropriate.

Table 6: Designation of particle shape (ISO 14688-2:2017)

Parameter	Term
Angularity/Roundness	Very angular
	Angular
	Subangular
	Subrounded
	Rounded
	Well rounded

Parameter	Term
Form	Cubic
	Flat (or tabular)
	Elongate
Surface Texture	Rough
	Smooth

Secondary Fractions

Table 7 presents terms for ranges of secondary fractions. If the secondary fraction is coarse, proportions are assessed by mass of different size fractions and the term 'slightly' or 'very' can precede the qualifying term.

Table 7: Mixtures of coarse and fine soils (BS 5930:2015+A1:2020)

Term	Principal Soil Type	Approximate Proportion of Secondary Fraction by Mass	
		Coarse Soil	Coarse and/or Fine Soil
-	SAND and GRAVEL	About equal proportions	-
Slightly clayey or slightly silty	SAND and/or GRAVEL	-	< 5 %
Clayey or silty		-	5 % to 20 %*
Very clayey or very silty		-	> 20 %*
Slightly sandy or slightly gravelly		< 5 %	-
Sandy or gravelly		5 % to 20 %	-
Very sandy or very gravelly		> 20 %	-
Slightly sandy and/or slightly gravelly	SILT [†] or CLAY [†]	< 35 %	-
Sandy or gravelly		35 % to 65 %	-
Very sandy or very gravelly		> 65 % [‡]	-

Notes:
* = Or described as fine soil depending on soil behaviour
† = Can be silty CLAY or clayey SILT
‡ = Or described as coarse soil depending on assessed soil behaviour

Soil Colour

Soil colours are described using a Munsell soil colour system (e.g. Gretag-Macbeth, 2000). The Munsell colour is arranged according to three variables known as Hue, Value and Chroma. The Hue notation of a colour indicates its relation to red, yellow, green, blue and purple. The Value notation indicates the relative lightness. The Chroma notation indicates the intensity of the colour.

Bedding and Interbedding

Layers of different soil types within a stratum are called bedding units. If beds of alternating or different soil types are too thin to be described as individual strata, the soil is described as interbedded or interlaminated, using the terms in Table 8, as appropriate. Where the soil types are approximately equal, 'thinly interlaminated SAND and CLAY' would, for example, be appropriate. Where one material is dominant, the subordinate material is described with a bed thickness and a bed spacing (using bedding and discontinuity spacing terms in Table 8 and Table 9 respectively), e.g. 'SAND with closely spaced thick laminae of clay'. Where two or more soils types are present in a deposit, arranged in an irregular manner, the soil is described as mixed, e.g. 'SAND with gravel size pockets (20 mm to 35 mm) of CLAY'. The spacing of sedimentary features (e.g. shell bands) and of minor structures (e.g. root holes in soils) are reported as measurements or using the spacing terms for discontinuities. These are descriptive terms that have no size connotation (e.g. pocket, lens, inclusion); where such terms are used their size, spacing and frequency are reported.

If the secondary fraction is fine, it is identified as 'clayey' or 'silty' on the basis of its plasticity. The terms 'silty' and 'clayey' are mutually exclusive, e.g. 'gravelly clayey fine SAND'. On the other hand, the terms 'sandy' and 'gravelly' may both be used, in which case the percentages are assessed separately, e.g. 'slightly gravelly slightly sandy CLAY' means that the soil contains up to 35 % sand and up to 35 % gravel (by dry weight).

The secondary fractions as adjectives are placed with the term describing the primary fraction in the order of increasing proportion when there are two coarse soil secondary features, or coarse and then fine if one of each.

Table 8: Bedding and interbedding thickness

Term	Thickness of Bedding Unit [mm]
Thinly (inter)laminated With [†] thin laminae	< 6
Thickly (inter)laminated With [†] thick laminae	6 to 20
Very thinly (inter)bedded [‡] With [†] very thin beds [‡]	20 to 60
Thinly (inter)bedded [‡] With [†] thin beds [‡]	60 to 200
Medium (inter)bedded [‡] With [†] medium beds [‡]	200 to 600
Thickly (inter)bedded [‡] With [†] thick beds [‡]	600 to 2000
Very thickly (inter)bedded [‡] With [†] very thick beds [‡]	> 2000

Notes:
† = Use 'with' or other quantifying term as appropriate
‡ = Use 'bedded' or other fabric name as appropriate

Discontinuities

The term discontinuity is used to describe surfaces that separate soils of different types or form planes of weakness within the soil. Discontinuities include fissures and shear planes, and the descriptor refers to the mean spacing between such discontinuities in a soil mass. A soil is 'fissured' when it breaks into blocks along unpolished discontinuities, and 'sheared' when it breaks into blocks along polished discontinuities (which is equivalent to a slickensided soil). The spacing description (Table 9) ranges from extremely closely spaced (< 20 mm) to very widely spaced (> 2000 mm). No other descriptive terms are

used. An example would be: 'firm grey very closely fissured fine sandy calcareous CLAY with frequent silt partings'.

The spacing terms are also used for distances between partings, isolated beds or laminae, desiccation cracks, rootlets, etc.

The surface texture of discontinuities is described, e.g. rough, smooth, or polished, as well as any colour changes or staining on discontinuities and any infilling.

Table 9: Discontinuity spacing (ISO 14688-2:2017)

Term	Spacing of Discontinuities [mm]
Extremely closely spaced	< 20
Very closely spaced	20 to 60
Closely spaced	60 to 200
Medium spaced	200 to 600
Widely spaced	600 to 2000
Very widely spaced	> 2000

Relative Density of Coarse Soils

Usually, soil description offers little evidence about the relative density of coarse soils. The reason for this is the substantial sampling disturbance incurred during conventional sampling operations such as push sampling, percussion sampling, and vibrocoring. Complementary investigation techniques, such as cone penetration tests (CPT), are usually necessary. Relative density is the ratio of the difference between laboratory index void ratios of a coarse (cohesionless) soil in its loosest state and existing in situ state to the difference between its void ratios in the loosest and densest states. Loosest and densest states are relative to laboratory test methods.

Relative density is referred to in BS 5930 in terms of N-values obtained by the standard penetration test (SPT). Results of such tests may not be available. Rather than using SPT-based values, it is common practice to interpret relative density on the basis of CPT results. Ranges of relative density are given in Table 10. These ranges are in common use in the industry. They were originally presented in Lambe and Whitman (1969).

Table 10: Relative density of coarse soils

Relative Density Term	Range of Relative Density [%]
Very loose	< 15
Loose	15 to 35
Medium dense	35 to 65
Dense	65 to 85
Very dense	> 85

Consistency and Undrained Shear Strength of Fine Soils

The consistency of fine soils can be described according to Table 11. Undrained shear strength can be classified using the terms given in Table 12.

Table 11: Description of consistency (ISO 14688-1:2017)

On-site Description Term	Definition
Very soft	Finger can be easily pushed in up to 25 mm Soil exudes between the fingers when squeezed in the hand
Soft	Finger can be pushed in up to 10 mm Soil can be moulded by light finger pressure

On-site Description Term	Definition
Firm	Thumb makes an impression easily Soil cannot be moulded by fingers, but rolls in the hand to 3 mm thick threads without breaking or crumbling
Stiff	Soil can be indented slightly by thumb Soil crumbles and breaks when rolling to 3 mm thick threads but is still sufficiently moist to be moulded to a lump again
Very stiff	Soil can be indented by thumb nail Soil cannot be moulded but crumbles under pressure

Table 12: Classification of strength (after BS 5930:2015+A1:2020)

Term Based on Measurement	Undrained Shear Strength, s_u [kPa]
Extremely low strength	< 10
Very low strength	10 to 20
Low strength	20 to 40
Medium strength	40 to 75
High strength	75 to 150
Very high strength	150 to 300
Extremely high strength	> 300

If a mineral cement appears to be present, the [nature and] degree of cementing is typically noted, e.g. 'slightly [iron oxide] cemented sand' or preferably using rock strength terms, e.g. 'very weak [carbonate] cemented SANDSTONE'.

Classification of cementation follows rock strength classification (Table 13) expressed as unconfined compressive strength σ_c :

Table 13: Cementation

Cementation	σ_c [MPa]
Slightly cemented	0.3 to 1.25
Moderately cemented	1.25 to 5.0
Well cemented	5.0 to 12.5

The term 'well cemented' in Table 13 applies to soil which also shows sublayers with little or no cementation. In case of further lithification, the soil description becomes a rock description.

Mineral Constituents and Tertiary Fractions

Mineral constituents are generally reported before the primary soil fraction, using qualitative terms such as 'slightly micaceous', 'glaucanitic' or 'very shelly'. For beds of material within a soil matrix, the terminology for spacing and thickness of beds is used. For individual particles of soil or material within a soil matrix, the terms 'partings' and 'pockets' may be used.

Tertiary fractions within the soil, such as shell or wood fragments, glauconite grains, plant remains, or small soil inclusions (such as partings or pockets), can be quantified using the terms 'with rare' (< 1 % by volume), 'with occasional' (1 % to 5 % by volume), 'with frequent' (5 % to 20 % by volume), 'with numerous' (20 % to 30 % by volume), and 'with abundant' (> 30 % by volume). These terms are usually added at the end of the primary soil description (e.g. 'with frequent shell fragments', 'with rare silt pockets'). The size of the tertiary constituents can be given in mm.

Soil Odour

For anthropogenic soils, odour can be described. Terms used to describe the odour are for example 'H₂S', 'musty', 'putrid', or 'chemical'. It is emphasised that soil odour descriptions are unlikely to be fully consistent, because of factors such as variations in sample handling, ambient conditions at time of sample description, and strong dependence on a person's ability to detect and identify odour.

Soil Description and Classification using ASTM D2487 and ASTM D2488

The ASTM standards for soil description and classification are applicable to naturally occurring soils passing a 3 inch (75 mm) sieve. The standards identify three major soil types: coarse-grained, fine-grained, and highly organic soils. The major soil types are further subdivided into 15 specific basic soil groups.

Before a soil can be classified according to these standards, generally the particle size distribution of the minus 75 mm material and the plasticity characteristics of the minus 0.425 mm sieve material are determined.

The identification and description of silica soils in the ASTM system consists primarily of a group name and symbol, which are based on particle size distribution and plasticity, and the results of other laboratory classification tests.

Based on the results of visual observations and prescribed laboratory tests, a soil is catalogued according to the basic soil groups, assigned a group symbol(s) and name, and thereby classified.

Soil Types

The initial classification of soils as coarse-grained or fine-grained is based on percentage fines. ASTM defines the fine-coarse boundary as 0.075 mm.

A soil can be classified as coarse-grained (sand or gravel) if the percentage fines is 50 % or less. Coarse-grained soils are further classified as either sand or gravel using the results of particle size distribution analyses.

Classification of fine-grained soils (silt or clay) is based on plasticity (liquid limit and plasticity index from Atterberg limits tests).

A soil is classified as highly organic when it contains sufficient quantities of dispersed organic matter that it has an influence on the liquid limit. The soil is an organic silt or organic clay if the liquid limit after oven drying is less than 75 % of the liquid limit of the original specimen determined before oven drying.

Peat is generally classified according to the degree of decomposition and strength. When encountered, reference can also be made to the classification given in ASTM standard D4427-18.

Soil Group Name and Group Symbol

Coarse-Grained Soils

For coarse-grained soils, the dominant soil fraction is sand if the dry weight of the sand fraction, i.e. particle sizes from 0.075 mm to 4.75 mm, exceeds that of the gravel fraction, i.e. particles ranging from 4.75 mm to 75 mm, and vice versa for gravel.

Coarse-grained soils are also described as well-graded or poorly-graded based on the particle-size distribution curve, using the coefficient of uniformity (C_u) and, to a lesser extent, the coefficient of curvature (C_c) as follows:

Particle size grading of coarse-grained soils with $\leq 12\%$ fines can be designated based on (C_u) and (C_c) from particle size distribution curves, as presented below:

- Sands are well-graded when $C_u \geq 6$ and C_c is between 1 and 3, and for $< 5\%$ fines ('SW')
- Sands are poorly-graded for other values of C_u and C_c , and for $< 5\%$ fines ('SP')
- Gravels are well-graded when $C_u \geq 4$ and C_c is between 1 and 3, and for $< 5\%$ fines ('GW')
- Gravels are poorly-graded for other values of C_u and C_c , and for $< 5\%$ fines ('GP').

For coarse-grained soils with fines contents $> 12\%$, these terms are not used. In this case, the soil is considered a coarse-grained soil with fines. The fines are determined as either clayey or silty based on the plasticity index versus liquid limit plot. Classify the soil as a clayey gravel, 'GC', or clayey sand, 'SC', if the fines are clayey. Classify the soil as a silty gravel, 'GM', or silty sand, 'SM', if the fines are silty (definition of 'clay(ey)' and 'silt(y)' as per section on fine-grained soils below).

If the fines are classified as a silty clay, 'CL-ML', classify the soil as a silty, clayey gravel, 'GC-GM', if it is a gravel or a silty, clayey sand, 'SC-SM', if it is a sand.

If the sample contains between 5 % and 12 % fines, the soil gets a dual classification using two group symbols. The first group symbol corresponds to that for a gravel or sand having $< 5\%$ fines ('GW', 'GP', 'SW', 'SP'), and the second symbol corresponds to a gravel or sand having $> 12\%$ fines ('GC', 'GM', 'SC', 'SM'). The group name corresponds to the first group symbol plus 'with clay' or 'with silt' to indicate the plasticity characteristics of the fines (for example: 'well-graded gravel with clay, GW-GC', 'poorly graded sand with silt, SP-SM').

If the specimen is predominantly sand or gravel but contains 15 % or more of the other coarse-grained constituent, the words 'with gravel' or 'with sand' is added to the group name.

Sands and gravels are sub-divided into coarse, medium, and fine, as defined in Table 14.

Table 14: Size fraction descriptions for coarse-grained soils

Soil	Particle Size Range [mm]		
	Coarse	Medium	Fine
Gravel	19 to 75	-	4.75 to 19
Sand	2.0 to 4.75	0.425 to 2.0	0.075 to 0.425

Fine-Grained Soils

Fine-grained soils are classified as clay or silt according to the results of Atterberg limits tests.

The soil is an inorganic clay if the liquid limit versus plasticity index plots on or above the A-line, $I_p > 4\%$, and the presence of organic matter does not influence the liquid limit (i.e. liquid limit after oven drying is $\geq 75\%$ of the liquid limit of the original specimen determined before oven drying).

The soil is then further classified as lean clay if $w_L < 50\%$, and given the group symbol 'CL', or as fat clay if $w_L \geq 50\%$ with group symbol 'CH'.

Soils are classified as silty clay where the liquid limit versus plasticity index plots on or above the A-line but where the plasticity index falls within the range $4 \leq I_p \leq 7\%$. Silty clays are given the group symbol 'CL-ML'.

The soil is an inorganic silt if the liquid limit versus plasticity index plots below the A-line or if $I_p < 4\%$, and the presence of

organic matter does not influence the liquid limit (i.e. liquid limit after oven drying is $\geq 75\%$ of the liquid limit of the original specimen determined before oven drying).

The soil is then further classified as silt if $w_L < 50\%$, and given the group symbol 'ML', or as elastic silt if $w_L \geq 50\%$, with group symbol 'MH'.

where:

I_p = plasticity index
 w_L = liquid limit

If a fine-grained soil contains between 15 % and 30 % coarse material, the words 'with sand' or 'with gravel' (whichever is predominant) is added to the group name. For example, 'lean clay with sand, CL', 'silt with gravel, ML'. If the percentage of sand is equal to the percentage of gravel, use 'with sand'.

If a fine-grained soil contains $> 30\%$ coarse material, the words 'sandy' or 'gravelly' are added to the group name (whichever is predominant). For example, 'sandy lean clay, CL', 'gravelly fat clay, CH'. If the percentage of sand is equal to the percentage of gravel, use 'sandy'.

Organic Soils

If fine-grained soil has a dark colour and an organic odour when moist and warm, a second liquid limit test is performed on a test specimen which has been oven dried at 105 °C to a constant mass. For both clay and silt, or the fines component of a coarse-grained soil, the additional term organic applies if the ratio of the liquid limit of a sample (or the fines portion of the sample) after oven drying at 105 °C to the liquid limit without oven drying is less than 0.75.

Organic soils are classified in a manner similar to that for inorganic soils for plots of the liquid limit (not oven dried) versus plasticity index with respect to the A-line. Organic clays and silts

Secondary Constituents

Table 16 presents a summary of terms used for ranges of secondary constituents. Applicable group symbols are defined above.

Table 16: Mixtures of coarse-grained soils and fine-grained soils

Term	Principal Soil Type	Term	Approximate Proportion of Secondary Constituent	
			Coarse-Grained Soils	Fine-Grained Soils
-	SAND and/or GRAVEL*	-	-	< 5 %
-	SAND and/or GRAVEL*	with clay or silt	-	5 % to 12 %
Clayey or silty	SAND and/or GRAVEL*	-	-	> 12 %
-	SAND and/or GRAVEL*	-	< 15 % gravel or sand	-
-	SAND and/or GRAVEL*	with sand or gravel	$\geq 15\%$ gravel or sand	-
-	SILT or CLAY	-	< 15 %	-
-	SILT or CLAY	with sand or gravel*	15 % to 29 %	-
Sandy and/or gravelly*	SILT or CLAY	-	$\geq 30\%$	-

Notes:
 * = Selection depends on which fraction has a higher percentage

Soil Colour

Soil colours are described using a Munsell soil colour system (e.g. Gretag-Macbeth, 2000).

Structure

Criteria for describing soil structure are provided in Table 17, along with additional terms in use in the geotechnical industry.

with liquid limit $w_L < 50\%$ are given the same group symbol 'OL'. Organic clays and silts with liquid limits $w_L \geq 50\%$ are given the group symbol 'OH'.

Coarse-grained soils containing fine organic material are described using the term 'with organic fines'.

Particle Shape

The description of particle shape includes references to shape and angularity. These terms are normally used only for gravels, cobbles, and boulders, though in some cases for coarse sands.

The shape of coarse particles is described as flat, elongated, or both.

- Flat: particles with width/thickness > 3
- Elongated: particles with length/width > 3
- Flat and elongated: particles meet criteria for both flat and elongated.

Angularity terms (Table 15) are usually only applied to particles of coarse sand size and larger. A range of angularity may be stated, such as 'subrounded to rounded'.

Table 15: Angularity of coarse-grained particles

Term	Criteria
Angular	Particles have sharp edges and relatively plane sides with unpolished surfaces
Subangular	Particles are similar to angular description but have rounded edges
Subrounded	Particles have nearly plane sides but have well-rounded corners and edges
Rounded	Particles have smoothly curved sides and no edges

Table 17: Criteria for describing structure

Description	Criteria
Stratified	Alternating layers of varying material or colour with the layers ≥ 6 mm thick
Laminated	Alternating layers of varying material or colour with the layers < 6 mm thick
Fissured	Breaks along definite planes of fracture with little resistance to fracturing
Slickensided	Fracture planes appear polished or glossy, sometimes striated

Description	Criteria
Blocky	Cohesive soil that can be broken down into small angular lumps which resist further breakdown
Lensed	Inclusion of small pockets of different soils, such as small lenses of sand scattered through a mass of clay
Homogeneous	Same colour and appearance throughout
Gassy*	Soil has a porous nature and there is evidence of gas, such as blisters
Expansive*	Visibly expands after sampling
Platy*	A stratified appearance when the soil can be broken into thin horizontal plates
Cemented*	Material grains bound together forming an intact mass
Notes: * = not part of ASTM D2488	

The distance between the fissures, shear planes and expansion cracks is noted using the terms in Table 9.

Consistency and Undrained Shear Strength of Fine-Grained Soils

The consistency of fine soils can be assessed on site, in case of no on-site laboratory. Table 18 shows terms for the designation of consistency of fine-grained soils in accordance with the results of manual tests.

Table 18: Criteria for describing consistency

Description	Criteria
Very soft	Thumb will penetrate soil more than 25 mm
Soft	Thumb will penetrate soil about 25 mm
Firm	Thumb will indent soil about 6 mm
Hard	Thumb will not indent soil but readily indented with thumbnail
Very hard	Thumbnail will not indent soil

Descriptions of undrained shear strength of fine-grained soils are not part of the ASTM classification system. If required by project specifications, undrained shear strength ranges according to Table 19 can be presented.

Table 19: Undrained shear strength of fine-grained soils

Term	Undrained Shear Strength*	
	[kPa]	[ksf] [†]
Very soft	< 12.5	< 0.25
Soft	12.5 to 25	0.25 to 0.50
Firm	25 to 50	0.50 to 1.0
Stiff	50 to 100	1.0 to 2.0
Very stiff	100 to 200	2.0 to 4.0
Hard [‡]	200 to 400	4.0 to 8.0
Very hard [‡]	> 400	> 8.0
Notes: * = From Terzaghi and Peck (1967) † = ksf used primarily for US projects ‡ = Upper boundary for 'hard', and a range for 'very hard' have been added		

Table 20: Description and classification of non-indurated carbonate soils (based on Clark & Walker, 1977)

Fine Soils		Coarse Soils		Carbonate Content (% CaCO ₃)
CLAY	SILT	Silica SAND	GRAVEL	< 10
Calcareous CLAY	Calcareous SILT	Calcareous silica SAND	Mixed carbonate and non-carbonate GRAVEL	10 to 50
Carbonate CLAY	Siliceous carbonate SILT	Siliceous carbonate SAND		50 to 90
Carbonate CLAY	Carbonate SILT	Carbonate SAND	Carbonate GRAVEL	> 90

Written Soil Descriptions

In a soil description, the main characteristics are typically given using the following standard word sequence, as applicable:

1. Relative density/consistency/undrained shear strength
2. Discontinuities
3. Bedding
4. Colour
5. Composite soil types: particle size distribution and grading, shape and size
6. Tertiary fractions either before or after the primary soil fraction as appropriate
7. PRIMARY SOIL FRACTION, based on grading and plasticity

For example: Firm closely fissured dark olive grey sandy calcareous CLAY with few silt pockets.

Description of Carbonate Soils using Clark & Walker (1977)

For carbonate soils, the classification system by Clark and Walker (1977) may be used to describe the carbonate content, particle size, and degree of induration.

Particle Size

Clark & Walker (1977) follows approximately the same boundaries between clay, silt, sand and, gravel fractions as used in BS 5930:2015+A1:2020 and ISO 14688-1:2017.

Carbonate Content

Carbonate content is used for non-indurated (unconfined compressive strength < 300 kPa) carbonate soils in the Clark & Walker classification system (Table 20). The description method does not distinguish between types of carbonate material and assumes that non-carbonate particles are siliceous.

Induration

Induration is the process of hardening of sediments through cementation and/or compaction. Degree of induration is classified by Clark & Walker (1977) by means of unconfined compressive strength. In Table 20, terms for non-indurated (unconfined compressive strength $\sigma_c < 0.3$ MPa) carbonate deposits are given, and in Table 21 for slightly ($\sigma_c = 0.3$ MPa to $\sigma_c = 12.5$ MPa) and moderately indurated ($\sigma_c = 12.5$ MPa to $\sigma_c = 100$ MPa) carbonate deposits.

Table 21: Description and classification of slightly to highly indurated carbonate soils and rocks (based on Clark & Walker, 1977)

Grain Size of Particulate Deposits				Carbonate Content [% CaCO ₃ of soil dry mass]	σ_c [MPa]
< 0.002 mm	0.002 mm to 0.06 mm	0.06 mm to 2 mm	2 mm to 60 mm		
Slightly Indurated					
CLAYSTONE	SILTSTONE	SANDSTONE	CONGLOMERATE or BRECCIA	< 10	0.3 to 12.5
Calcareous CLAYSTONE	Calcareous SILTSTONE	Calcareous SANDSTONE	Calcareous CONGLOMERATE	10 to 50	
Clayey CALCILUTITE	Siliceous CALCISILTITE	Siliceous CALCARENITE	Conglomeratic CALCIRUDITE	50 to 90	
CALCILUTITE	CALCISILTITE	CALCARENITE	CALCIRUDITE	> 90	
Moderately Indurated					
CLAYSTONE	SILTSTONE	SANDSTONE	CONGLOMERATE or BRECCIA	< 10	12.5 to 100
Calcareous CLAYSTONE	Calcareous SILTSTONE	Calcareous SANDSTONE	Calcareous CONGLOMERATE	10 to 50	
Fine-grained argillaceous LIMESTONE	Fine-grained siliceous LIMESTONE	Siliceous detrital LIMESTONE	Conglomeratic LIMESTONE	50 to 90	
Fine-grained LIMESTONE		Detrital LIMESTONE	Conglomerate LIMESTONE	> 90	

The Clark & Walker system does not include reef limestone (biolithite). Reef limestone represents an in situ accumulation of biological origin (e.g. coral reef) and consists largely of carbonate skeletal material of colonising organisms. The carbonate content normally exceeds 90 %. Classification of strength follows rock description procedures.

Particulate Deposits

The geological origin of a single particle type allows the following descriptions (optional).

Clastic

Sediment transported and deposited as grains of inorganic origin. Typical clastic particles are:

- quartz grains: clear or milky white and ranging from very angular to very rounded; commonly a frosted surface for wind-blown grains;
- feldspar grains: varying in colour from milky white to light yellowish brown;
- mica flakes: varying in colour from gold-coloured to dark brown;
- dark mineral grains: usually of igneous or metamorphic origin with undetermined mineralogy;
- silicate grains: undetermined mineralogy;
- rock fragments: including fragments of carbonate rock;
- debris: deposit of rock fragments of a variety of particle sizes which may include sand and finer fractions; typical examples are rock debris and coral debris.

Organic

Remains of plants and animals that consist mainly of carbon compounds.

Bioclastic

Sediment transported and deposited as grains of organic origin. Examples of bioclastic particles are:

- Calcareous algae: crustal or nodular growths or erect and branching forms produced by lime-secreting algae; microstructures include layered, rectangular structures and internal fine tube-like structures;

- Foraminifera: hard sediment test (external skeleton) consisting of calcite or aragonite and produced by unicellular organisms; commonly less than 1 mm in diameter, multi-chambered and intact;
- Sponge spicules: spicules of siliceous sponges in a variety of rayed shapes; dimensions ranging from less than 1 mm to over 1 cm in length but usually less than 1 mm in width;
- Corals: commonly consisting of small fibres set perpendicular to the walls and septal surfaces; mainly aragonite composition for relatively recent forms; conversion of aragonite to calcite for earlier corals, usually with consequent loss of original structural details;
- Echinoids: hard part of echinoids consisting of a plate or skeletal element forming a single crystal of calcite; five-rayed internal symmetry for spines of echinoids; typical widths ranging from several mm to a few cm;
- Bryozoans: chambered cell-like structures that are considerably coarser than those of calcareous algae; either aragonite or calcite composition; possible cell in-fill consisting of clear calcite and/or micrite;
- Bivalves and gastropods: mollusk shells, chiefly of aragonite composition; inner layer of aragonite protected by an outer layer of calcite for some bivalve shells and gastropods.

Oolitic

Sediment consisting of solid, round or oval, highly polished and smooth coated grains, which may or may not have a nucleus. The coating consists of chemically precipitated aragonite, possibly converted to calcite. Oolites have concentric structures and may also have radial structures. The grains are generally less than 2 mm diameter.

Pelletal

Sediment consisting of well-rounded grains of ellipsoidal shape and no specific internal structure. The composition is clay to silt-sized carbonate material, which is probably the excretion product of sediment-eating organisms. Pellets may have an oolitic crust. The grains are generally less than 2 mm diameter.

Structure of Non Particulate Deposits

Reef

Soil or rock formed by in situ accumulation or build-up of carbonate material by colonial organisms such as polyps (coral), algae (algal mats or balls) and sponges.

Orthochemical

Orthochemical components precipitated during or after deposition. These components can include: (1) pyrite spherulites and grains, (2) crystal euhedra of anhydrite or gypsum, (3) replacement patches and nodular masses of anhydrite and gypsum. Single grains are rare.

Geological Information

Specific geological terms can assist the geotechnical soil description by providing information on stratigraphy, origin (genesis) or regional significance (optional). Examples are:

- Time stratigraphy, such as Eemian and Pleistocene
- Lithostratigraphy, such as Yarmouth Roads Formation
- Depositional environment, such as marine, glacio-lacustrine and residual soil
- Regional significance, such as chalk and mud.

References

ASTM International (2017). *Standard practice for classification of soils for engineering purposes (unified soil classification system)* (ASTM D2487 - 17). <https://www.astm.org/Standards/D2487>

ASTM International (2017). *Standard practice for description and identification of soils (visual-manual procedure)* (ASTM D2488 - 17e1). <https://www.astm.org/Standards/D2488.htm>

ASTM International (2018). *Standard classification of peat samples by laboratory testing* (ASTM D4427-18). <https://www.astm.org/Standards/D4427.htm>

BSI (2020). *Code of practice for ground investigations* (BS 5930:2015+A1:2020). <https://shop.bsigroup.com/ProductDetail/?pid=000000000030400754>

Casagrande, A. (1947). Classification and Identification of Soils. In *Proceedings of the American Society of Civil Engineers*,. 73, 6, 783-810.

Clark, A.R., & Walker, B.F. (1977). A proposed scheme for the classification and nomenclature for use in the engineering description on Middle Eastern sedimentary rocks. *Géotechnique*, 27(1), 93–99.

Gretag-Macbeth (2000). *Munsell Soil Color Charts*. Year 2000 revised washable edition. New Windsor.

International Organization for Standardization (2017). Geotechnical investigation and testing - identification and classification of soil - part 1: identification and description (ISO 14688-1:2017). <https://www.iso.org/standard/66345.html>

International Organization for Standardization (2017). Geotechnical investigation and testing - identification and classification of soil - part 2: principles for a classification (ISO 14688-2:2017). <https://www.iso.org/standard/66346.html>

International Organization for Standardization (2014). *Petroleum and natural gas industries – specific requirements for offshore structures – part 8: marine soil investigations* (ISO 19901-8:2014). <https://www.iso.org/standard/61145.html>

Lambe, T.W., & Whitman, R.V. (1969). *Soil mechanics*. John Wiley & Sons.

Terzaghi, K. & Peck, R.B. (1967). *Soil Mechanics in Engineering Practice*. (2nd ed.), John Wiley & Sons.

Cone Penetration Test

Introduction

The cone penetration test (CPT) involves the measurement of the resistance of ground to steady and continuous penetration of a cone penetrometer equipped with internal sensors. The measurements comprise penetration depth, cone resistance, sleeve friction and, optionally, pore pressure and inclination from vertical. These measurements permit interpretation of ground conditions.

CPT apparatus and procedures adopted by Fugro are in general accordance ISSMGE (1999), ASTM (2020), ISO (2012) and ISO (2014). BS 5930 (BSI, 2015) refer to ISSMGE (1999). General agreement also applies to Eurocode 7 (CEN, 2007).

Fugro offers CPT systems operated from (1) ground surface and seafloor (non-drilling deployment mode) and (2) downhole in a borehole (drilling deployment mode).

CPT Apparatus

General

CPT apparatus includes various parts as described below:

- Thrust machine: apparatus providing thrust to the push rods so that the recommended rate of penetration (20 mm/s) is controlled;
- Reaction equipment: reaction for the thrust machine;
- Push rod: thick-walled cylindrical tube used for advancing the penetrometer to the required test depth. Push rods may also consist of drill pipe;
- Friction-cone penetrometer (CPT): cylindrical terminal body mounted on the lower end of the push rods, including a cone, a friction sleeve and internal sensing devices for the measurement of cone resistance, sleeve friction and, optionally, inclination;
- Piezocone penetrometer (CPTU or PCPT): cylindrical terminal body mounted on the lower end of the push rods, including a cone, a friction sleeve, a filter and internal sensing devices for the measurement of cone resistance, sleeve friction, pressure and, optionally, inclination;
- Measuring system: apparatus and software, including sensors, data transmission apparatus, recording apparatus and data processing apparatus.

Deployment from ground surface or seafloor

Specific additional apparatus for CPT deployment from ground surface and seafloor can include:

- Push rod casing: guide for the part of the push rods protruding above the soil, and for the push rod length exposed in water or soil, to prevent buckling when the required penetration pressure increases beyond the safe limit for the exposed upstanding length of push rods;
- Friction reducer: ring or special projections fixed on the outside of the push rods, with an outside diameter larger than the base of the cone, to reduce soil friction acting on the push rods.

Downhole Borehole Deployment

Downhole CPT systems latch into a bottom hole assembly at the lower end of a drill pipe. System options are:

1. Operation of a downhole thrust machine by applying mud pressure in the borehole;

2. Remote control of a downhole thrust machine by hydraulic pressure transmitted through an umbilical cable connected to a surface-based pump unit, together with;
3. Application of thrust to drill rods where CPT apparatus and a short push rod are latched in the bottom hole assembly; the thrust machine is at ground surface or seafloor.

Data recording can be surface-based and/or downhole.

Downhole CPTs require drilling apparatus for advancing the borehole. The maximum CPT stroke is generally 1.5 m or 3 m.

Cone Penetrometer

Typical features of Fugro penetrometers (Figure 1) include:

- Cone base areas of 500 mm², 1000 mm² or 1500 mm²; other sizes are also in use, e.g. 3300 mm²;
- Cone and friction sleeve sensors placed in series, i.e. subtraction-type penetrometers;
- Pore pressure measurements either at the face of the cone (u_1) or at the cylindrical extension of the cone (u_2). Multiple-sensor penetrometers (u_1 , u_2 and u_3) are also available. The u_3 location is immediately above the friction sleeve;
- Incliner;
- Storage of signals from the penetrometer in digital form for subsequent computer-based processing and presentation.

Procedure

Figure 2 summarises the test procedure. The procedure includes several stages. The stage of Additional Measurements is optional.

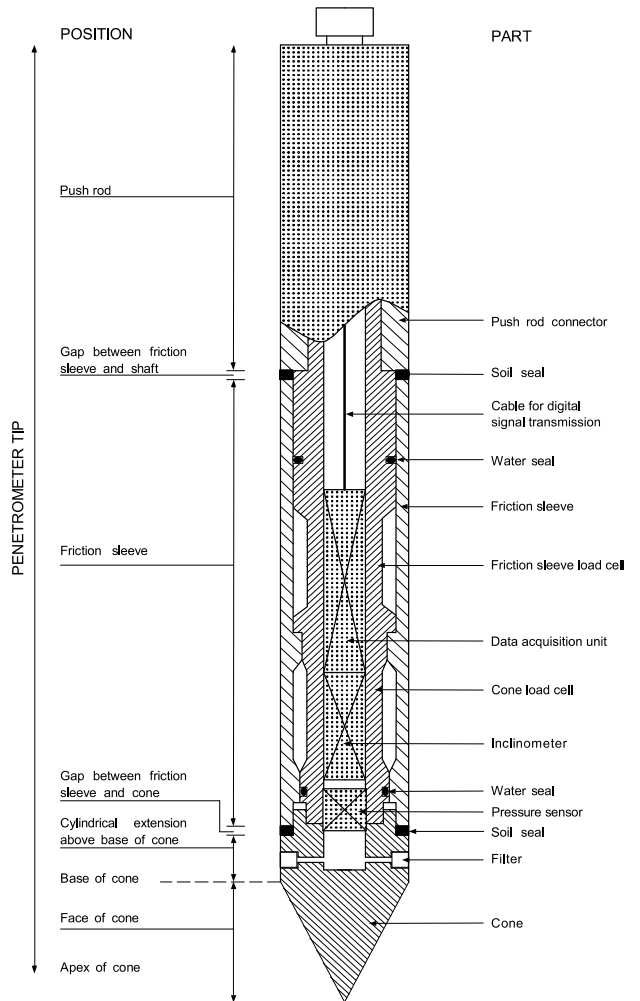


Figure 1: Piezocone Penetrometer

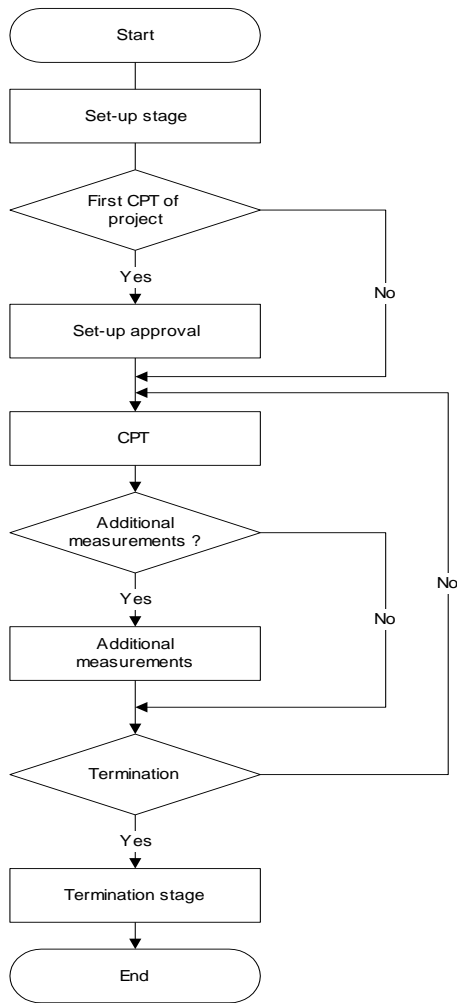


Figure 2: Flow chart

The set-up stage is at discretion of the equipment operator, particularly considering suitability of expected ground type(s), accessibility, risk of damage to equipment and safety of persons.

Set-up requires a reasonably flat, accessible, ground surface with a slope of 5° or less. Most onshore thrust machines have levelling facilities allowing a vertical start of penetration. Seabed frames used for offshore CPT activities have no levelling facilities, i.e. start of penetration may not be vertical.

For over-water (marine/ offshore activities), additional accessibility considerations include:

- Minimum water depth for the selected pontoon, jack-up or vessel and the selected test equipment;
- Maximum water depth for the selected pontoon, jack-up or vessel;
- Maximum depth below water (sea) level of selected test equipment;
- Metocean conditions, particularly wind, waves, currents.

The set-up stage typically includes selection of equipment and procedures according to a required accuracy class or application class, type of cone penetrometer and data processing/ submission. Tables 1 and 2 summarise ISO application classes. The allowable minimum accuracy of a measured parameter is the larger value of the two quoted. A percentage value applies to the measured value and not to the measuring range. The concept of application classes considers intended soil conditions for selection of an application class. For example, Application Class 1 of ISO (2014) can be selected for 'very soft to soft soil deposits',

which is approximately equivalent to $q_c < 0.5$ to $q_c < 1$ MPa. In other words, Application Class 1 should not apply to 'mixed bedded soil profiles with weak to strong layers'.

The accuracy values apply to ground surface or seafloor as reference. They are uncoupled from uncertainty of spatial position below ground surface or seafloor.

The set-up stage or the termination stage includes the location survey, i.e. the determination of the coordinates and the ground surface elevation (or the water depth).

The set-up stage and the termination stage for a downhole CPT include lowering of the CPT apparatus into the borehole and lifting respectively. Most projects require multiple downhole tests in a single borehole.

Table 1: Application Classes (ISO, 2014)

Application Class	Parameter	Allowable Minimum Accuracy
1	Cone resistance	35 kPa or 5 %
	Sleeve friction	5 kPa or 10 %
	Pore pressure	25 kPa or 5 %
2	Cone resistance	100 kPa or 5 %
	Sleeve friction	15 kPa or 15 %
	Pore pressure	50 kPa or 5 %
3	Cone Resistance	200 kPa or 5 %
	Sleeve friction	25 kPa or 15 %
	Pore pressure	100 kPa or 5 %

Table 2: Application Classes (ISO, 2012)

Application Class	Parameter	Allowable Minimum Accuracy	Maximum Length between Measurements
1	Cone resistance	35 kPa or 5 %	20 mm
	Sleeve friction	5 kPa or 10 %	
	Pore pressure, Inclination	10 kPa or 2 % 2°	
	Penetration length	0.1 m or 1 %	
2	Cone resistance	100 kPa or 5 %	20 mm
	Sleeve friction	15 kPa or 15 %	
	Pore pressure, Inclination	10 kPa or 3 % 2°	
	Penetration length	0.1 m or 1 %	
3	Cone resistance	200 kPa or 5 %	50 mm
	Sleeve friction	25 kPa or 15 %	
	Pore pressure, Inclination	50 kPa or 5 % 5°	
	Penetration length	0.2 m or 2 %	
4	Cone resistance	500 kPa or 5 %	50 mm
	Sleeve friction	50 kPa or 20 %	
	Penetration length	0.2 m or 2 %	

For piezocone testing, the set-up stage also includes the following steps:

- Office-based or site-based: de-airing of the filter in glycerine by application of 24-hour vacuum and storage in a glycerine-filled container;
- On-site: glycerine filling of hollow space in the cone penetrometer and subsequent mounting of the filter;
- On-site: application of a flexible membrane around the filter to prevent loss of saturating fluid prior to the start of a test.

Land-based tests may include specific measures to help retention of filter saturation during penetration of partially saturated zones. Relaxation of requirements typically applies to offshore tests where water pressures will force entrapped air into solution.

Criteria for test termination are as follows, unless specifically agreed otherwise:

- As instructed by client;
- Reaching target penetration;
- Reaching maximum capacity of the thrust machine, reaction equipment, push rods and/or measuring sensors;
- Sudden increase in penetrometer inclination;
- Risk of damage to apparatus or safety of persons, at discretion of equipment operator or as determined by software algorithms;

whichever occurs first and as applicable. Note that ASTM and ISO standards provide no specific requirements for maximum penetrometer inclination from vertical. A value of 15° is commonly considered.

Special apparatus and procedures may apply to:

- Specific additional measurements (for example shear wave velocity);
- Specific applications (for example offshore tests and measurements for application/accuracy Classes 1 and 2).

Results

CPT Parameters

Presentation of results from cone penetration tests typically includes:

- CPT parameters q_c , f_s and R_f versus depth below ground surface or versus elevation;
- Additional CPTU parameters u_1 or u_2 and, optionally, q_t , q_n , B_q , Q_v , Q_{tv} , F_r and I_c for tests with pore pressure measurements;
- Optionally, inclination i for tests with inclination measurements;
- Standard graphical format and optional ASCII and AGS formats.

Most standards specify scales for graphical presentation as follows:

- Axis for penetration depth z : 1 scale unit = 1 m;
- Axis for cone resistance q_c , corrected cone resistance q_t and net cone resistance q_n : 1 scale unit = 2 MPa or 0.5 MPa;
- Axis for sleeve friction f_s : 1 scale unit = 50 kPa;
- Axis for friction ratio R_f : 1 scale unit = 2 %;
- Axis for pore pressure u : 1 scale unit = 0.2 MPa or 0.02 MPa;
- Axis for pore pressure ratio B_q : 1 scale unit = 0.5.

Graphical presentation aims for these scale units and scale ratios, where suitable and practicable.

The reference level of a test is (1) the ground surface for onshore tests, (2) the seafloor for nearshore and offshore tests. Historically, the bottom of the borehole was used as the reference level of downhole tests. Data processing presumes a hydrostatic pore pressure profile relative to seafloor, unless specifically indicated otherwise. The definition of CPT parameters is as follows:

z = penetration depth relative to ground surface or seafloor, corrected for inclination from vertical (i) where a test includes inclination measurements, as follows:

$$z = \int_0^l \cos i \cdot dl$$

where:

z = penetration depth for the conical base of the cone penetrometer

l = recorded penetration length

i = recorded inclination from vertical

q_c = cone resistance relative to the reference level of the test.

f_s = sleeve friction relative to the reference level of the test. A calculated depth correction applies so that the presented sleeve friction corresponds with the cone depth.

f_t = corrected sleeve friction relative to the reference level of the test. Sleeve friction is corrected for pore pressures acting on the end areas of the friction sleeve

$$f_t = f_s - \frac{(u_2 * A_{sb} - u_3 * A_{st})}{A_s}$$

or simplified to:

$$f_t = f_s - u_2 \frac{(A_{sb} - A_{st})}{A_s} \quad \text{or}$$

$$f_t = f_s - (u_2 * a_{fs})$$

where:

A_{sb} = cross sectional area in the gap between the friction sleeve and the cone

A_{st} = cross sectional area in the gap above the friction sleeve

A_s = surface area of the friction sleeve

a_{fs} = net area ratio of the friction sleeve $(A_{sb} - A_{st})/A_s$

R_f = ratio of sleeve friction to cone resistance (f_s/q_c). This calculated ratio is for the cone depth.

R_{ft} = corrected friction ratio (f_t/q_t). The ratio f_t/q_t applies if f_t is known.

I_{SBT} = non-normalized soil behaviour type index (Robertson, 2010)

$$I_{SBT} = [(3.47 - \log(q_c/P_a))^2 + (\log R_f + 1.22)^2]^{0.5}$$

where:

P_a = atmospheric pressure

u_1 = pore pressure at the face of the cone, relative to the reference level of the test.

u_2 = pore pressure at the cylindrical extension above the base of the cone or in the gap between the friction sleeve and the cone, relative to the reference level of the test.

u_3 = pore pressure immediately above the friction sleeve or in the gap above the friction sleeve, relative to the reference level of the test.

q_t = corrected cone resistance (also called total cone resistance). This includes corrections for hydrostatic and transient pore pressures, and cone construction. The corrected cone resistance is relative to ground surface or seafloor:

$$q_t = q_c + (1-a)u_2 \text{ or}$$

$$q_t = q_c + (1-a)[K(u_1 - u_0) + u_0]$$

Historically, equations for downhole tests were:

$$q_t = q_c + (1-a)u_2 + u_{0i} \text{ or}$$

$$q_t = q_c + (1-a)[K(u_1 + u_{0i} - u_0) + u_0] + a * u_{0i}$$

where:

a = net area ratio of the cross-sectional steel area at the gap between cone and friction sleeve to the cone base area. This ratio is penetrometer-type dependent. The a -factor indicates the effect of pore pressure on unequal cross-sectional areas of the cone.

u_0 = hydrostatic pore pressure at the cone, relative to the phreatic surface or the seafloor. This is a calculated value.

u_{0i} = hydrostatic pore pressure at the bottom of the borehole, relative to seafloor. This is a calculated value.

K = adjustment factor for the ratio of pore pressure at the cylindrical extension above the base of the cone to pore pressure on the cone face $K = (u_2 - u_0)/(u_1 - u_0)$

The term $u_2 - u_0$ refers to excess pore pressure (with respect to hydrostatic pore pressure). Common symbols for excess pore pressure are du_2 or Δu_2 . Similarly, du_1 or Δu_1 can represent the term $u_1 - u_0$.

The K -factor is only of interest for processing of CPTU results with pore pressure measurement at the cone face (u_1). The factor depends on soil characteristics such as fabric, overconsolidation ratio, compressibility and crushability. The K -factor (Peuchen et al., 2010) can be estimated from:

$$K = 0.91e^{-0.09Q_t^{0.47}} \left(\frac{1}{1 + F_r(0.17 + 0.061(Q_t - 21.6)^{1/3})} - e^{-2F_r} \right)$$

q_n = $q_t - \sigma_{vo}$ = net cone resistance. This includes corrections for hydrostatic and transient pore pressures, in situ stress, and cone construction. The symbol for q_n may also be q_{net} .

where:

σ_{vo} = total in situ vertical stress at the cone base, relative to ground surface or seafloor. This is a calculated value.

Q_t = q_n/σ'_{vo} = normalized cone resistance

where:

σ'_{vo} = effective in situ vertical stress at the cone base, relative to ground surface or seafloor. This is a calculated value.

Q_{tn} = normalized cone resistance with variable stress exponent n , where:

$$Q_{tn} = [(q_t - \sigma_{vo})/P_a](P_a/\sigma'_{vo})^n$$

$$n = 0.381(I_c) + 0.05(\sigma'_{vo}/P_a) - 0.15 \text{ and } n \leq 1 \text{ (Zhang et al., 2002)}$$

I_c = soil behaviour type index (Robertson and Wride, 1998)

$$I_c = [(3.47 - \log Q_{tn})^2 + (\log F_r + 1.22)^2]^{0.5}$$

F_r = f_t/q_n = normalized friction ratio.

B_q = pore pressure ratio $B_q = (u_2 - u_0)/q_n$ or

$$B_q = K(u_1 - u_0)/q_n$$

Presented values for u_2 , q_t , q_n and B_q may be denoted by u_2^* , q_t^* , q_n^* , B_q^* , Q_t^* and F_r^* if u_2 is derived rather than measured, for example if derived by applying a K -factor.

Pore pressure u_2 at the cylindrical extension is commonly assumed equal to u_{2g} in the gap. The assumption $u_2 = u_{2g}$ is probably reasonable for deepwater CPTs and associated high values of ambient pressure that promote saturated conditions in the gap. A similar comment applies to u_3 . Note that CPTU saturation procedures apply to the pore pressure measuring system only. These procedures exclude the gaps below and above the friction sleeve.

Some deployment systems allow monitoring of CPT parameters in reverse mode, i.e. upon retraction of the cone penetrometer. This optional feature presents additional information that can improve interpretation of ground behaviour, for example strength sensitivity of fine-grained soil.

Accuracy Classes and Application Classes

Cone penetration test standards can follow a 'prescriptive' approach, whereby specific detailed measures provided a 'deemed to comply' practice. ASTM (2020) is an example of this approach.

ISO (2012, 2014) specify 'performance' criteria for cone penetration test measurements. The test results should meet the requirements of one of the application classes. Historically, the concept of application classes was based on an international reference test procedure (ISSMGE, 1999). The ISO standards are under revision (2021). The ISO revision will probably lead to replacement of application classes by a prescriptive approach, i.e. method-based requirements and cone penetrometer classes. These method-based requirements will rely on detailed laboratory calibration and verification to be performed for cone penetrometers. The results of these activities will determine that a cone penetrometer complies with one of the standardised cone penetrometer classes. Compliance with a particular cone penetrometer class then provides some indication for uncertainty of CPT results.

The ISO standard on metrological confirmation (ISO, 2003) provides the general framework for assessment of performance compliance.

The following comments apply:

- Accuracy is the 'closeness of a measurement to the true value of the quantity being measured'. It is the accuracy as a whole that is ultimately important not the individual parts. Precision is the 'closeness of each set of measurements to each other'. The resolution of a measuring system is the 'minimum size of the change in the value of a quantity that it can detect'. It will influence the accuracy and precision of a measurement.
- Accuracy Class 3 and Application Class 3 typically represents industry practice. They are approximately equivalent to the more implicit requirements of ASTM International. Class 3 applies, unless specifically agreed otherwise.

So-called 'zero drift' of a measured parameter is an approximate performance indicator for the measuring system (Peuchen and Terwindt, 2014). Zero drift is the absolute difference of the zero readings, reference readings or zero reference reading of a measuring system between the start and completion of the cone penetration test. The reference readings can be taken at (1) atmospheric pressure at ground surface or above water level or (2) under hydrostatic water pressure close to seafloor. The zero drift of the measured parameters can be compared with the

allowable minimum accuracy according to the selected application class, per test. This comparison considers the maximum range of values of q_c , f_s and, where applicable, u_1 or u_2 for calculation of the percentage box values (Tables 1 or 2).

Differences in interpretation about compliance with the ISO box values for accuracy became apparent after publication of ISO 22476-1:2012 and, subsequently, publication of ISO 19901-8:2014. Unfortunately, the interpretational challenges emerged from contractual disputes, unnecessary re-work and CPT results assigned higher confidence than actual (Peuchen and Parasie, 2019).

Peuchen and Terwindt (2014, 2015) provide guidance on uncertainty estimation for cone penetration test results. The calculation model for uncertainty estimates for q_c , f_s and u considers the following uncertainty contributions, where applicable: (1) force and pressure sensors, (2) geometry of the cone penetrometer, (3) effects from ambient and transient temperature, (4) non-axial force on cone penetrometer (bending moment), (5) ambient fluid pressure in soil and (6) zero offsets for q_c , f_s and u relative to seafloor.

Accuracy considerations for strongly layered soils should allow for heat flux phenomena. Heat flux gives an apparent shift in cone resistance (Post and Nebbeling, 1995). For example, friction in dense sand causes a cone to heat by about 1°C/MPa cone resistance. Resulting heat flux decreases cone resistance by an apparent shift in the order of 100 kPa to 200 kPa for a penetrating probe going from dense sand into clay. This is a temporary decrease lasting about 5 minutes. Penetration interruption can serve as mitigation measure for transient temperature effects. The incorporation of one or more add-on temperature sensors in a cone penetrometer, and associated data algorithms, can reduce the effects from ambient and transient temperature fluctuations.

Pore Pressures

A CPTU pore pressure measuring system is intended for use in water-saturated uncemented fine-grained soil. Pore pressure measurements (u) are commonly assumed to represent pore water pressures. This assumption is reasonable for soils saturated under in situ stress conditions and remaining saturated during penetration of the cone penetrometer.

Pore pressure results obtained for ground conditions such as partially saturated soils, very dense sands and cemented soils may not be representative and/or repeatable. For example, stiffness differences between the steel components of the cone penetrometer and the piezocone filter can affect results for very dense sands.

Loss of saturation of the pore pressure measuring system can occur during a test (Lunne et al., 1997; Peuchen and Terwindt, 2014). Loss of saturation usually causes a sluggish pore pressure response during penetration of ground below the zone causing desaturation of the pore pressure measuring system. Reasons for loss of saturation include:

- penetration of partially saturated ground, for example ground containing significant amounts of gas;
- reduction of pore pressure to below in situ pore pressure, causing gas in solution to become free gas;
- measurement of negative pore pressures such that cavitation occurs; for example, this is not uncommon for a piezocone filter located at the cylindrical extension above the base of the cone (u_2 location), at the time of penetration of dense sand or overconsolidated clay layers.

Re-saturation of a pore pressure measurement system can take place upon further penetration into soil. Particularly, re-saturation may take place in saturated low-permeability soils (clays) that are normally consolidated or lightly overconsolidated and where the gap can become saturated by adequate supply of water and/or water pressure.

Measured pore pressures affected by desaturation of the pore pressure measurement system may not be representative of soil behaviour. Consequently, derived parameters that use pore pressure may also not be representative.

Shallow Penetration

Shallow penetration will affect CPT measurements. Values of q_c , f_s and u for initial penetration of a cone penetrometer below ground surface, seafloor or bottom of a borehole will differ from a fully embedded cone penetrometer. As a general guide, initial penetration effects can be expected for a distance of about 8 times the diameter of the cone penetrometer for q_c , u_1 and u_2 , and for a distance of about 15 times the diameter of the cone penetrometer for f_s . Initial penetration effects can be deeper for downhole borehole deployment. This is because of (1) complex ground stress conditions immediately below the required borehole and (2) borehole-induced ground disturbance that cannot be avoided.

Use of reaction equipment will affect stress conditions for shallow penetration. Particularly, offshore conditions may include extremely soft ground at seafloor. Soil disturbance, pore pressure build-up and consolidation of near-surface soft soil may take place.

Penetration Rate

CPT standards typically provide limits of ± 5 mm/s for a nominal penetration rate of 20 mm/s. Considerations include:

- A typical thrust machine provides a push speed with an uncertainty within ± 5 mm/s under favourable conditions. Under adverse conditions, penetration rates may be outside these limits, for example with strongly varying thrust and towards the thrust limit of a thrust machine;
- The penetration rate is not necessarily equal to the push speed because of inevitable vertical movements of the thrust machine and length variation and bending of the push-rod string.

Penetration Interruption

A penetration interruption may be unavoidable, for example to add a push rod or to perform a pore pressure dissipation test. This will affect test results.

Consolidation of low-permeability soil around a cone tip is of particular interest. A stationary cone penetrometer can apply local stresses that approach failure conditions, i.e. about 9 times the undrained shear strength or about 2 times the in situ mean effective stress. Pore pressure re-distribution and dissipation occur, resulting in a local increase in undrained shear strength and hence cone (bearing) resistance. A doubling of cone resistance may not be unreasonable for 100 % consolidation. Supplementary considerations include:

- Small downward movement of a penetrometer (order of millimetres) during a test can contribute to maintaining local stresses approaching failure conditions;
- Soil consolidation around a cone penetrometer may lead to soil/penetrometer adhesion that is sufficient to give an increase in 'cone' diameter. Resumption of penetration will

lead to loss of adhered soil, usually within an equivalent distance of a few times the cone diameter;

- A low B_q value may imply partially drained penetration conditions. It is likely that any steady-state penetration conditions will not apply instantaneously upon resumption of penetration;
- Measuring sensors in a probe generate heat, but this is probably not significant for any stationary measurement. Fugro's strain-gauge load sensors are compensated for ambient temperature fluctuations.

Depth Measurement for Offshore Conditions

Table 3 presents depth accuracy classes. Peuchen and Wemmenhove (2020) present a probabilistic approach to depth uncertainty assessment for in situ testing data points, with reference to these accuracy classes.

Offshore definition of the seafloor (ground surface) is difficult for extremely soft ground at seafloor (ISO, 2014). Penetration of the reaction equipment into a near-fluid zone of the seabed may take place unnoticed. Such settlement affects the start of penetration depth z . Also, settlement may continue at the time of testing.

Downhole CPT systems rely on depth control applicable to borehole drilling. Depth control according to Z2 of Table 3 is typically feasible for drilling systems deployed from a fixed platform, for example a jack-up. This value excludes uncertainty associated with determination of seafloor level. Drilling control from floating equipment, for example a geotechnical survey vessel, may be subject to the additional influence of waves and tides. Z2 is typically feasible for favourable conditions. Z3 or Z4 may apply for adverse conditions.

Table 3: Depth Accuracy Classes according to ISO (2014)

Depth Accuracy Class	Maximum Data Point Depth Uncertainty [m]
Z1	0.1
Z2	0.5
Z3	1.0
Z4	2.0
Z5	> 2.0

Zero-Correction for Offshore Conditions

Water pressures generate significant values of cone resistance and pore pressure. The standardised practice is to correct these reference readings to zero at seafloor. CPT systems for non-

drilling mode and for seafloor drilling mode allow zero-correction to hydrostatic conditions prior to the start of a test, typically with a zero-correction uncertainty approaching the resolution of the CPT system. Downhole borehole CPT systems latch into the lower end of a drill pipe. The pressure conditions in the drill pipe may not be in full equilibrium with the surrounding ground water pressure and zero-correction will be subject to increased uncertainty, i.e. uncertainty for pore pressure in the order of 100 kPa for deepwater tests (Peuchen, 2000). This uncertainty depends on factors such as the free-flow and viscosity of drill fluid between the drill bit and the seafloor. The uncertainty typically decreases with decreasing depth of the drill bit below sea level and below seafloor. Uncertainty for the zero-correction of cone resistance is approximately equivalent, but by a factor representing the net area ratio effect.

Deepwater Tests

A deepwater environment presents some favourable conditions for cone penetration tests, notably temperature. Ambient temperature conditions are practically constant and the measuring system has ample time to adjust to these temperatures. In addition, transient heat flow phenomena in a cone penetrometer are usually not applicable. This is because a cone penetrometer accumulates negligible (frictional) heat when penetrating the generally prevalent soils of very soft consistency.

Deepwater (piezocone) pore pressure measurements are essentially similar to shallow-water measurements, with the exception of an increased measuring range for pore pressure leading to some reduction in sensor accuracy. Saturation of a pore pressure measuring system is excellent for a deepwater environment, as the high pressures will force any gas bubbles into solution.

Currently available evidence indicates that a high-quality subtraction-type cone penetrometer is adequate for very soft soil characterisation to a water depth of 3000 metres and probably beyond.

Additional Measurements

Friction-cone and piezocone penetrometers allow specific additional measurements, such as friction set-up tests, pore pressure dissipation tests and measurements of ground water pressure. These additional measurements require a penetration interruption or may be feasible at the end of a test. It is also common to add other in situ test devices to a cone penetrometer. Table 4 presents the more common types.

Table 4: Probes for additional In Situ Tests

Type of Probe	Properties	Units
Electrical Conductivity Penetrometer (ECPT)	Electrical conductivity, K	S/m
Temperature Cone Penetrometer (TCPT)	Temperature, T , and thermal conductivity, k	K, W/(m·K)
Seismic Cone Penetrometer (SCPT)	S-wave velocity, v_s , and P-wave velocity, v_p	m/s
Cone Pressuremeter (CPMT)	Shear stress-strain-time response, σ, ϵ, t	MPa, τ, s
Natural Gamma Penetrometer (GCPT)	Natural gamma ray, γ	CPS
Cone Magnetometer (CMMT)	Magnetic flux density B , magnetic field horizontal angle θ and vertical angle ϕ	$\mu T, ^\circ, ^\circ$
Hydraulic Profiling Tool (HPT)	Permeability, k	m/s
S = Siemens		s = second
m = metre		Pa = Pascal
K = Kelvin (or °C)		CPS = counts per second
W = Watt		T = Tesla

References

- ASTM International (2020). *Standard test method for electronic friction cone and piezocone penetration testing of soils* (ASTM D5778-20). <https://www.astm.org/Standards/D5778.htm>.
- BSI (2015). *Code of practice for ground investigations* (BS 5930:2015). <https://shop.bsigroup.com/ProductDetail?pid=000000000030268443>.
- European Committee for Standardization (2010). *Eurocode 7 – geotechnical design – part 2: ground investigation and testing* (EN 1997-2:2007+ AC:2010) https://standards.cen.eu/dyn/www/f?p=204:110:0:::FSP_PROJECT,FSP_ORG_ID:23735,6231&cs=14A2DCCA6BF367BFBD54D9FC0822BE0ED.
- International Organization for Standardization (2003). *Measurement management systems - requirements for measurement processes and measuring equipment* (ISO 10012:2003) <https://www.iso.org/standard/26033.html>
- International Organization for Standardization (2012). *Geotechnical investigation and testing – Field testing – Part 1: Electrical cone and piezocone penetration test* (ISO 22476-1:2012). <https://www.iso.org/standard/57728.html>
- International Organization for Standardization (2014). *Petroleum and natural gas industries – specific requirements for offshore structures – part 8: marine soil investigations* (ISO 19901-8:2014). <https://www.iso.org/standard/61145.html>
- International Society for Soil Mechanics and Geotechnical Engineering (1999). International reference test procedure for the cone penetration test (CPT) and the cone penetration test with pore pressure (CPTU): Report of the ISSMGE technical committee 16 on ground property characterisation from in-situ testing. In F.B.J. Barends et al. (eds.) *Geotechnical engineering for transportation infrastructure: proceedings of the twelfth European conference on soil mechanics and geotechnical engineering, Amsterdam, Netherlands, 7-10 June 1999, Vol. 3* (pp. 2195-2222). Balkema.
- Lunne, T., Robertson, P.K. & Powell, J.J.M. (1997). *Cone penetration testing in geotechnical practice*. Blackie Academic & Professional.
- Peuchen, J. (2000). Deepwater cone penetration tests. In *32nd Annual Offshore Technology Conference, 2000: OTC Paper 12094* <https://doi.org/10.4043/12094-MS>
- Peuchen, J., VandenBerghe, J.F. & Coulais, C. (2010), Estimation of u_1/u_2 conversion factor for piezocone. In *CPT'10: 2nd International symposium on cone penetration testing, Huntington Beach, California: conference proceedings*.
- Peuchen, J. & Terwindt, J. (2014). Introduction to CPT accuracy. In *3rd International symposium on cone penetration testing CPT14 : May 12-14 (2014) - Las Vegas, Nevada*.
- Peuchen, J. & Terwindt, J. (2015). Measurement uncertainty of offshore cone penetration tests. In V. Meyer (ed.) *Frontiers in offshore geotechnics III: proceedings of the third international symposium on frontiers in offshore geotechnics (ISFOG 2015), Oslo, Norway, 10-12 June 2015*. (pp. 1209-1214) CRC Press..
- Peuchen, J. & Parasie, N. (2019). Challenges for CPT accuracy classes. *Proceedings of the XVII ECSMGE-2019: geotechnical engineering foundation of the future*. IGS publishing https://www.ecsmge-2019.com/uploads/2/1/7/9/21790806/0049-ecsmge-2019_peuchen.pdf
- Peuchen, J. & Wemmenhove, R. (2020). Depth accuracy of data points in marine soil investigation. In Z. Westgate (ed.). *4th International Symposium on Frontiers in Offshore Geotechnics (ISFOG 2020): proceedings* (pp. 1036-1045). Deep Foundations Institute.
- Post, M.L. & Nebbeling, H. (1995). Uncertainties in cone penetration testing. In *International Symposium on Cone Penetration Testing CPT'95, Linköping, Sweden, October 4-5, 1995, Vol. 2* (SGF Report, No. 3:95) (pp. 73-78). Swedish Geotechnical Society.
- Robertson, P.K. & Wride (Fear), C.E. (1998). Evaluating cyclic liquefaction potential using the cone penetration test. *Canadian Geotechnical Journal*, 35(3), 442-459. <https://doi.org/10.1139/t98-017>
- Robertson, P.K. (2010). Soil behaviour type from the CPT: an update. In *2nd International symposium on cone penetration testing, Huntington Beach, CA, Vol. 2*. (pp. 575-583)
- Zhang, G., Robertson, P.K. & Brachman, R.W.I. (2002). Estimating liquefaction induced ground settlements from CPT for level ground. *Canadian Geotechnical Journal*, 39(5) 1168-1180. <https://doi.org/10.1139/t02-047>

Cone Penetration Test Interpretation

Scope

This document presents a summary of interpretation methods for cone penetration test (CPT) results. The project-specific selection of methods depends on the agreed project requirements. Some of the methods suit computer-based interpretation of CPT data records.

Parameter Interpretation

Interpretation of cone penetration test results helps provide parameters for geotechnical models. Conventional models are typically based on plasticity theory for ultimate limit states, and on elasticity theory and consolidation theory for serviceability limit states. Features of these geotechnical models are:

- analysis of either drained (sand model) behaviour or undrained (clay model) behaviour for plasticity models;
- analysis for the ultimate limit state differs from that for the serviceability limit state.

CPT interpretation methods are mostly based on empirical correlations with limited theoretical backing. Data integration with other, complementary investigation techniques (such as geological analysis, borehole/sample logging and laboratory testing) can improve confidence levels.

The interpretation techniques discussed below are subject to limitations such as:

- CPT measurements, including measurement uncertainty (Peuchen & Terwindt, 2014 & 2015) and effects resulting from deployment method, initial embedment of a cone penetrometer, penetration interruption and inevitable loss of saturation of a pore pressure measuring system;
- Most interpretation methods apply a transformation model to "conventional" sands (drained soil behaviour) and clays (undrained soil behaviour). Conventional methods may not be appropriate for silts, sand/clay/gravel mixtures, varved or layered soils, gassy soils, underconsolidated soils, peats, carbonate soils, cemented soils and residual soils. These non-conventional soils warrant a more specific approach;
- Drained or undrained behaviour for the geotechnical analysis at hand may or may not coincide with respectively drained or undrained behaviour during fixed-rate penetration testing. This interpretation difficulty remains largely unresolved at this time;
- CPT interpretation techniques can be indirect, i.e. requiring estimates of various other parameters. This is consistent with an integrated geotechnical investigation approach. Inevitably, this approach also includes some redundancy of data;
- Empirical correlations can rely on data pairing, for example pairing of CPT net cone resistance at a point in space with laboratory undrained shear strength applicable to another, nearby spatial position. Data pairing uncertainty can be limited by applying judgement;
- Empirical correlations can use reference parameters such as the undrained shear strength determined from a laboratory single-stage isotropically consolidated undrained triaxial compression test on an undisturbed specimen obtained by means of push sampling techniques (e.g. Van der Wal et al., 2010). The reference parameter may not be appropriate for the selected geotechnical model, and adjustment may be

necessary. Also, adjustment for test conditions may be necessary, for example in situ temperature versus laboratory temperature;

- The cone penetration test offers limited direct information on serviceability limit states (deformation), as the penetration process imposes large strains in the surrounding soil. In comparison to ultimate limit states, better complementary data will usually be required;
- The interpretations typically apply to conditions as encountered at the time of the geotechnical investigation. Geological, environmental and construction/operational factors may alter as-found conditions.

Penetration Behaviour

Soil behaviour during cone penetration testing shows large displacements in the immediate vicinity of the penetrometer, and small elastic displacements further away from the penetrometer. Density/structure, stiffness and in situ stress conditions significantly affect the measured parameters.

The measured cone resistance (q_c) includes hydrostatic water pressures as well as induced pore pressures resulting from stresses and strains related to the penetration process. The induced pore pressures are usually negligible for clean sand because the ratio of effective stress to pore pressure is high. This ratio can be low for penetration into normally consolidated and slightly overconsolidated clays. Knowledge of pore pressures around the penetrometer can thus be important. CPT parameters that take account of pore pressure effects include corrected cone resistance (q_t), net cone resistance (q_n) and pore pressure ratio (B_q). These parameters can be calculated if piezocone penetration test (PCPT or CPTU) data are available. The influence of pore pressures on sleeve friction f_s is relatively small. It is common to ignore this influence. Calculation of friction ratio R_f (defined as f_s/q_c) includes no allowance for pore pressure effects.

The penetration rate with respect to soil permeability determines whether soil behaviour is primarily undrained, drained or partially drained. Partial drainage may also be denoted as partial consolidation. In general, soil behaviour during cone penetration testing is:

- Drained in clean sand, i.e. no measurable pore pressures because of (1) soil displacements and (2) soil volume change depending on dilative/contractive soil behaviour;
- Undrained in clay, i.e. no significant soil volume change immediately around the cone penetrometer and pore pressure change depending on dilative/contractive soil behaviour;
- Partially drained in soils with intermediate permeability, such as sandy silt, i.e. potential for (1) some soil volume change depending on dilative/contractive soil behaviour and (2) potential for pore pressure change depending on dilative/contractive soil behaviour.

Results of a pore pressure dissipation test can provide indications for partial drainage conditions. Particularly, partial drainage conditions should be considered when t_{50} is less than about 100 s (DeJong and Randolph, 2012). The term t_{50} represents the time for 50 % dissipation of excess pore pressure at the u_2 location of a cone penetrometer.

CPT parameters can be influenced by the presence of thin (< 0.2 m thick) layers in a ground profile. Boulanger and DeJong (2018) proposed a method that provides estimates of corrected q_c and f_s values based on an inverse filtering procedure that accounts for thin layer and transitional effects during cone penetration.

The following sections mostly consider interpretation of drained soil behaviour (sand) and undrained soil behaviour (clay).

Soil Behaviour Identification

Identification of soil stratigraphy in terms of general soil behaviour (and to a lesser degree soil type) is a more important feature of CPT than other investigation techniques.

Figures 1 and 2 show soil behaviour identification according to procedures given by Robertson (2009), representing an update of Robertson (1990) by exchange of Q_t with Q_{tn} . The procedures consider a normalised soil behaviour classification that provides general guidance on likely soil type (silty sand for example) and a preliminary indication of parameters such as angle of internal friction ϕ' , overconsolidation ratio (OCR) and clay sensitivity (S_t). Classification is possible for $1 \leq Q_{tn} \leq 1000$, $0.1 \leq F_r \leq 10$ and $-0.2 \leq B_q \leq 1.4$. The procedures require piezocone test data:

$$Q_{tn} = [(q_t - \sigma_{vo})/P_a](P_a/\sigma'_{vo})^n \quad Q_t = \frac{q_t - \sigma_{vo}}{\sigma'_{vo}}$$

$$F_r \text{ or } nR_f = \frac{f_s}{q_t - \sigma_{vo}} 100\% \quad B_q = \frac{u - u_0}{q_t - \sigma_{vo}}$$

where:

- B_q = pore pressure ratio
- F_r = normalised friction ratio
- Q_{tn} = normalised cone resistance with variable stress exponent
- Q_t = normalised cone resistance
- q_t = corrected cone resistance
- σ_{vo} = total in situ vertical stress
- σ'_{vo} = effective in situ vertical stress
- P_a = atmospheric pressure
- n = stress exponent
- f_s = measured sleeve friction
- u = measured pore pressure
- u_0 = theoretical hydrostatic pore pressure.

The stress exponent n is according to Zhang et al. (2002):

$$n = 0.381 (I_c) + 0.05 (\sigma'_{vo} / P_a) - 0.15$$

where $n \leq 1$.

Robertson and Wride (1998) defined soil behaviour type index I_c (Figure 2) as follows:

$$I_c = [(3.47 - \log Q_{tn})^2 + (\log F_r + 1.22)^2]^{0.5}$$

Soils with $I_c < 2.05$ are generally cohesionless, coarse grained, where cone penetration is generally drained and soils with $I_c > 2.60$ are generally cohesive, fine grained, where cone penetration is generally undrained (Robertson & Wride, 1998). Cone penetration in soils with $2.05 < I_c < 2.60$ is often partially drained.

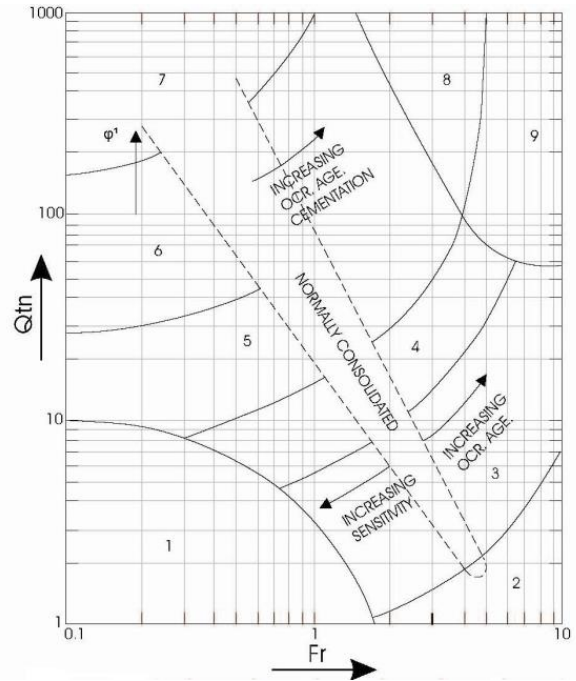


Figure 1: Classification chart Robertson (2009)

1. Sensitive, fine grained
 2. Organic soils - peats
 3. Clays - clay to silty clay
 4. Silt mixtures - clayey silt to silty clay
 5. Sand mixtures - silty sand to sandy silt
 6. Sands - clean sand to silty sand
 7. Gravelly sand to sand
 8. Very stiff sand to clayey sand*
 9. Very stiff, fine grained*
- (*) Heavily overconsolidated or cemented

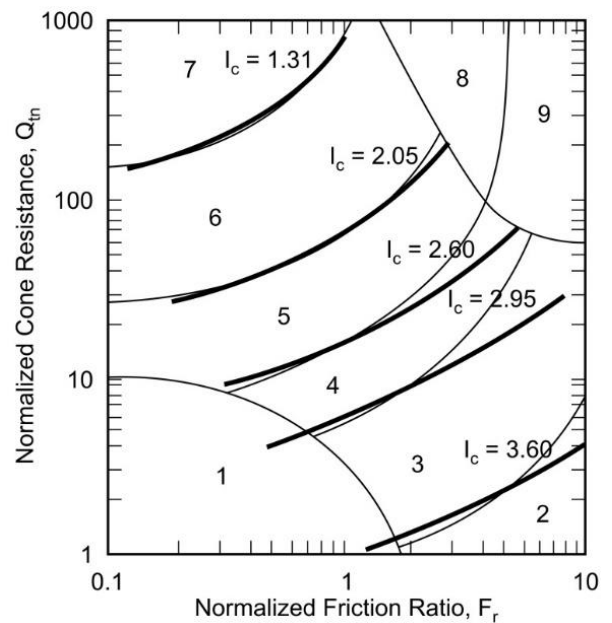


Figure 2: Soil behaviour type index I_c superimposed on Robertson (2009) classification chart

Figure 3 presents a classification chart for friction cone data according to Robertson (2010). This procedure requires no pore pressure input. A non-normalised soil behaviour type index, I_{SBT} applies:

$$I_{SBT} = [(3.47 - \log(q_c/P_a))^2 + (\log R_f + 1.22)^2]^{0.5}$$

I_{SBT} is similar to I_c . Values for I_{SBT} and I_c are typically comparable for effective in situ vertical stress between 50 kPa and 150 kPa.

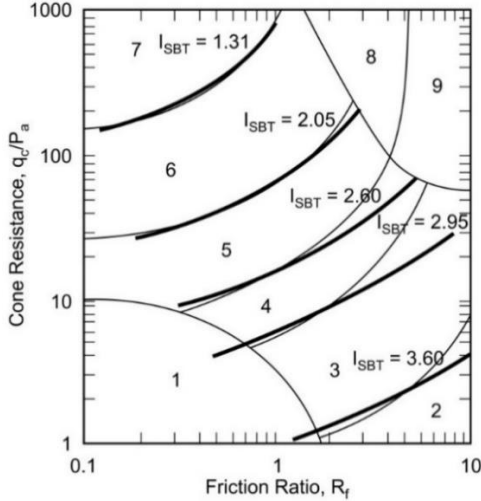


Figure 3: Robertson (2010) classification chart including I_{SBT}

Figure 4 presents a classification chart focusing on contractive and dilative soil behaviour, according to Robertson (2016a). The equations for the contractive-dilative boundary (CD) and modified soil behaviour type index (I_B) are as follows:

$$CD = (Q_{tn} - 11)(1 + 0.06F_r)^{17} \text{ and}$$

$$I_B = 100(Q_{tn} + 10)/(70 + Q_{tn}F_r)$$

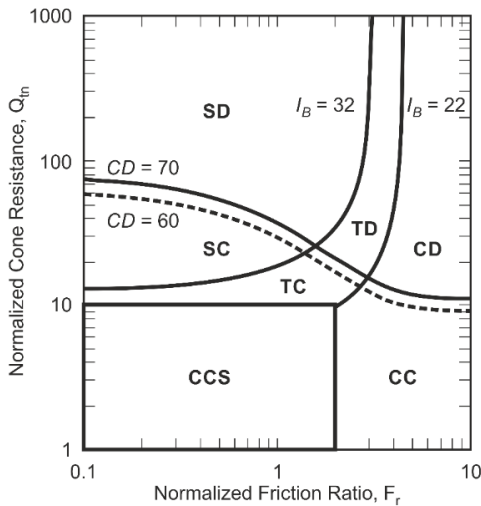


Figure 4: Classification chart according to Robertson (2016a)

- CCS Clay-like – Contractive - Sensitive
- CC Clay-like – Contractive
- CD Clay-like – Dilative
- TC Transitional – Contractive
- TD Transitional – Dilative
- SC Sand-like Contractive
- SD Sand-like Dilative

Suggested values of CD are $CD = 60$ (low value) and $CD = 70$ (high value). Suggested values for I_B are $I_B = 32$, representing a low value for sand-like soil behaviour types and $I_B = 22$

representing a high value for clay-like soil behaviour types. The region between $I_B = 32$ and $I_B = 22$ represents soils typically showing transitional or intermediate soil behaviour types.

Sand Model

Unit Weight – Sand

Unit weight of uncemented (silica) sand, silt and clay soils may be derived according to Mayne et al. (2010):

$$\gamma = 1.95\gamma_w \left(\frac{\sigma'_{vo}}{P_a}\right)^{0.06} \left(\frac{f_t}{P_a}\right)^{0.06}$$

where total unit weight γ and unit weight of water γ_w are in kN/m^3 and effective in situ vertical stress σ'_{vo} is in kPa. The symbol f_t refers to sleeve friction corrected for pore pressures acting on the end areas of the friction sleeve, with units in kPa. Atmospheric pressure P_a is in kPa.

Unit weight may also be derived according to Lengkeek et al. (2018):

$$\gamma = \gamma_{ref} - \beta \cdot (\log(q_{t,ref}/q_t)) / (\log(R_{f,ref}/R_f))$$

where γ_{ref} is a reference unit weight at which q_t is constant regardless of friction ratio R_f , β is a factor for unit weight contouring, $q_{t,ref}$ is a reference for total cone resistance q_t at which γ is constant regardless of R_f , and $R_{f,ref}$ is a reference friction ratio. The default values are: $\gamma_{ref} = 19 \text{ kN/m}^3$, $\beta = 4.12$, $q_{t,ref} = 5 \text{ MPa}$, and $R_{f,ref} = 30 \%$. The correlation allows development of project-specific estimation of unit weight.

Shear Wave Velocity – Sand

If no in situ measurements of shear wave velocities (v_s) are available, then empirical correlation with CPT parameters may be considered. Hegazy and Mayne (2006) published a statistical correlation derived from 73 sites worldwide representing a range of soil types including sands, clays, soil mixtures and mine tailings (Figure 6). The correlation considers a normalized cone resistance (q_{c1N_hm}) and a soil behaviour type index (I_{c_hm}) as follows:

$$v_s = 0.0831q_{c1N_hm}(\sigma'_{vo}/P_a)^{0.25} e^{(1.786I_{c_hm})} \quad (\text{Hegazy \& Mayne, 2006})$$

where shear wave velocity v_s is in m/s and q_{c1N_hm} and I_{c_hm} are dimensionless. Calculations for q_{c1N_hm} and I_{c_hm} require iteration, and consider cone resistance q_c or corrected cone resistance $q_{t,c}$, sleeve friction f_s , total in situ vertical stress σ_{vo} , effective in situ vertical stress σ'_{vo} and atmospheric pressure P_a .

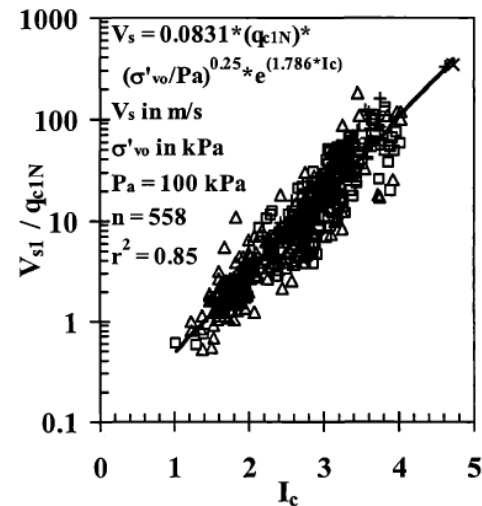


Figure 6: $v_s - q_c$ correlation according to Hegazy and Mayne (2006)

Robertson and Cabal (2015) present a v_s correlation incorporating net cone resistance $q_n (= q_t - \sigma_{vo})$ and soil behaviour type index (I_c) as defined by Robertson and Wride (1998):

$$v_s = [\alpha_{vs}(q_t - \sigma_{vo})/P_a]^{0.5} \text{ where } \alpha_{vs} = 10^{(0.55 I_c + 1.68)} \quad (\text{Robertson \& Cabal, 2015})$$

where shear wave velocity v_s is in m/s and corrected cone resistance q_t , total in situ vertical stress σ_{vo} and atmospheric pressure P_a are in kPa. The method can be applied to a wide range of soil behaviour types, notably uncemented Holocene to Pleistocene age soils. Older deposits could have a higher shear wave velocity. Exceptions are Zones 1, 8 and 9 of Robertson (1990 and 2009).

Baldi et al. (1989) derived a correlation between shear wave velocity v_s and cone resistance q_c for uncemented silica sands. This correlation is based on data from CPT, cross-hole and Seismic Cone Penetration Tests (SCPT) performed in quaternary deposits of the predominantly silica Po river sand and Gioia Tauro sand with gravel.

$$v_s = 277 q_c^{0.13} \sigma'_{vo}{}^{0.27} \quad (\text{Baldi et al., 1989})$$

where shear wave velocity v_s is in m/s and cone resistance q_c and effective in situ vertical stress σ'_{vo} are in MPa.

Shear wave velocity may be normalised according to Robertson and Cabal (2015):

$$v_{s1} = v_s \cdot (P_a/\sigma'_{vo})^{0.25} \quad (\text{Robertson \& Cabal, 2015})$$

In Situ Stress Conditions - Sand

A knowledge of in situ stress conditions is required for estimation of parameters such as relative density D_r and angle of internal friction of a sand deposit ϕ' . The effective in situ vertical stress σ'_{vo} may be calculated with a reasonable degree of accuracy but the effective in situ horizontal stress $\sigma'_{ho} = K_0 \cdot \sigma'_{vo}$ is generally unknown. Usually, it is necessary to consider a range of conditions for K_0 (coefficient of earth pressure at rest). The range can consider overconsolidation as inferred from a geological assessment, preconsolidation pressures of intermediate clay layers and/or theoretical limits of K_0 .

Geological factors concerning overconsolidation include ice loading, soil loading and groundwater fluctuations (influence from desiccation). Possible subdivisions for these factors are mechanical, suction, cyclic and ageing consolidation.

The following approach can be applied for direct estimation of K_0 based on Agaiby and Mayne (2019):

$$K_0 = 0.45\sqrt{OCR}$$

$$\text{using: } OCR = \frac{\sigma'_p}{\sigma'_{vo}} \quad \sigma'_p = 0.33 \cdot q_n^{m'} \quad m' = 1 - \frac{0.28}{1 + (\frac{I_c}{2.65})^{2.5}}$$

where OCR is overconsolidation ratio, σ'_p is effective preconsolidation stress, σ'_{vo} is effective in situ vertical stress, q_n is net cone resistance in kPa and I_c is soil behaviour type index.

The $K_0 - OCR$ relationship represents a schematisation of $K_0 = (1 - \sin\phi') \cdot OCR^{\sin\phi'}$ proposed by Mayne and Kulhawy (1982). Mayne and Kulhawy (1982) investigated mechanical overconsolidation of reconstituted laboratory specimens for over 170 different soils. For many soil types (e.g. Mayne, 2020), it can be shown that the $K_0 = 0.45\sqrt{OCR}$ equation provides similar statistics to the Mayne and Kulhawy correlation using ϕ' (effective angle of internal friction):

$$K_0 = (1 - \sin\phi') \cdot OCR^{\sin\phi'}$$

Figure 5 presents an approximate CPT-based correlation for K_0 according to Robertson (2016b). K_0 limits are typically set to 0.5 and 2. Linear interpolation is applied for the region between $K_0 = 0.5$ and $K_0 = 2$.

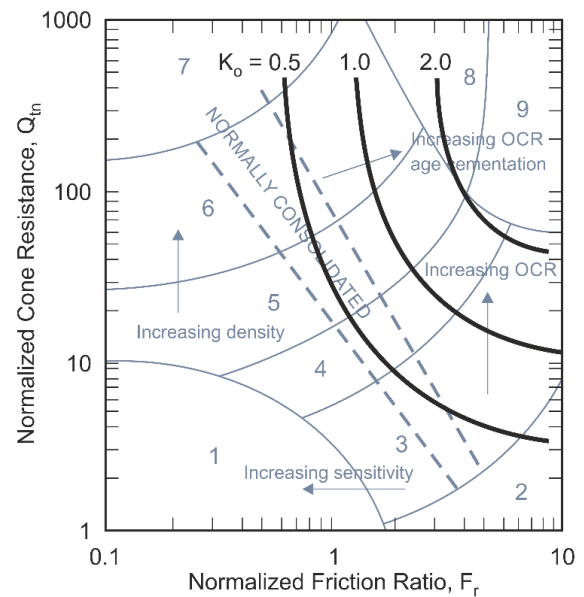


Figure 5: K_0 correlation according to Robertson (2016b)

No laboratory study can fully capture in situ behaviour. Particularly, K_0 may be underestimated if effects such as ageing and cyclic loading are relevant.

In general, in situ K_0 values are limited to the range $K_0 = 0.5$ to $K_0 = 1.5$. For many situations, K_0 values are believed to be relatively low at greater depths (say $K_0 < 1$ for depths exceeding 50 m). Jamiolkowski et al. (2003) recommend using a limiting value $K_0 = 1$ in practice, for limit states where low values of soil resistance and soil stiffness are critical.

Relative Density - Sand

The relative density concept applies to sands with a percentage fines of less than about 15 %.

Relative density is defined as $D_r = (e_{max} - e)/(e_{max} - e_{min})$, where e_{max} is maximum index void ratio, e represents in situ void ratio and e_{min} is minimum index void ratio. Maximum and minimum index void ratios are defined by laboratory testing. Relative density can exceed 100 %, because in situ void ratio can be lower than laboratory values for minimum index void ratio.

CPT-based correlations are commonly used for estimation of in situ relative density. These correlations rely on database results of CPTs carried out in sand samples reconstituted in laboratory calibration chamber tests. Use of such correlations implies dependence on, for example:

- soil type of database versus soil type in situ;
- reference laboratory test method for determination of index void ratios, particularly sensitivity to minimum index void ratio;
- range of stress levels and K_0 values for calibration testing;
- results applicable to reconstituted sand samples, sample preparation method and soil stress history simplifications.

Jamiolkowski et al. (2003) proposed the following relationship between q_c and D_r for normally and overconsolidated silica (dry) sands:

$$D_{r(dry)} = \frac{1}{2.96} \ln \left[\frac{\frac{q_c}{P_a}}{24.94 \left(\frac{\sigma'_{vo} \left(\frac{1+2K_0}{3} \right)}{P_a} \right)^{0.46}} \right]$$

and for saturated sands:

$$D_{r(sat)} = \left(\frac{-1.87 + 2.32 \ln \frac{q_c}{(P_a * \sigma'_{vo})^{0.5}}}{100} + 1 \right) \frac{D_{r(dry)}}{100}$$

where relative density D_r is a fraction. The correlation for saturated sands results in relative densities that can be up to about 10% higher compared to the correlation for dry sands.

Kulhawy and Mayne (1990) proposed:

$$D_r^2 = Q_{tm*} / Q_f \quad \text{where: } Q_{tm*} = \left(\frac{q_c}{P_a} \right) / \left(\frac{\sigma'_{vo}}{P_a} \right)^{0.5}$$

and q_c is corrected cone resistance, P_a is atmospheric pressure, σ'_{vo} is effective in situ vertical stress. Kulhawy and Mayne (1990) suggested using $Q_f = 280$ for highly compressible normally consolidated sands and $Q_f = 450$ for highly compressible overconsolidated sands (overconsolidation ratio of > 8) based on their dataset. Robertson and Cabal (2015) suggested $Q_f = 350$ for clean, uncemented, medium compressible quartz sands of about 1 000 years old. Values for Q_f can be closer to 300 for fine sands and closer to 400 for coarse sands. Furthermore, Q_f increases with age and increases significantly when age exceeds 10 000 years.

Determination of laboratory minimum and maximum index void ratios forms the basis for the relative density concept (loose, dense sand, etc.). No internationally agreed procedure is available. It is understood that Jamiolkowski et al. (2003) used results from one of the ASTM vibratory table methods for determination of minimum index void ratio. It is not clear which specific ASTM method was used, i.e. a vibratory table method requiring oven-dried soil or wet soil.

Calibration chamber test results apply to a limited range of stress conditions; typically:

$$\begin{array}{ccccccc} 50 \text{ kPa} & < & \sigma'_{vo} & < & 400 \text{ kPa} \\ 0.4 & < & K_0 & < & 1.5 \end{array}$$

Sample preparation for laboratory chamber tests is usually by means of dry pluviation. Soil stress history application is by mechanical overconsolidation.

Effective Angle of Internal Friction - Sand

The effective shear strength parameter ϕ' is not a true constant. It depends on factors such as density, stress level, shearing mode and mineralogy. There is evidence that overconsolidation ratio, method of deposition and in situ stress anisotropy is less important.

Correlation of angle of internal friction ϕ' to cone resistance q_c may be done at various levels of sophistication. Simple procedures rely on a conservative assessment of soil behaviour classification. A more sophisticated empirical correlation consists of:

- Estimation of in situ stress conditions σ'_{vo} and σ'_{ho}
- Estimation of relative density D_r
- Empirical correlation of angle of internal friction ϕ' with D_r , σ'_{vo} and σ'_{ho} .

Estimation of stress conditions and relative density has been discussed above.

The empirical procedure proposed by Bolton (1986 and 1987) is used for estimation of ϕ' . This correlation applies to clean sands and considers peak secant angle of internal friction in Isotropically Consolidated Drained triaxial compression (CID) of reconstituted sand. This procedure requires estimation of the dilatancy index and the critical state angle of internal friction.

Kulhawy and Mayne (1990) determined an equation based upon 20 data sets obtained from calibration chamber tests. This equation is almost identical to the empirical formula determined earlier by Trofimenkov (1974) which was based on mechanical cone data. Mayne (2007) validated the use of total cone resistance q_t instead of cone resistance q_c used in the equation from Kulhawy and Mayne (1990).

$$\phi' = 17.6 + 11.0 \log \left(\frac{q_t}{P_a} \right) / \left(\frac{\sigma'_{vo}}{P_a} \right)^{0.5} \quad (\text{Mayne, 2007})$$

Undrained Shear Strength - Sand

Undrained shear strength of cohesionless soil can be important for assessment of cyclic mobility and liquefaction potential. Geotechnical procedures other than the conventional limit state models are employed.

Constrained Modulus - Sand

Kulhawy and Mayne (1990) derived two formulas for the determination of the constrained modulus for both normally consolidated and overconsolidated sands by indicating that the modulus is a function of relative density. The determination of relative density can be done with, for example, the methods indicated above.

$$M = q_c * 10^{1.09 - 0.0075 D_r}$$

(normally consolidated sands, Kulhawy & Mayne, 1990)

$$M = q_c * 10^{1.78 - 0.0122 D_r}$$

(overconsolidated sands, Kulhawy & Mayne, 1990)

where D_r is in %, and q_c and M in kPa respectively.

Young's Modulus - Sand

A common guideline is an empirical correlation given by Baldi et al. (1989). The correlation is for silica-based sand and considers cone resistance q_c , in situ stress conditions and secant Young's modulus for drained stress change E' . The ratio of E'/q_c typically ranges from about 3 to 5 for recently deposited normally consolidated sands up to about $E'/q_c = 6$ to $E'/q_c = 25$ for overconsolidated sands. The correlation has been inferred from laboratory conditions; including CPTs in a calibration chamber and conventional triaxial compression tests on reconstituted sand samples. It takes account of the degree of deformation and overconsolidation. In this regard, it is noted that secant deformation moduli are strongly dependent on strain level: the elastic modulus increases with decreasing strain to an upper limit at about 10^{-4} % strain.

Shear Modulus at Small Strain - Sand

For estimation of initial (small strain) or dynamic shear moduli, ratios of G_{max}/q_c of between about 4 and 20 can be considered, in accordance with Baldi et al. (1989). The basis for this correlation is similar to that of secant Young's modulus, except that laboratory resonant column tests serve as reference instead of triaxial compression tests. Results of limited in situ seismic cross-hole and downhole tests provide an approximate check of this correlation.

Interpretation of small strain shear modulus can also be estimated from a correlation proposed by Rix and Stokoe (1991) in which data from calibration test measurements is compared to the correlation obtained between G_{max} and q_c by Baldi et al. (1989).

$$G_{max} = 1634(q_c)^{0.25}(\sigma'_{vo})^{0.375} \quad (\text{Rix \& Stokoe, 1991})$$

where G_{max} , q_c and σ'_{vo} are in kPa.

CLAY MODEL

Unit Weight – Clay

Empirical correlation between unit weight of clay and CPT parameters is as described in "Unit Weight – Sand" above.

Shear Wave Velocity – Clay

Hegazy and Mayne (2006) and Roberson and Cabal (2015) present empirical correlations between shear wave velocity and CPT parameters for a wide range of soils including clays, as described in "Shear Wave Velocity v_s – Sand" above. The Hegazy and Mayne correlation is sensitive to use of q_c or q_t . It should be used with caution for soils showing undrained or partially drained CPT response.

Mayne and Rix (1995) derived a correlation between shear wave velocity v_s and cone resistance q_c for intact and fissured clays. A database from Mayne and Rix (1993) was used including 31 different clay sites.

$$v_s = 1.75q_c^{0.627} \quad (\text{Mayne \& Rix, 1995})$$

where shear wave velocity v_s is in m/s and cone resistance q_c is in kPa.

In Situ Stress Conditions - Clay

Similar to sand, a knowledge of in situ stress conditions is generally necessary for estimation of other parameters such as consistency (soft, stiff, etc.) of a clay deposit and compressibility.

Calculation of the effective in situ vertical stress σ'_{vo} is reasonably accurate. A more approximate estimate applies to the effective in situ horizontal stress σ'_{ho} , or K_0 as $\sigma'_{ho} = K_0 \cdot \sigma'_{vo}$.

Direct correlations for interpretation of the coefficient of earth pressure at rest K_0 are the same as described for the Sand Model.

For normally consolidated clays and silts, K_{0nc} may be correlated with angle of internal friction, in accordance with Jaky (1944), or more simply, in accordance with Mayne and Kulhawy (1982):

$$K_0 = (1 - \sin\phi') \cdot OCR^{\sin\phi'}$$

where OCR is overconsolidation ratio and ϕ' is effective angle of internal friction. For many types of clay (e.g. Agaiby and Mayne, 2020), this equation can be approximated by $K_0 = 0.45\sqrt{(OCR)}$.

The plasticity index together with OCR may also be used for preliminary estimates of K_{0oc} as indicated by Brooker and Ireland (1965).

Overconsolidation Ratio - Clay

Overconsolidation ratio is defined as $OCR = \sigma'_p / \sigma'_{vo}$ where σ'_p is the effective preconsolidation stress considered to correspond with the maximum vertical effective stress to which the soil has been subjected in the past, and σ'_{vo} is the current effective in situ vertical stress. The effective preconsolidation stress approximates a stress level where relatively small strains are separated from relatively large strains occurring on the virgin compression stress range. The reference OCR is usually based on laboratory

oedometer tests carried out on undisturbed samples. It may thus be influenced by factors such as sample disturbance, strain rate effects and interpretation procedure.

The following approach can be applied (Agaiby and Mayne, 2019):

$$OCR = \frac{\sigma'_p}{\sigma'_{vo}} \quad \sigma'_p = 0.33 \cdot q_n^{m'} \quad m' = 1 - \frac{0.28}{1 + \left(\frac{I_c}{2.65}\right)^{2.5}}$$

where OCR is overconsolidation ratio, σ'_p is effective preconsolidation stress, σ'_{vo} is effective in situ vertical stress, q_n is net cone resistance in kPa and I_c is soil behaviour type index.

Chen and Mayne (1996) presented the following correlation for 205 clay sites around the world:

$$OCR = 0.317 \cdot Q_t$$

Overconsolidation ratio may also be inferred indirectly from a geological assessment and from undrained strength ratios. Geological factors concerning overconsolidation have been discussed under "in situ stress conditions - sand". An empirical procedure for estimation of OCR based on undrained strength ratio s_u / σ'_{vo} is given by Wroth (1984). The procedure uses the strength rebound parameter λ . Guidance for selection of λ and normally consolidated undrained strength ratio is given by Mayne (1988). Historically, much use has also been made of the Skempton (1957) relationship between normally consolidated undrained strength ratio and plasticity index I_p . This equation is useful for preliminary estimates, considering that I_p probably relates to ϕ' in some complex manner.

Undrained Shear Strength - Clay

No single undrained shear strength exists. The in situ undrained shear strength s_u depends on factors such as mode of failure, stress history, anisotropy, strain rate and temperature.

Various theoretical and empirical procedures are available to correlate q_c with s_u . Theoretical approaches use bearing capacity, cavity expansion or steady penetration solutions, all of which require several simplifying assumptions. Empirical approaches are more common in engineering practice because of difficulties in realistic soil modelling. An empirical correlation for soft to stiff, intact and relatively homogeneous clays is given by Battaglio et al. (1986) as follows:

$$s_u = (q_c - \sigma_{vo}) / N_c$$

where s_u , σ_{vo} and q_c are in kPa. N_c is an empirical factor that typically ranges between 10 and 25. The higher N_c factors typically apply to clays with a relatively low plasticity index and/or apply to heavily overconsolidated clays. Lower N_c factors are generally appropriate for normally consolidated and slightly overconsolidated clays. The reference undrained shear strength is that determined from in situ vane test results. The term σ_{vo} (total in situ vertical stress) becomes insignificant for stiff clays at shallow depth so that the equation reduces to $s_u = q_c / N_c$.

For specific design situations, a different s_u reference strength should be used. For example, offshore axial pile capacity predictions in accordance with API (2011) recommend s_u to be based on undrained triaxial compression tests, which are likely to yield lower s_u values than in situ vane tests. A site-specific or regional approach should generally be preferred.

If piezocone test data are available, then improved correlations are feasible because of the pore pressure information. Empirical correlations of piezocone test results with laboratory undrained shear strengths are commonly expressed, as follows:

$$s_u = q_n / N_{kt}$$

N_{kt} ranges typically between 8 and 30 with the higher N_{kt} factors applying to heavily overconsolidated clays.

Mayne and Peuchen (2018) account for N_{kt} variation according to B_q :

$$N_{kt} = 10.5 - 4.6 \cdot \ln(B_q + 0.1)$$

where $B_q > -0.1$. The equation is based on 407 paired CPT and laboratory test results, particularly anisotropically consolidated triaxial compressive strength. Factoring of N_{kt} can be applied by multiplying the calculated N_{kt} factor by, for example, 0.85 and 1.2.

Mayne et al. (2015) recommend a mean $N_{kt} = 12$ with a standard deviation of 2.8 for correlation with laboratory anisotropically consolidated triaxial compressive strength. The recommendations are based on a study of 51 onshore and offshore clays and apply to normally consolidated to slightly overconsolidated clays with q_n values of typically less than 8 MPa. Slightly higher N_{kt} values can be expected for average laboratory undrained shear strength, defined as the average of laboratory triaxial compression, simple shear and triaxial extension.

Clay Sensitivity

The sensitivity of a clay (S_t) is the ratio of undisturbed undrained shear strength to remoulded undrained shear strength. Sensitivity may be assessed from the CPT friction ratio R_f , in accordance with Schmertmann (1978):

$$S_t = N_s / R_f$$

where N_s is a correlation factor typically ranging between 5 and 10. The correlation is expected to be inaccurate for sensitive clays where uncertainty in very low values for sleeve friction may dominate results.

The reference S_t value is often taken to be that determined from undisturbed and remoulded laboratory unconsolidated undrained triaxial tests. This reference S_t value may differ from that determined from other tests, for example laboratory miniature vane tests. This is partly related to the definition of sensitivity. For vane tests, several measurements of undrained shear strength are possible:

- Intact (I) = undisturbed undrained shear strength as measured on an intact/undisturbed specimen;
- Intact-Residual (I-R) = measured post peak during initial shearing of the intact specimen;
- Intact-Vane Remoulded (I-VR) = measured after multiple-quick rotations of the vane after completion of the intact test;
- Hand Remoulded (HR) = steady state (post-peak if exists) resistance of hand remoulded test specimen;
- Hand Remoulded – Vane Remoulded (HR-VR) = steady state resistance of hand remoulded specimen measured after applying multiple-quick vane rotations.

Skempton and Northey (1952) present a correlation of sensitivity and laboratory liquidity index I_L . This correlation may allow a check on CPT-based interpretation of sensitivity.

Effective Shear Strength Parameters - Clay

Measurement of pore water pressures during penetration testing has led to development of interpretation procedures for estimation of effective stress parameters of cohesive soils. Background information may be found in Sandven (1990). Currently available procedures are evaluated to be "experimental" and are yet not commonly adopted.

In general, CPT interpretation of effective shear strength parameters for clay and silt relies on soil behaviour-type classification.

It is noted that significant silt and sand fractions in a clay deposit will increase ϕ' , while a significant clay fraction in silt will decrease ϕ' .

Masood and Mitchell (1993) provide an equation for the determination of ϕ' by combining sleeve friction with the Rankine earth-pressure theory. The equation is based on the following assumptions:

- Unit adhesion between soil and sleeve is negligible;
- Friction angle between soil and sleeve = $\phi'/3$;
- Lateral earth pressure coefficient during penetration is equal to the Rankine coefficient of lateral earth pressure under passive conditions.

$$\frac{f_s}{\sigma'_{vo}} = \tan^2(45^\circ + \frac{\phi'}{2}) \tan(\frac{\phi'}{3})$$

(Masood & Mitchell, 1993)

Mayne (2001) proposed an approximation of the Masood and Mitchell equation, as follows:

$$\phi' = 30.8 \left[\log\left(\frac{f_s}{\sigma'_{vo}}\right) + 1.26 \right] \quad (\text{Mayne, 2001})$$

Mayne (2001) also proposed the following approximation of friction angle ϕ' based on pore pressure ratio B_q and the cone resistance number N_m (Senneset, Sandven and Janbu, 1989):

$$\phi' = 29.5B_q^{0.121}(0.256 + 0.336B_q + \log N_m)$$

(Mayne, 2001)

where

$$N_m = \frac{q_t - \sigma_{vo}}{\sigma'_{vo} + a}$$

where the cone resistance number N_m is dimensionless, total cone resistance q_t , total in situ vertical stress σ_{vo} and effective in situ vertical stress σ'_{vo} are in kPa.

Senneset et al. (1989) use the attraction value a as a function of soil type. In general, the attraction value ranges from 5 to > 50 for both sands and clays and may be estimated directly from CPT results. The correlation is valid if the angle of plastification β is zero. In general, a plastification angle of zero applies to medium sands and silts, sensitive clays and highly compressible clays.

Constrained Modulus - Clay

Mitchell and Gardner (1976) present an approximate correlation of cone resistance with constrained modulus M (or coefficient of volume compressibility m_v , where $M = 1/m_v$). Typical ratios of M/q_c range between 1 and 8 for silts and clays. Refinements include q_c ranges and soil type (silt, clay, low plasticity, high plasticity, etc.). The correlation relies on the results of conventional laboratory oedometer tests carried out on undisturbed clay and silt samples.

Kulhawy and Mayne (1990) correlated constrained modulus M with net cone resistance data. This relationship is based on data from 12 (clay) test sites, with constrained moduli up to 60 MPa. The published standard deviation is 6.7 MPa.

$$M = 8.25 q_n \quad (\text{Kulhawy & Mayne, 1990})$$

Young's Modulus – Clay

Young's modulus E_u can be derived as follows:

- Estimation of undrained shear strength s_u from CPT data, as outlined above;

- Estimation of secant Young's moduli for undrained stress change in general accordance with correlations based on s_u , as presented by Ladd et al. (1977).

Laboratory undrained triaxial tests carried out on undisturbed clay specimen form the basis for the E_u versus s_u correlations. Typical E_u/s_u ratios at a shear stress ratio of 0.3 range between about 300 and 900 for normally consolidated clays and $E_u/s_u = 100$ to $E_u/s_u = 300$ for heavily overconsolidated clay. Higher E_u/s_u ratios would apply to lower shear stress ratios, and vice versa.

Shear Modulus at Small Strain - Clay

Mayne and Rix (1993) determined a relationship between G_{max} and q_c by studying 481 data sets from 31 sites all over the world. G_{max} ranged between about 0.7 MPa and 800 MPa.

$$G_{max} = 2.78 q_c^{1.335} \quad (\text{Mayne \& Rix, 1993})$$

where G_{max} and q_c are in kPa.

References

- Agaiby, S.S. & Mayne, P.W. (2019). CPT evaluation of yield stress in soils. *Journal of Geotechnical & Geoenvironmental Engineering* 145(12): doi.org/10.1061/(ASCE)GT.1943-5606.0002164
- American Petroleum Institute [API] (2014). *Planning, designing and constructing fixed offshore platforms - working stress design*. (API RP 2A-WSD, 22nd Edition) <https://www.apiwebstore.org/publications/item.cgi?b9e32dec-268b-404d-988e-5cda65c27757>
- Baldi, G., Bellotti, R., Ghionna, V.N., Jamiolkowski, M., & Lo Presti, D.C.F. (1989). Modulus of sands from CPTs and DMTs. In *Proceedings of the 12th international conference on soil mechanics and foundation engineering, Rio de Janeiro, 13–18 August 1989* (pp. 165–170). Balkema.
- Battaglio, M., Bruzzi, D., Jamiolkowski, M., & Lancellotta, R. (1986). Interpretation of CPTs and CPTUs, part 1: Undrained penetration of saturated clays. In *Field instrumentation and in-situ measurements: Proceedings of the fourth international geotechnical seminar, 25–27 November 1986, Mandarin Hotel, Singapore* (pp. 129–143). Nanyang Technological Institute.
- Bolton, M.D. (1986). The strength and dilatancy of sands. *Géotechnique*, 36(1), 65–78. http://www-civ.eng.cam.ac.uk/geotech_new/people/bolton/mbd_pub/14_Geotechnique_No36_Is1_65_78.pdf
- Bolton, M.D. (1987). Author's reply to discussion of the strength and dilatancy of sands. *Géotechnique*, 37(2) 225-226 <https://doi.org/10.1680/geot.1987.37.2.219>
- Boulanger, R.W. & DeJong, J.T. (2018). Inverse filtering procedure to correct cone penetration data for thin-layer and transition effects. In M.A. Hicks, F. Pisanò & J. Peuchen. (eds.) *Cone Penetration Testing 2018: Proceedings of the 4th International Symposium on Cone Penetration Testing (CPT18): Delft, The Netherlands, 21-22 June 2018* (pp. 25-44). CRC Press
- Brooker, E.W. & Ireland, H.O., 1965. Earth pressures at rest related to stress history. *Canadian Geotechnical Journal*, 2(1), 1–15. <https://doi.org/10.1139/t65-001>
- Chen, B.SY., & Mayne, P.W. (1996). Statistical relationships between piezocone measurements and stress history of clays. *Canadian Geotechnical Journal*, 33(3), 488–498. doi.org/10.1139/t96-070
- DeJong, J.T. & Randolph, M.F. (2012). Influence of partial consolidation during cone penetration on estimated soil behavior type and pore pressure dissipation measurements. *Journal of Geotechnical and Geoenvironmental Engineering*, 138(7) 777-788: doi.org/10.1061/(ASCE)GT.1943-5606.0000646
- Hegazy, Y.A., & Mayne P.W. (2006, June). *A global statistical correlation between shear wave velocity and cone penetration data* [conference presentation]. GeoShanghai International Conference, Shanghai, China. ASCE. [https://doi.org/10.1061/40861\(193\)31](https://doi.org/10.1061/40861(193)31)
- Jaky, J. (1944). The coefficient of earth pressure at rest. *Magyar Mérnök és Építész Egylet Közlönye*, 78(22) 355-358. (in Hungarian).
- Jamiolkowski, M., Lo Presti, D.C.F., & Manassero, M. (2003). Evaluation of relative density and shear strength of sands from CPT and DMT. In J.T. Germaine, T.C. Sheahan & R.V. Whitman (Eds.), *Soil behavior and soft ground construction* (pp. 201–238). American Society for Civil Engineers. <https://doi.org/10.1061/9780784406595>
- Kulhawy, F.H., & Mayne, P.W. (1990). *Manual on estimating soil properties for foundation design*. (Report EL-6800). Electric Power Research Institute.
- Ladd, C.C., Foott, R., Ishihara, K., Schlosser, F. & Poulos, H.G. (1977). Stress-deformation and strength characteristics. In *Proceedings of the ninth international conference on soil mechanics and foundation engineering, 1977, Tokyo* (volume 2) (pp. 421-494). Japanese Society of Soil Mechanics and Foundation Engineering
- Lengkeek, H.J., De Greef, J. & Joosten, S. (2018). CPT based unit weight estimation extended to soft organic soils and peat. In M.A. Hicks, F. Pisanò & J. Peuchen (eds.) *Cone Penetration Testing 2018: Proceedings of the 4th International Symposium on Cone Penetration Testing (CPT18): Delft, The Netherlands, 21-22 June 2018* (pp. 389-394). CRC Press
- Masood, T. & Mitchell, J.K. (1993). Estimation of in situ lateral stresses in soils by cone-penetration test. *Journal of Geotechnical Engineering*, 119(10) 1624-1639: doi.org/10.1061/(ASCE)0733-9410(1993)119:10(1624)
- Mayne, P.W. (1988). Determining OCR in clays from laboratory strength. *Journal of Geotechnical Engineering*, 114(1) 76-92: doi.org/10.1061/(ASCE)0733-9410(1988)114:1(76)
- Mayne, P.W. (2001). *Geotechnical site characterization using cone, piezocone, SCPTu, and VST*. Georgia Institute of Technology.
- Mayne, P.W. (2020). The 26th Széchy Lecture: Use of in-situ geotechnical tests for foundation systems. *Proceedings of the Széchy Károly Emlékkonferencia*, published by the Hungarian Geotechnical Society, Budapest: 12-73
- Mayne, P.W. (2007). In-situ test calibrations for evaluating soil parameters. In T.S. Tan, K.K. Phoon, D.W. Hight & S. Leroueil (eds.) *Characterisation and Engineering Properties of Natural Soils* (Volume 3) (pp. 1601-1652). Taylor & Francis.
- Mayne, P.W., & Kulhawy, F.H. (1982). K_0 -OCR relationships in soil. *Journal of the Geotechnical Engineering Division*, 108(6), 851–872.
- Mayne, P.W. & Rix, G.J. (1993). G_{max} - q_c relationships for clays. *Geotechnical Testing Journal*, 16(1) 54-60 <https://doi.org/10.1520/GTJ10267J>

Mayne, P.W., & Rix, G.J. (1995). Correlations between shear wave velocity and cone tip resistance in natural clays. *Soils and Foundations*, 35(2), 107–110.
https://doi.org/10.3208/sandf1972.35.2_107

Mayne, P.W., Peuchen, J. & Bouwmeester, D. (2010). Soil unit weight estimation from CPTs. In CPT'10: 2nd International symposium on cone penetration testing, Huntington Beach, California: conference proceedings.

Mayne, P.W., Peuchen, J. & Baltoukas, D.B. (2015). Piezocone evaluation of undrained strength in soft to firm offshore clays. In V. Meyer (ed.) *Frontiers in Offshore Geotechnics III: proceedings of the Third International Symposium on Frontiers in Offshore Geotechnics (ISFOG 2015), Oslo, Norway, 10-12 June 2015*. (pp. 1091-1096) CRC Press.

Mayne, P.W. & Peuchen, J. (2018). Evaluation of CPTU N_{kt} cone factor for undrained strength of clays. In M.A. Hicks, F. Pisanò & J. Peuchen (eds.) *Cone Penetration Testing 2018: Proceedings of the 4th International Symposium on Cone Penetration Testing (CPT18): Delft, The Netherlands, 21-22 June 2018*. (pp. 423-429) CRC Press.

Mitchell, J.K. & Gardner, W.S. (1976). In situ measurement of volume change characteristics. In Proceedings of the conference on in situ measurement of soil properties, June 1-4, 1975, Raleigh, North Carolina: Specialty Conference of the Geotechnical Engineering Division, ASCE, II (pp. 279-345). American Society of Civil Engineers.

Peuchen, J. & Terwindt, J. (2014). Introduction to CPT accuracy. In 3rd International symposium on cone penetration testing CPT14 : May 12-14 (2014) - Las Vegas, Nevada.

Peuchen, J. & Terwindt, J. (2015). Measurement uncertainty of offshore cone penetration tests. In V. Meyer (ed.) *Frontiers in offshore geotechnics III: proceedings of the third international symposium on frontiers in offshore geotechnics (ISFOG 2015), Oslo, Norway, 10-12 June 2015*. (pp. 1209-1214) CRC Press.

Rix, G.J., & Stokoe, K.H. (1991). Correlation of initial tangent modulus and cone penetration resistance. In A.-B. Huang (Ed.), *Proceedings of the 1st international symposium on calibration chamber testing, ISOCCT1* (pp. 351–362). Elsevier.

Robertson, P.K. (1990). Soil classification using the cone penetration test. *Canadian Geotechnical Journal*, 27(1), 151–158.
<https://doi.org/10.1139/t90-014>

Robertson, P.K. (2009). Performance based earthquake design using the CPT. In T. Kokusho, Y. Tsukamoto, & M. Yoshimine (Eds.), *Performance-based design in earthquake geotechnical engineering: From case history to practice* (pp. 3–20). CRC Press.

Robertson, P.K. (2010). Soil behaviour type from the CPT: an update. In 2nd International symposium on cone penetration testing, Huntington Beach, CA, Vol. 2. (pp. 575-583)

Robertson, P.K. (2016a). Cone penetration test (CPT)-based soil behaviour type (SBT) classification system — an update. *Canadian Geotechnical Journal*, 53(12) 1910-1927
<https://doi.org/10.1139/cgj-2016-0044>

Robertson, P.K. (2016b). Estimating K_0 in sandy soils using the CPT. In B.M. Lehane, H.E. Acosta-Martinez & R.B. Kelly (eds.) *Geotechnical and geophysical site characterization 5: proceedings of the fifth international conference on geotechnical and geophysical site characterization (ISSMGE TC-102 - ISC'5), Gold Coast, Queensland, Australia, 5-9 September 2016* (pp. 515-518). Australian Geomechanics Society

Robertson, P.K. & Cabal, K.L. (2015) *Guide to cone penetration testing for geotechnical engineering*. (6th ed.) Gregg Drilling & Testing.

Robertson, P.K. & Wride (Fear), C.E. (1998). Evaluating cyclic liquefaction potential using the cone penetration test. *Canadian Geotechnical Journal*, 35(3), 442-459. <https://doi.org/10.1139/t98-017>

Robertson, P.K., Woeller, D.J. & Finn, W.D.L. (1992). Seismic cone penetration test for evaluating liquefaction potential under cyclic loading. *Canadian Geotechnical Journal*, 29(4) 686-695
<https://doi.org/10.1139/t92-075>

Sandven, R. (1990). *Strength and deformation properties of fine grained soils obtained from piezocone tests* [Thesis]. Norwegian Institute of Technology, Department of Civil Engineering

Schmertmann, J.H. (1978). *Guidelines for cone penetration test: Performance and design* (Report no. FHWA-TS-78-209). Federal Highway Administration, US Department of Transportation.

Senneset, K., Sandven, R., & Janbu, N. (1989). The evaluation of soil parameters from piezocone tests. *Transportation Research Record*, 1235, 24–37.
<http://onlinepubs.trb.org/Onlinepubs/trr/1989/1235/1235-003.pdf>

Skempton, A.W. (1957). Discussion on Airport Paper No. 35: The planning and design of the new Hong Kong Airport. *Proceedings of the Institution of Civil Engineers*, 7(2) 306.

Skempton, A.W., & Northey, R.D. (1952). The sensitivity of clays. *Géotechnique*, 3(1), 30–53.
<https://doi.org/10.1680/geot.1952.3.1.30>

Trofimenkov, J.G. (1974). Penetration testing in USSR: state-of-the-art report. in *Proceedings of the European symposium on penetration testing ESOPT, Stockholm, June 5-7, 1974*, 1 (pp. 147-154). National Swedish Building Research.

Van der Wal, T., Goedemoed, S. & Peuchen, J. (2010). Bias reduction on CPT-based correlations. In *CPT'10: 2nd international symposium on cone penetration testing, Huntington Beach, CA: conference proceedings*.

Wroth, C.P. (1984). The interpretation of in situ soil tests. *Géotechnique*, 34(4), 449–489.
<https://doi.org/10.1680/geot.1984.34.4.449>
<https://www.icvirtuallibrary.com/doi/pdf/10.1680/geot.1984.34.4.449>

Zhang, G., Robertson, P.K. & Brachman, R.W.I. (2002). Estimating liquefaction induced ground settlements from CPT for level ground. *Canadian Geotechnical Journal*, 39(5) 1168-1180.
<https://doi.org/10.1139/t02-047>

Positioning Survey and Depth Measurement

Introduction

This document describes survey of horizontal and elevation/depth reference points for geotechnical and/or environmental data acquisition in a marine environment.

National and international standards for geotechnical and/or environmental data acquisition (as ASTM, BSI, CEN and ISO) require such surveys. This document summarises common practice.

Procedure

The procedure for positioning survey and depth measurement depends on the agreed project specifications. For example, water level correction and subsurface positioning may not be part of the activities agreed upon. Some or all of the following steps can apply:

- definition of the type of survey and the target location;
- set-up and initial checks of the survey system and depth measurement system;
- surface positioning survey of the reference point, i.e. the determination of grid coordinates;
- sub-sea positioning survey, i.e. adjustment of the surface positioning results for underwater offset;

- sub-seafloor positioning survey, i.e. estimation of the spatial position of a data point below seafloor;
- measurement of the water depth;
- estimation of depth below water level for a data point applicable to the water column;
- estimation of depth below seafloor for a data point applicable to the seabed;
- calculation of elevation of seafloor relative to a vertical datum, e.g. water level correction;
- calculation of elevation of a data point relative to a vertical datum.

This document uses the terms seafloor and seabed. Seafloor is the underwater ground surface, i.e. the plane separating water and ground (soil, rock, made ground). The seabed is the ground below seafloor. A synonym for seabed is sub-seafloor (ISO, 2021).

IHO Classification for Horizontal Positioning and Water Depth

Positioning surveys require specific systems and procedures, such as those summarised below for marine applications. The International Hydrographic Organization (IHO, 2020) defines 5 orders of hydrographic survey (Table 1).

The term 'depth' refers here to water depth, i.e. the vertical distance between water level and seafloor and referenced to a vertical datum such as Lowest Astronomical Tide LAT. Note that a water level such as LAT depends on the calculation model used for determining the vertical datum.

The term 'uncertainty' considers a confidence level of 95 %.

Table 1: Summary of IHO Classification

Parameter Order	IHO Order				
	2	1b	1a	Special	Exclusive
Area description	Areas where a general description of the seafloor is considered adequate	Areas where under-keel clearance is not considered to be an issue for the type of surface shipping expected to transit the area	Areas where under-keel clearance is less critical but features of concern to surface shipping may exist	Areas where under-keel clearance is critical	Areas where there is strict minimum under-keel clearance and manoeuvrability criteria
Depth – total horizontal uncertainty	20 m + 10 % of depth	5 m + 5 % of depth	5 m + 5 % of depth	2 m	1 m
Depth – total vertical uncertainty	$a = 1.0$ m $b = 0.023$	$a = 0.5$ m $b = 0.013$	$a = 0.5$ m $b = 0.013$	$a = 0.25$ m $b = 0.0075$	$a = 0.15$ m $b = 0.0075$
Feature search	Not applicable	Not applicable	100 %	100 %	200 %
Bathymetric coverage	4 %	5 %	100 %	100 %	200 %
Feature detection	Not applicable	Not applicable	Cubic features > 2 m in depths up to 50 m; 10 % of depth beyond 50 m	Cubic features > 1 m	Cubic features > 0.5 m

Note: The use of coefficients a and b is as follows:

$$\pm\sqrt{[a^2 + (b * d)^2]}$$

where:

- a represents that portion of the uncertainty that does not vary with water depth
- b is a coefficient which represents that portion of the uncertainty that varies with water depth
- d is the water depth
- $b * d$ represents that portion of the uncertainty that varies with water depth.

Figure 1 illustrates the effect of coefficients *a* and *b*.

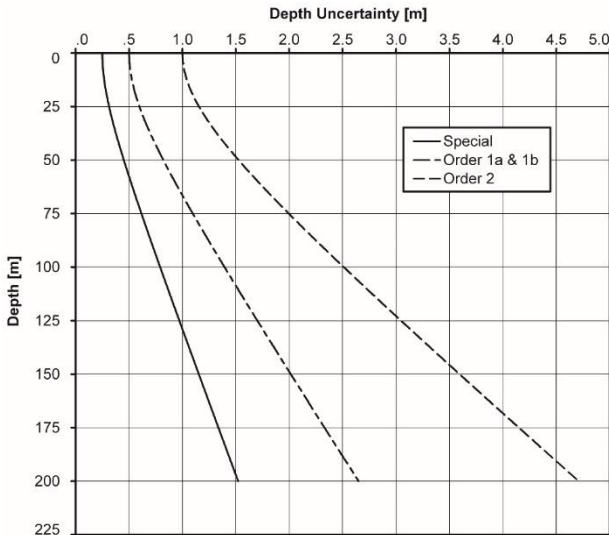


Figure 1: IHO water depth uncertainty

The IHO Special Order and Exclusive Order surveys are uncommon in geotechnical and/or environmental data acquisition. A Special Order system set-up may consist of: RTK DGPS; a multibeam echosounder; a motion compensator, and a conductivity temperature depth (CTD) probe. Subsurface positioning is uncommon in limited water depths.

An IHO Order 1a and 1b survey system set-up may include: high-accuracy DGPS; long baseline (LBL) subsurface positioning; a CTD probe with Digiquartz pressure sensor; a barometer; and a tide gauge.

IHO Order 2 surveys are common in geotechnical and/or environmental data acquisition. Such system set-ups could include: DGPS; ultra short baseline (USBL) subsurface positioning (IMCA, 2017); CTD probe; single beam echosounder or direct sounding by drill pipe; a motion compensator; and predicted tide correction.

These are examples of the simplest set-ups. Independent measurements are often made using a redundant system (IOGP, 2011; ISO, 2021). For example, surface position may be determined by two independent DGPS systems or direct sounding by drill pipe and echosounding.

ISO Classification for Seafloor Mapping

The International Organization for Standardization (ISO, 2021) defines three types of seafloor mapping:

- Reconnaissance seafloor mapping;
- Engineering seafloor mapping;
- Detailed engineering seafloor mapping.

The mapping types are primarily defined by cell sizes for digital terrain models.

ISO Depth Accuracy Classes

ISO (2014) provides depth accuracy classes, as shown in Table 2. These classes apply to depth below seafloor of a data point or measurement point acquired by borehole logging, in situ testing, and physical sampling and laboratory testing. ISO (2014) includes guidance on factors to consider for data point depth uncertainty. One of the factors is the position of a sample or test specimen within a sampler.

Class Z4 applies as default, except for samplers with no fixed seafloor reference, where Z5 applies as default.

Note that ISO (2014) uses accuracy class and application class interchangeably. A definition is given for application class and not for accuracy class. Application classes are defined in terms of 'classification of equipment based on achievable level of accuracy'. This is interpreted to mean achievable under favourable conditions.

Table 2: Depth Accuracy Classes for Data Point Measurements Relative to Seafloor

Depth Accuracy Class	Maximum Data Point Depth Uncertainty [m]
Z1	0.1
Z2	0.5
Z3	1.0
Z4	2.0
Z5	> 2.0

Guidance on use of Results

General

Use of results should consider that relatively complex uncertainty budgets (uncertainty estimates) can apply. Uncertainty budgets are typically project-specific, for example:

- Horizontal positioning of a tool at seafloor implies use of multiple instruments contributing to the uncertainty budget, e.g. (1) DGPS antenna position and (2) offset between antenna and actual position of the tool at seafloor;
- Soft soils can introduce uncertainty in underwater vertical position. A water pressure measurement tool mounted on an underwater frame may sink into the soil, thus affecting the measurement;
- Insufficient acoustic contrast between water and soft can affect echosounder water depth measurements;
- An irregular or sloping seafloor may affect echosounder measurements. An echosounder determines the earliest arrival of acoustic waves within the beam area. The highest points within the beam are assumed to correlate with the seafloor position, and thus yield the 'water depth'.

Horizontal positioning

- DGPS - antenna position uncertainty typically in the order of 1 to 2 metres;
- High accuracy DGPS - antenna position uncertainty typically in the order of 0.2 ;
- RTK DGPS – antenna position uncertainty typically in the order of centimetres;
- Gyro compass – uncertainty typically in the order of 0.5° to 1°;
- Directional inclinometer - uncertainty typically in the order of 1° to 2° (relative to vertical) and in the order of 5° to 10° (orientation relative to North).

DGPS uncertainty contributions include the geodetic network, vessel dynamics and antenna offset. Continuous logging on location allows some quantification of position uncertainty.

The acquisition and analysis of directional inclinometer data for sub-seafloor positioning can apply to a drill string or a cone penetration test. This practice is uncommon.

Sub-sea positioning

- LBL system: receiver position uncertainty typically in the order of 1 metre;
- USBL system: uncertainty of typically 0.5 m plus 1 % of distance between transducer and transceiver.

Uncertainty contributions include timing, ray bending, sound absorption, noise and offset.

Water depth measurement

- Direct sounding by drill pipe: uncertainty of typically about 1 m plus 0.5 % of measured mean water depth;
- Echosounder: uncertainty of typically about 0.3 m plus 1 % of measured mean water depth;
- Digiquartz probe: probe position uncertainty of typically about 0.2 m plus 0.1 % of measured mean water depth;
- Motion compensator: heave measurements have a typical uncertainty of 0.05 m, and roll and pitch an uncertainty of about 0.1°, relative to the mounting of the unit itself.

The pressure sensor estimates are corrected for atmospheric pressure. The echosounder estimate typically incorporates CTD sound velocity checks, motion compensation, and transducer draught, including vessel squat correction. Vessel squat is a vertical displacement of the hull as a vessel moves, and is determined by water depth and the vessel shape and size. The direct sounding estimate includes uncertainties related to tape measurement, heave, drill pipe length variation due to self-weight and temperature change, drill pipe bending and offset from vertical axis.

Tide correction

- Predicted tides: correction uncertainty typically in the order of 0.2 m to 1 m, depending on tidal range and meteorological circumstances;
- High accuracy DGPS: antenna position uncertainty typically in the order of 0.1 m;
- Tide gauge: correction uncertainty typically in the order of 0.1 m;
- RTK DGPS: antenna position uncertainty typically in the order of 0.1 m.

Depth below seafloor – marine soil investigation

Peuchen et al. (2005) present the following expression for depth uncertainty assessment for in situ testing, i.e. excluding considerations for sampling and laboratory testing:

$$\Delta z = \pm \sqrt{[a^2 + (b * d)^2 + (c * z)^2]}$$

where:

- a* constant depth uncertainty, i.e. the sum of all uncertainties that do not vary with depth below seafloor in metres
- b* uncertainty dependent on water depth, i.e. the sum of all uncertainties that are water depth dependent
- c* uncertainty dependent on data point depth below seafloor, i.e. the sum of all uncertainties that are data point depth dependent
- d* water depth in metres
- z* data point depth in metres below to seafloor
- Δz data point depth uncertainty in metres (95 % confidence level)

Tables 3 to 5 present coefficients and accompanying premises.

Table 3: Coefficients for Data Point Uncertainty Assessment – In Situ Testing

Deployment System	Data Point Depth Uncertainty Δz		
	<i>a</i>	<i>b</i>	<i>c</i>
Vessel drilling – favourable	0.4 m	0.003	0.003
Vessel drilling – adverse	1.0 m	0.005	0.004
Non-drilling – favourable	0.2 m	0	0.01
Non-drilling – adverse	0.8 m	0	0.02

Note: resolution estimated at 50 % of uncertainty

Table 4: Premise to Estimated Data Point Depth Uncertainty – In Situ Testing and Vessel Drilling Deployment

Characteristics	Marine Setting	
	Favourable	Adverse
Vessel - horizontal position	Variation within 5 m of target	Variation within 5 m of target
Vessel heave	1 m at 'hook' point	3 m at 'hook' point
Tidal variation	1.5 m, with correction for tidal variation by pressure sensor mounted on seabed frame	3 m, with correction for tidal variation by pressure sensor mounted on seabed frame
Seafloor	Firm and level	Very soft seabed soils or very rugged seafloor
Drill pipe checkpoint	Touchdown on seabed frame at borehole start	Touchdown on seabed frame at borehole start
Drill pipe bending	None	Minor
Borehole orientation	Vertical	Inclined at average 2° from vertical from sea level to test depth z

Table 5: Premise to Estimated Data Point Depth Uncertainty – In Situ Testing and Non-Drilling Deployment

Characteristics	Marine Setting	
	Favourable	Adverse
Vessel - horizontal position	Variation within 5 m of target	Variation within 5 m of target
Vessel heave	1 m at 'hook' point	3 m at 'hook' point
Tidal variation	1.5 m	3 m
Seafloor	Firm and level	Very soft seabed soils or very rugged seafloor
Orientation of Penetration	Vertical at start, with correction for measured inclination	Inclined at average 5° from vertical from seafloor to test depth z

Peuchen and Wemmenhove (2020) present a probabilistic approach to depth uncertainty assessment for in situ testing data points and for sample depths, including sample recovery considerations.

Note that definition of seafloor is difficult for extremely soft ground. Reaction equipment may penetrate unnoticed into a near-fluid zone of the seabed. Settlement may also continue during testing (Bouwmeester et al., 2009).

Seabed frame settlement is likely to be governed by the following factors:

1. Descent velocity and penetration into seabed, including possible erosion (scouring) caused by seabed frame descent and resulting water overpressures;
2. Non-centric loading during touchdown and testing;
3. Variable on-bottom weight of reaction equipment, because of drilling, sampling and testing activities and because of tensioning and hysteresis forces in a heave compensation system;
4. Consolidation of seabed soil.

Depth below seafloor – marine geophysical investigation

ISO (2021) includes some guidance on uncertainties for depth below seafloor for data acquired by marine geophysical investigation, such as seismic reflection survey.

Uncertainties can typically be reduced by ground truthing, i.e. comparison and depth correction on the basis of marine soil investigation data.

References

Bouwmeester, D., Peuchen, J., Van der Wal, T., Sarata, B., Willemse, C.A., Van Baars, S. & Peelen, R. (2009). Prediction of breakout forces for deepwater seafloor objects. In *OTC.09: Proceedings 2009 Offshore Technology Conference, 4-7 May, Houston, Texas, USA, OTC Paper 19925*
<https://doi.org/10.4043/19925-MS>.

International Association of Oil and Gas Producers & IMCA International Marine Contractors Association. (2011). *Guidelines for GNSS positioning in the oil & gas industry*. (Geomatics Guidance Note 19, IMCA S 015, IOGP Report No. 373-19) IOGP & IMCA

International Hydrographic Organization. (2020). *IHO standards for hydrographic surveys (S-44 Edition 6.0.0)*. IHO

International Marine Contractors Association. (2017). *Guidance on vessel USBL systems for use in offshore survey, positioning and DP operations* (IMCA M 244 (Rev 1)). IMCA (also IMCA S 017).

International Organization for Standardization. (2014). *Petroleum and natural gas industries – specific requirements for offshore structures – part 8: marine soil investigations*. (ISO 19901-8:2014).
<https://www.iso.org/standard/61145.html>

International Organization for Standardization. (2021). *Petroleum and natural gas industries - specific requirements for offshore structures – Part 10: Marine geophysical investigations*. (ISO 19901-10). <https://www.iso.org/standard/77017.html>

Peuchen, J., Adrichem, J. & Hefer, P.A. (2005). Practice notes on push-in penetrometers for offshore geotechnical investigation. In S. Gourvenec and M. Cassidy (Eds.) *Frontiers in offshore geotechnics ISFOG 2005: proceedings of the first international symposium on frontiers in offshore geotechnics, University of Western Australia, Perth, 19-21 September 2005*. (pp. 973-979). Taylor & Francis.

Peuchen, J. & Wemmenhove, R. (2020). Depth accuracy of data points in marine soil investigation. In Z. Westgate (ed.). *4th International Symposium on Frontiers in Offshore Geotechnics (ISFOG 2020): proceedings* (pp. 1036-1045). Deep Foundations Institute.

Marine Reflection Seismics

Introduction

Marine geophysical investigation by seismic reflection methods provides a continuous acoustic record of the seafloor and seabed (ground below seafloor). The acquired data are typically interpreted for site characterisation, particularly mapping of stratigraphic, geomorphological, structural and geohazard features of the seabed.

This document covers 2D high resolution (HR), ultra-high resolution (UHR) and ultra-ultra-high resolution (UUHR) seismic and sub-bottom profiler (SBP) seismic reflection methods.

- HR seismic: method that acquires data containing frequencies between 75 Hz and 300 Hz; expected vertical resolution range: 1 m to 7 m;
- UHR seismic: method that acquires data containing frequencies between 250 Hz and 800 Hz; expected vertical resolution range: 0.5 m to 2 m;
- UUHR seismic: method that acquires data containing frequencies between 750 Hz and 2000 Hz; expected vertical resolution range: 0.2 m to 1 m;
- SBP: method that acquires data containing frequencies between 1000 Hz and 15000 Hz; expected vertical resolution range: < 0.5 m.

These methods are commonly required to provide input for design, installation, operation and decommission of offshore structures (ISO, 2015; ISO, 2019)

Apparatus and procedures adopted by Fugro are in general accordance with ISO 19901-10:2021 (ISO, 2021) and ISSMGE (2005). The scope of marine geophysical investigation is according to agreed project specifications.

A marine geophysical investigation is commonly followed by marine soil investigation (ISO, 2014).

Apparatus

Overview

Reflection seismic survey spreads comprise the following components:

- Survey platform;
- Source to produce a discrete and repeatable acoustic pulse;
- Receiver (array) to receive the reflected signals;
- Positioning equipment;
- Recording/display unit(s).

Survey Platforms

Examples of survey platforms are:

- Geophysical survey (surface) vessel;
- Autonomous surface vessel (ASV);
- Remotely operated vehicle (ROV);
- Autonomous underwater vehicle (AUV).

Selection of a survey platform depends on factors such as scope of investigation, water depth and seafloor terrain (including gradients).

Sources

Acoustic sources are commonly classified on the basis of power levels and operation frequency. In general, higher power levels

result in lower frequencies and imply greater penetration in the seabed but with less resolution. Acoustic sources include:

- Pinger: a low energy device with an array of acoustic transducers that convert an electric pulse into an acoustic pulse within the frequency range of 3 kHz to 7 kHz;
- Chirp: type of pinger that emits a frequency-modulated pulse over a specified range of frequencies;
- Boomer: source powered by a rapid high-voltage discharge of capacitor banks through a spark gap. Combinations of energy supply and energy discharge units give available power levels ranging from 100 Joules to more than 1 000 Joules with a frequency range of 50 Hz to a few kHz;
- Sparker: a seismic source that operates by producing an electric discharge in water. The heat generated by the discharge vaporises the water at the electrode tips, creating an effect equivalent to a small explosion of bubbles, which oscillate and collapse after a few milliseconds. Sparker sources are generally limited to an energy range of 200 Joules to 10 000 Joules, though there is generally little advantage to be gained in increasing the energy level beyond 3 000 Joules;
- Airgun: source which injects a bubble of highly compressed air into the water.

In some systems, a source is combined with a receiver in a single unit (transducer), e.g. a pinger system mounted in the hull of a survey platform.

In many cases, a source is towed behind a geophysical survey vessel, either at the sea surface or at some depth below the sea surface.

Receivers

Receivers convert the transmitted acoustic energy (i.e. seabed reflections) into electric signals. Receivers include:

- Hydrophones;
- Geophones;
- Accelerometers.

Receiver configurations can comprise a single receiver (single channel), multiple receivers (ocean bottom nodes/ cables) or a group of receivers (array; multichannel). A group of receivers is incorporated in a flexible streamer, which is towed by the survey platform, either at the sea surface or at some depth below the sea surface.

Positioning Equipment

Positioning equipment typically includes multiple GNSS systems, mounted on the survey platform and in some cases on the source and receiver systems. For example, a streamer may be fitted with a tail buoy that includes a GNSS positioning system.

AUV and ROV survey platforms include subsea positioning systems.

Recording/ Display Units

A control unit is an integrated source trigger and recorder unit, which records the electrical signals from the receivers. The control unit may allow initial processing to the recorded data including:

- Overall and time varied gain (TVG);
- Swell filters;
- trace stacking;
- band-pass filters.

Signals are displayed in real-time and recorded digitally.

Procedure

Overview

The procedure for marine reflection seismics generally includes activities ranging from survey design to integrated geosciences. The agreed project specifications can cover some or all of the steps in the procedure.

Survey Design and Selection of Apparatus

Survey design depends on the required level of seabed detail. Particularly, it includes selection of apparatus and layout of survey track lines.

One or more seismic reflection methods can be selected, for example a combination of SBP and UHR methods. This selection phase takes account of factors such as:

- Feasible combinations of required resolution and penetration depth into the seabed;
- Inherent limitations, e.g. detailed imaging of the upper 0.5 m below seafloor (Peuchen and Westgate, 2018); this depth interval can be important for design of sub-sea templates, surface-laid pipelines and cables.

Survey platform, source and receiver (single or multiple) configurations are then selected. In general, such selection depends on expected wave heights, (tidal) currents, water depths, seabed conditions and sustainability considerations.

Where applicable, the tow depths of a source and of a receiver array (streamer) can be selected to minimise metocean effects (e.g. swell) on data quality of the recorded signals.

The survey line plan (i.e. survey design) typically considers:

- Required spatial detail of the ground model as function of survey track line spacing, e.g. lateral delineation of soil provinces, ground units and geological features;
- Detection of isolated seabed features, smaller than the distance between survey track lines (e.g. isolated boulders, shallow gas pockets, anthropogenic debris below seafloor etc.);
- Survey line orientations, taking into account seafloor morphological features that may impair adequate transmittal of seismic waves (e.g. survey track lines perpendicular to steep slopes to reduce unwanted noise in seismic data);
- Sustainability considerations including use of energy (e.g. reduction of negative effects on marine life).

Equipment Deployment

Equipment can be deployed (1) as integral part of the survey platform, (2) launched and towed behind a surface vessel and (3) by detached operations (e.g. for ocean bottom nodes).

For AUV and ASV operations, the survey line plan is uploaded in an internal navigation computer of these survey platforms. Following deployment, these systems autonomously acquire data along a programmed line plan, using a suite of acoustic sensors to avoid obstacles and maintain a specified speed and (in case of AUV) a near-constant elevation above seafloor.

For ROV operations, a ROV operator controls the survey platform from a vessel or from an onshore remote operations centre.

Equipment deployment can include a verification and testing programme for key components of the apparatus, for example by data acquisition along a line within the site. This line can be surveyed several times to adjust acquisition parameters (e.g. operating frequency and/or energy levels, equipment tow depth)

for local conditions to optimise trade-off between resolution and depth of penetration.

Data Processing

SBP data can be processed either in real-time or separately as a post-acquisition exercise. Basic processing steps include:

- Adding detailed geodetic positions to the acquired seismic traces;
- Applying a correction for tidal effects during data acquisition.

Additional processing typically applies to HR, UHR and UUHR seismic reflection data. Processing steps will vary according to agreed project specifications and site-specific conditions. The focus of the processing is typically on maintaining the relative amplitude relationships and preserving the high frequency content for the depth zone(s) of interest.

Processing techniques include (ISO, 2021):

- Gain recovery/amplitude manipulation;
- Velocity analysis;
- Mute;
- Normal moveout (NMO) correction and common mid-point (CMP) stack;
- Designature techniques;
- Demultiple techniques;
- Deconvolution before stack (DBS);
- Pre-stack time migration (PSTM);
- Post-stack coherent noise attenuation;
- Zero-phase conversion;
- Time varying filter (TVF);
- Time-depth conversion.

Assessment of Data Quality

For surface vessels, the quality of the data can depend on sea state, e.g. wave height during data acquisition. An example would be 'tugging' of a towing cable caused by large waves, having a detrimental effect on data quality.

Data acquisition in shallow coastal water may be impaired by surface breaking waves (i.e. surf zone). Acquisition in such areas is challenging and may require an exceptionally calm sea state.

Shallow gas in the seabed can make it impossible for seismic reflection methods to obtain adequate resolution at and below the upper surface of shallow gas. The presence of even a small amount of gas in the seabed causes substantial soil can drastically increase the attenuation of the acoustic signal, causing (acoustic) blanking.

Information from the data interpretation phase and the integrated geosciences phase can support assessment of data quality.

Data Interpretation

The data interpretation phase can make use of specialist interpretation software, allowing interrogation of seismic records or lines. Seismic reflectors, that correspond to geological and/or geotechnical ground units can be mapped as horizons. Furthermore, data interpretation allows mapping and assessment of potential geohazards, for example:

- Cemented coarse soil layers;
- Shallow gas;
- Buried channels (i.e. spatial variation in soil conditions).

Reflectors mapped in the time domain (e.g. two-way travel time as depth scale) can be converted to depth using an estimate for seismic velocity. Velocity estimates can be obtained from general

knowledge of the seabed, nearby marine geophysical investigation, a (seismic) velocity model and, preferably, by correlation (ground truthing) with site-specific geotechnical data (e.g. cone penetration test data showing distinct changes in cone resistance at soil unit boundaries) and data derived from borehole geophysical logging. Ground truthing increases reliability of data interpretation.

Integrated Geosciences

Integration of seismic reflection data with other methods of investigation can be done at different levels:

- Stratigraphic Zonation: integration focussing on achieving stratigraphic alignment between seismic profiles obtained by non-intrusive techniques and stratigraphic interpretation from results of intrusive ground investigation;
- Geotechnical Zonation: integration providing a vertical and horizontal zonation and includes mapping of 'soil provinces', with each soil province having a representative vertical soil profile and distinct seismic character;
- Geotechnical Zonation and Analysis – integration as per Geotechnical Zonation, additionally including engineering assessments for specific project requirements.

Results

Reporting Scope and Format

The results of a marine reflection seismics typically include documentation of data acquisition, data processing steps and interpretive features (e.g. seismic data character of the seabed and illustrative data examples). In addition, the following can be provided, depending on agreed project specifications:

- Track charts presenting positions of the survey track lines;
- Shallow structure maps, presenting depth to top or base of interpreted ground units;
- Isopach maps, presenting thickness range of interpreted ground units;
- Geological features maps, presenting positions of e.g. interpreted buried channels, shallow gas anomalies, etc.
- Cross sections;
- GIS data base;
- Digital, seismic interpretation project (e.g. Kingdom Suite project, Petrel project);
- Voxel ground model for GIS-type visualisation.

Reflection Amplitude

Reflection amplitude (high, medium, low) is the deviation of a seismic wave from the zero-crossing along a trace. It provides a measure of relative reflection strength and can provide an indication of lithological contrast (seismic velocity - density of ground), ground layer spacing, possible pore fluid/gas content etc.

In general, high amplitude events correlate to strong vertical variation of contrasting lithologies (e.g. sand / clay), while low amplitude indicates more comparable lithologies on both sides of an interface (e.g. sand / silty sand).

High amplitudes typically occur at seafloor, where there is a large contrast in density (unit weight) and velocity between seawater and seabed. A boundary between soil and rock is generally also associated with high amplitude reflectors. High amplitude reflections can also be associated with soil including (free, undissolved) gas, due to the low velocities for gassy soil.

A reversed (polarity) amplitude – as in "polarity reversal" – is an amplitude feature characterised by reversal of the seismic

reflection polarity along a horizontal interface, when followed from trace to trace. This may be due to a change in fluid/gas contents of pore space. Reversed polarity is commonly associated with gas in soil.

Seismic Frequency

Seismic frequency (high, medium, low) is commonly associated with resolution of seismic data. Resolution is the ability to distinguish two seabed features from one another (e.g. top and base of a ground layer and interbedding).

The vertical resolution (limit of separability) can be taken as $\frac{1}{4}$ of the seismic wavelength (λ). The wavelength in turn can be calculated from seismic velocity v , i.e. $\lambda = v/F$ where F is seismic frequency.

Seismic frequency decreases with increasing depth, as high frequencies in a seismic signal are more quickly attenuated. Conversely, seismic velocity generally increases with depth. As a result, vertical resolution of seismic data is depth dependent (Brown, 2004).

In general, high frequency seismic data imply reduced signal penetration below seafloor, but with greater overall vertical resolution.

Reflection Configuration

Reflection configuration can be described as parallel or sub-parallel, divergent, wavy, hummocky, chaotic, transparent etc.

Reflection configuration is related to the geometry/ pattern of ground layering/ bedding pattern resulting from specific depositional processes, original palaeotopography and post-depositional processes. For example, a high energy depositional environment (e.g. fluvial environment, debris flows) generally results in a more chaotic seismic response.

Reflection Continuity

Reflection continuity (continuous, discontinuous, truncation of reflectors) describes continuity of ground layers. It is directly related to sedimentation processes and post-sedimentation processes (e.g. erosion) and hence, to geological setting.

In general, the less energetic the environment, the more continuous the seismic response. Continuity also indicates greater lateral extent of certain depositional conditions, while discontinuities may suggest rapid changes in energy levels during deposition and/or effects of post-depositional erosion.

For example, flood plain deposits are generally associated with a low energy environment that may be laterally continuous. The reflections associated with a flood plain are generally continuous (parallel bedded reflectors). The reflections associated with a (meandering) stream or fluvial channel are localised and of low lateral continuity.

Multiple Reflections

'Multiples' are commonly associated with seismic datasets. Multiple reflections are reflections generated by acoustic waves travelling several times (reverberation) between two strong interfaces (e.g. seafloor and a boundary between rock / soil layers) before they arrive at the receiver. Multiple reflections can be strong and can interfere with reflections of geological interfaces, whereby the latter are obscured in the depth interval where the multiples appear.

For example, an acoustic wave traveling from its source may be reflected off the seafloor, the sea surface and the seafloor again before arriving at the receiver (seafloor multiples). The "ray-path"

of this multiple is approximately twice that of a normal source-seafloor-receiver ray-path.

If two strong subsurface reflectors are present, acoustic signals may “bounce” several times between them, before the wave-front can be recorded at the receiver (peg-leg multiples).

Seismic Artefacts

Seismic artefacts may be caused by lateral variation of seabed conditions, including buried boulders and steeply dipping ground strata. Examples are:

- Pull-up effects below seafloor sand waves, where seismic reflectors can appear at slightly higher elevations than where sand waves are not present. This is due to small seismic velocity variations and steep-sided slopes of the sand waves;
- Acoustic transparency and signal attenuation below crests of sand waves and enhanced amplitude reflections or signal tuning at the troughs of the sand waves. These feature can mask seismic signal;
- Pull-down effects as indicator for the presence of free gas in the seabed. Gassy soils have lower seismic velocity and hence acoustic waves travel slower than in fluid-saturated soils, causing seismic reflectors to (locally) occur lower than in non-gassy soils;
- Hyperbole-shaped reflections (i.e. diffraction hyperbolae) originating from “point sources” in the seabed. Typical point sources are buried boulders, pipelines and cables.

Bibliography

Brown, A. (2004). *Interpretation of three-dimensional seismic data*. (6th ed.) American Association of Petroleum Geologists (AAPG); Society of Exploration Geophysicists (AAPG Memoir ; 42)(SEG Investigations in Geophysics ; No. 9)

International Organization for Standardization. (2015). *General principles on reliability for structures*. (ISO 2394:2015). <https://www.iso.org/standard/58036.html>

International Organization for Standardization. (2019). *Petroleum and natural gas industries – general requirements for offshore structures*. (ISO 19900-2019). <https://www.iso.org/standard/69761.html>

International Organization for Standardization. (2014). *Petroleum and natural gas industries – specific requirements for offshore structures – part 8: marine soil investigations*. (ISO 19901-8:2014). <https://www.iso.org/standard/61145.html>

International Organization for Standardization. (2021). *Petroleum and natural gas industries - specific requirements for offshore structures – part 10: marine geophysical investigations*. (ISO 19901- 10:2021). <https://www.iso.org/standard/77017.html>.

International Society for Soil Mechanics and Geotechnical Engineering, Technical Committee 1. (2005). *Geotechnical & geophysical investigations for offshore and nearshore developments*. International Society for Soil Mechanics and Geotechnical Engineering. (ISSMGE)

Peuchen, J. and Westgate, Z.J. (2018). Defining geotechnical parameters for surface-laid subsea pipe-soil interaction. In M.A. Hicks, F. Pisanò & L.J. Peuchen, L.J. (eds.) *Cone Penetration Testing 2018: Proceedings of the 4th International Symposium on Cone Penetration Testing (CPT18): Delft, The Netherlands, 21-22 June 2018*. (pp. 519-524) CRC Press.

Site Characterisation

Introduction

Site characterisation may be defined as a fit-for-purpose model of a site. For the context of this document, site is defined as a geographical part of the earth at a particular time or period, that:

- Incorporates the surface of the earth and ground below this surface;
- Can include water and air above the ground surface;
- Can include man-made objects and structures in or connected to the ground.

Ground is defined as soil and rock, including made ground, pore fluid and pore gas.

A fit-for-purpose site model is fundamental to managing ground risks and optimizing opportunities. The model is a prediction and a reduction of reality and can be used to:

- Provide sound information with which to define and assess the suitability of a site for proposed facilities;
- Detect and assess the possible effects of geohazards and changes in seabed conditions with time;
- Choose parameter values for verification of limit states and to assess the feasibility of building/installing, operating, and/or decommissioning a structure.

The model has interpretive limits that typically depend on:

- Structure characteristics and project phase such as conceptual design, installation and structure re-assessment;
- Data selected and available at the time of study:
 - Stratigraphic schematisation, e.g. partial data coverage or detection limits of deployed investigation tools and an interface between strata being more gradual than indicated;
 - Level of detail and accuracy in interpretation of geotechnical parameter values, which can be affected by test data, sample size, quality, and coverage;

- Public-domain information such as geological understanding;
- Data visualisation algorithms, e.g. for data contouring.

Other terms used in practice for (parts of) site characterisation include integrated study, integrated geosciences, desk study, and seabed characterisation.

Site characterisation can also refer to the activities required to create the model of the site (e.g. Evans, 2010; Peuchen, 2012). Ideally, site characterisation benefits from integration of multidisciplinary data (e.g. geotechnical and geophysical data integration).

This document focuses on marine projects. Site characterisation is an integral part of offshore structure design and operation according to reliability principles covered by standards and codes of practice; for instance API (2014a, 2014b and 2015), ASTM (2018), DNV GL (2017), RenewableUK (2013), CEN (2009 and 2015); ISO (2014, 2016a, 2016b, 2017, 2019 and 2021).

Table 1 shows levels of integration that can be considered.

The terms seabed and seafloor are according to ISO (2016a):

- Seabed comprises materials below the sea in which a structure is founded, whether of soils such as sand, silt or clay, cemented materials or, of rock
- Seafloor is defined as the interface between the sea and the seabed.

This document also uses the geological term 'sediments' as synonym of uncemented soil.

Table 1: Levels of Integration for Marine Site Characterisation

Integration Level	Integration Type	Description
1	Bundled Information	Each data acquisition activity is interpreted and reported separately. No specific effort is made to consider and reconcile potential conflicts between information sources.
2	Stratigraphic Integration	This level of integration specifically focusses on achieving stratigraphic alignment between (1) sub-surface/sub-bottom profiles obtained by non-intrusive geophysical techniques (e.g. seismostratigraphy) and (2) stratigraphic interpretation from results of ground investigation obtained at specific locations (e.g. geotechnical soil unitisation). The stratigraphic alignment considers vertical zonation of a site.
3	Geotechnical Zonation	This level of integration provides a vertical and horizontal geotechnical zoning of a site. The horizontal zonation comprises a delineation and mapping of 'soil provinces'. Each soil province has a representative vertical soil profile and envelopes of ground characterisation such as shear strength, relative density, friction angle, unit weight, etc. The 'horizontal and vertical zoning' facilitates selection of engineering criteria (e.g. geotechnical parameter values/ranges) for analysis of trenchability, anchor holding capacity, foundation bearing resistance, etc.
4	Geotechnical Zonation and Analysis	This level of integration not only provides geotechnical zonation but also incorporates engineering assessments for specific project requirements such as bearing resistance, trenching resistance, anchor holding capacity, upheaval buckling resistance, scour potential etc. These requirements are usually specific to the type of facility, construction method and project phase.

Procedure

Figure 1 summarises the general procedure. Decisions on scope and adequacy are project-specific and depend on input such as project specifications, management of site risk, sustainability considerations and schedule constraints.

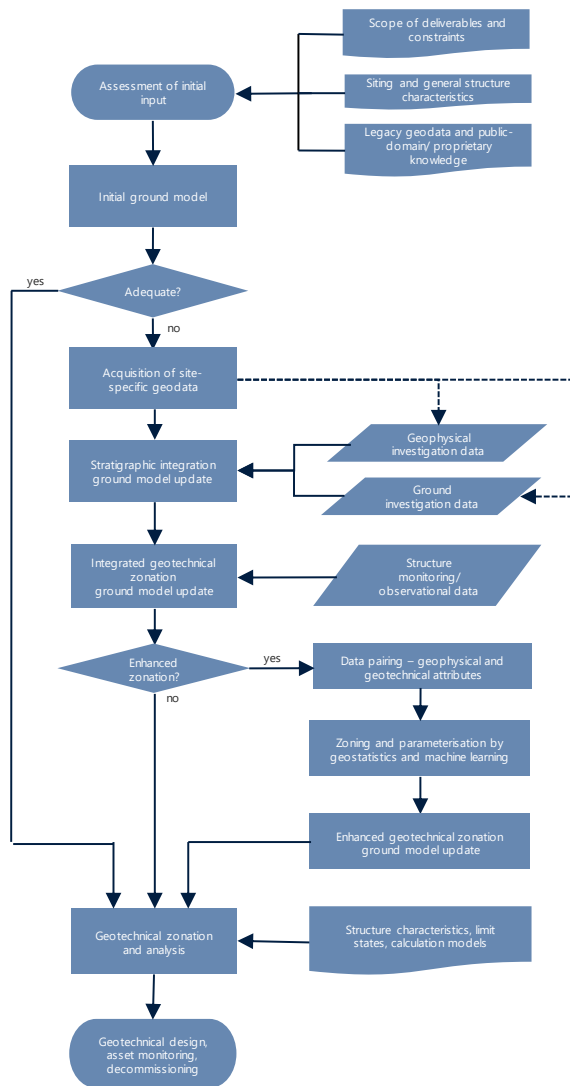


Figure 1: General procedure

Figure 1 includes terms of Table 1. The procedure item “enhanced zonation” is relatively novel to industry and ISO (2021) recommends appropriate caution.

Visualisation of Ground Model

Diagrams, still images, video and 3-D visualisation can communicate and convey site characterisation to experts, users of the model, and the public at large.

For Integration Levels 2, 3 and 4 (Table 1), a common approach for data management and imaging is combining a GIS (geographical information system) with one or more separate software packages. SubsurfaceViewer software for 3-D voxel visualisation, IHS Markit® Kingdom software for geophysical data and GeODin® software for geotechnical data are examples of such software packages for nearshore and offshore projects.

Site Hazards

Types of Hazards, Risk and Mitigation

Site hazards may be grouped into:

- Natural geohazards;
- Man-made hazards.

Natural geohazards are commonly referred to as geohazards or geological hazards. They are about past geological processes and events that have shaped the seafloor and seabed. Some of these processes may still be active today. The resulting seafloor topography, and geological and geotechnical conditions within the seabed can be hazardous when installing offshore structures including infrastructure (e.g. Clayton and Power, 2002; IOGP, 2009, 2017; API, 2014a).

Man-made hazards include shipwrecks, fallen objects, seafloor debris and unexploded ordnance. Within the context of this document, man-made hazards exclude accidental events such as vessel impact, sabotage, well drilling problems, and fishing activities.

In relation to offshore activities, geohazards can be defined as local and/or regional site conditions and ground conditions having a potential of developing into a condition (e.g. irregular seafloor topography) or process (e.g. currents, submarine slides) that could cause loss of life or damage to health, environments and/or assets. The event-triggering sources can be ongoing geological processes or human induced changes (IOGP, 2009). Figure 2 presents a schematic overview of offshore geohazards.

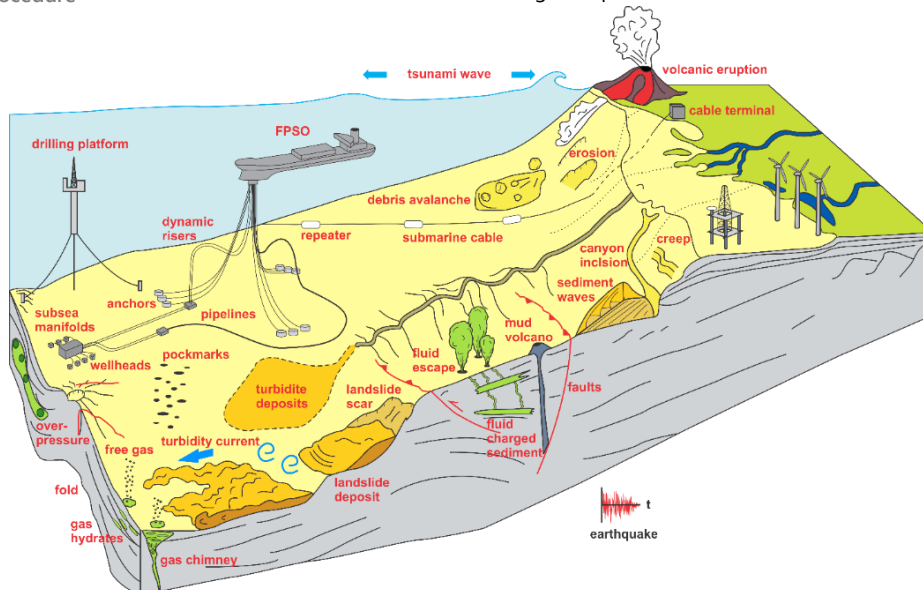


Figure 2: Offshore natural geohazards (modified after Campbell et al., 1986)

The damage potential of site hazards can range from, for example, local effects on pipelines and subsea structures to complete loss of all installations in a license areas and third party losses (IOGP, 2009).

The table below presents an overview of potential impacts and/or consequence associated with natural geohazards (and man-made hazards) occurring offshore.

Table 2: Potential Impact/Consequence Associated with Site Hazards

Impact/Consequence	Natural Geohazards and Man-made Hazards															
	Irregular Seafloor Topography	Seafloor Bedforms	Seafloor Outcrops and Hard Seafloor	Soil Liquefaction	Shallow Gas and Gassy Soils	Gas Hydrates	Gas and Fluid Seepage	Diapirs (e.g. Mud /Salt) and Mud Volcanoes	Earthquakes	Faults	Tsunamis	Slope Failure	Submarine Mass Movement	Wind, Waves and Currents	Seafloor Scour and Sediment Mobility	Man-Made Hazards
Uneven support (foundation instability)		x				x				x	x				x	
Loss of support (structural stresses)				x			x		x		x	x	x			
Spanning (pipeline and flowlines)	x	x	x							x						
Increased foundation settlements, reduced access				x	x											
Burial/embedment leading to additional loading and reduced access		x		x									x		x	
Reduced soil strength and bearing resistance				x	x		x									
Lateral loading of structure leading to overstressing of foundation/structure components									x		x	x	x	x		x
Structure displacement and structural damage				x					x	x	x	x	x			x
Increased potential for soil liquefaction					x	x	x		x		x			x		
Increased potential for shallow soil instability and submarine sliding					x	x	x	x	x		x			x	x	
Foundation and structure installation difficulties	x	x	x		x	x	x									x
Steel abrasion, gouging and denting; excessive wear of trenching equipment			x													
Gas and fluid migration (excess pore pressures)					x	x	x	x		x	x			x		
Corrosion of steel structures, pipelines, flowlines					x		x	x								
Well (borehole) instability					x	x	x			x						
Mud losses (well/borehole drilling)										x						
Damage to casing string and pile foundations										x						
Presence of environmentally protected chemosynthetic communities					x		x	x								
Explosions leading to changed site conditions																x

Site hazards can generally not be treated on a statistical basis applying solely historical data. The nature of a hazard is often site and time dependent. In addition, natural geohazards are often interrelated. This may be due to a common trigger mechanism (e.g. earthquake, slope failure), or that one geohazard occurrence or process forms a trigger for other geohazards.

For instance:

- Earthquakes will induce dynamic actions on a structure and may induce elevated pore pressures leading to increased susceptibility to soil liquefaction;

- Slope failures and their deposits may result in irregular seafloor topography;
- Mud and salt diapirs are commonly associated with radial fault patterns, and continuous diapirism may result in (shallow) slope failures.

Table 3 highlights some relations between natural geohazards.

Table 3: Related Offshore Natural Geohazards

	Irregular Seafloor Topography	Seafloor Bedforms	Seafloor Outcrops and Hard Seafloor	Soil Liquefaction	Shallow Gas and Gassy Soils	Gas Hydrates	Gas and Fluid Seepage	Diapirs (e.g. Mud /Salt) and Mud Volcanoes	Earthquakes	Faults	Tsunamis	Slope Failure	Submarine Mass Movement	Wind, Waves and Currents	Seafloor Scour and Sediment Mobility
Irregular Seafloor Topography		x	x							x		x	x	x	x
Seafloor Bedforms	x													x	x
Seafloor Outcrops and Hard Seafloor	x				x		x	x				x			x
Soil Liquefaction					x	x	x	x	x					x	
Shallow Gas and Gassy Soils			x	x		x	x	x		x		x	x		
Gas Hydrates				x	x		x					x	x		
Gas and Fluid Seepage			x	x	x	x		x		x		x	x		
Diapirs (e.g. Mud /Salt) and Mud Volcanoes			x	x	x		x			x		x			
Earthquakes				x						x	x	x	x		
Faults	x				x		x	x	x		x	x	x		
Tsunamis									x	x		x	x	x	x
Slope Failure	x		x		x	x	x	x	x	x	x		x	x	x
Submarine Mass Movement	x				x	x	x		x	x	x	x		x	x
Wind, Waves and Currents	x	x		x							x	x	x		x
Seafloor Scour and Sediment Mobility	x	x	x								x	x	x	x	

Assessment of hazard probability of occurrence and frequency can be based on geomechanical modelling taking into account uncertainty in modelling of site conditions, ground parameter values, ongoing geological processes, actions and applied analysis methods (Clayton and Power, 2002; IOGP, 2009).

The risk of a site hazard is the sum of the product of the probability of a hazard event affecting a structure and damage consequence. The damage consequence can depend on factors such as structure robustness and vulnerability. The information in this document covers the nature of hazards and their potential implications, not the risk. Power et al. (2005) and Galavazi et al. (2006) describe risk analysis methodology.

Risk mitigation can include avoidance (e.g. a certain standoff distance to avoid structure interaction) and design for robustness.

Irregular Seafloor

Seafloor morphology can be irregular as a result of past or present geological processes. Human activities can also affect the seafloor topography. Irregular seafloor may be caused by (or be associated with) a number of natural and man-made phenomena. These include:

- Canyons and channels;
- Boulders (e.g. drop stones);
- Spudcan footprints;
- Anchor scars;
- Trawl marks and ice gouging;
- Drill cuttings.

The scale of morphological features varies (e.g. scour marks, submarine canyons). The impact can differ per structure type and geometry.

Seabed Scour and Sediment Mobility

Seabed scour relates to the erosion of seabed sediments. Such erosion can occur under normal metocean conditions or can be enhanced as a result of a structure or multiple structures interrupting a natural flow regime above seafloor, thereby increasing flow velocities. Scour can be enhanced or initiated by secondary processes such as rocking of a structure.

Especially non-cohesive sandy (and silty) sediments are susceptible to scour. Erosion and transport of fine sand can start at a flow velocity in excess of 0.2 m/s. Local scour pits (or scour holes) can form shortly after installation of a structure. Their dimensions will usually vary in time depending on the flow regime.

Scour can occur in any water depth (from shoreline to deep sea). The flow regime due to wave- and tidal influence is generally stronger in shallow water than in deep water (Soulsby, 1997; Sumer and Fredsoe, 2002). In general, tide- and wave action, in combination with fluvial discharge of fresh water, determine the natural flow regime in coastal areas. Deepwater bottom current activity may result from density differences between water

Table 4: Seafloor Bedforms

Bedform Type	Related Flow	Wavelength [m]	Amplitude [m]	Time-scale	Migration Rate	Source
Ripple	Instant flow	0.1 to 1	0.01 to 0.1	Hours	> 1 m/day	2, 3, 4
Megaripple	Storm surges	10 to 20	0.1 to 1.5	Days	100 m/year	1, 3
Sand wave	Tidal currents	50 to 1000	2 to 18	Decades	1 m/year to 10 m/year	1, 2, 3, 4
Long bed wave	Unknown	1500 to 2500	1 to 5	Unknown	Unknown	2, 3, 4
Sand bank	Tidal currents	5000 to 10000	5 to 50	Centuries	m/year	2, 3, 4

1. Ashley (1990)
 2. Dodd et al. (2003)
 3. Morelissen et al. (2013)
 4. Reineck and Singh (1980)

For structure design it is important to know which part of the seabed and/or the bedforms is actually mobile. For example, cable trenching can modify bedforms. The rate at which the bedforms recover after cable trenching will depend on sediment transport rate and supply of sediment.

Seafloor Outcrops and Hard Seafloor

Seafloor outcrops and hard seafloor ground conditions commonly include:

- Shell and coral banks, reefs, which are common in shallow waters in the tropical zones;
- Local patches of cemented soil (e.g. hard ground, cap rock). Examples are authigenic carbonates around pockmarks, Kurkar ridges (cemented aeolian dunes) in the eastern Mediterranean Sea, beach rocks (cemented beach sediments) in the Caribbean Sea, sabkha deposits (evaporitic-tidal floodplain deposits) in the Arabian/Persian Gulf and Gulf of Suez;
- Crust composed of precipitated metal sulphides associated with hydrothermal activity (e.g. black and white smokers) in vicinity of tectonic plate boundaries and faults;
- Outcrops of rock. Examples are pre-Quaternary sand- and limestone beds offshore West Africa, sedimentary and metamorphic rocks exposed in the Irish Sea.

masses and from global thermohaline ocean circulation. Resulting sedimentary accumulations are known as contourite drifts (Faugeres et al., 1999).

Seafloor variation can usually be characterized as some combination of the following (Whitehouse, 1998):

- Local scour and sedimentation; usually a steep-sided scour pit around a structure or structural element;
- Global (or general) scour; a (shallow) scoured basin of large extent around a structure, possibly due to overall structure effects, multiple structure interaction, or wave-soil-structure interaction;
- Overall seabed movement; erosion, deposition, bedform migration that would also occur in the absence of a structure (i.e. regional scour).

Seafloor Bedforms

A seafloor bedform is a morphological feature formed by interaction of wave action and (tidal) currents and cohesionless sediment (i.e. sand/silt). Bedforms are typically found in sandy areas at a continental shelf.

A characteristic of bedforms is their mobility (Table 4). Sand waves tend to move slowly (metres per year) or flex their crests with (tidal) currents. Smaller-scale ripples tend to be more mobile, in the order of metres per day.

It should be noted that seafloor outcrops and hard seafloor may have environmental protection status or legislative implications.

Cementation of soil may result from sub-marine cementation processes. Cementation may also have resulted from past sub-aerial exposure of a continental shelf during low sea level stands under arid climate conditions. Cementation generally occurs in carbonate-rich and hyper-saline environments.

Diapirs and Mud Volcanoes

A diapir is a domal upwelling of sediment, rock or salt that forms in response to tectonic forces, density differences, and high overburden pressures. Diapirs can pierce through a stratigraphic overburden and create an envelope of overconsolidated soils, deformed rock, and sediments around a diaper core (e.g. salt). Generally, a circular dome-shaped topographic feature develops when a diapir approaches the seafloor. Diapirs are commonly associated with radial faulting patterns and locally increased seafloor slopes.

Salt diapirs are known to be present in, for example, the Gulf of Mexico, offshore Brazil and West Africa, and the North Sea.

Mud diapirs and mud volcanoes are usually associated with rapidly-deposited sediments and in situ pore pressure conditions

significantly higher than hydrostatic (overpressured). Additionally, high vertical and horizontal stresses typically apply, caused by faulting, folding and uplift processes.

Mud diapirs and mud volcanoes occur mostly in (historic) delta areas: Nile Delta (offshore Egypt), Absheron Ridge (offshore Azerbaijan, Caspian Sea), Makran Ridge (offshore Iran, Arabian Sea), and Niger Delta (offshore Nigeria).

Release of pressure is commonly provided by faults and folding of the strata. Sediments mixed with over-pressured fluid and gas (mud) migrate upward through the stratigraphic overburden in vertical columnar zones (diapirs). Usually the over-pressured muds enter fault planes, thus causing diapirism along faults. A mud volcano can form when a mud diapir breaks the seafloor.

In general, mud volcanoes are conical, as tall as 65 m and up to 2 km across. The size and shape of a mud volcano depends on the frequency of expulsion and the type of material ejected. This can be unconsolidated soils, overconsolidated material, fractured rock (e.g. breccia), oil, gas, and water (Snead, 1972; Newton et al., 1980; Delisle et al., 2002; Delisle, 2004; Delisle, 2005). Not all offshore mud volcanoes are active. Eruptions are believed to be episodic.

Shallow Gas and Gassy Soils

Gas may be present (trapped) in the seabed (e.g. gassy soils). Shallow gas can comprise a mixture of different gases, such as carbon dioxide, hydrogen sulphide, ethane, and methane. In general, the gases originate from bacterial decay of organic matter (biogenic gases) within a few metres of the seafloor. Gas may also come from sources much deeper in the stratigraphy and migrates upwards through pores and cracks in the soil and rock (petrogenic gases).

Shallow gas may be present dissolved in pore water, as free gas in gas-filled voids or bubbles, and as gas hydrates. Over time, gas in soil may increase the in situ pore pressures and result in excess pore pressures.

Migration of gas in soil can result in accumulation of gas in the seabed below a foundation. Shallow gas in the pore water can have a serious effect on foundation behaviour.

In addition, shallow gas can be toxic to humans, can combust and explode.

Soil property measurements on geotechnical samples containing shallow gas may not be representative of in situ properties.

Gas Hydrates

Gas hydrates are ice-like crystalline solids composed of water molecules surrounding a molecule of gas, generally methane. Gas hydrates can only form when gas is over-saturated in water. Gas hydrates are stable under high pressure and low temperature conditions, and may be present at seafloor and in shallow sediments, generally in deep water environments in excess of 500 m below Mean Sea Level (Rastogi et al., 1999; Von Rad et al., 2000).

Stable gas hydrate acts as cement and increases strength and rigidity of soil.

Natural gas hydrates are regarded as a geohazard when they dissociate, start 'melting'. Both water and gas are released into soil when gas hydrates dissociate. This can result in formation of 'gassy soils'. The addition of water and gas may decrease soil strength and form a weak layer (Orange and Breen, 1992; Judd and Hovland, 2007). Gas hydrate dissociation may be initiated by

human activities, e.g. flow of 'hot' hydrocarbons through well production casings, pipelines and flowlines.

Gas hydrates may form as a result of human activity. Gas hydrates can be a by-product of hydrocarbon production, forming hydrate plugs in the wellbore, around leaking joints and in pipelines. If a deep water exploration or production well is leaking, gas introduced into the shallow soils may react with water molecules to form hydrate layers or nodules.

Gas and Fluid Seepage

Gas and fluid seepage at seafloor is commonly associated with pockmarks. Pockmarks are roughly circular or conical depressions in the seafloor, generally 1 m to 350 m wide and up to 35 m deep (Newton et al., 1980; Von Rad et al., 2000; Judd and Hovland, 2007).

Pockmarks form by disruption of a pore pressure environment. This disruption may be triggered by natural or human causes, and can form on time scales of less than a year. Pockmarks can be intermittently active over long periods of time or can grow with explosive eruption events. The sediments in a pockmark are generally variable and may be overconsolidated.

When gas seeps continue over a long period of time, biological processes may cause cementation of the seabed sediments. Formation of authigenic carbonates can take place around the seeps (Judd and Hovland, 2007; Ding, 2008). In some cases, unique ecological habitats form in and around pockmarks. Such habitats may be protected by environmental legislation.

Authigenic carbonates may form thin crusts of weakly cemented sediments (hard grounds). They can be continuous over distances of several hundreds of metres (Von Rad et al., 2000). Locally more massive, competent layers of authigenic carbonates can be present as hard cemented layers or 'lenses'. They may form large build-ups and seafloor mounts (Judd and Hovland, 2007).

Apart from natural seeps, gas seepage may also be induced by drilling activities (e.g. geotechnical drilling, hydrocarbon exploration drilling). The drilling process may cause fracturing of soil and rock, when drilling mud pressures exceed the fracture pressure of the soil or rock (i.e. hydraulic fracturing). These fractures may form pathways for fluid and gas migration into the wellbore and up to seafloor. A wellbore or leaking well casing may form a pathway to the surrounding rock and soil formations, introducing gas into sand layers in the shallow subsurface. Overtime, the introduced gas may affect the geotechnical properties of a soil and have serious effects on foundation behaviour.

Drilling-induced fluid flows (e.g. shallow water flows) occur when a pressurised sand body (aquifer) encapsulated in clay is penetrated by the drilling process. Shallow water flows are common offshore large river deltas, such as the Mississippi Delta (Gulf of Mexico) and the Nile Delta (offshore Egypt). The sand bodies are commonly derived from sediment deposition out of turbidity currents.

Earthquakes

An earthquake, or seismic event, occurs after stresses in the earth's crust that have gradually built up, are suddenly released by movements along a fault. The movement generates seismic waves which propagate away from the earthquake epicentre. Most earthquakes occur along tectonic plate boundaries.

The location, magnitude, and frequency (recurrence) of earthquakes cannot be reliably predicted. The probability of

seismic events can be assessed on the basis of historic records of earthquake activity.

Seismic impact depends on geotechnical conditions at the site and structure design. Seismic activity may induce faulting, soil liquefaction, slope failure, and tsunamis.

Soil Liquefaction

Two types of liquefaction may be distinguished:

- Gravitational (sometimes called static- or flow-) liquefaction, usually occurring in submerged slopes;
- Cyclic liquefaction, usually generated through strong cyclic forces.

Soil liquefaction or cyclic mobility represents a decrease of soil strength and stiffness caused by an increase in pore water pressure in saturated soil. Soil liquefaction usually occurs in response to sudden change in stress condition, causing it to behave like a liquid. Examples of cyclic and dynamic actions include earthquake shaking, storm wave loading, structure displacements upon cyclic load application, pile installation by driving, and vortex vibrations due to fluid flow around a structure.

Liquefaction potential can be significant for loose cohesionless soils present close to ground surface (seafloor) and below the water table. Dense sands, loose unsaturated sands, and some sensitive cohesive materials can also liquefy under some conditions. In addition, the presence of gas in loose sands can change soil behaviour and may potentially cause liquefaction (Grozic, 2003).

Faults

A fault is a planar fracture or discontinuity in a volume of soil or rock along which significant vertical and/or horizontal displacement has occurred (Figure 3) (i.e. faulting). Fault zones are areas where multiple fractures and faults occur in close proximity, with similar moment direction.

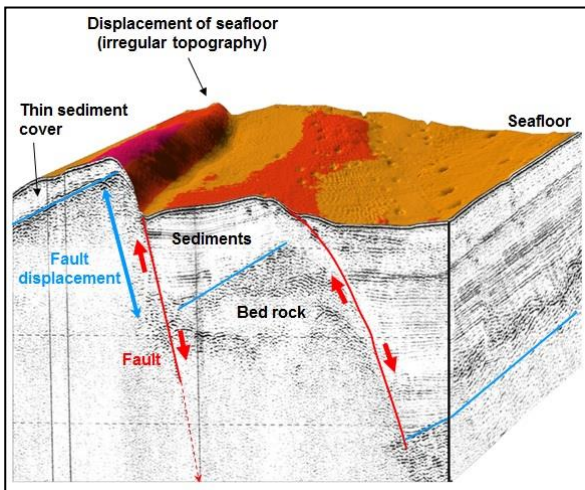


Figure 3: Surface and subsurface expression of fault displacement

Faults can be associated with:

- Tectonic activity (e.g. at tectonic plate boundaries, earthquake zones);

- Laterally variable soil subsidence and compaction;
- Soil contractions (e.g. polygonal faulting in North Sea and West African seabed sediments);
- Diapirism (e.g. radial faulting);
- Slope failure (e.g. headwall scarp, failure planes, tension cracks).

Movement along the fault plane (and hence soil displacement) is a semi-continuous process acting on time scales ranging from years to millions of years. Faults are commonly considered to be inactive if there has been no observed movement or evidence of seismic activity during the last 10,000 years. In this case a fault can be covered by a uniform layer of soil (i.e. without a clear discontinuity surface being present). Depending on crustal stresses and changes therein, apparently inactive faults may be reactivated causing further soil displacements and even seismic events.

Faults may result in a displaced, stepped seafloor and/or irregular linear topographic features on the seafloor (e.g., headwall scarps). In addition, stratigraphic sequences are displaced in the seabed.

Deep-seated faults, with lengths of hundreds to thousands of metres, may be associated with earthquakes. The build-up of stresses due to differential movement in the earth's crust may be released along these deep-seated faults, whereby large amounts of energy move through rock and soils in the form of pressure waves and shear waves. These deep-seated, earthquake-generating faults are sometimes referred to as seismic faults.

Tsunamis

A tsunami (or surge wave) is a series of ocean waves of long wave lengths which are created when a large volume of water is suddenly displaced by a submarine earthquake, landslide, or volcanic eruption (Figure 4). In the open ocean, tsunami waves travel at high speeds (in excess of 800 km/h) with heights of, say, less than 0.05 m. As they approach the coast the velocity decreases (to approximately 50 km/h) and the wave height increases up to several metres or tens of metres. At the coastline, the force of a tsunami wave can cause loss of life, damage to buildings and infrastructure, large scale erosion (scour) and flooding of low-lying areas.

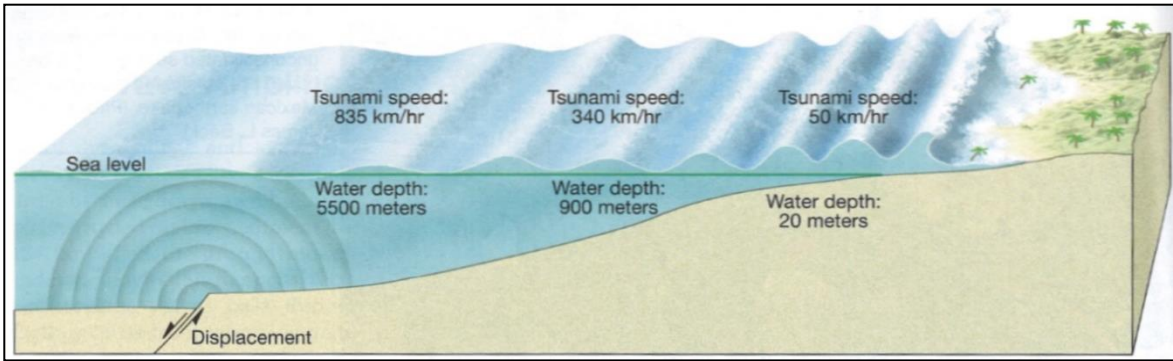


Figure 4: Tsunami generated by fault displacement offshore

Slope Failure

Slope failure occurs when downslope driving forces acting on seabed exceed resistance. In general, slope failure results in the down-slope movement of a soil mass (see section titled 'Submarine Mass Movements'). Slopes may be unstable at any water depth.

Slopes may develop due to tectonics, high sedimentation rates, or incision and erosion by seafloor currents and flows.

Slope failure can be triggered by earthquakes, strong currents, storms (wave actions), tsunamis, volcanism, and human activity (Hampton et al., 1996; Mulder and Cochonat, 1996; Locat and Lee, 2005; Judd and Hovland, 2007; Rogers and Goodbred, 2010).

Usually a combination of two or more factors influences slope failure, e.g. presence of shallow gas and an earthquake (Orange and Breen, 1992; Judd and Hovland, 2007). Slopes can be unstable due to low shear strength and overpressured strata (e.g. shallow gas). Seabed may fail on slight slopes as little as 0.5° (Hampton et al., 1996; Judd and Hovland, 2007).

Failure scarps and oversteepened slopes are commonly associated with past slope failures. Past slope failures may be reactivated if a trigger (e.g. pore pressure build-up, earthquake)

is present. The seafloor morphology resulting from a slope failure may be irregular and undulating (see section titled 'Irregular Seafloor Topography').

Submarine Mass Movements

A submarine mass movement is a displacement of seabed material driven directly by gravity or other body forces, rather than stresses associated with fluid flow. The deposits of submarine mass movements are commonly referred to as mass transport deposits (MTD).

Submarine mass movements commonly follow from slope failures and include the following processes (Figure 5) (Lee et al., 2007):

- Slides:
 - Translational slide
 - Rotational slide
- Mass flows:
 - Debris flow
 - Debris avalanche
 - Mud flow
 - Liquefaction flow
 - Turbidity current

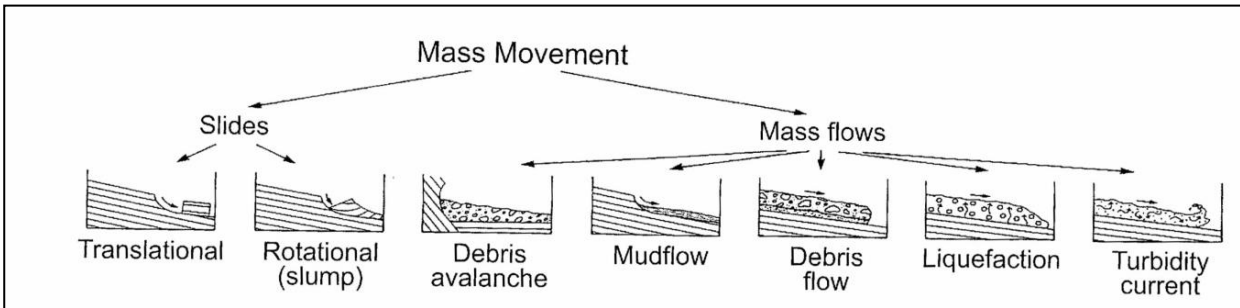


Figure 5: Submarine mass movement classification (after Lee et al., 2007)

Slides are movements of essentially rigid, undeformed masses along discrete failure/slip planes. If slip occurs along a planar surface the slide is referred to as a translational slide. If slip occurs along a curved failure plane and the rigid mass shows rotation, the slide is referred to as rotational.

If moving sediments take a form of viscous fluid, the feature is referred to as mass flow or gravity flow. Mass flow deposits show considerable internal deformation with many invisible or short-lived internal slip surfaces. Submarine slides can become mass flows as the failed material progressively disintegrates, gets entrained with surrounding water and moves downslope.

Debris flows are mass flows in which sediments are heterogeneous and may include larger clasts supported by a

fine-grained soil matrix. Mud flows involve predominantly fine-grained (mud) sediments. Turbidity currents involve downslope transport of a relatively dilute suspension of sediment grains that are supported by an upward component of fluid turbulence. Turbidity currents often evolve from disintegration and dilution of debris and mud flows. Liquefaction flows occur when loosely packed sandy sediments collapse under environmental conditions (e.g. cyclic actions by waves or earthquakes; see section titled Soil Liquefaction). Debris avalanches occur where slides collapse and disintegrate into smaller pieces. They move rapidly without following pre-existing channels or valleys.

The potential impact of submarine mass movements on a structure depends upon the location or orientation of the structure in relation to the movement direction (Figure 6).

Mass Movement Mechanism	Profile View	Plan View	Impact		
			Structure	Pipeline / Flowline / Cable	
				Orientation of mass movement	
				Parallel	Perpendicular
Creep			Rotation About Base	Dragging Rupture Spanning	Dragging Rupture Spanning
Translational Slide			Translation Downdrag at Crest Uplift at Toe	Stretching at Crest Compression at Toe Loss of Support Rupture Spanning	Dragging Loss of Support Rupture Spanning
Rotational Slide			Rotation About Top Downdrag at Crest Uplift at Toe	Stretching at Crest and Toe Loss of Support Rupture Spanning	Dragging Loss of Support Rupture Spanning
Debris Avalanche			Translation/Rotation +/- Downdrag +/- Uplift	Compression and Stretching Loss of Support Rupture Spanning, Burial	Dragging Loss of Support Rupture Spanning Burial
Debris Flow			Loading Burial Scour	Compression Burial Loading Scour	Dragging Burial Loading Scour
Liquefied Flow			Loading Burial Scour	Compression Burial Loading Scour	Dragging Burial Loading Scour
Fluidised Flow			Loading Burial Scour	Compression Burial Loading Scour	Dragging Burial Loading Scour
High Density Turbidity Current			Loading? Burial? Scour	Burial Loading Scour	Burial Loading Scour
Low Density Turbidity Current			Scour?	Scour	Scour

Profile view

 Structure
 ● Pipeline / flowline / cable

Plan view

 Foundation
 — Pipeline / flowline / cable (parallel)

} Pipeline / flowline / cable (perpendicular)

Figure 6: Potential impacts of submarine mass movements on platform foundation and pipeline (modified after Thomas et al., 2009)

Wind, Waves and Currents

Periods of extreme weather conditions, such as (tropical) storms, monsoons, peak wind, waves, and current regimes can cause lateral and cyclic actions on the seafloor and any seabed-supported structure. In addition, adverse weather conditions may complicate structure installation activities.

Peak wave and (seafloor/bottom) current regimes can also cause changes in seafloor conditions due to scour and burial (i.e. sediment remobilisation), winnowing of seafloor sediments (i.e. removal of fine/clay-size materials) and development of irregular seafloor topography.

Tidal variation and atmospheric pressure fluctuations as a result of storms are known to change pore pressure conditions in the seabed, potentially creating circumstances leading to soil failure and liquefaction.

Estimation of environmental actions is relatively inaccurate. It normally involves statistical data for a specific geographic region and various procedures for modelling the interaction of a structure and its environment.

Man-Made Hazards

Human activities and anthropogenic (i.e. man-made/man-induced) features, debris, or obstructions can have an adverse effect on an offshore structure.

Seafloor features and objects have been left by human activities since the dawn of mankind. Shipwrecks can form archaeological sites, war graves, enhance ecological diversity, and may be restricted areas.

In addition, offshore energy activities such as drilling, (jack-up) platform installation and decommissioning and resulting footprints may alter seafloor topography and/or potentially alter seabed conditions (e.g. drill spoils, gas charging as a result of gas migration along exploration wells).

Commonly encountered man-made hazards include:

- Unexploded ordnance (UXO);
- Existing energy facilities (e.g. fixed platforms, pipelines, manifolds, wellheads, power cables etc.);
- Telecommunication cables;
- Shipwrecks;
- Fallen objects (e.g. shipping containers).

These hazards can complicate structure installation and design if not identified at an early stage.

Activities such as hydrocarbon extraction and deep salt mining can change site conditions, for example causing regional subsidence of the seabed and/or trigger fault activity (Barton et al., 1987; Broughton et al., 1998; Broughton et al., 1997; Gebara et al., 2000). Subsidence can range from millimetres to tens of metres. It typically depends on reservoir size, mechanical properties of reservoir and overlying ground, reservoir depth, production rate, pressure drawdown, and duration.

References

American Petroleum Institute [API]. (2014a). Geotechnical and foundation design considerations: ISO 19901-4:2003 (modified), petroleum and natural gas industries-specific requirements for offshore structures, part 4-geotechnical and foundation design considerations: addendum 1. (ANSI/API RP 2GEO First Edition, with Addendum)
<https://www.apiwebstore.org/publications/item.cgi?b6c6e7f5-6da7-46c2-97bb-54bd470f0401>.

American Petroleum Institute [API]. (2015). *Design, construction, operation, and maintenance of offshore hydrocarbon pipelines (limit state design)*. (API RP 1111 5th Edition).
<https://www.apiwebstore.org/publications/item.cgi?3fb25780-bd91-43e0-8959-e064621d198f>.

American Petroleum Institute [API]. (2014b). *Planning, designing and constructing fixed offshore platforms - working stress design*. (API RP 2A-WSD, 22nd Edition)
<https://www.apiwebstore.org/publications/item.cgi?b9e32dec-268b-404d-988e-5cda65c27757f>.

Ashley, G.M. (1990). Classification of large-scale subaqueous bedforms: a new look at an old problem [research symposium].

Journal of Sedimentary Petrology, 60(1) 160-172
<https://doi.org/10.2110/jsr.60.160>.

ASTM International. (2018). *Standard guide to site characterization for engineering, design, and construction purposes*. (ASTM D420-18).
<https://www.astm.org/Standards/D420.htm>.

Barton, N., Hårvik, L., Christianson, M., Bandis, S.C., Makurat, A., Chryssanthakis, P. & Vik, G. (1987). Rock mechanics modelling of the Ekofisk reservoir subsidence. *Proceedings of the 27th symposium on rock mechanics, Alabama, 1986* (pp. 267-274)

Broughton, P., Aldridge, T.R. & Komaromy, S. (1998). Steel jacket structures for the new Ekofisk complex in the North Sea. *Proceedings of the Institution of Civil Engineers. Civil Engineering*, 126(2), 54-64. <https://doi.org/10.1680/icien.1998.30433>

Broughton, P., Aldridge, T.R. & Nagel, N.B. (1997). Geotechnical aspects of subsidence related to the foundation design of Ekofisk platforms. *Proceedings of the Institution of Civil Engineers. Geotechnical Engineering*, 125(3) 129-140.
<https://doi.org/10.1680/igeng.1997.29464>

Campbell, K.J., Hooper, J.R. & Prior, D.B. (1986). Engineering implications of deepwater geologic and soil conditions, Texas-Louisiana slope. In *Eighteenth annual offshore technology conference, May 5-8, 1986, Houston, Texas: Proceedings, 1, OTC Paper 5105* (pp. 225-232) <https://doi.org/10.4043/5105-MS>

Clayton, C. & Power, P. (2002). Managing geotechnical risk in deepwater. In M. Cook et al. (eds.) *Offshore site investigation and geotechnics: diversity and sustainability: proceedings of an international conference, 26-28 november 2002* (pp. 425-443). Society for Underwater Technology.

Delisle, G. (2004). The mud volcanoes of Pakistan. *Environmental Geology*, 46(8) 1024-1029. <https://doi.org/10.1007/s00254-004-1089-x>

Delisle, G. (2005). Mud volcanoes of Pakistan — an overview: a report on three centuries of historic and recent investigations in Pakistan. In G. Martinelli & B. Panahi (eds.) *Mud volcanoes, geodynamics and seismicity* (pp. 159-169). Springer.

Delisle, G., Von Rad, U., Andruleit, H., Von Daniels, C.H., Tabrez, A.R. & Inam, A. (2002). Active mud volcanoes on- and offshore eastern Makran, Pakistan. *International Journal of Earth Sciences*, 91(1) 93-110. <https://doi.org/10.1007/s005310100203>

Ding, F. (2008). *Near-surface sediment structures at cold seeps and their physical control on seepage: a geophysical and geological study in the Southern Gulf of Mexico and at the frontal makran accretionary prism/Pakistan*. [Dissertation] Universität Bremen.

DNV GL AS (2017, August). *Offshore soil mechanics and geotechnical engineering. Recommended practice* (DNVGL-RP-C212). <https://standards.globalspec.com/std/10183661/DNVGL-RP-C212>.

Dodd, N., Blondeaux, P., Calvete, D., De Swart, H.E., Falqués, A., Hulscher, S.J.M.H., Róznyski, G. & Vittori, G. (2003). Understanding coastal morphodynamics using stability methods. *Journal of Coastal Research*, 19(4) 849-865.

European Committee for Standardization. (2009). *Eurocode 7: geotechnical design - part 1: general rules (with corrigendum EN 1997-1:2004/AC, February 2009)*. (EN 1997-1:2004).
https://standards.cen.eu/dyn/www?fp=204:110:0:::FSP_PROJECT_FSP_ORG_ID:12442,6231&cs=1D03CC06CB9166EAAA1C6CE997CDA87C2.

European Committee for Standardization. (2015). *Petroleum and natural gas industries - pipeline transportation systems ISO 13623:2009 modified.* (EN 14161+A1:2015) https://standards.cen.eu/dyn/www/f?p=204:110:0:::FSP_PROJECT_FSP_ORG_ID:60145,5996&cs=1CB24029A869268F9A5290800D2D8C0A6.

Evans, T.G. (2010). A systematic approach to offshore engineering for multiple-project developments in geohazardous areas. In S. Gourvenec & D. White (Eds.), *Frontiers in offshore geotechnics II: proceedings of the 2nd international symposium on frontiers in offshore geotechnics, Perth, Australia, 8-10 November 2010* (pp. 3-32). CRC Press.

Faugères, J.-C., Stow, D.A.V., Imbert, P. & Viana, A. (1999). Seismic features diagnostic of contourite drifts. *Marine Geology*, 162(1) 1-38. [https://doi.org/10.1016/S0025-3227\(99\)00068-7](https://doi.org/10.1016/S0025-3227(99)00068-7)

Galavazi, M., Moore, R., Lee, M., Brunnsden, D. & Austin, B. (2006). Quantifying the impact of deepwater geohazards. In *2006 Offshore technology conference, 1-4 May, Houston, OTC Paper 18083*. <https://doi.org/10.4043/18083-MS>

Gebara, J.M., Dolan, D., Pawsey, S., Jeanjean, P. & Dahl-Stamnes, K.H. (2000). Assessment of offshore platforms under subsidence—part I: approach. *Journal of Offshore Mechanics and Arctic Engineering*, 122(4) 260-266. <https://doi.org/10.1115/1.1313530>

Grozic, J.L.H. (2003). Liquefaction potential of gassy marine sands. In J. Locat & J. Mienert (eds.), *Submarine mass movements and their consequences* (pp. 37-45). Kluwer Academic Publishers.

Hampton, M.A., Lee, H.J. & Locat, J. (1996). Submarine landslides. *Review of Geophysics*, 34(1), 33-59. <https://doi.org/10.1029/95RG03287>.

International Association of Oil and Gas Producers. (2009). *Geohazards from seafloor instability and mass flow*. (IOGP Report No. 425) IOGP.

International Association of Oil and Gas Producers. (2017). *Guidelines for the conduct of offshore drilling hazard site surveys* (Version 2.0). (IOGP Report No. 373-18-1) IOGP.

International Organization for Standardization. (2014). *Petroleum and natural gas industries – specific requirements for offshore structures – part 8: marine soil investigations*. (ISO 19901-8:2014). <https://www.iso.org/standard/61145.html>.

International Organization for Standardization. (2016a). *Petroleum and natural gas industries – specific requirements for offshore structures – part 4: geotechnical and foundation design considerations*. (ISO 19901-4:2016). <https://www.iso.org/standard/61144.html>.

International Organization for Standardization. (2016b). *Petroleum and natural gas industries – specific requirements for offshore structures – part 1: jack-ups*. (ISO 19905-1:2016). <https://www.iso.org/standard/68135.html>.

International Organization for Standardization. (2017). *Petroleum and natural gas industries - pipeline transportation systems*. (ISO 13623:2017). <https://www.iso.org/standard/61251.html>

International Organization for Standardization. (2019). *Petroleum and natural gas industries – general requirements for offshore structures*. (ISO 19900-2019). <https://www.iso.org/standard/69761.html>.

International Organization for Standardization. (2021). *Petroleum and natural gas industries - specific requirements for offshore*

structures – part 10: marine geophysical investigations. (ISO 19901-10:2021). <https://www.iso.org/standard/77017.html>

Judd, A.G. & Hovland, M. (2007). *Seabed fluid flow: the impact on geology, biology, and the marine environment*. Cambridge University Press.

Lee, H.J., Locat, J., Desgagnés, P., Parsons, J.D., McAdoo, B.G., Orange, D.L., Puig, P., Wong, F.L., Dartnell, P. & Boulanger, E. (2007). Submarine mass movements on continental margins. In C.A. Nittrouer et al. (eds.) *Continental margin sedimentation: from sediment transport to sequence stratigraphy* (pp. 213-274). (Special Publication of the International Association of Sedimentologists, No. 37) Blackwell

Locat, J. & Lee, H.L. (2005). Subaqueous debris flows. In M. Jakob & O. Hungr (eds.), *Debris-flow hazards and related phenomena* (pp. 203-245). Springer-Verlag.

Morelissen, R., Hulscher, S., Knaapen, M.A.F., Németh, A.A. & Bijker, R. (2003). Mathematical modelling of sand wave migration and the interaction with pipelines. *Coastal Engineering*, 48(3) 197-209. [https://doi.org/10.1016/S0378-3839\(03\)00028-0](https://doi.org/10.1016/S0378-3839(03)00028-0)

Mulder, T. & Cochonat, P. (1996). Classification of offshore mass movements. *Journal of Sedimentary Research*, 66(1), 43-57. <https://doi.org/10.1306/D42682AC-2B26-11D7-8648000102C1865D>

Newton, R.S., Cunningham, R.C. & Schubert, C.E. (1980). Mud volcanoes and pockmarks: seafloor engineering hazards or geological curiosities? In *Twelfth annual offshore technology conference*, May 5-8, Houston, Texas: proceedings, 1, OTC Paper 3729 (pp. 425-429) <https://doi.org/10.4043/3729-MS>

Parker, E.J., Traverso, C., Moore, R., Evans, T. & Usher, N. (2008). Evaluation of landslide impact on deepwater submarine pipelines. OTC.08: proceedings 2008 offshore technology conference, 8 May, Houston, Texas, USA, OTC Paper 19459. <https://doi.org/10.4043/19459-MS>

Peuchen, J. (2012). Site characterization in nearshore and offshore geotechnical projects. In R.Q. Coutinho & P.W. Mayne (eds.) *Geotechnical and geophysical site characterization 4: proceedings of the fourth international conference on site characterization ISC-4, Porto de Galinhas-Pernambuco, Brazil, 17-21 September 2012, volume I* (pp. 83-111). CRC Press.

Power, P., Galavazi, M. & Wood, G. (2005). Geohazards need not be: redefining project risk. In *Offshore technology conference*, 2-5 May 2005, Houston, Texas, U.S.A., OTC Paper 17634. <https://doi.org/10.4043/17634-MS>.

Rastogi, A., Deka, B., Budhiraja, I.L. & Agarwal, G.C. (1999). Possibility of large deposits of gas hydrates in deeper waters of India. *Marine Georesources & Geotechnology*, 17(1), 49-63. <https://doi.org/10.1080/106411999274007>.

Reineck, H.-E. & Singh, I.B. (1980). *Depositional sedimentary environments* (2nd ed.). Springer.

Renewable UK (2013). *Guidelines for the selection and operation of jack-ups in the marine renewable energy industry: version 2: full technical and regulatory update*. RenewableUK.

Rogers, K.G. & Goodbred, S.L. (2010). Mass failures associated with the passage of a large tropical cyclone over the swatch of no ground submarine canyon bay of Bengal. *Geology*, 38(11) 1051-1054. <https://doi.org/10.1130/G31181.1>.

Skipp, B.O. & Mallard, D.J. (1995). Site investigations with earthquakes in mind. In A.S. Elnashai (ed.) *European seismic design practice: research and application: proceedings of the*

fifth SECED conference on european seismic design practice, Chester, United Kingdom, 26-27 October 1995 (pp. 151-161). Balkema.

Snead, R.E. (1972). Mud volcanoes of the Makran Coast. *Explorers Journal*, 50(1) 22-28.

Soulsby, R. (1997). *Dynamics of marine sands: a manual for practical applications*. Thomas Telford.

Sumer, B.M. & Fredsøe, J. (2002). *The mechanics of scour in the marine environment*. World Scientific.

Thomas, S., Hooper, J.R. & Clare, M. (2009). Constraining geohazards to the past: impact assessment of submarine mass movements on seabed developments. In D.C. Mosher et al. (eds.), *Submarine mass movements and their consequences: 4th international symposium* (pp. 387-398). Springer.

Von Rad, U., Berner, U., Delisle, G., Dooze-Rolinski, H., Fechner, N., Linke, P., Lückge, A., Roeser, H.A., Schmaljohann, R., Wiedicke, M. & SONNE 122/130 Scientific Parties (2000). Gas and fluid venting at the Makran accretionary wedge off Pakistan. *Geo-Marine Letters*, 20(1) 10-19.
<https://doi.org/10.1007/s003670000033>

Wells, D.L. & Coppersmith, K.J. (1994). New empirical relationships among magnitude, rupture length, rupture width, rupture area, and surface displacement. *Bulletin of the Seismological Society of America*, 84(4), 974-1002.

Whitehouse, R. (1998). *Scour at marine structures: a manual for practical applications*. Thomas Telford.

Yuan, F., Wang, L., Guo, Z. & Shi, R. (2012). A refined analytical model for landslide or debris flow impact on pipelines. part I: surface pipelines. *Applied Ocean Research*, 35, 95-104.
<https://doi.org/10.1016/j.apor.2011.12.001>.

Geotechnical Analysis

Approach

A geotechnical design situation or a re-assessment of an existing structure requires geotechnical analysis, including evaluation of hazards and verification of relevant limit states. Geotechnical analysis follows design philosophies included in standards and codes of practice, where available. All consider that the resistance (or capacity) of a geotechnical system must be greater than the actions (demands or loads) on the system for an acceptable or required level of safety or reliability (ISO, 2015).

The approach for geotechnical analysis typically includes these steps:

- selection of procedures and models for geotechnical analysis;
- processing and integration of geotechnical information, e.g. by preparation of geotechnical logs, cross sections, geographical information system GIS and/or 3D ground model;
- site characterisation including hazard identification;
- selection of geotechnical parameter values for calculation models;
- application of calculation models and evaluation of results.

The approach for geotechnical analysis includes assumptions and premises. One premise is that the client's activities are state-of-the-practice in all areas, including planning, engineering, construction, operation and maintenance of a geotechnical system or structure.

Hazard Evaluation

Hazards are situations or events with potential to cause damage (ISO 2000; 2013). Hazard evaluation typically includes classification, estimation of probability of occurrence and measures for countering the hazard. Examples of hazards are abnormal environmental events, accidental events, geohazards and man-made site hazards. Note that event probability differs from risk, where risk is defined as the product of probability and consequence.

In many geotechnical situations, hazard evaluation will not be complete and exact. It will be necessary to draw on so-called tacit expert knowledge. This means senior expertise, with access to geotechnical knowledge and experience. Judgement and opinion are inevitable and a senior expert or a team of senior experts is more likely to arrive at a correct understanding and an appropriate way forward. Judgement is qualitative and subjective. Table 1 shows probability expressions intended for a context of approximate and subjective probability of the occurrence of a hazardous event during a defined exposure period.

Measures for countering a hazard include source elimination, avoidance, implementation of a barrier, minimising consequences and design for the hazard.

Table 1: Expressions for Approximate and Subjective Probability (adapted from Peuchen et al., 2015)

Short Descriptor	Verbal Descriptor	Approximate Probability for Exposure Period
Negligible	Unlikely, although the possibility cannot be ruled out completely	0 to 0.01
Low	Not probable, although uncertain	0.01 to 0.1
High	Credible, possibility can be described with reasonable confidence by known physical conditions or processes	0.1 to 1

Limit States

Limit states may be grouped into Ultimate Limit States (ULS, for example for structure stability), Serviceability Limit States (SLS, for example for avoiding excessive settlement), Fatigue Limit States (FLS, for example for structural integrity of a pile) and Accidental Limit States (ALS, for example for impact of an object).

Limit states can consider (1) global behaviour, i.e. the structure as a whole, (2) structural components, e.g. the behaviour of a shallow foundation and (3) localised features such as buckling of a pile tip during penetration into ground including boulders.

Verification of a limit state usually involves one or more of the following approaches:

- calculation models;
- prescriptive measures;
- experimental models and load tests;
- observational method.

Features of a calculation model typically include:

- method of analysis typically including simplifications;
- actions, such as (a sequence of) imposed loads or imposed displacements;
- geometrical data, such as the shape of a geotechnical structure, geometry of the ground surface, water levels and ground strata;
- values of geotechnical parameters of ground (soil, rock, pore fluid, pore gas) and other materials;
- limiting values of, for example, deformations and vibrations;
- results that are (1) accurate, predictive, (2) approximate, subject to model uncertainty/ bias, or (3) cautious, err on the safe side;
- partial factors or safety factors, with or without specific factors for model uncertainties and dimensional variations.

Prescriptive measures generally involve (1) conventional and conservative details in the design and (2) attention to specification and control of materials, workmanship, protection and maintenance procedures. Their use is often applicable where calculation models are not available or not necessary. Examples are prescriptive measures for ensuring durability against chemical attack or frost action.

Experimental models and load tests can help to justify a design approach. Important considerations for evaluation of the results include differences in ground conditions, time effects and scale effects.

Prediction of geotechnical behaviour is often difficult. The observational method allows carefully planned monitoring during construction and includes planned contingency measures

where necessary. Assessment of the monitoring results takes place at appropriate stages.

Design Philosophies

Design philosophies typically incorporate geotechnical calculation models and corresponding (partial) factors. These partial factors or safety factors may vary depending on the specific design scenario.

Design philosophies for the ULS may be grouped as follows:

1. Working Stress Design (WSD) or Allowable Stress Design (ASD);
2. Partial Factor Design (PFD) or Limit State Design (LSD);
 - a. Factored material properties;
 - b. Factored resistance.

The WSD method uses global safety factors applied to unfactored values (or ultimate values) of resistance.

The PFD methods for the ULS use partial action factors and partial factors applied to resistance. The partial action factors are applied to unfactored values of actions. This results in design values for actions. The factored material properties and factored resistance methods differ by their calculation of resistance. The method for factored material properties applies partial material factors to unfactored values of material properties such as undrained shear strength of soil. The factored values are then used in the calculation model to obtain a design value for resistance (factored resistance). The factored resistance method uses unfactored values of material properties in the calculation model and then applies a partial resistance factor to obtain a design value for resistance. Some PFD approaches allow the use of partial factors that specifically include or exclude model uncertainties (e.g. CEN, 2009). A separate partial factor can also be considered to account for model uncertainty or other uncertainties not covered by other partial factors (e.g. ISO, 2019 and CEN, 2009).

API RP 2A-WSD Fixed Offshore Platforms (API, 2014a) is an example of the WSD approach for the ULS. Eurocode 7 Geotechnical Design (CEN, 2009; 2010), ISO Offshore Structures ISO 19900 and ISO 19901-4 (ISO 2019; 2016) and API RP 2GEO Geotechnical and Foundation Design Considerations (API, 2014b) provide design principles according to the PFD approaches.

Design philosophies for the ALS, SLS and FLS are similar to the ULS. Global safety factors and partial factors will differ from the ULS.

Geotechnical Parameter Values

Design Process

Assignment of geotechnical parameter values or soil property values is according to the following steps:

1. Site characterisation and stratigraphic schematisation;
2. Evaluation of derived values of geotechnical parameters;
3. Selection of representative values of geotechnical parameters and application in a calculation model.

The selection of representative values of geotechnical parameters takes place within the context of a calculation model and thus includes consideration of limit states, actions, geometry, limiting values and partial factors or safety factors. Divorcing the selection of representative geotechnical values from the actual use and evaluation of a calculation model can lead to errors.

The presentation of geotechnical parameter values is typically in graphical format and/or tabular format. Graphical formats include data plots versus depth, values presented in Cartesian

coordinates diagrams, colour bars and histograms. Tabular data for a ground unit or ground stratum can include linear representation. Typically, linear interpolation applies between two increasing depths, each with corresponding parameter values. A step change applies when two (tabular) parameter values are assigned to a single depth.

Stratigraphic Schematisation

General site characterisation is necessary before stratigraphic schematisation and before evaluation of the results of specific tests and observations. Such site characterisation comprises a general assessment of the character and basic constituents of the ground (soil and rock classification) and their possible change in time.

Typical parameters for soil classification include particle size distribution, water content, carbonate content, Atterberg limits, unit weight, relative density and undrained shear strength. Typical parameters for rock classification include mineralogy, water content, unit weight and uni-axial compressive strength.

The extent of stratigraphic schematisation depends on the nature of the actions, geometrical quantities of the structure that interacts with the ground, volume of ground that represents the domain of influence with respect to the limit state, spatial ground variability, simplification of ground conditions, e.g. undrained versus drained foundation response.

Two competing factors apply to spatial ground variability: (1) the spatial averaging of properties over a potential failure surface, which reduces the coefficient of variation of property values (i.e. with respect to that for the location under consideration) and (2) the tendency for a failure surface to follow the path of least resistance.

Stratigraphic schematisation can include evaluation of:

- basic parameters such as undrained shear strength and relative density;
- geological and hydro-geological setting;
- results of a geophysical survey;
- hazards such as potential instability of the ground;
- water levels;
- ground and ground water, with respect to structure durability.

Derived Values of Geotechnical Parameters

This document considers Eurocode 7 EN 1997-1:2004 for definition of *derived value*: "value of a geotechnical parameter obtained by theory, correlation or empiricism from test results". Where applicable, this document considers derived values to include measured values, test results, correlation values, theoretical values and empirical values. Borehole geophysical logging, in situ testing, laboratory test measurements and other relevant data provide a basis for obtaining derived values of geotechnical parameters.

Laboratory test standards often specify procedures for obtaining derived values, particularly where it is possible to obtain a derived value by means of a conversion model or theory. Such derived values are thus part of the laboratory test report. An example is the unconsolidated undrained triaxial compression test. Normalised load and displacement data are the basic measured values. The measured values and the use of theory allow the calculation of a derived value of undrained shear strength by consideration of principal stress conditions and a theoretical deformation model.

Standards for in situ tests can require reporting of (normalised) derived values that can serve as direct input for some calculation models. An example is the use of CPT cone resistance for the calculation of axial pile resistance. A more common approach is to obtain derived values of geotechnical parameters from in situ tests on the basis of empiricism or (simplified) theory or a combination thereof.

This document considers *low estimate*, *best estimate* and *high estimate* values for derived values. The use of statistical methods can help to identify outliers and can support selection of best, low and high estimates. In statistical terms, this document considers a best estimate value as a mean value of data points acquired for a soil province, ground unit, stratum or multiple soil layers. Low and high estimates aim for the quantile associated with the 5 % fractile. Comments are as follows:

- Low, best and high estimates consider a reference method or procedure. This is because a test result or a derived value typically depends on the method(s) selected to obtain the parameter value. For example, undrained shear strength derived from a triaxial test on an intact soil specimen will depend on the sampling method, sample handling practice, laboratory test procedure and whether undrained shear strength is derived from maximum deviator stress or maximum principal stress ratio;
- Low, best and high estimates can include judgement and opinion, particularly for a limited quantity or absence of test results and derived values. This implies that outliers may be ignored and that a bias may be introduced relative to the available data. Judgement and opinion consider physically credible values, comparison of data with results from other tests and *a priori* knowledge such as geological setting and comparable experience;
- A wide spread of data can indicate spatial variability of soil. This means that averaging of test results and derived values can obscure a weaker or stronger zone;
- A calculation model usually requires specific schematisation of soil stratigraphy and model-specific selection of parameter values. This is not covered by low, best and high estimates.

Representative Values of Geotechnical Parameters

Industry uses multiple terms for unfactored values of geotechnical parameters that are applied in a calculation model, for example:

- CEN (2009) considers “characteristic value”, representing a cautious estimate for the value affecting the occurrence of a limit state;
- DNV GL (2017a and 2019) consider “characteristic value”, generally a low value with a prescribed probability of being favourably exceeded; sub-groups are “best estimate”, “lower bound” and “upper bound”;
- ISO (2019) considers “representative value” for a parameter used in a calculation model, with sub-groups “characteristic value” and “nominal value”; nominal value is defined as a value assigned to a basic variable determined on a non-statistical basis, typically from acquired experience or physical conditions;
- ISO (2015) considers “characteristic value” and “nominal value”, with emphasis on characteristic value defined as “value specified preferably on statistical bases, so it can be considered to have a prescribed probability of not being exceeded”. A footnote to the definition of characteristic value refers to a nominal value that may be specified in cases where a statistical distribution is not known.

The text below uses *representative value* according to ISO (2013) for the value of a geotechnical parameter required for a calculation model.

The selection of a representative value takes account of probable differences between derived values of a geotechnical parameter and the geotechnical parameter that actually affects the behaviour of a geotechnical structure. In most cases, this is because no reliable and affordable geotechnical methods are available for direct and accurate representative values required for a calculation model. In other words, (multiple) test methods for derived values are typically selected based on feasibility in terms of available technology, economics and schedule. This limits applicability for the selection of representative values. For example, in situ relative density is defined relative to in situ void ratio and index void ratios. In situ void ratio can be obtained from laboratory tests on undisturbed, intact soil specimens. This is technically feasible for a marine setting, but considerations for economics and schedule lead to substitute, approximate, CPT-based correlations for relative density and their associated statistical distributions.

Other reasons for differences between derived values and representative values can include inhomogeneity of the ground, extent of the zone governing a particular limit state, uncertainties in geometrical data and analytical model, time effects, brittle or ductile response of the ground, influence of construction activities.

Representative values can be lower values, which are less than the most probable value, or upper values, which are greater. Each calculation requires the most unfavourable combination of lower and/or upper values for independent geotechnical parameters. Appropriate judgement should be applied for selection of representative values of parameters that are interdependent.

Selection of a statistical representative value is typically such that the calculated probability of a worse value governing the occurrence of a limit state is not greater than 5 %. A representative value is, in most cases, a nominal value based on an estimate of a statistical distribution for the representative value of the geotechnical parameter required for a particular calculation model. This estimate is mainly based on a small amount of derived values and general experience. Note that the statistics for derived values are not necessarily representative of in situ conditions. Aleatory uncertainties are covered to some degree. Epistemic uncertainties are not. Furthermore, an estimate of a statistical distribution for a representative value should typically differ from that for a derived value. Where cautious, statistical equivalence is sometimes accepted in practice.

Uncertainty modelling such as described in DNV GL (2017a) will typically require quantification of the epistemic uncertainties of derived values. Such quantification is challenging as it will require large data sets within a 3D context and judgement on selection of adjustment factors.

Hicks (2013) and Baecher and Christian (2003) illustrate that statistical methods for selection of a representative value can be feasible in some situations. Usually, such methods should allow for incorporation of a-priori knowledge of comparable experience with geotechnical parameters, for example by Bayesian methods, as necessary. Variance reduction methods may be applied where appropriate.

In principle, spatial ground variability affects:

- The mean (X_m), standard deviation (SD) and probability density function (pdf) of the ground property for the location under consideration, including any depth trend;

- The scale of fluctuation (θ) of the ground property, which is the distance over which the property values are significantly correlated; the scale of fluctuation in the (near) horizontal plane is often much larger than in the vertical direction, i.e. $\theta_h \gg \theta_v$, for example due to the process of deposition;
- The limit state under consideration, particularly relating to the geometrical quantities of the structure that interacts with the ground, the nature of the applied actions and the volume of ground that represents the domain of influence with respect to the limit state.

The pdf required for the representative value(s) should take account of the spatial variability of ground property values and the limit state under consideration, and thus may differ considerably from the underlying pdf for the location under consideration (Figure 1).

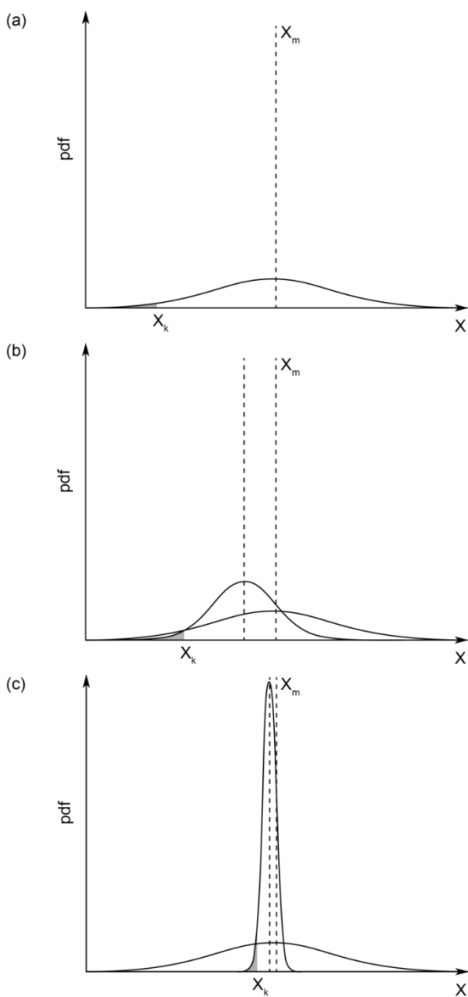


Figure 1: Estimation of representative value and pdf (after Hicks, 2013): (a) X_k based on underlying pdf (for large θ/D); (b) X_k based on modified pdf (for intermediate θ/D); (c) X_k based on modified pdf (for small θ/D)

If the domain of influence is represented by the dimension D , the representative value will be a function of the ratio θ/D and will generally lie within the following limits:

- For relatively large values of θ/D , there may be considerable uncertainty regarding the property value governing the structure response. Specifically, although the occurrence of the limit state will generally be governed by the “local” mean,

there will be uncertainty about what that mean actually is. The representative value may then be represented by the 5 percentile of the underlying pdf (Figure 1a);

- For intermediate values of θ/D , the representative value may be estimated from a pdf with a reduced variance to account for averaging of properties. However, account should also be taken of any apparent reduction in the property mean due to the tendency for failure to follow the path of least resistance (Figure 1b);
- For small values of θ/D , there is considerable averaging of property values over potential failure surfaces and the response of the structure may be reasonably represented by a cautious estimate of the mean over the failure surface. For the assumption of a normal distribution of X , this is equivalent to a cautious estimate of X_m , the mean of the underlying distribution (Figure 1c).

References

American Petroleum Institute [API] (2014a). *Planning, designing and constructing fixed offshore platforms - working stress design*. (API RP 2A-WSD, 22nd Edition) <https://www.apiwebstore.org/publications/item.cgi?b9e32dec-268b-404d-988e-5cda65c27757>

American Petroleum Institute [API] (2014b). Geotechnical and foundation design considerations: ISO 19901-4:2003 (modified), petroleum and natural gas industries-specific requirements for offshore structures, part 4-geotechnical and foundation design considerations: addendum 1. (ANSI/API RP 2GEO First Edition, with Addendum) <https://www.apiwebstore.org/publications/item.cgi?b6c6e7f5-6da7-46c2-97bb-54bd470f0401>

Baecher, G.B., and Christian, J.T. (2003). *Reliability and statistics in geotechnical engineering*. Wiley.

DNV GL AS, (2017). Statistical representation of soil data (DNVGL-RP-C207). <https://standards.globalspec.com/std/10159282/DNVGL-RP-C207>

DNV GL AS (2019). *Offshore soil mechanics and geotechnical engineering. Recommended practice* (DNVGL-RP-C212). <https://standards.globalspec.com/std/10183661/DNVGL-RP-C212>

European Committee for Standardization (2009). Eurocode 7: geotechnical design - part 1: general rules (with corrigendum EN 1997-1:2004/AC, February 2009) (EN 1997-1:2004). https://standards.cen.eu/dyn/www/f?p=204:110:0:::FSP_PROJECT,FSP_ORG_ID:12442,6231&cs=1D03CC06CB9166EAAA1C6CE997CDA87C2

European Committee for Standardization (2010). *Eurocode 7 - geotechnical design - part 2: ground investigation and testing* (EN 1997-2:2007+ AC:2010) https://standards.cen.eu/dyn/www/f?p=204:110:0:::FSP_PROJECT,FSP_ORG_ID:23735,6231&cs=14A2DCCA6BF367BFBD54D9FC0822BE0ED.

Hicks, M.A. (2013). An explanation of characteristic values of soil properties in Eurocode 7. In P. Arnold, G.A. Fenton, M.A. Hicks, T. Schweckendiek and B. Simpson (eds.) *Modern geotechnical design codes of practice: implementation, application and practice* (pp. 36-45). IOS Press. DOI 10.3233/978-1-61499-163-2-36.

International Organization for Standardization (2015). *General principles on reliability for structures* (ISO 2394:2015). <https://www.iso.org/standard/58036.html>

International Organization for Standardization (2016). Petroleum and natural gas industries – specific requirements for offshore structures – part 4: geotechnical and foundation design considerations (ISO 19901-4:2016). <https://www.iso.org/standard/61144.html>

International Organization for Standardization (2019). *Petroleum and natural gas industries – general requirements for offshore structures* (ISO 19900-2019).

<https://www.iso.org/standard/69761.html>

International Organization for Standardization (2016). *Petroleum and natural gas industries – offshore production installations – guidelines on tools and techniques for hazard identification and risk assessment* (ISO 17776:2016).

<https://www.iso.org/standard/63062.html>

Peuchen, J., Meijninger, B.M.L. & Drummen, T.W.A. (2015). Reassessment of geotechnical conditions after an offshore well incident. Invited lecture. In *Proceedings of the XVI ECSMGE: geotechnical engineering for infrastructure and development* (pp. 195-206). ICE Publishing.

Appendix D

Supplementary Information
about Document

Contents Appendix D: Supplementary Information about Document

List of Documents

D.1 Quality Management Record

D.2 Document Issue Record

D.1 Quality Management Record

Fugro Project Lead: B.B. Klosowska
Principal Geologist

Report Review and Approval: L.J. Peuchen
Principal Geotechnical Engineer

Document Section	Prepared By	Checked By
Main Text	BBK/KKS	LJP
Appendix A	KWA	BBK
Appendix B	EGM	BBK
Appendix C	BBK	LJP

Project Team

Initials	Name	Role
BBK	B. Klosowska	Principal Geologist
KKS	K. Kaltekis	Senior Geotechnical Engineer
LJP	J. Peuchen	Principal Geotechnical Engineer
KWA	K. Wojtaszekova	GIS specialist
EGM	E. Gómez Meyer	Geotechnical Engineer

D.2 Document Issue Record

Section	Page No.	Plate No.	Issue	Revision
Main Text	all	-	02	Editorial amendment

- The definitive copy of this document is held in Fugro's information system
- Document distribution is restricted to project participants approved by the client
- The Issue number of this document is shown on the Document Control page presented after the title page of this document; some (unchanged) pages and plates can show a lower issue number
- The reference at the bottom left-hand corner of each page shows the Fugro document no. and the page issue number